PAX2/3 IN NORMAL KIDNEY DEVELOPMENT AND AS THERAPEUTIC TARGETS IN RENAL CANCER.

by

Pierre-Alain Hueber

A thesis submitted to Graduate and Postdoctoral Studies Office of McGill University in partial fulfillment of the requirements of the Degree of Doctor of Philosophy.

December 2007

Department of Medicine
McGill University
Montreal, Quebec
Canada

Your file Votre référence
ISBN: 978-0-494-50830-5
Our file Notre référence
ISBN: 978-0-494-50830-5

ABSTRACT

The *PAX* gene family of transcription factors plays a prominent role during embryogenesis however can be aberrantly re-activated during tumorigenesis and contributes to the malignant phenotype.

During embryonic kidney development, *PAX2* exerts an anti-apoptotic function however its expression typically attenuates during the post-natal period. On the other hand, PAX2 aberrant expression is observed in the majority of Renal Cell Carcinomas (RCC). RCC is resistant to chemotherapy; up-regulation of anti-apoptotic genes is recognized to contribute to tumor resistance to chemotherapy. We hypothesized that the anti-apoptotic effect of the *PAX2* gene that is expressed in RCC cells contributes to RCC and their resistance to chemotherapy-induced cell death.

Human embryonic kidney (HEK293) cells transfected with a *PAX2* expression vector and exposed to cisplatin, were protected from apoptosis compared to control cells. Conversely, murine collecting duct cells stably transfected with *PAX2* antisense cDNA had twofold increases in cisplatin-induced apoptosis. Similarly, PAX2 knockdown using PAX2 siRNA in RCC cells CAKI-1 and ACHN enhances cisplatin-induced apoptosis *in vitro*.

To test the combination of *PAX2* expression silencing and cisplatin teatment *in vivo* we developed a model of renal tumors by injecting ACHN cells as a xenograft under the skin of nude mice. I showed that a *PAX2* shRNA successfully knocks down PAX2 mRNA and protein levels in a RCC cell line (ACHN). ACHN cells stably transfected with shRNAs targeted against the PAX2 homeodomain, are more susceptible to cisplatin-induced caspase-3 activation than the control ACHN cell line. Furthermore, growth of subcutaneous ACHN/shPAX2 xenografts in nude mice is significantly more responsive to cisplatin therapy than control of ACHN cell tumors. This work proposes *PAX2* as a potential therapeutic gene target in metastatic renal cell carcinoma and suggests that

adjunctive PAX2 knockdown may enhance the efficacy of chemotherapeutic agents such as cisplatin.

Wilms tumor, the most common pediatric renal cancer, is thought to arise from a progenitor cell of the metanephric mesenchyme that fails to complete nephrogenesis. In addition to its characteristic triphasic histology, WT can exhibit myogenic differentiation. Myogenic programming during muscle development is controlled by a PAX3 transciption factor determinant for muscle development; unexpectedly PAX3 transcriptional activity has been recently identified in the embryonic mouse kidney. These observations led us to hypothesize that *PAX3* plays a role during kidney development. Furthermore, we predict that if PAX3 expression is verified during renal development, PAX3 may also be expressed in Wilms tumor with a myogenic component.

I showed that PAX3 is expressed in the metanephric mesenchyme and stromal compartment of the developing mouse kidney. In a panel of 20 Wilms tumors, PAX3 was identified in tumor samples with myogenic histopathology. Furthermore, mutations of WT1 were consistently associated with PAX3 expression in Wilms tumors and modulation of WT1 expression in HEK293 cells was inversely correlated with the level of endogenous PAX3 protein.

This work supports a novel model of normal renal development in which progenitor cells of the metanephric blastema express PAX3 when targeted toward the stromal cell fate. Suppression of PAX3 is integral to the mesenchyme-to-epithelium transition, which defines the nephrogenic cell fate and may be accomplished, in part, by WT1. Conversely, failure to suppress PAX3 may account for the myogenic phenotype in a subset of WT1-negative Wilms tumors.

RESUME

Les programmes génétiques qui contrôlent le développement embryonnaire peuvent êtres réactivés durant l'oncogenèse ou ils contribuent à l'acquisition du cancer.

PAX2 encode un facteur de transcription essentiel au développement embryonnaire du rein qui a pour fonction de contrôler l'apoptose ou mort cellulaire programmé. Après complétion de l'organogenèse, la répression transcriptionnelle de ce facteur durant la période postnatale permet la différenciation normale de l'épithélium rénal. Cependant, la réactivation aberrante de PAX2 est observée dans la majorité des cas de carcinome rénal.

Les cancers du rein sont extrêmement résistants aux traitements actuels et aucun agent de chimiothérapies n'a, à ce jour, prouvé son efficacité contre ce type de cancer. Ainsi il est impératif d'identifier les voies moléculaires impliquées dans la résistance à la chimiothérapie des cellules de carcinomes rénaux de manière à définir une nouvelle stratégie thérapeutique efficace. Un des mécanisme notoire qui cause la résistance a la mort cellulaire des cellules cancéreuses est l'expression de gènes anti-apoptotiques.
En s'appuyant sur la fonction anti-apoptotique de PAX2, nous supposons que l'expression de PAX2 dans les adénocarcinomes rénaux contribue à leur résistance à la mort cellulaire programmee induite par la chimiothérapie.

Nous montrons que l'expression de PAX2 dans des cellules embryogéniques rénales leurs confère une protection significative contre l'apoptose induite par l'agent de chimiothérapie cisplatin. Réciproquement l'inhibition de l'expression endogène de gène PAX2 dans les cellules d'adénocarcinomes rénaux CAKI-1 et ACHN, par siRNA, entraîne l'apoptose et une susceptibilité des cellules tumorales a la mort cellulaire induite par le traitement de cisplatin *in vitro*.

Pour tester *in vivo* le potentiel de PAX2 comme cible thérapeutique, nous avons développé un Model de tumeur rénal dans des souris athymiques en les injectant avec des xénogreffes des cellules de carcinome rénal ACHN en sous-cutanés. Afin d'inhiber l'expression de PAX2, nous avons généré des lignées cellulaires de carcinome rénal stable contenant un vecteur d'expression de PAX2 shRNA. En mesurant la croissance des tumeurs +/-PAX2 dans des souris athymiques traités avec du cisplatin (en injection intra-péritonéale) nous avons pu montrer que l'inhibition de PAX2 dans les tumeurs ACHN-shPAX2 augmente leur susceptibilité a l'effet thérapeutique du cisplatin résultant en une réduction significative du volume tumoral. Ce travail met en évidence le rôle de PAX2 dans la résistance à la chimiothérapie des cellules de carcinomes rénaux et identifie le potentiel des stratégies thérapeutiques visant à moduler l'expression de PAX2.

La tumeur de Wilms est l'une des plus fréquentes des tumeurs solides de l'enfant. Une différentiation myogènes est présente dans 5 à 10% des cas. PAX3 est un facteur de transcription qui joue un rôle central dans la myogenèse. Récemment et de façon inattendue la présence de PAX3 a été suggérée dans le rein embryonnaire. Nous avons émis l'hypothèse suivante : si l'expression de PAX3 est confirmée dans le rein embryonnaire, il est envisageable que PAX3 soit également exprimé dans les tumeurs de Wilms dans lesquels il est peut être responsable de la différentiation musculaire parfois observée.

J'ai montré que PAX3 est exprimé dans le rein embryonnaire où il marque la lignée stromale. PAX3 est exprimé dans les cellules du mésenchyme (MK4) mais pas dans les cellules épithéliales (IMCD).
En sur exprimant PAX3 dans une lignée cellulaire de rein embryonnaire HEK293 j'ai montré que la fonction de PAX3 incluse la prolifération et la migration cellulaires.
Nous avons démontré l'expression de PAX3 dans les tumeurs de Wilms qui ont une composante myogénique. Nous avons aussi mis en évidence l'association entre l'expression de PAX3 dans la composante stromale des tumeurs de Wilms et la présence d'une mutation dans le gène WT1. Cette observation fut confirmée *in vitro* dans des cellules de reins embryonnaires, dans lesquels l'inhibition de WT1 via WT1-siRNA

résulte en une augmentation de l'expression de PAX3. Réciproquement la transfection de l'isoforme WT(-/+) entraîne réduction de l'expression de PAX3.

L'ensemble de ces observations soutient l'hypothèse que WT1 inhibe l'expression de PAX3 dans les cellules rénales durant le développement rénal normal mais qu'en présence d'une mutation dans le gène WT1 acquise lors de la formation d'une tumeur de Wilms, PAX3 est exprimé de façon anormale. De plus, nous proposons et que l'expression de PAX3 est typiquement responsable du potentiel de différentiation musculaire des tumeurs de Wilms qui ont une mutation dans *WT1* et une histologie stromale.

TABLE OF CONTENTS

ABSTRACT 2
RESUME 4
TABLE OF CONTENTS 7
LIST OF FIGURES 10
LIST OF TABLES 11
ABBREVIATIONS 12
ACKNOWLEDGEMENTS 13
PREFACE 14
CONTRIBUTIONS OF AUTHORS 15

CHAPTER I: INTRODUCTION 16

1.1 Renal Cell Carcinoma (RCC) 17
1.1.1 Epidemiology 18
1.1.2 Risk factors 21
1.1.3 Genetic factors 23
1.1.3.1 Familial Clear Cell RCC 26
1.1.3.2 Familial Papillary RCC 29
1.1.3.3 Familial Chromophobe RCC and Oncocytoma 31
1.1.3.4 Diagnostic and management of hereditary renal cancer 31
1.1.4 Histopathology 32
1.1.5 Molecular biology of RCC 36
1.1.5.1 VHL/HIF pathway 36
1.1.5.2 MET pathway 37
1.1.5.3 PTEN, Akt and mTOR pathway 38
1.1.6 Diagnosis staging and prognosis 40
1.1.7 Treatment 43
1.1.7.1 Surgical care 43
1.1.7.2 Chemotherapy 44
1.1.7.3 Modifiers of biological response 46
1.1.7.4 Therapies targeting molecular pathways 47
1.1.8 RCC Summary: 50

1.2 Wilms Tumor 51
1.2.1 Epidemiology 51
1.2.3 Genetic predispositions 52
1.2.4 Genetic syndromes 53
1.2.5 Familial Wilms Tumor 57
1.2.6 Diagnosis and clinical presentation 57
1.2.7 Histology 58
1.2.8 Staging/prognosis 59
1.2.9 Treatment 61
1.2.9.1 Overview 61

1.2.9.2 Surgery 61
1.2.9.3 Chemotherapy 62
1.2.9.4 Treatment long-term sequelae 65
1.2.10.1 WT1 (chromosome 11p13) 66
1.2.10.2 WT2 (Chromosome 11p15) 67
1.2.10.3 CTNNB1 (chromosome 3p21) 68
1.2.10.4 WTX (chromosome Xq11.1) 69
1.2.10.5 Other loci 70
1.2.12 Wilms tumor as an aberration of normal nephrogenesis 74

1.3 Kidney development 76
1.3.1 Overview 76
1.3.2 PAX2/8 and WT1 in kidney development 77
1.3.3 The WNT canonical pathway in kidney development 79
1.3.4 Renal stem cells and cancer stem cell 79

1.4 PAX genes in development and cancer 81
1.4.1 Overview 81
1.4.2 PAX2 84
1.4.2.1 Overview 84
1.4.2.2 Human Renal Coloboma Syndrome and the *Pax2*^{1Neu} mouse 84
1.4.2.3 Genomic structure of *PAX2* 85
1.4.2.4 PAX2 expression during development 85
1.4.2.5 PAX2 function during development 86
1.4.2.6 Expression in cancer 88
1.4.2.7 PAX2 function in cancer 89
1.4.3 PAX3 90
1.4.3.1 Overview 90
1.4.3.2 The Splotch Mouse and the Waardenburg syndrome 91
1.4.3.3 Gene structure 92
1.4.3.4 Expression during development 93
1.4.3.4 PAX3 function during development 94
1.4.3.5 Expression in cancer 97
1.4.3.6 Function in cancer 97

1. 5 Research aims 99

CHAPTER II: PAX2 as a therapeutic target for renal cancer 100

2.1 Overview: 101

PAX2 inactivation enhances cisplatin-induced apoptosis in renal carcinoma cells 102
2.1.1 ABSTRACT 103
2.1.2 INTRODUCTION 104
2.1.3 RESULTS 106

2.1.4 DISCUSSION 118
2.1.5 METHODS 121

In Vivo validation of PAX2 as a target for renal cancer therapy 128
2.2.1 ABSTRACT 129
2.2.2 INTRODUCTION 130
2.2.3 RESULTS 131
2.2.4 DISCUSSION 138
2.2.5 METHODS 142

CHAPTER III: PAX3: from kidney development to Wilms tumor 151

3.1 ABSTRACT 153
3.2 INTRODUCTION 154
3.3 RESULTS 155
3.4 DISCUSSION 168
3.5 METHODS 172

CHAPTER IV: DISCUSSION AND FUTURE DIRECTIONS 179

4.1 DISCUSSION 180
4.1.1 Paradigm 180
4.1.2 PAX2 confers resistance to cisplatin-induced apoptosis 181
4.1.3 Suppression of PAX2 enhances cisplatin-induced apoptosis in RCC cells 182
4.1.4 Suppression of PAX2 enhances *in vivo* response of renal tumor to cisplatin 186
4.1.5 Other PAX genes in cancer 188
4.1.6 *PAX3* is expressed in the developing kidney 188
4.1.7 PAX3 expression is identified in myogenic Wilms Tumors 190
4.1.8 PAX3 is regulated by WT1 during renal development 191
4.1.9 PAX3 function 191
4.1.10 A novel WT1(-) primary Wilms tumor cell line 192
4.1.11 A novel model of renal development and Wilms tumor 192

4.2 SUMMARY 194

4.3 FUTURE DIRECTIONS 195

4.4 ORIGINAL CONTRIBUTIONS 197

LIST OF FIGURES

Figure 1.1 World map of kidney cancer incidence..... 19
Figure 1.2 Kidney cancer rate in Canada 1983-1997..... 20
Figure 1.3 RCC Histological appearances..... 35
Figure 1.4 Molecular pathway in RCC..... 39
Figure 1.5 Staging and Prognosis of RCC..... 42
Figure 1.6 Molecular pathways and targeted therapies..... 49
Figure 1.7 Wilms tumor histology.....58
Figure 1.8 Wilms tumor pathogenesis..... 72
Figure 1.9 Stages of kidney development and nephrogenesis..... 78
Figure 2.1.1.PAX2 expression confers resistance to cisplatin-induced apoptosis..... 108
Figure 2.1.2. Reduced PAX2 expression sensitizes IMCD cells to cisplatin..... 109
Figure 2.1.3. Genetic reduction of PAX2 increases susceptibility to cisplatin-induced apoptosis..... 110
Figure 2.1.4. Endogenous PAX2 protein expression by CAKI-1 and ACHN renal carcinoma cells is suppressed by PAX2-siRNA..... 113
Figure 2.1.5. Inhibition of PAX2 induces apoptosis of Renal Cell Carcinoma cell lines. 114
Figure 2.1.6. Annexin V staining..... 115
Figure 2.1.7. RCC cell death caused by PAX2 siRNA and cisplatin are additive..... 116
Figure 2.1.8. Combined killing induced by PAX2 inhibition plus cisplatin is caspase-dependent..... 117
Figure 2.2.1 Diagram of Pax2 shRNA construct..... 132
Figure 2.2.2 Stable knockdown of PAX2 mRNA and protein in ACHN cells expressing shRNA constructs..... 133
Figure 2.2.3: Stable knockdown of PAX2 sensitizes ACHN cells to Caspase-3 induced by treatment with cisplatin..... 135
Figure 2.2.4 Effect of PAX2 knockdown on the growth of ACHN tumor xenografts in nude mice treated with cisplatin..... 137
Figure 3.1. *PAX3* mRNA and PAX3 protein are expressed in mouse embryonic kidney and in renal cell lines..... 157
Figure 3.2 PAX3 protein localizes in the stromal and the mesenchymal compartments of developing mouse kidney..... 158
Figure 3.2 PAX3 mRNA transcript and protein is up regulated in a panel of Wilms Tumor with myogenesis..... 161
Figure 3.4 WT1 inhibits PAX3 promoter transcriptional activity in human embryonic kidney (HEK293) cells..... 162
Figure 3.5 Function of PAX3 in HEK293 cells..... 165
Figure 3,6 Characterization of a primary Wilms tumor cell line (WiTP3)..... 166
Figure 3.7 Development model of Wilms tumor molecular pathogenesis..... 167

LIST OF TABLES

Table 1.1 Inherited syndromes associated with the development of renal neoplasia. 25
Table 1.2 Genetic syndromes predisposing to Wilms tumor 54
Table 1.3 Staging of Wilms tumors: 60
Table 1.4 Treatment of favorable histology Wilms tumor: 63
Table 1.5 PAX genes structure, chromosomal location and human syndromes: 82
Table 1.6 PAX genes expression and function in cancer: 83

ABBREVIATIONS

APAF-1	apoptosis protease activating factor-1
BAX	BCL2 associated X protein
BCL2	B-cell lymphoma 2
β-GAL	beta-galactosidase
cDNA	complementary DNA
DMR	DNA methylated region
DNA	deoxyribonucleic acid
E	embryonic day
EGF	epidermal growth factor
EGFR	epidermal growth factor receptor
FGF	fibroblast growth factor
FOXC	forkhead box C
FOXD	forkhead box D
GAPDH	glyceraldehydes-3-phosphate dehydrogenase
GDNF	glial-cell derived neurotrophic factor
HEK 293	human embryonic kidney 293 cells
HGF	hepatocyte growth factor
IAP	inhibitors of apoptosis
IMCD	inner medullary collecting duct cells
MAPK	mitogen-activated protein kinase
MM	metanephric mesenchyme
mRNA	messenger ribonucleic acid
NAIP	neuronal apoptosis inhibitory protein
OMIM	online Mendelian inheritance in man
P	post-natal day
PAX	paired-box gene
PBS	phosphate buffered saline
PCR	polymerase chain reaction
RAR	retinoic acid receptor
RCC	renal cell carcinoma
RCS	renal-coloboma syndrome
RNA	ribonucleic acid
RNAi	RNA interference
RT-PCR	reverse transcripation PCR
ShRNA	short hairpin RNA
SiRNA	short/small RNA
TGFα	transforming growth factor alpha
TUNEL	terminal deoxynucleotidyl transferase-mediated dUTP nick end labelling
UB	ureteric bud
VHL	Von-Hippel Lindau gene
WNT	homologue of the *Drosophila* wingless-type gene
WT1	Wilm's tumor gene 1
XIAP	X-linked IAP

ACKNOWLEDGEMENTS

Firstly, I would like to thank my supervisor, Dr. Paul Goodyer. Thank you for providing me with a stimulating lab environment with constant openness and enthusiasm for novel ideas and for your help ensuring the achievement of my PhD.

Thank you to my lab colleagues and friends, it has been a pleasure working with you. Thank you Lee Lee for your technical support, expertise and patience with a member of the 'kit' generation like me. To Dave Myburgh, thank you for being my IT guru. Dr. Diana Iglesias, your Latin spirit, endless enthusiasm for science and your friendship were a true support. Thank you Dr. Dziarmaga for your intensity, leadership and your attempt to "polish' my lab skills. Thank you Dr. Xhang for your pleasant demeanour and humorous spirit. Merci Dr Elkares, pour ton aide et pour prendre la releve de l'unite du cancer des reins du PG lab.

Thank you to the entire Nephrology team; you will be remembered. Tiffany Cohen (for your efficiency), Anne-Marie Patenaude (for your biology "de fer"), Jacklyn Quinlan (for your Caribbean spirit), Elena Pasquet (for your pragmatism), Inga Murawski (for your cookies), Tristan Alie (for your sense of adventure) and Nicholas Haddad (for your poise).

Domo aligato gozaïmass to Dr. Ryugi Fukuzawa from our New Zealand collaborators, for your work and valuable insight on Wilms tumor pathogenesis.

Thank you to my supervisory committee members, both past and present; Dr.'s Nada Jabado, Jacques Galipeau, Lawrence Panasci, Gordon Shore, Harry Goldsmith and Maxime Bouchard. Your insight and constructive criticisms contributed to the achievement of my research project.

Finally, a sincere thank you to my friends, family, wife Angela and above all, my grandfather, for your continuous support during this scientific venture.

PREFACE

This thesis is written in accordance with the guidelines of the Faculty of Graduate Studies at McGill University. It is comprised of four chapters and two appendices. Chapter I is an introduction consisting of the rationale for the research as well as background information relevant to this thesis. Chapters II and III are data chapters and are in the form in which they were submitted for publication. Part I of Chapter II has been published in *Kidney International April 2006* and Part II has been submitted to C*ancer Letters*. Chapter III has been submitted to *Proceedings of the National Academy of Sciences* (PNAS). Connecting text between Chapters II and III is provided in accordance with Section C of the Guidelines for Submitting a Doctoral or Master's Thesis in the manuscript-based format. Chapter IV consists of a general discussion of the results presented in Chapter II and future directions. Appendix I consists of publications that arose during the course of the candidate's graduate work. Appendix II consists of permissions and compliance forms.

Gene and protein nomenclature was assigned following the guidelines provided by HGNC (HUGO Gene Nomenclature Committee) (www.gene.ucl.ac.uk/nomenclature) for human genes and proteins and on guidelines from Mouse Genome Informatics – The Jackson Laboratory (www.informatics.jax.org/mgihome/nomen) for mouse genes and proteins.

CONTRIBUTIONS OF AUTHORS

Dr. Paula Waters was responsible for the engineering and the IMCD cells stably transfected with a *PAX2* antisense (Figure 2.2). Patsy Clark was responsible for the experiment of *Pax2+/-* embryonic kidney explants treated with cisplatin (Figure 2.3). Dr. Suhje He was responsible for PAX3 staining of the embryonic kidney at stage E11.(Figure 3.2). Dr. Ryugy Fukuzawa was responsible for performing all experiments on the Wilms tumor panel including PAX3 immunostaining and QRT-PCR (Figure 3.3). Dr. Myriam Blumentkrantz was responsible for the H&E and WT1 staining of the tumors from which the WiTP3 cells were derived (Figure 6a). Dr. Reyan Elkares was responsible for the genetic analysis of the WiTP cells (Figure 6b).

The candidate was responsible for all other experiments participated actively in experimental design strategies, the preparation all of the manuscripts and figures included. Chapter V is a discussion of all results presented in this thesis, as well as potential future studies and a list of original contributions by the candidate.

CHAPTER I: INTRODUCTION

INTRODUCTION

Foreword:

Of the many challenges of medicine, rarely a malady has experienced more hard-fought progress than the treatment and cure of cancer. According to the World Health Organization (WHO), the projections of cancer deaths is rising with an estimated 9 million people dying from cancer in 2015, and 11.4 million dying in 2030 (http://www.who.int/cancer/en/). This statistic can be translated into more concrete facts: in Canada one person out of four will develop a cancer; we all know someone that has been taken by this disease. It has regrettably become a cliché to highlight the need for cancer research and the imperative necessity of finding better treatment.

Kidney cancer is the 7th leading malignant condition among men and the 12th among women worldwide, accounting for almost 3% of all cancers worldwide with 200,000 new cases and 78,000 deaths annually (Curado. M. P., 2007). In adults, 80 to 85 percent of kidney tumors are classified as renal-cell carcinoma, arising from the renal parenchyma in adults and 10% are transitional-cell carcinomas from the renal pelvis. Children may develop Wilms tumors (nephroblastoma) of the kidney during the first years of life.

1.1 Renal Cell Carcinoma (RCC)

Renal-cell carcinoma arises from the renal epithelium and is the most common renal malignancy. At the time of diagnosis, a quarter of the patients present with advanced metastatic disease. Due to resistance to current therapy, the median 5 year survival rate for patients with metastatic RCC is only between five and ten per cent. Understanding the kidney cancer molecular pathways underlying RCC resistance to therapy is imperative to identify targets for novel drug therapy.

1.1.1 Epidemiology

In Canada in 2006, 4600 patients were diagnosed with renal cancer and 1550 died from this disease (Canadian Cancer Statistic 2006, www.cancer.ca). The male to female ratio in incidence is 1.6:1 and the median age is in the sixth decade of life. The incidence age adjusted for the world population is variable depending on the geographical location. In 2002, the incidence rate in Canada was about 11 per 100,000 men and 5.8 per 100,000 women which is comparable to the incidence rate in the US or Western Europe. Rates are generally high in Europe, North America and Scandinavia, intermediate in the Middle East and South America and low in Asia and Africa **(Fig.1.1)** (Scelo & Brennan, 2007). During the last two decades, kidney cancer incidence rates have been rising in nearly all regions of the world. For example, in Canada the incidence has increased by more than 50% between 1977 and 1996 **(Fig1.2)** (Perkin et al.). This trend is partly explained by improvements in detection and diagnostic but also correlates with an increased prevalence of risk factors. In the US, kidney cancer is more frequent in the black population (13.3 per 100,000 men and 7.1 per 100,000 women) than in the white population (11.1 per 100,000 and 5.6 per 100,000 women). A reason for this difference may be explained by the higher frequency of obesity and hypertension among the black than in the white population, both recognized as risk factors for RCC (Chow *et al.*, 1999).

Figure 1.1 World map of kidney cancer incidence.

For both male and female, a high incidence of RCC is observed in Europe and North America and a low incidence is found in Asia and Africa (Curado. M. P., 2007). (Data from Globocan 2002 Cancer Incidence, Mortality and Prevalence Worldwide, IARC Cancer Base No. 6, Lyon, IARC Press, 2002)

Kidney cancer Age-Standardized incidence rate per 100,000 females

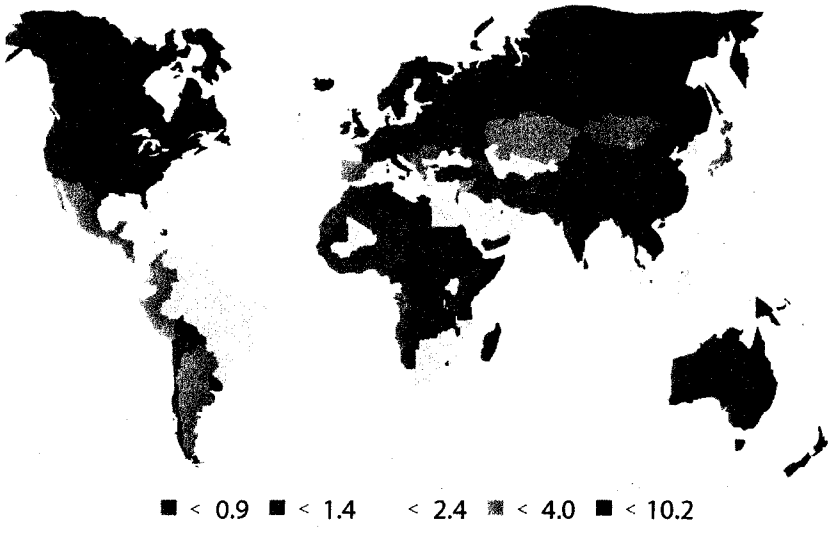

Kidney cancer Age-Standardized incidence rate per 100,000 males

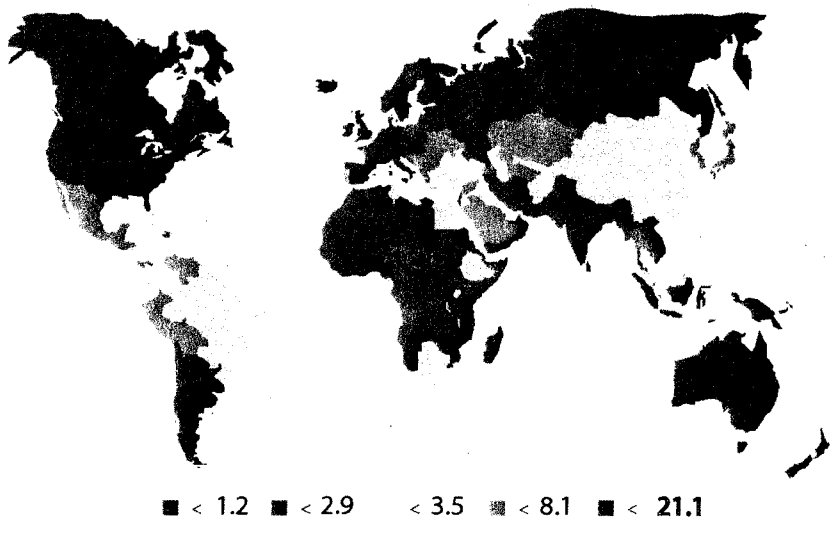

Fig. 1.1

Figure 1.2 Kidney cancer rate in Canada 1983-1997.

The kidney cancer rate has steadily increased over time in Canada in both males and females for the last two decades (Curado. M. P., 2007). (Graphic built using the data from Arkin, D.M., Whelan, S.L., Ferlay, J., and Storm, H. Cancer Incidence in Five Continents, Vol. I to VIII IARC CancerBaseNo. 7, Lyon, 2005).

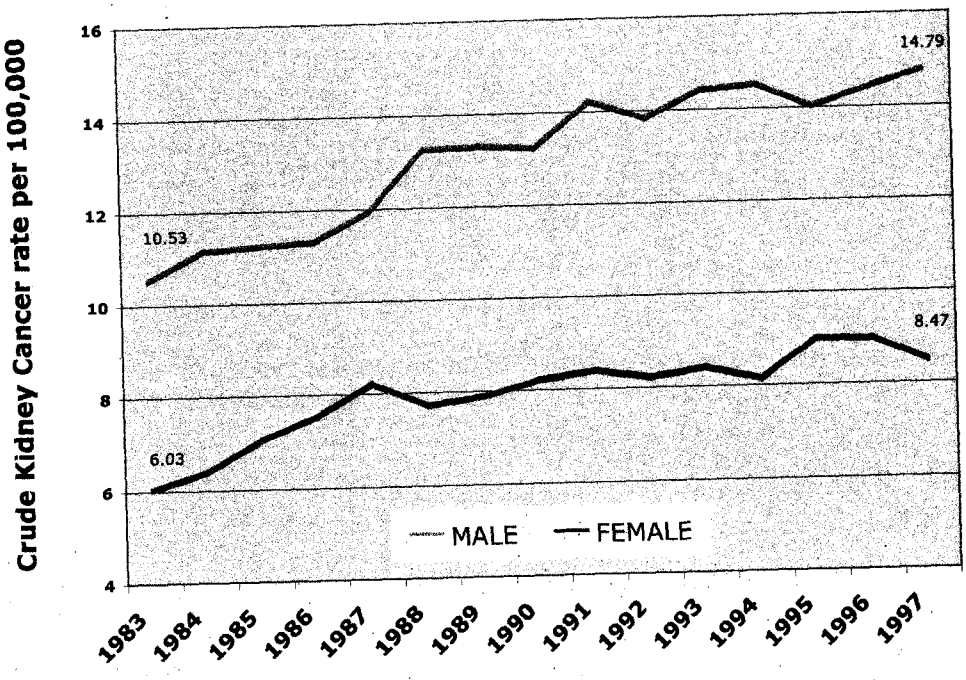
Crude Kidney Cancer rate per 100,000
16
14
12
10
8
6
4
14.79
10.53
8.47
6.03
MALE
FEMALE
1983
1984
1985
1986
1987
1988
1989
1990
1991
1992
1993
1994
1995
1996
1997

Fig.1.2

1.1.2 Risk factors

Overview:

Cigarette smoking and obesity are the most consistently established causal risk factors and estimated to account together for about 60 % of all renal cell cancer cases. Hypertension, rather than antihypertensive drugs, appears to influence renal cell cancer development. In general, there appears to be a protective effect of fruit and vegetable consumption, although no particular component of diet has been clearly implicated. There are sporadic reports of occupational exposures such as Polycyclic Aromatic Hydrocarbon (PAH) being associated with this cancer but the evidence for association with a specific occupation is still inconclusive.

Cigarette Smoking:

Several studies have clearly demonstrated that cigarette smoking is a risk factor for developing renal cancer. Smokers are at 50% increased risk of developing renal cancer compared with non-smokers. This risk has been shown to significantly decrease with years of cessation (Hunt *et al.*, 2005). It is estimated that smoking is responsible for 20-30% of renal cancer in men and 10-20% in women (McLaughlin *et al.*, 1995).

The mechanism by which cigarette smoking increases the risk of kidney cancer is not fully understood yet. Cigarette smoke has been shown to cause specific DNA alteration. For instance, Korenaga and colleagues found a significant association between smoking and allelic imbalance at chromosome 5q22.2-22.3 in RCC (Korenaga *et al.*, 2005). Interestingly, a study conducted in the Netherlands concluded that smoking was not associated with *VHL* specific mutation implying that smoking may cause or promote RCC independently of the VHL pathway (van Dijk *et al.*, 2006).

Obesity:

A linear relationship between kidney cancer and increasing weight gain has been established in several case-control and cohort studies both in men and women equally.

A review concludes that the relative risk for RCC is 1.07 per each unit Body Mass Index (BMI) increase above the obesity threshold (Bergstrom *et al.*, 2001). The mechanism by

which obesity triggers renal cancer is unclear although hormonal factors such as increased levels of estrogen associated with weight gain may be implicated (Calle & Kaaks, 2004). In the overall population it is estimated that 25% of all kidney cancer cases stem from being overweight and obese. Therefore obesity is designated as major player underlying the increase incidence of renal cancer in North America for the last past 20 years (Calle & Kaaks, 2004)

Hypertension:

A history of hypertension has been consistently associated with kidney cancer.

This association between blood pressure and increased risk cancer seems to occur in a dose dependent manner. Since reduction of blood pressure has been shown to reduce RCC risk, hypertension appears to have a causal relationship to renal cancer (Scelo & Brennan, 2007). About 20-40% of renal cancer can be attributed to hypertension (Scelo & Brennan, 2007).

Diabetes mellitus:

Diabetes mellitus has been associated with an increased risk of several cancers however its relation with RCC risk is controversial. A slight, increased risk was found in patients with a history of diabetes mellitus but further studies of this issue are required (Zucchetto *et al.*, 2007).

Use of Analgesics:

An association between chronic use of phenacetin containing analgesics and cancers of the renal pelvis has been clearly established (Scelo & Brennan, 2007). However, the effect on development of renal cell carcinoma is less clear. In any event, this is no longer a major concern since phenacetin-containing analgesics are currently no longer on the market. Extensive studies have been conducted on acetaminophen (the major metabolite phenactin) and have concluded that there is no relationship between renal cancer and acetaminophen use. Similarly studies have ruled out the use of aspirin as a potential cause of increased risk for renal cancer (McCredie *et al.*, 1995).

Kidney Transplantation and Dialysis:

A higher incidence of RCC is observed in patients undergoing long-term renal dialysis. RCC seems to arise in those dialysis patients who develop renal cystic disease of the native kidneys. Patients with kidney transplants who develop cysts in their native kidneys also have increased likelihood of developing RCC. It is estimated that 30-40% of kidney transplant patients will develop acquired cystic disease and this confers a 30-fold increase in the risk of developing RCC (Stewart *et al.*, 2003).

Diet:

A study has concluded that increased intake of both fruits and vegetables possibly reduce the risk of kidney cancer (Rashidkhani *et al.*, 2005). However other studies found no correlation between fruits and vegetable intake and risk of developing RCC (Weikert *et al.*, 2006). Overall, the results of analytical studies indicate that coffee and tea consumption does not increase the risk of renal cell cancer (Lee *et al.*, 2006).

Epidemiologic studies have investigated the association between alcohol consumption and the incidence of RCC, with somewhat controversial results. In the past, studies have found no relation between alcohol consumption and RCC, however, several recent studies have shown a protective effect of ethanol consumption. It was confirmed in a pooled analysis of 12 prospective studies that moderate alcohol consumption was associated with a lower risk of renal cell cancer among both women and men (Lee *et al.*, 2007).

1.1.3 Genetic factors

Several studies have reported an increased risk of developing renal cancer for individuals with a first-degree relative affected by this disease (Chow *et al.*, 2000).Although most cases of RCC occur sporadically, an inherited predisposition to renal cancer is estimated to account for 1-4% of all cases. Interestingly, these inherited genetic factors can involve some of the same genes that cause sporadic renal cancer. Typically, familial renal cancers

are characterized by an early onset compared with sporadic cases and frequently comprise bilateral and multifocal tumors. So far seven hereditary renal cancer syndromes and 5 predisposing genes associated with these have been identified (summarized in **table 1.1).**

Table 1.1 Inherited syndromes associated with the development of renal neoplasia. Von Hippel–Lindau (VHL) disease, associated with clear-cell renal-cell carcinomas and multi-organ neoplasia, is caused by germline mutations in the *VHL* tumor-suppressor gene and loss of the wild-type *VHL* allele; Patients with hereditary papillary renal carcinoma (HPRC) harbor germline activating mutations in the *MET* proto-oncogene, which can cause renal cancers with papillary type-1 histology. Papillary type-2 renal carcinomas and cutaneous and uterine smooth-muscle tumors are associated with the syndrome of hereditary leiomyomatosis and renal-cell cancer (HLRCC), which is caused by germline loss-of-function mutations in the Fumarate-Hydratase (*FH*) gene. The Birt–Hogg–Dubé syndrome (BHD) predisposes to cutaneous nodules (benign tumors of the hair follicle), spontaneous pneumothorax and an increased risk for renal cancers such as chromophobe renal-cell carcinoma and oncocytic hybrid renal tumor. BHD is caused by germline mutations in the tumor-suppressor gene *BHD*. Hyperparathyroidism-jaw tumor syndrome (HPT-JT) is associated with parathyroid adenomas, fibro-osseous tumors of the jaw, and unusual renal tumors containing a mixture of epithelial and stromal elements. This syndrome is caused by germline mutations in the gene *HRPT2* (Pavlovich & Schmidt, 2004).

Table 1.1 Heritable syndromes associated with renal cancer:

Syndrome	Gene	RCC type
Von Hippel-Lindau (VHL)	*VHL*, 3p35	**Clear-cell RCC** (solid and/or cystic, multiple and bilateral)
Hereditary papillary renal cacinoma (HLRCC)	*MET*, 7q31	**Papillary RCC type 1** (solid, multiple and bilateral)
Hereditary leimyopmatosis renal-cell cancer (HLRCC)	*FH*, 1q42-43	**Papillary RCC type 2** (collecting-duct carcinoma, solitary, aggressive)
Birt-Hogg-Dube (BHD)	*BHD*, 17p11.2	**Hybrid oncocytic RCC, chromophobe RCC, clear-cell RCC, Oncocytoma** (multiple, bilateral)
Hyperparathyroidism-jaw tumor (HP-JT)	*HRPTC2*, 1q25-32	**Mixed epithelial and stromal tumor, papillary RCC** (cyst)
Constitutional chromosme-3 translocation	Unknown gene Possibly *VHL*	**Clear-cell RCC** (multiple bilateral)
Familial papillary thyroid cancer (FPTC)	Unknown gene, 1q21	**Papillary RCC, oncocytoma**

1.1.3.1 Familial Clear Cell RCC

1.1.3.1.1 VHL: Von Hippel–Lindau (VHL) disease

Von Hippel-Lindau disease (OMIM 19330) is a rare, autosomal dominant, familial cancer syndrome consisting chiefly of retinal angiomas, hemangioblastomas of the central nervous system (CNS), pheochromocytomas and renal-cell carcinoma of the clear-cell type. Kidney cancer develops in 75% of VHL patients by the age of 60 and is the leading cause of death in the VHL patient population. Following the classic Knudson two hit hypothesis of a hereditary cancer syndrome (Knudson, 1997), one mutated *VHL* allele is inherited and renal cell neoplasia arises when the normal *VHL* allele is inactivated. While *Vhl-/-* mice are embryonic lethal due to a defect of placental vasculogenesis, *Vhl+/-* mice do not display a significant phenotype. Transgenic mice heterozygous for liver targeted deletion of *Vhl* (generated from the cross between a floxed *Vhl* mouse and a mouse line carrying an albumin-*cre* driven recombinase), develop hemangioblastoma but do not exhibit any of the renal lesions typical of human VHL disease (Haase *et al.*, 2001). Nonetheless, it has been recently reported that conditional inactivation of *VHL* in the mouse kidney, using Cre recombinase under the control of the phosphoenolpyruvate carboxykinase promoter (active in the renal proximal tubule), causes the development of polycythemia and renal cysts (Rankin *et al.*, 2006).

In humans, the *VHL* tumor suppressor gene maps to the chromosome 3p24-25 and encodes for pVHL protein (or VHL). Demonstrating VHL tumor suppressor functions, the reintroduction of VHL protein into *VHL -/-* carcinoma cell lines has been shown sufficient to suppress their growth as renal tumor xenografts in nude mice (Iliopoulos *et al.*, 1995). The tumor suppressor function of VHL relates to its ability to target specific proteins for destruction. VHL is the substrate recognition component of an E3 ubiquitin ligase complex that includes elongin B, elongin C, Cul2, and Rbx1. This complex is capable of directing the covalent attachment of polyubiquitin tails to specific proteins, which serve as signals for such proteins to be degraded by the proteasome. Several VHL targets have been identified, including the members of the hypoxia-inducible factor HIF–

alpha family (HIF-1alpha, HIF-2alpha, and HIF-3alpha). Under normal conditions, HIF-alpha proteins are hydroxylated by members of the EGLN family of enzymes and subsequently recognized by pVHL that orchestrates their destruction. When oxygen is low or in cells that lack pVHL, HIF-alpha is not tagged for destruction and is free to heterodimerize with its constitutively expressed partner HIF-beta. Together, they activate the transcription of a panel of genes involved in adaptation to hypoxia. These genes include the vascular endothelial growth factor (VEGF) that regulates angiogenesis and the transforming growth factor alpha (TGF-alpha that controls cell proliferation) (Kaelin, 2002).

Downstream of VHL, HIF-2alpha plays an instrumental role with respect to *VHL-/-* renal carcinogenesis. This is first illustrated by the fact that the elimination of HIF-2alpha, like the restoration of pVHL function, is sufficient to suppress *VHL-/-* tumor growth *in vivo* (Kaelin, 2007; Kondo *et al.*, 2002). In addition, the over-expression of HIF-2alpha in *VHL-/-* renal cancer cells is able to override the reintroduction of pVhl (Kondo *et al.*, 2003). HIF-1 is also a target of VHL but is not as potent as HIF-2alpha in driving tumorigenesis; inhibition of HIF-1alpha alone in VHL-/- tumor does not suppress tumorigeneicity in nude mice.

VHL disease is clinically divided into two types based on the presence (type 2) or the absence (type 1) of pheochromocytoma. Type 2 disease is further subdivided into three subtypes: type 2A (low risk of RCC), type 2B (high risk of RCC), and type 2C (pheochromocytoma only). VHL disease shows clear genotype-phenotype correlations. Type 1 disease is associated with large deletions or protein-truncating mutations that directly compromise pVHL's functions, including its ability to regulate HIF-alpha. In contrast, type 2 disease is almost always linked to *VHL* missense mutations. Interestingly, both type 2A and type 2B *VHL* mutations measurably compromise pVHL's ability to regulate HIF. Therefore, it is still not fully understood why type 2A and type 2B *VHL* mutations are associated with markedly different risks of developing renal carcinoma. In this regard, a number of HIF-independent functions have been ascribed to pVHL, some of which might conceivably be linked to renal tumorigenesis. On the other hand, a recent

report suggested that type 2A mutants bind to HIF-alpha with higher affinity than do type 2B mutants. This suggests that quantitative differences between type 2A and type 2B mutants, with respect to HIF binding, translate into different risks of renal carcinoma in humans (Knauth *et al.*, 2006). Li et al. showed that type 2A mutant is less compromised quantitatively with respect to the regulation of HIF2-alpha and HIF target genes, compared to type 2B mutants. In addition, the increased levels of HIF2-alpha and its downstream targets in cells producing type 2B mutants, correlated with increased tumor formation in nude mice. This demonstrates that HIF2-alpha is a critical component in VHL-/- renal carcinogenesis (Li *et al.*, 2007). It is important to note that a specific germline *VHL* mutation affecting both alleles, was found to cause a recessive form of polycythemia affecting a population living in the Chuvas region of Russia (Ang *et al.*, 2002).The occurrence of this cancer-free VHL-/- population clearly suggests that VHL mutations alone are not always sufficient to cause renal cancer.

Functions of VHL that are not related to HIF have also been identified. For instance, VHL is clearly involved in assembly of the extracellular fibronectin matrix and has been implicated as a regulator of epithelial-cell differentiation and cell-cycle exit, perhaps through its ability to downregulate cyclin kinase inhibitors p27 and p21(Mack *et al.*, 2005). Moreover, VHL is also responsible for suppressing the expression of the chemokine receptor CXCR4, which is implicated in the RCC cells capacity to metastasize (Staller *et al.*, 2003). Similarly *VHL* loss of function leads to up-regulation of metalloproteases known to play an important role in cancer cell metastasis (Petrella & Brinckerhoff, 2006). Furthermore, VHL has been shown to stabilize another tumour suppressor, jade-1 that is known to suppress renal cancer cell growth, in part by increasing apoptosis (Zhou *et al.*, 2004; Zhou *et al.*, 2002). However, how the function of jade-1 is related to the development of VHL-defect associated tumors remains yet to be clarified.

To summarize, VHL disease is the primary cause of hereditary clear cell RCC. It has also been very useful to decipher the molecular biology of sporadic RCC as *VHL* mutation is estimated to be present in as much as 80% of clear cell RCC. In addition, the

molecular players of the VHL pathway have served successfully as a therapeutic target for new agents for the treatment of RCC.

1.1.3.1.2 Other loci associated with familial clear cell RCC

Distinct from patients with VHL disease, multifocal bilateral clear-cell RCC has been reported in patients with translocation of chromosome 3 at a fragile site (3p14). Loss of the translocated chromosome 3p by non-disjunction probably implicates a *VHL* gene. The remaining allele is typically mutated or silenced by hypermethylation (Chen *et al.*, 2003). Few families have been reported worldwide with a hereditary solitary tumor without *VHL* mutation or linkage with chromosome 3p. No other clinical manifestations have been detected in these patients; this Familial Clear Cell Renal cancer is associated with unknown loci (Teh *et al.*, 1997).

Three cases of early onset renal call carcinoma have been reported in SDHB-associated heritable paraganglioma (OMIM 18479 & 60573). Hereditary multiple paraganglioma is associated with mutation in the mitochondrial enzyme succinate dehydrogenase B located at 1p36 locus (Vanharanta *et al.*, 2004). Finally, patients affected with tuberous sclerosis (OMIM 191100) have multiple renal angiolipomas and cysts. RCC is also observed in 1-2% of these cases (Lendvay & Marshall, 2003).

1.1.3.2 Familial Papillary RCC

1.1.3.2.1 MET: Hereditary Papillary Renal Cell Carcinoma (HPRCC)

Hereditary Papillary Renal Cell Carcinoma (OMIM 605074) is a hereditary cancer syndrome, inherited in an autosomal dominant fashion, in which affected individuals are

at risk of the development of bilateral, multifocal and type 1 (low grade and favorable prognosis) papillary renal carcinoma (Schmidt *et al.*, 1997). Approximately 20 % of HPRCC patients develop multiple, bilateral papillary tumors at a later age, than patients with VHL disease. *MET* maps to chromosome7q31, and encodes for Receptor Tyrosinase Kinase. Binding of the MET receptor by its ligand, hepatocyte growth factor (HGF) induces receptor dimerization and transphosphorylation of the tyrosine kinase domain leading to conformational changes and phosphorylation of the docking domain. Phosphorylation of the docking domain at Y1349 and Y1356 allows for the recruitment and activation of a downstream intracellular pathway resulting in promotion of cell proliferation, inhibition of apoptosis and increased motility. Most of the mutation occurs in the activation loop of the ATP binding site leading to constitutive MET receptor activation. Duplication of chromosome 7 carrying the mutation is generally the second event leading to tumorigenesis. MET activating mutation also occurs in 15% of the cases of sporadic papillary RCC (Pavlovich & Schmidt, 2004).

1.1.3.2.2 FH: Hereditary Leimyomatosis Renal Cell Cancer (HLRCC)

First described by Reed et al in 1973, patients affected with HLRCC (**OMIM 605839**) are prone to develop multiple cutaneous and uterine leimyomas and solitary papillary type II RCC (high grade, very aggressive and with a bad prognosis) (Reed *et al.*, 1973). Germline mutation in the gene located at locus 1q42-43 coding for the Krebs cycle enzyme Fumarate Hydratase (FH) predisposes to this dominantly inherited syndrome (Tomlinson *et al.*, 2002). It is believed that the FH gene acts as a tumor suppressor gene but the exact mechanism leading to tumor development remains to be clarified. One proposed mechanism is that impaired mitochondrial function leads to severe energy deficits and the formation of oxygen free radicals. This is sensed by the mitochondria as hypoxia and leads to stabilization of HIF-1α with consequences similar to the one of VHL inactivation (Pavlovich & Schmidt, 2004). Depending on the studies, it can be estimated that the risk of developing renal cancer in FH carriers ranges anywhere

between 1 and 5%. This tumor has a very aggressive course and a total nephrectomy is indicated at an early stage. This is unlike the case of VHL patients where nephron-sparing surgery is the desired treatment (Refae *et al.*, 2007).

1.1.3.3 Familial Chromophobe RCC and Oncocytoma

BHD: Birt-Hogg-Dube syndrome (OMIM 135150):

BHD syndrome is a genodermatosis that predisposes to benign cutaneous lesions of the face and neck, spontaneous pneumothorax and/or lung cysts. In addition, 15-30% of the patient carriers of a germlime mutation in the BHD gene (17p11.2) develop RCC with diverse histology including chromophobe and mixed chromophobe-oncocytic types at various ages. The BHD tumor suppressor gene encodes the protein folliculin (Pavlovich & Schmidt, 2004). A recent study suggests Folliculin may be involved in the AMPK and mTOR signaling pathways, but further clarification with respect to Folliculin function as a tumor suppressor is definitely needed (Baba *et al.*, 2006).

1.1.3.4 Diagnosis and management of hereditary renal cancer

Effective clinical management of hereditary renal cancer syndrome relies on early diagnosis. Therefore, early onset, bilateral tumors, familial or personal history of cancer should immediately warrant suspicion and clinical investigation for hereditary renal cancer. Genetic testing is available for the known causative genes (*VHL*, *MET*, *FH* and *BHD*) and should be performed according to the histological subtype. In clear cell RCC cases, the first step is *VHL* genomic analysis and if normal, a karyotype assessing chromosome 3 translocation should be performed. Patients with papillary type I should be screened for *MET* mutation and patients affected with type papillary RCC should be checked for *FH* mutation. In patients presenting with chromophobe and/or oncotyoma,

analysis of the *BHD* gene is wanted. For patients with inherited RCC (multiple, bilateral and recurrent tumors), nephrons sparing surgery is the standard treatment. Promising results have been obtained with radiofrequency ablation and cryotherapy and therefore might be considered for treating small renal tumors (Richard *et al.*, 2004).

1.1.4 Histopathology

RCC malignancies are heterogeneous and exhibit several distinct histologies (**Figure 1.3**). According to the current WHO classification, there are 4 major histological subtypes of renal cell carcinoma: clear cell (≥75% of cases), papillary type (15%, subdivided into type 1 and type 2), chromophobe tumors (4%) and collecting duct tumors (1%). Oncocytoma (4%) is another form of benign renal neoplasm that follows a more indolent course.

Clear cell RCC (75%):

The classification "Clear Cell" refers to the clear appearance of the cytoplasm under light microscopy examination after hematoxylin/eosin (H & E) staining. This is the result of an intensive intracytoplasmic accumulation of glycogen, phospholipids and neutral lipids. Macroscopically, a clear cell carcinoma typically presents as a multinodular mass with yellow-colored surface speckled by gray or white foci (Storkel & van den Berg, 1995).

Papillary RCC (15%):

Papillary renal cell carcinomas have a chromophilic appearance on H&E staining under the light microscope. The tumor epithelium is either cuboidal (type A papillary RCC) or columnar (type B papillary RCC). This is of interest as studies have suggested that type B is more advanced at presentation and has a worse prognosis than type A. Generally speaking, papillary RCC are of a low nuclear grade although the type B may exhibit pleomorphism and significant mitotic activity. Positive staining for cytokeratin 7 is the

most useful immunohistochemical marker of papillary renal cell carcinoma, as it is not seen in any other renal carcinomas (Fleming & O'Donnell, 2000).

Chromophobe RCC (5%):

Macroscopically, the tumour has a uniform soft grey appearance. Under light microscopy, chromophobe RCC is weakly stained with eosin (as suggested by the name) and the cytoplasm is seen to be composed of pale membrane-bound vesicles with perinuclear halo formation. Chromophobe RCCs show an irregular reactivity for cytokeratin but are usually vimentin negative. Cytogenetic analysis typically shows multiple monosomies but no chromosome 3 loss or trisomies of chromosome 7 and 17. Also, mutation in p53 is more common than in other renal tumors and is seen in about 30% of the cases (Fleming & O'Donnell, 2000).

Oncocytoma (5%):

This is a benign renal neoplasm. Oncocytoma usually presents as a well-circumscribed and tan colored mass with a central stellate scar. Upon microscopic examination, oncocytomas are seen to be composed of cuboidal cells with intensely eosinophilic granular cytoplasm. Oncocytomas may occasionally be multifocal and is then referred as 'oncocytomatosis'.

Collecting duct RCC (<1)%:

Collecting duct Carcinomas are usually large tumors located in the medulla of the kidney with extension into the perinephric fat and the renal pelvis. The white colored surface is interspersed with necroses and presents an irregular border with peri-tumoral cortical satellite nodules as a result of severe angio-invasiveness. Regional spread with infiltration of the adrenals and lymph-node metastases are common (Storkel & van den Berg, 1995).

The tumors may have tubular papillary architecture but the most characteristic feature is of an infiltrating ductal pattern exciting a desmoplastic stromal response. The infiltrating ducts are lined by a single layer of epithelium, often showing extreme pleomorphism with mitotic activity and nuclei with prominent nucleoli. In some instances the infiltrating

ducts form microcysts and this is frequently seen in metastatic collecting duct carcinoma. Collecting duct carcinoma appears to occur in a younger age group than most other renal carcinomas. In establishing the diagnosis, immunohistochemistry for cytokeratins and for lectins may be helpful; collecting duct carcinomas are vimentin negative (Storkel & van den Berg, 1995).

Unclassified RCC:

It is estimated that 3-5% of renal carcinoma are difficult to classify within this scheme. These may be tumors with an unusual mixture of components, tumors with an unrecognizable architecture or cytological pattern or sarcomatoid renal carcinomas in which the original epithelial element cannot be identified (Storkel & van den Berg, 1995).

Figure 1.3 RCC Histological appearances.

75% of RCC have clear cell histology; 5% have papillary Type I histology; 10% papillary type II; 5% Chromophobe; 5% Oncocytoma and less than 1% are of Collecting Duct type histology (Zucchi et al., 2003).

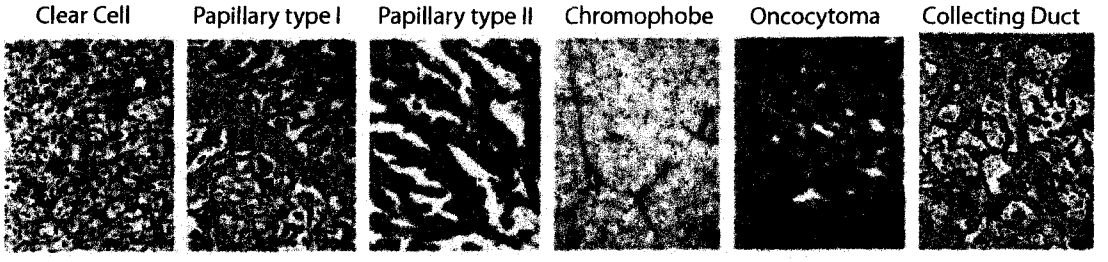
Clear Cell
Papillary type I
Papillary type II
Chromophobe
Oncocytoma
Collecting Duct

Fig.1.3

1.1.5 Molecular biology of RCC

1.1.5.1 VHL/HIF pathway

Between 60% and 80% of sporadic clear cell renal carcinomas are linked to biallelic genomic inactivation of the *VHL* gene. In a number of *VHL*+/+ clear cell renal carcinomas, little or no *VHL* mRNA is produced as a result of promoter hypermethylation (Herman *et al.*, 1994; Kim and Kaelin, 2004). VHL protein, the product of the *VHL* gene, functions as a tumor suppressor, inhibiting growth when reintroduced into cultures of renal-cell carcinoma cells. In normal cells, the VHL protein plays a key role in the regulation of the hypoxia-inducible factor, which controls the expression of several genes in response to hypoxic stress (Latif *et al.*, 1993). Under normoxic conditions (i.e. normal oxygen tension), HIF-1alpha is hydroxylated allowing its ubiquination by the VHL protein complex, enabling its proteosomal degradation. Under hypoxic conditions, HIF-1alpha is not hydroxylated and cannot be ubiquitinated by the VHL protein complex. Similarly, biallelic inactivation of *VHL* as it occurs in RCC cells, prevents degradation of HIF-1alpha (Kamura *et al.*, 2000; Kim and Kaelin, 2004; Latif *et al.*, 1993).

Once stabilized, HIF-1alpha translocates into the nucleus, where it dimerizes with constitutively present HIF-1 beta to form the active transcriptional factor HIF-1 heterodimer. HIF-1 activates transcription of hypoxia-inducible genes, including proangiogenenic factors such as vascular endothelial growth factor (VEGF), cellular growth factors such as transforming growth factor alpha (TGFalpha) and its cognate receptor, the epidermal growth factor receptor (EGFR).

When VHL protein function is compromised, these HIF target genes are overexpressed, creating a microenvironment favorable for cell transformation. The importance of angiogenesis in the biology of renal cancer is well established. RCC must induce the formation of novel blood vessels to supply nutrient and oxygen needed for tumor growth and malignant progression. VEGF, one of the best-known pro-angigenic factors is expressed at high levels in the majority of renal cancer; VEGF overexpression is linked to

molecular aberrant activation of the VHL/HIF pathway due to genetic lesions in the *VHL* gene.

Accumulation of HIF also leads to abnormal production of TGF-alpha. This in combination with the overexpression EGF receptor, perhaps via increase of *EGFR* mRNA translation, provides a molecular autocrine mechanism for unregulated growth of renal cells (de Paulsen *et al.*, 2001; Franovic *et al.*, 2007; Gunaratnam *et al.*, 2003) (**Figure 1.5**). The importance of the EGFR mitogenic pathway in renal cancer cell is confirmed by the fact that inhibition of EGFR expression via RNA interference suppresses VHL-/- RCC cells tumorigenicty in nude mice (Smith *et al.*, 2005). However, EGFR inhibitors such as Iressa have shown no improvement in overall survival of patients with metastatic RCC (Jermann et al. 2006).

1.1.5.2 MET pathway

Mutations in the tyrosine kinase domain of the MET gene produced constitutive phosphorylation of MET receptor protein. Activating mutation of the MET proto oncogene is associated with hereditary papillary RCC. In addition MET is mutated in 14% of sporadic papillary cancer (Schmidt *et al.*, 1997; Schmidt *et al.*, 1999). More recently, it has been shown that in clear cell renal carcinoma, MET can be constitutively phosphorylated as a consequence of VHL inactivation, leading to cell growth released from contact inhibition and in tumorigenesis (Nakaigawa *et al.*, 2006). HGF and MET protein are frequently observed in clear cell RCC and are associated with progression of the disease (Miyata *et al.*, 2006). Alltogether theses studies validate MET as a major pathway implicated in renal cancer biology (Linehan *et al.*, 2004).

1.1.5.3 PTEN, Akt and mTOR pathway

Recent data from a large series of metastatic renal cell carcinoma (RCC) patients have identified mTOR pathway activation as an adverse prognostic factor (Lam *et al.*, 2007) . The mTOR signaling pathway was originally discovered during studies of the immunosuppressive agent rapamycin. This highly conserved pathway regulates cell proliferation and metabolism in response to environmental factors, linking a cell growth factor receptor signaling via phosphoinositide-3-kinase (PI3K) to cell proliferation, and angiogenesis. A link of the mTOR pathway to the tumor suppressor PTEN has also been established.

PTEN loss of function through mutation, deletion, or epigenetic silencing results in increased activation of Akt and mTOR. This results, downstream, in enhanced activity of eukaryotic translation initiation factor 4E binding protein (4EBP1) and the S6K1 kinase. The net effect is the stimulation of cellular protein synthesis and entry of cells into the G1 phase of the cell cycle. Yet another product of this pathway is an increase in hypoxia inducible factor (HIF)1-alpha and HIF2-alpha expression, thus linking the mTOR pathway to angiogenesis. Accordingly, akt activation is frequently observed in RCC and in combination with a decreased PTEN expression (Hara *et al.*, 2005).

In addition, activation of mTOR in RCC can be the results of mutations that disrupt the tuberous sclerosis complex 1 and 2 genes (*TSC1* and *TSC2,* respectively). Like pVHL, the TSC1/TSC2 complex functions to regulate HIF as part of an oxygen sensing pathway and its disruption confers a predisposition to renal-cell carcinoma associated with increased HIF activity (Kaelin, 2007).

Figure 1.4 Molecular pathway in RCC.

Von Hippel–Lindau (VHL) is mutated in 75% of RCC. VHL normally encodes a protein (pVHL) that targets hypoxia-inducible factor (HIF) for proteolysis. As a result of VHL inactivation, a defective pVHL is produced and HIF is up-regulated, translocates to the nucleus and results in the transcription of several genes involved in angiogenesis and tumor growth. These genes include vascular endothelial growth factor (VEGF), platelet-derived growth factor (PDGF), epidermal growth factor (EGF) and the transforming growth factor alpha (TGF-a) (Cohen & McGovern, 2005). (Adapted from Cohen et al. used with permission of New England Journal of Medicine, 2005 Copyright Massacussets Medical Society. All right reserved).

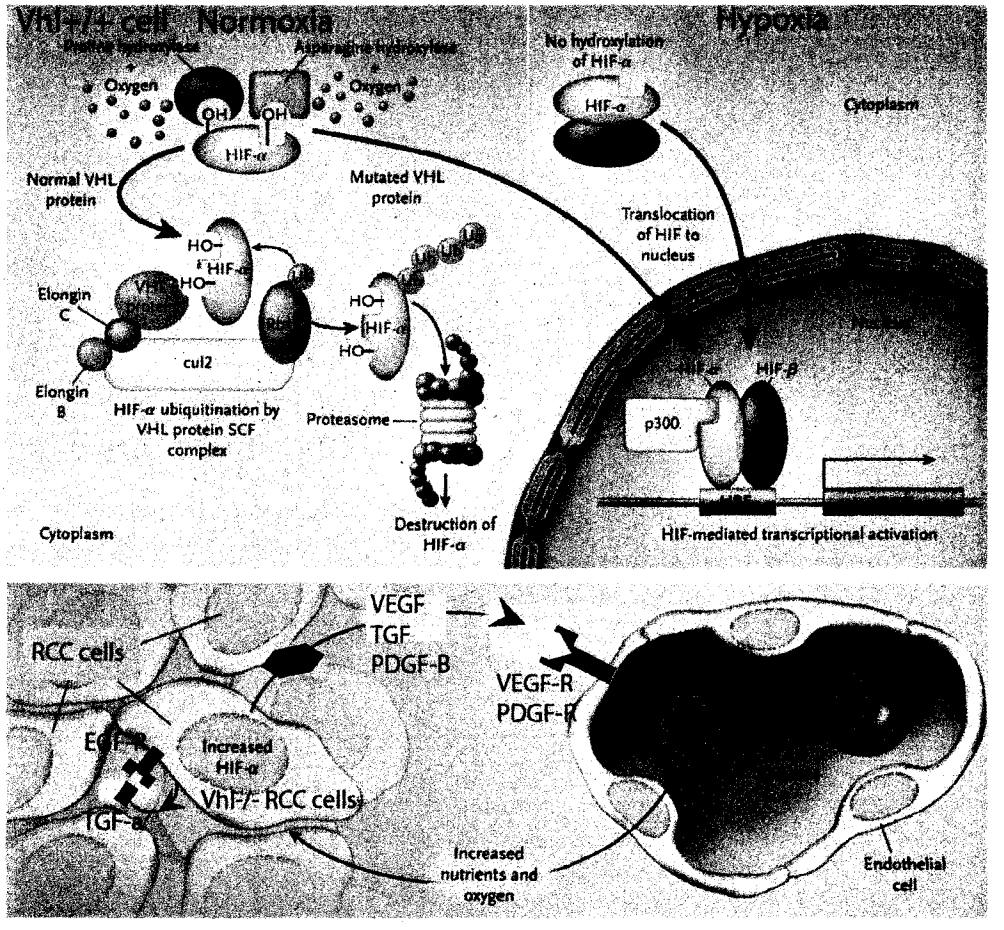
Vhl+/+ cell Normoxia
Oxygen
OH
HIF-α
Normal VHL protein
Mutated VHL protein
HO
HIF-α
Elongin C
Elongin B
cul2
HIF-α ubiquitination by VHL protein SCF complex
Proteasome
Destruction of HIF-α
Cytoplasm
Hypoxia
No hydroxylation of HIF-α
Cytoplasm
Translocation of HIF to nucleus
HIF-β
p300
HIF-mediated transcriptional activation
RCC cells
VEGF
TGF
PDGF-B
VEGF-R
PDGF-R
Increased HIF-α
Vhl-/- RCC cells
TGF-α
Increased nutrients and oxygen
Endothelial cell

Fig.1.4

1.1.6 Diagnosis staging and prognosis

RCC is a challenging diagnosis, as it remains clinically silent most of its course.
The classic presentation of renal-cell carcinoma includes the triad of flank pain, hematuria and a palpable abdominal mass (seen in only 10% of cases and is indicative of an advanced disease). In fact, 30% of the cases are asymptomatic and are detected incidentally as a renal mass on radiographic examination.

Clinical staging requires radiological assessment to evaluate the extent of the disease. Imaging of the chest, abdomen and pelvis should be performed with Computed Tomography (CT) or a combination of CT with Magnetic Resonance Imaging (MRI) or standard chest radiograph. Staging of RCC is performed worldwide according to the tumor-node-metastasis (TNM) classification (**Figure 1.5A)** (AJCC, 2002; Fuhrman *et al.*, 1982). To grade tumours, the most widely used system is the Fuhrman scheme (Fuhrman *et al.*, 1982) which distinguishes four grades based on nuclear size and shape and the prominence of nucleoli of RCC cells when examined under high power (x400 magnification).

Several integrated systems have been developed to establish prognosis (Ficarra *et al.*, 2007). A system that is widely used and has been successfully validated in 400 patients at 8 international centers is the University of California, Los Angeles (UCLA) Integrating Staging System (**Figure 1.5C**) (Patard *et al.*, 2004a; Zisman *et al.*, 2002). This system takes into account TNM staging, the patient's score on the Eastern Cooperative Oncology Group (ECOG) performance status (ECOG scale measures functional impairment in patients with cancer from 1 to 5: 1 = Fully active, able to carry on all pre-disease performance without restriction to 4 = Completely disabled, cannot carry on any selfcare and totally confined to bed or chair; 5=dead (Oken *et al.*, 1982), and the Fuhrman nuclear grading system which assesses histological grading of the tumor cells. Accordingly, the

UISS classifies patients with RCC into 2 categories distinguishing non-metatstatic and metastatic. Each of these 2 categories is sub-classified into 3 risk levels: low, medium and high. Survival analysis shows a 5 year survival rate of 97% (low), 81% (med) and 63% (high) for non-metastatic and 39% (low), 17% (med) and 7% (high) for metastatic disease (Patard *et al.*, 2004a). (**Figure 1.6C**)

Other studies have highlighted the additional prognostic value of a panel of molecular markers, which may correlate disease status and response to treatment. The majority of clear cell RCC expresses XIAP protein and a significant inverse correlation between XIAP levels and tumor aggressiveness. This is indicated by patients' survival, validating XIAP as an independent prognostic parameter (Ramp *et al.*, 2004). It is well established that deregulation of apoptosis plays an important role in tumor progression and resistance to chemotherapy. Therefore it is not suprising that XIAP that is the most potent caspase inhibitor of all known IAP (inhibitor of apoptosis) family members is independent prognostic marker for RCC. It is important to mention that contrary to previous beliefs, Carbonic anhydrase IX has been recently proven not to be an independent predictor of outcomes for patients with clear cell renal cell carcinoma (Leibovich *et al.*, 2007).

Figure 1.5 Staging and Prognosis of RCC.

A) Staging of RCC is performed worldwide according to the tumor-node-metastasis (TNM) classification (AJCC, 2002).

B) Visualization of Tumor staging depending on the extend of the disease (adapted from Cohen et al. used with permission of New England Journal of Medicine, 2005 Copyright Massacussets Medical Society. All right reserved).

C) The University of California Los Angeles, (UCLA) Integrating Staging System.
The University of California Los Angeles integrated staging system can predict survival in renal cell carcinoma taking into account TNM staging, the patient's score on the Eastern Cooperative Oncology Group (ECOG) performance status and the Fuhreman nuclear grading (Klatte *et al.*, 2007).

A

2002 TNM Classification of Renal Cell Carcinoma

Primary Tumor (T)

T1a Tumor 4 cm or less in greatest dimension, limited to the kidney

T1b Tumor more than 4 cm but not more than 7 cm in greatest dimension, limited to the kidney

T2 Tumor more than 7 cm in greatest dimension, limited to the kidney

T3a Tumor directly invades adrenal gland or perirenal and/or renal sinus fat but not beyond Gerota's fascia

T3b Tumor grossly extends into the renal vein or its segmental (muscle-containing) branches, or the vena cava below the diaphragm

T3c Tumor grossly extends into the vena cava above the diaphragm or invades the wall of the vena cava

T4 Tumor invades beyond Gerota's fascia

Regional Lymph Nodes (N)

N0 No regional lymph node metastasis

N1 Metastasis in a single regional lymph node

N2 Metastasis in more than 1 regional lymph node

Distant Metastasis (M)

M0 No distant metastasis

M1 Distant metastasis

B

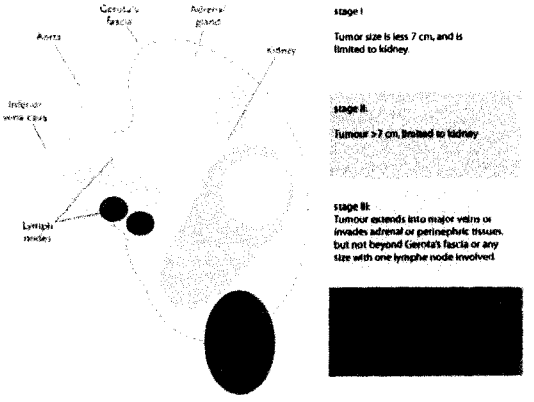

C

Non metastatic RCC (N0M0)

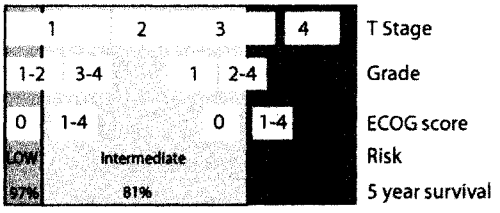

Metastatic RCC (N + M0 or M1)

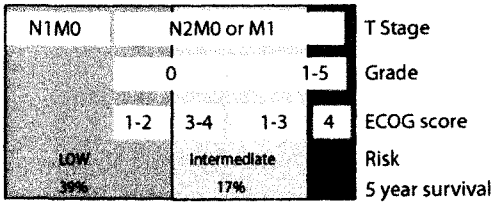

Fig.1.5

1.1.7 Treatment

Overview:

Surgery is the treatment of choice for initial presentation of RCC. There is no proven role for radiation and there is no standard chemotherapy. Immunotherapy is appropriate for selected patients with metastatic disease and research protocol including novel targeted therapy, are appropriate for many patients.

1.1.7.1 Surgical care

Radical Nephrectomy, which includes removal of the kidney with Gerota's fascia, the ipsilateral adrenal gland and regional lymph nodes, has been the standard of care for many years. But adrenal involvement can be identified preoperatively by CT scan and therefore be reserved for patients with large upper-pole lesions or abnormal appearance of the adrenal gland. Resection of the lymph node is limited to prognosis information since virtually all patients positive for distance metastasis will relapse later, regardless of lymphoadenectomy (Phillips & Messing, 1993).

Nephron-sparing surgery is the standard of care for small tumors less than 4cm and should be performed in patients with a functionally solitary kidney and is indicated in hereditary renal cancer, in bilateral tumours and in selected patients with whom the contralateral kidney is threatened by an associated disease such as diabetes, mellitus or hypertension.

Partial nephrectomies have excellent survival rates and are accompanied by a low risk of local (3.2%) and distant (5.8%) recurrence, with preservation of renal function in 98% of cases (Patard et al., 2004).

Laparoscopic surgery is becoming the standard of care for radical and partial nephrectomy. It is a minimally invasive procedure appropriate for most patients with

kidney cancer. Long-term oncologic outcomes of laparoscopic surgery and open surgery are similar. The benefits of a laparoscopic approach include decreased hemorrhage, reduced postoperative pain, shorter hospitalization and better cosmesis (Al-Qudah *et al.*, 2007).

Percutaeous thermal ablative therapy is becoming an available option for small tumors. The tumor cells are destroyed by radiofrequency, heat ablation or cryoablation. A needle probe is advanced through the skin and directed into the tumor using image guidance. Studies indicate that radiofrequency ablation can reliably eradicate RCCs smaller than 3.7 cm. Treatment of larger RCCs will expose the patient at an increased risk of residual RCC. Because identification of the RCC type is important, a core biopsy should be performed as part of the procedure (Permpongkosol *et al.*, 2006). The rate of complication is relatively low but postoperative hemorrhage, urinary leakage and damages to adjacent structures have been reported. Altogether, radiofrequency ablation seems to be a promising new modality for the minimally invasive treatment of renal cell carcinoma (Boss *et al.*, 2007).

1.1.7.2 Chemotherapy

Because RCC is often metastatic at the time of diagnosis, medical therapy is usually required. However, results of chemotherapy in RCC have been very disappointing with response rates less than 10% (Yagoda *et al.*, 1995). RCC is resistant to a variety of cytotoxic drugs with diverse structures and different mechanism of action. This phenotype has been termed Multi Drug Resistance (Mickisch, 1994). Multi drug resistance of the renal carcinoma cells can be caused by expression of the *mdr1* gene that encodes for 179kDa membrane P-glycoprotein. This P-glycoprotein functions as a transport channel that extrudes hydrophobic drugs outside of the cells (Pastan & Gottesman, 1987). Mdr1 is highly expressed in proximal tubule cells— the cells from which clear-cell and papillary renal-cell carcinoma may originate. Indeed, mdrI is

expressed in 90% of RCC (van Kalken *et al.*, 1991). The MDR resistance associated with P-glycprotein expression can be reversed with agents such as Verapamil and Cyclosporine, but clinical trials with these agents have not shown an enhanced anti-tumor effect of the chemotherapy (Motzer *et al.*, 1995).Another mechanism that contributes to renal tumor cell resistance is increased expression of drug metabolizing enzymes such as glutathione transferase (Chuang *et al.*, 2005).

Despite its suboptimal efficacy, chemotherapy is nevertheless of some benefit in renal-cell carcinomas of the collecting-duct subtype (Gollob *et al.*, 2001; Milowsky *et al.*, 2002; Peyromaure *et al.*, 2003). In a Phase II study, the combination of carboplatin and paclitaxel has shown a clinical response in aggressive collecting duct renal cancer (Oudard *et al.*, 2007).

Both cisplatin and carboplatin have broad antitumor activity that is attributed primarily to their ability to form DNA-platinum adducts resulting in cancer cell apoptosis. Again, clinical effectiveness can be limited by up-regulation of anti-apoptotic genes by RCC cells. The classical apoptotic pathway consists of activation of the caspase family cascade. The effector caspase serves to cleave the cellular protein substrates resulting in programmed cell death. The caspase X-linked inhibitor of apoptosis protein (XIAP) has the potential to inhibit the activation of caspases enzymes and slows down the process at this step. XIAP is expressed in the majority of RCC cells and predicts a worse prognosis; Knocking out XIAP expression sensitizes RCC cells to chemotherapy *in vitro* (Mizutani *et al.*, 2005). Similarly Smac/DIABLO expression is downregulated in RCC and transfection with Smac/DIABLO sensitized RCC to TRAIL/cisplatin-induced apoptosis (Mizutani *et al.*, 2005; Yan *et al.*, 2004). These results suggest that expression of antiapoptotic genes in RCC tissue may be markers of chemoresistance. More importantly, however, it is conceivable that modulation of the apopototic pathway might render RCCs more responsive to standard chemotherapeutic agents.

1.1.7.3 Modifiers of biological response

Overview:

Renal cancer is one of the few cancers where stabilization and even spontaneous regression has been reported in the absence of systematic treatment. One explanation is that the host immune response might occasionally control renal tumor growth. Immunotherapy function has been proposed to enhance the antigenicity of the tumor and enhances host immune surveillance (Oliver *et al.*, 1989).

Interferon-alpha (INF-alpha):

Interferon alpha has a direct antiproliferative effect on renal cancer cells and can also stimulate host mononuclear cells while enhancing expression of MHC molecules. The overall response achieve by interferon alpha treatment is 12% and can be as high as 30% in patient with advanced disease (lung metastasis) with prior nephrectomy (Minasian *et al.*, 1993). However, IFN-alpha has significant side effects and is rarely considered as a single agent for treatment of advanced RCC (Atkins *et al.*, 2007).

Interleukin 2 (IL-2):

High dose IL-2 was first approved by the Food and Drug Administration (FDA) for use in patients with RCC in 1992 after initial overall response rates of around 15% and durable, complete responses were reported. Until 2005, high-dose interleukin-2, was the only treatment FDA-approved for metastatic renal cancer (Fyfe *et al.*, 1995). IL-2 acts by activating lymphocytes (NK and activator T cells) without affecting cancer cells directly. IL 2 treatment alone can achieve a response rate of 20% in patients with metastatic RCC and a complete remission in 5% of the cases (Rosenberg, 2007). The major toxicities of high-dose IL-2 aside from fever and malaise are related to increased vascular permeability including hypotension and oliguria. Careful monitoring and fluid replacement can control symptoms of this capillary leakage syndrome but has been nevertheless implicated in 4% of treatment-related death. As a consequence, IL-2 is often not the first choice of treatment of patients with metastatic RCC (Rosenberg, 2007).

Tumor Vaccine:

Tumor vaccine strategy is to enhance the host immunity against the tumor.One of the most promising a vaccine has been with autologous or sibling donor dendritic cells (DC) transplatation. Dendritic cells are the most potent antigen-presenting cells in activating pro-inflammatory tumour specific immune pathways. Immature DC process antigens and then migrate to lymphoid organs where they activate specific cytotoxic T-cells targeted against tumor antigens (Holtl *et al.*, 2002). However, the overall efficacy of immunotherapy for advanced RCC remains modest.

1.1.7.4 Therapies targeting molecular pathways

Aberrant VHL/HIF/VEGF pathway activity is seen in the majority of RCCs. This provides a strong rational for exploring therapeutic agents that inhibit HIF-regulated genes. One phase II study in patients with metastatic RCC showed tumour shrinkage in most patients treated with Bevacizumab, a humanized VEGF-neutralizing antibody. The treatment was generally well tolerated. In a randomized, placebo-controlled, phase 2 trial of bevacizumab in patients with metastatic clear-cell renal-cell carcinoma, partial responses were observed in 10% of patients who were given a high dose of the antibody. There was a statistically significant improvement in progression-free survival. Although overall patient survival was not improved, blockade of VEGF does inhibit tumour growth (Yang *et al.*, 2003).

Sunitinib and Sorenafib are small molecule oral inhibitors of the tyrosinase kinase portion of the VEGf and PFGF receptors and are now approved by the FDA for use in advanced renal cell carcinoma. A phase II study of Sorenafib in cytokine-refractory RCC patients (TARGETs trial) showed significant differences in disease progression-free disease compared with placebo. (5.5 vs 2.8 months). A phase II study of Sunitinib showed an objective response in 34% of the patients; a phase III study shows a better response rate

with Sunitinib than with INF-alpha. Neither Sunitinib nor Sorafenib had a significant effect on initial survival, but the final long-term analysis has not yet been reported. An important point in evaluating these trials is that both Sunitinib and Sorafenib caused clinically significant toxic effects including hypertension.

Temsirolimus and Everolimus are derivatives of rapamycin and function to inhibit the mTOR pathway. Everolimus was shown to be effective in patients with advanced RCC and is now being further explored as a single agent and in combination with other therapies (Cho *et al.*, 2007). Temsirolimus showed antitumor activity in Phase II and Phase III trials; temsirolimus achieved increased overall survival compared to INF-alpha alone (Hudes *et al.*, 2007).

Figure 1.6 Molecular pathways and targeted therapies.

A) Bevacizumab is a humanized monoclonal antibody that targets VEGF ligand. Both Sunitinib and Sorafenib inhibit the VEGF and PDGFβ pathways, at least in part by acting on the VEGF receptor 2 (VEGFR2) and the PDGF receptor β (PDGFRβ), which are receptor tyrosine kinases. Finally, Temsirolimus and Sirolimus inhibit the mammalian target of rapamycin (mTOR) (Brugarolas, 2007). Figure adapted adapted from New England Journal of Medicine, 2007 Copyright Massacussets Medical Society. All right reserved).

B) Several targeted drugs are in the pipeline for the treatment of RCC either targeting angiogenesis or the mTOR pathways (Larkin et al., 2007)

A

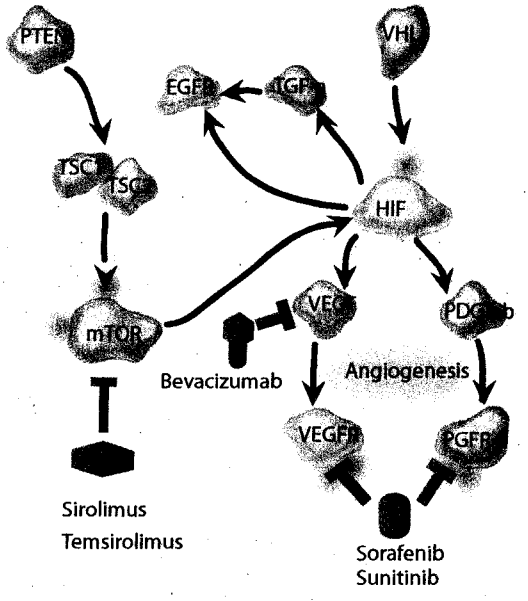

B

Agent	Mechanism of Action	Manufacturer	Status
Sunitinib	*VEGF-R, PDGF-R, c-kit, Raf kinase inhibitor*	*Pfizer*	*FDA approved*
Sorafenib	*VEGF-R, PDGF-R, c-kit, Raf kinase inhibitor*	*Bayer/Onyx*	*FDA approved*
Temsirolimus	*mTOR inhibitor*	*Wyeth*	*FDA approved*
Bevacizumab	*VEGF ligand inhibitor*	*Genetech/Roche*	*Phase III*
Everolimus	*mTOR inhibitor*	*Novartis*	*Phase III*
Pazopanib	*VEGF-R, PDGF-R, c-kit, tyrosine kinase inhibitor*	*GlaxoSmithKline*	*Phase III*
Axitinib	*VEGF-R, PDGF-R, tyrosine kinase inhibitor*	*Pfizer*	*Phase II*
Vatalanib	*VEGF-R, PDGF-R, tyrosine kinase inhibitor*	*Novartis*	*Phase II*

Fig.1.6

1.1.8 RCC Summary:

RCC is one of the most resistant tumors to therapy. Only high doses of IL-2 have been shown to be able to cause complete remission in patients with advanced renal-cell carcinoma and this in only 5% of the cases and along with tricky management of side effects. Overall, treatment of RCC is currently moving from the cytokine era to the targeted agent era. Small inhibitors targeting the VEGF or mTOR pathway have shown significantly improved effects on tumor growth in virtually all patients with RCC. Although more patients seem to benefit from this targeted treatment, it is only Temsirolimus, which results in an increased overall survival, and this only in limited cases. Many questions still remain regarding the efficacy of combination treatments and on the best way to achieve complete remission. Nevertheless the promising clinical outcome progress of these targeted drugs validates the idea that new treatments can emerge from an understanding of the molecular biology of the renal tumors. At the moment, the chance of survival for patients afflicted with advanced renal cancer remains unacceptably low. Therefore we have to continue further the exploration of the molecular pathways implicated in this disease and continue to identify targets for the development of novel agents (Larkin *et al.*, 2007).

1.2 Wilms Tumor

Overview:

Wilms tumor (WT) is a childhood cancer of the kidney that arises in 1/10,000 children from a progenitor cell in the undifferentiated fetal metanephric mesenchyme. WT recapitulates in its histology the developmental differentiation process of nephrogenesis. The mixture of renal cellular lineages that characterize WT was noticed by Max Wilms who first described WT as "die mischgeschwulste der Niere" in 1899 (Wilms, 1899) (Wilms, 1899). Since then, WT has remarkably served to define the paradigm of pediatric cancer: Knudson and Strong establish the two-hit hypothesis model using WT bimodal age distribution. WT was also one of the first cancers in which a tumor suppressor (WT1) was mapped by positional cloning and one of the first malignancies described in association with epigenetic modification (Willins, 2003). Finally, the multidisciplinary management of Wilms tumor has become an example of successful cancer therapy that progressed from 30% survival in the 1930s to a more than 85% cure rate today (1991).

1.2.1 Epidemiology

In North America, the incidence rate of Wilms tumor is 8.1 cases per million in Caucasian children. The incidence rate is about three times higher for blacks in the United States and Africa (9-12 cases per millions) than for East Asians (3 cases per millions), with rates for white populations in Europe and North America intermediate between these extremes (Breslow *et al.*, 1994). The variations in the incidence of Wilms tumor vary according to ethnicity; the incidence of Wilms tumor does not exhibit geographic variation, suggesting that environmental factors do not play an important role (Stiller & Parkin, 1990). The incidence of Wilms tumor over time has been relatively constant for the last 20 years (Linet *et al.*, 1999). Although most tumors are sporadic and unilateral, bilateral or multifocal tumors account for 10% of the cases (Knudson & Strong, 1972). The male-to-female ratio for patients with a unilateral tumor is 0.92 to

1.00 and for those with bilateral tumors is 0.60 to 1.00. The mean age at diagnosis for those with unilateral tumors is 41.5 months for males and 46.9 months for females, compared with 29.5 months for males and 32.6 months for females with bilateral tumors (Breslow *et al.*, 1993).

1.2.3 Genetic predispositions

The average age at diagnosis of WT is 42–47 months for children with unilateral tumors and 30–33 months for children with bilateral disease (Breslow *et al.*, 1993). An earlier age at diagnosis and an increased frequency of bilateral disease is characteristic of syndromic WT and in familial WT (Knudson & Strong, 1972). In order to explain this bimodal distribution of WT (also observed in Retinoblastoma and Neuroblastoma) Knudson and Strong elaborated the 2 hit hypothesis which attempts to model the rate-limiting events required to initiate tumorigenesis (Knudson & Strong, 1972). They hypothesized that WT arises from the occurrence of two sequential genetic events ("hits") that inactivate a recessive tumor suppressor gene. Patients born with a germline mutation (or first hit) need acquire only a single somatic mutation, inducing a Wilms tumor at an early stage and increasing the likelihood of multifocal tumors. In contrast, patients without a germline mutation must acquire two *de novo* hits in a single somatic cell; the much lower probability of two independent events occurring in the same cell accounts for the later age of onset and unilateral tumors. However, familial forms constitute only 2% of Wilms tumors (Diller *et al.*, 1998) and many children exhibit bilateral WT without family history. Thus, Knudson's 2-hit model may be an oversimplification. *De novo* events altering the stability of several different Wilms tumor genes has also been suggested (Narod & Lenoir, 1991).

1.2.4 Genetic syndromes

Overview:

Studies of patients affected by genetic syndrome predisposing to Wilms Tumor have been fundamental in identifying genetic factors involved in Wilms tumorigenesis **(Table 1.2)**. Patients with these syndromes tend to develop multiple tumors.

Table 1.2 Genetic syndromes predisposing to Wilms tumor.

Patients affected by these genetic syndromes tend to develop ealy onset multiple and bilateral tumor. The strongest associations are linked to deletions and mutation in the gene *WT1* in the WAGR syndrome and Denys-Drash Syndrome respectively. The Beckwith–Wiedemann syndrome (BWS) locus at 11p15 has also been associated with Wilms tumor due to both germline overexpression of paternally imprinted insulin-like growth factor 2 (IGF2). Other rare syndrome caused by mutation in genes not identified can also predispose the patients affected by these diseases to the development of Wilms tumor.

Table 1.2 Heritable syndromes associated with Wilms tumor:

Syndrome	Locus/Gene	Renal Phenotype
WAGR (Wilms tumor, aniridia, genitourinary abnormalities and menta retardation)	11p13/WT1:large deletion (also involving PAX6)	30% of the patients develop ilms Tumor.
Denys-Drash	11p13/WT1 point mutation (in the Zn finger domain)	90% of the patients develop Wilms tumor.
Frasier	11p13/WT1:point mutations (in the KTS splicing donor site)	Patients rarely develop Wilms tumor.
Beckwith-Wiedemann	11p15 (IGF2,H!9,p57)	5% of patients develop Wilms tumor.
Simpson-Golabi-Behmel	Xq26/GPC3	7.5% of the patients develop Wilms tumor
Sotos	5q35/NNSD1	Les than 5% of patients develop Wilms tumor
Perlman	Unknown	30% of patients develop Wilms tumor
Familial Wilms Tumor 1 (FWT1)	17q12-21	20% of patients develop Wilms tumor
Familial Wilms Tumor 2 (FWT2)	19q13.4	70% of patients develop Wilms tumor

WAGR (WT is present 30% of the cases):

Initial insights into the molecular biology of Wilms tumor were derived from the observation that patients with Aniridia (absence or malformation of the iris), genitourinary malformations, and mental retardation (WAGR syndrome), were at 30% risk of developing the tumor. Cytogenetic analysis of individuals with this syndrome showed deletions at chromosome 11p13, which was later found to be the locus of a contiguous set of genes including *PAX6*, the gene causing aniridia, and *WT1*, one of the Wilms' tumor genes. Reduced dosage of *PAX6* gene underlies the defect in ocular development while constitutional germline hemizygosity for the *WT1* gene is associated with the genitourinary malformations. Wilms tumors arise when a renal cell acquires an additional somatic point mutation in the remaining WT1 wild-type allele (Call *et al.*, 1990; Gessler *et al.*, 1990).

Denys Drash (WT present in 90% of the cases):

The Denys–Drash Syndrome (DDS) (OMIM number 194080) is characterized by male pseudohermaphroditism and progressive glomerular nephropathy leading to end-stage renal disease. Normal glomerular development is disturbed and affected patients exhibit proteinuira in association with diffuse mesangial sclerosis and severe alterations of the podocytes. In addition, DDS patients have 95% chance of developing Wilms tumor (Habib *et al.*, 1985). DDS is caused by point mutations in the zinc-finger DNA-binding region of the *WT1* gene, resulting in loss or alteration of DNA binding ability, as demonstrated by *in vitro* studies (Pelletier *et al.*, 1991a). The most common *WT1* lesion is a mutation (Arg394Trp) affecting the third zinc finger domain of the WT1 protein (Bruening *et al.*, 1992). Other point mutations in the second Zinc finger lead to similar DDS phenotype (Baird *et al.*, 1992; Sakai *et al.*, 1993). Pelletier has suggested that DDS is the result of WT1 mutations, which cause a dominant negative effect on the wildtype allele. One mechanism to explain this phenomenon might be that WT1 proteins dimerize via their N-Terminal domains (Englert *et al.*, 1995; Moffett *et al.*, 1995; Reddy *et al.*, 1995).

Beckwith-Widemann Syndrome:

Beckwith–Wiedemann syndrome (BWS) (MIM 130650) is a developmental disorder with an incidence of about 1 per 20,0000 births, characterized by somatic overgrowth, macroglossia, abdominal wall defects and increased incidence of embryonal tumors. Approximately 5% of BWS patients develop Wilms tumors. Although the precise genetic mechanism causing Wilms tumor remains undefined, defective expression of imprinted genes at locus 11p15.5 have been implicated. Regional genes with aberrant imprinting include insulin-like growth factor-2 (IGF2), *H19* untranslated RNA, and *CDKN1C*, which encodes a cyclin-dependent kinase inhibitor, $p57^{KIP2}$. BWS patients often show altered DNA methylation of the 11p15 region associated with decreased expression of *CDKN1C* and increased expression of IGF2. These aberrations in gene expression are thought to alter cellular proligferation and may underlie the somatic overgrowth phenotype of BWS (Maher & Reik, 2000).

Hyperparathyroidism–jaw-tumor syndrome:

Hyperparathyroidism–jaw-tumor syndrome (OMIM 145001) is a very rare disease that predisposes to multiple parathyroid adenomas, a fibro-osseous tumor of the jaw, renal cyst, harmatomas and mesoblastic nephroma. In addition, affected individuals have hereditary hyperparathyroidism (with consequent nephrolithiasis) and can develop a late onset Wilms tumor (Kakinuma *et al.*, 1994). Germline mutation in *HRPT2* located at 1q25–32 has been identified and encoded for the protein parafibromin, which is thought to act as a tumor suppressor, but its exact function remains to be determined (Pavlovich & Schmidt, 2004).

Li–Fraumeni syndrome:

Li-Fraumeni (OMIM 151623) is a rare syndrome caused by a mutation in the *TP53* tumor-suppressor gene that encodes p53 protein, an important regulator of the cell cycle and apoptosis. Patients with Li–Fraumeni syndrome have a strong predisposition to develop a variety of cancers and Wilms tumor has been reported in affected individuals (Hartley *et al.*, 1993).

1.2.5 Familial Wilms Tumor

Overview:

Familial WT is relatively rare, occurring in 1–2% of all cases of WT. Typically Wilms tumor family pedigrees are small, with only two or three affected relatives, and there is usually no associated congenital abnormality or predisposition to other tumor types (Ruteshouser & Huff, 2004).

WT1:

Germline *WT1* mutations are usually de novo mutations identified in WT patients with no family history (Pelletier et al., 1991). WT1 mutational analysis of familial cases demonstrated that only 2 out of 30 families carried an inherited alteration in WT1 (McDonald *et al.*, 1998). Thus, germline WT1 mutations are rarely observed in a family context, and most individuals with germline WT1 mutations are ''sporadic'' cases (Ruteshouser & Huff, 2004).

FWT1 and FWT2:

Genetic linkage studies of WT families have led to the identification of two familial predisposition loci at 17q12-q21 (FWT1) (McDonald *et al.*, 1998; Rahman *et al.*, 1996), and 19q13.4 (FWT2). However, other Wilms tumor families show no linkage to either locus, implying the existence of additional familial Wilms tumor susceptibility genes (Rapley *et al.*, 2000; Ruteshouser and Huff, 2004).

1.2.6 Diagnosis and clinical presentation

Approximately one third of patients present with abdominal pain, anorexia, vomiting, malaise, or a combination of these symptoms, but the most common clinical presentation of WT is an asymptomatic abdominal mass. About 30% of patients have haematuria, 10% have a coagulopathy and 25% develop hypertension. Abdominal CT-scan and ultrasonography are used to detect abnormal renal mass. X-Ray or CT scan of the chest is

recommended to assess lung metastases (Kalapurakal *et al.*, 2004). Wilms tumors may be either a solid or cystic mass within the kidney, visibly displacing the collecting system. They may be encapsulated and may undergo central necrosis with hemorrhage. The tumor extends into the renal vein in 40% of cases. Wilms tumors rarely extend into the ureter and bladder. Partially differentiated cystic nephroblastomas (i.e. multilobular cystic nephroma) may mimic Wilms tumor appearance, but are considered benign lesions.

1.2.7 Histology

Favorable histology:

The classic untreated Wilms' tumor consists of varying proportions of three (triphasic) cell types: blastemal, stromal, and epithelial, commonly recapitulating various stages of normal renal development (**Figure 1.7**). Less commonly, heterologous epithelial or stromal components are identified, including mucinous or squamous epithelium, skeletal muscle, cartilage, osteoid, or fat elements. A significant number of stromal Wilms tumors exhibit skeletal-muscle differentiations, varying from well differentiated (rhabdomyomatous) to poorly differentiated (rhabdomyoblastic).

Anaplastic (Unfavorable histology):

Anaplastic foci, characterized by greatly enlarged polyploid nuclei, arise within Wilms tumors in 5% of cases. Anaplastic tumors are more frequent in African-Americans than in Caucasian patients (Bardeesy *et al.*, 1994; Bonadio *et al.*, 1985). They are more resistant to chemotherapy and correlate with the presence of secondary p53 mutations (Beckwith, 1997).

Blastemal vs Epithelial:

Blastemal-predominant tumors are often invasive and present at an advanced stage, but they respond relatively well to chemotherapy. In contrast, predominantly epithelial or myogenic Wilms tumors are often localized at the time of presentation, but tend to be

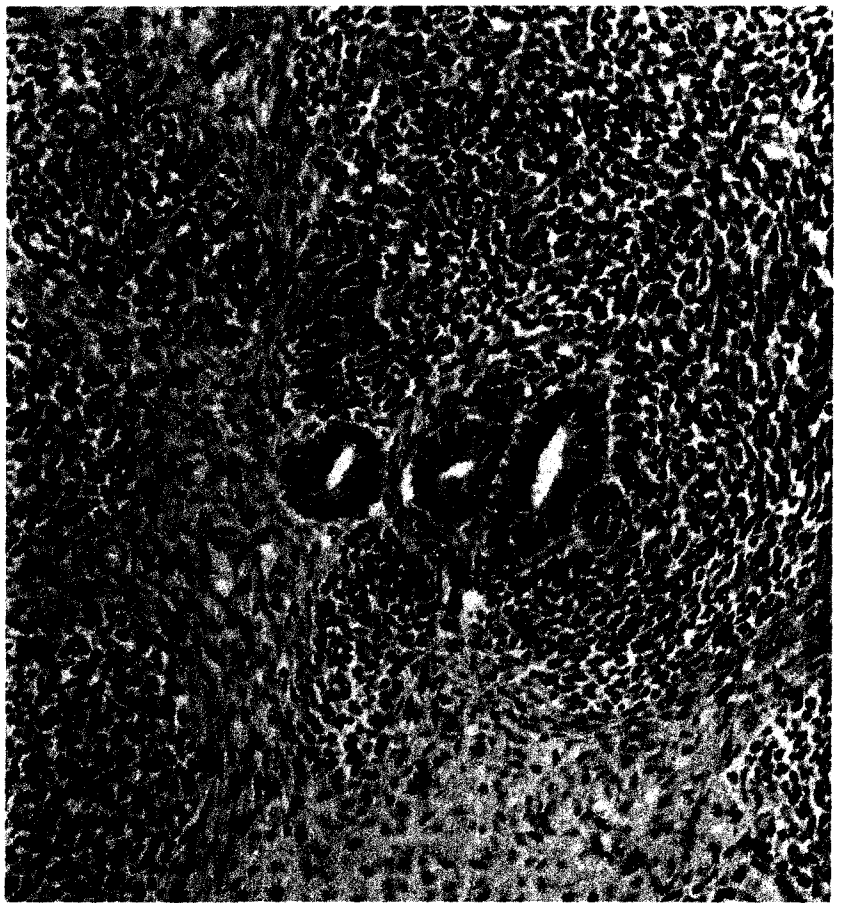

Wilms tumor triphasic histology

Fig.1.7

quite resistant to chemotherapy (Anderson *et al.*, 2002).

1.2.8 Staging/prognosis

The North American National Wilms Tumor Study Group (NWTSG) has established staging system for Wilms tumor. The stage is defined on the basis of tumor size, gross anatomy and presence of metastatic disease (**Table 1.3**) (Kalapurakal *et al.*, 2004). In addition, genetic features have been proven useful to predict treatment outcome. Patients with loss of heterozygosity (LOH) at chromosomes 1p and 16q at 16q are at greater risk of relapse and mortality than children without this lesion. This result was confirmed in the fifth National Wilms Tumor Study (NWTS-5) that prospectively analyzed LOH in primary Wilms tumors. Tumor-specific LOH for both chromosomes 1p and 16q occurs in 5% of patients with a favorable histology and correlates with a significantly increased risk of relapse and death (Grundy *et al.*, 2005b). Other prognostic markers are an increase in gene copy number at chromosome 1q (Hing *et al.*, 2001; Lu *et al.*, 2002). Gene expression profiling has demonstrated signature gene expression patterns associated with bad prognosis and relapse and may in the future help to identify patients at high risk (Li *et al.*, 2005b; Williams *et al.*, 2004). In addition, high telomerase RNA expression in Wilms Tumor have been correlated with tumor recurrence (Dome *et al.*, 2005; Dome *et al.*, 1999).

Table 1.3 Staging of Wilms tumors:

NWTSG recommends surgical staging in every case and is based on the tumor size, lymphe nodes involments and metastasis (1991) .

Table 1.3 Wilms tumor staging:

Stage I (43% of patients) Tumor is limited to the kidney and is completely resected. The renal capsule is intact. The tumor is not ruptured or biopsied prior to removal. No involvement of renal sinus vessels. No evidence of the tumor at or beyond the margins of resection.
Stage II (23% of patients) There is regional extension of the tumor (i.e., penetration of the renal sinus capsule, or extensive invasion of the soft tissue of the renal sinus, as discussed below). Blood vessels within the nephrectomy specimen outside the renal parenchyma, including those of the renal sinus, contain tumor.
Stage III (23% of patients) Lymph nodes within the abdomen or pelvis are involved by tumor. (Lymph node involvement in the thorax, or other extra-abdominal sites is a criterion for Stage IV.) The tumor has penetrated through the peritoneal surface. Tumor implants are found on the peritoneal surface. Gross or microscopic tumor remains postoperatively The tumor is not completely resectable because of local infiltration into vital structures. Tumor spillage occurs either before or during surgery. The tumor was biopsied before removal. The tumor is removed in more than one piece
Stage IV (10% of patients) In stage IV Wilms' tumor, hematogenous metastases (lung, liver, bone, brain, etc.), or lymph node metastases outside the abdominopelvic region are present. (The presence of tumor within the adrenal gland is not interpreted as metastasis and staging depends on all other staging parameters present.)
Stage V (5% of patients) In stage V Wilms' tumor, bilateral involvement by tumor is present at diagnosis. An attempt should be made to stage each side according to the above criteria on the basis of the extent of disease. The 4-year survival is 94% for those patients whose most advanced lesion is stage I or stage II, and 76% for those whose most advanced lesion is stage III.
Stage I-IV Anaplasia Anaplastic histology accounts for about 10% of Wilms' tumors. Children with anaplastic tumors have a worse prognosis than children with favorable histology when compared stage to stage. These tumors are more resistant to the chemotherapy traditionally used in children with Wilms' tumor (favorable histology).

1.2.9 Treatment

1.2.9.1 Overview

The mainstay of Wilms tumor therapy is a combination of surgery and chemotherapy. Radiation therapy is added for patients with advanced disease. The National Wilms Tumor Study group, now Children Oncology Group (COG), advocate early nephrectomy and then chemotherapy and radiation when indicated. SIOP trials suggest the use of pre-operative chemotherapy followed by surgery.

1.2.9.2 Surgery

The NWTSG has conducted five trials where primary surgical resection of the tumor is the initial treatment of most children. As a result, complete nephrectomy is recommended in North America. One of the main challenges of WT surgery is to avoid tumor spillage, which increases the risk of local abdominal relapse and a subsequent poor outcome (Shamberger *et al.*, 1999).Regional lymph nodes should be assessed at the time of nephrectomy (Shamberger *et al.*, 1999). It is worth to mention that partial nephrectomy is generally not recommended for a unilateral tumor; the rate of renal failure in patients with unilateral tumor is less than 1% (Ritchey *et al.*, 1996)

A retrospective analysis of the NWTS-4 study suggested that patients younger than 2 years old with favorable histology and a stage I, small tumor, might be treated without receiving adjuvant chemoatherapy after nephrectomy, reducing treatment burden. However, in the NWTS-5 trial of 75 children with small (<550 g) stage I, favorable histology tumors, nephrectomy alone led to relapse by 2 years in 13.5% of subjects and the trial was abandoned (Green *et al.*, 2001). Survival was still 98% since relapses were successfully treated by chemotherapy, but surgery alone will be restricted to selected cases in a future trial planned by the Children Oncology Group (COG) (Grundy et al., 2005).

1.2.9.3 Chemotherapy

The COG now advocates up-front resection of the primary Wilms tumor before chemotherapy. In contrast, Societe international d'oncologie pediatrique (SIOP) recommends that chemotherapy be given before surgery. Both approaches yield excellent clinical outcomes but the debate about the relative merits of each approach is ongoing`(Green, 2007). The NWTSG recommends preoperative chemotherapy for specific cases, including bilateral Wilms tumor, tumor in a horseshoe kidney, tumor in a solitary kidney, tumor thrombus in the inferior vena cava above the level of the hepatic veins and respiratory distress resulting from the presence of an extensive metastatic tumor.

Treatment of WT with favorable histology:

Overall the NWTS-5 treatment approach is considered a reasonable standard of care for Wilms tumor with favorable histological features (Green *et al.*, 1998) (summarized in **Table 1.4**). Treatment of high-risk patients including WT with anaplastic histology, bilateral tumor and recurrent Wilms tumor, needs specific considerations.

Table 1.4 Treatment of favorable histology Wilms tumor:

The protocols for the treatment favorable histology WTs are summarized here. The National Wilms Tumor Study Group (NWRSG), which is now part of the Children's Oncology Group (COG), has established standard treatment for Wilms tumor in North America which consists of surgery followed by chemotherapy and, in some patients, radiation therapy depending on the stage of the tumor (Metzger & Dome, 2005).

Table 1.4 Treatment regimens for WT with favorable histology from completed NWTSG trials:

Stage	Chemotherapy (NWTS-5)	Radiation Therapy (NWTS-5)	OS% (NWTS-4)
I	VA X 18 weeks	-	98.7 (2-year)
II	VA X 18 weeks	-	93.8 (8-year)
III	VDA X 24 weeks	10.8 Gy flank	93.0 (8-year)
IV	VDA X 24 weeks	12 Gy lung (if lung metastasis)	89.5 (2-year)

A, dactinomycin; D, doxorubicin; V, vincristine; OS, Overall survival.

Treatment of anaplastic WT:

The NWTS-5 study treated patients with stage I anaplastic Wilms tumor and obtained encouraging results using vincristine and dactinomycin. However, preliminary analysis showed unexpectedly low survival of 70% and 83% respectively. As a consequence, future therapeutic regimen for these patients will include the additional administration of Doxorubicin and radiation therapy in COG studies. For patients with stage II, III or IV diffuse anaplasia, the treatment regimen includes cyclophosphamide. Such patients receive abdominal radiation therapy and a novel chemotherapy regimen consisting of vincristine, doxorubicin and cyclophosphamide, alternating with cyclophosphamide and etoposide. Survival for this group is 55%. Patients with stage II–IV focal anaplasia are treated with abdominal irradiation, vincristine, doxorubicin and dactinomycin. The survival estimates for patients with focal anaplasia is 75% (Metzger & Dome, 2005).

Treatment of recurrent WT:

Salvage therapy includes multi-agent protocols using cyclophosphamide, ifosfamide, cisplatin, carboplatin and etoposide. In particular, the combination (ifosfamide, carboplatin and etoposide), has significantly improved survival after relapse with a 50% to 60% rate (Metzger & Dome, 2005).

The role of high dose therapy with autologous stem cell rescue in relapse WT needs further clarification. Several studies have shown promising results with overall survival between 60 and 75% (Metzger & Dome, 2005).

Treatment of bilateral WT:

Synchronous bilateral Wilms tumors account for 6% of all Wilms tumors. The main challenge of this stage V tumor is the preservation of the renal function without compromising cancer control. This is the only group in which the NWTSG recommends pre-treatment with chemotherapy after biopsy confirmation. The role of preoperative chemotherapy is to reduce tumor size, thereby facilitating nephron-sparing surgery. Local recurrence for these patients is 8.2%. Long-term survival rates for patients with synchronous bilateral Wilms tumors are approximately 70%–80% (Metzger & Dome, 2005).

Metachronous bilateral Wilms tumor accounts for approximately 2% of all Wilms tumors. The NWTSG has reported lower survival rates for patients with metachronous compared to patients with synchronous bilateral tumors. It is estimated that overall survival for patients with metachronous bilateral Wilms tumor is about 50%. Children younger than 12 months who have perilobar nephrogenic rests are at markedly increased risk of contralateral disease and require frequent and regular surveillance for several years (Metzger & Dome, 2005).

1.2.9.4 Treatment long-term sequelae

Increasing data on the long term side effects of WT treatments have emerged as survival has improved. In bilateral Wilms tumor, nephron-sparing surgery is often attempted but about 4% of these patients still develop end-stage renal failure when total nephrectomy is required or radiation-induced damage compromises residual renal tissue. Congestive heart failure is a common complication after anthracyclines and the risk is further increased when whole-lung irradiation is given for metastases. Radiotherapy can also injure the lung and radiation nephritis is associated with malignant hypertension. Women who have received abdominal radiotherapy for Wilms tumor are at higher risk of adverse pregnancy outcomes. Finally, there is increased risk of developing a second malignant neoplasm (Kalapurakal *et al.*, 2004).

The treatment of Wilms tumor is one of the great success stories in oncology. Modern treatment regimens yield survival rates of 90%. However, there remain some patients for whom current treatment is unsatisfactory including those with anaplastic, bilateral or recurrent disease with favorable histologic features. This represents about 25% of patients who have Wilms tumor and highlight the need for a continued effort to develop novel treatment. Thus, therapy for Wilms tumor is not yet optimal and there remains considerable motivation to improve on current therapeutic strategies (Kalapurakal *et al.*, 2004).

1.2.10 Pathogenesis of Wilms tumor

1.2.10.1 WT1 (chromosome 11p13)

Only 5% of WT cases involve germline mutations of *WT1*, but WT1 mutations were found in about 20% of 600 sporadic Wilms tumors (Little & Wells, 1997) (updated *WT1* mutational database maintained at http://www.umd.necker.fr). Approximately two-thirds of sporadic *WT1* mutations are caused by deletion of *WT1* or mutations which produce a truncated protein with disrupted DNA-binding domain. This is consistent with the view that *WT1* acts as a recessive tumor suppressor gene. Interestingly, specific missense mutations of WT1 may act as dominant-negative properties, as discussed above (Little *et al.*, 1993; Pritchard-Jones, 1997).

Wilms tumours caused by *WT1* mutation appear to represent a discrete malignant subtype with mesenchymal (stromal) phenotype (Schumacher *et al.*, 1997; Schumacher *et al.*, 2003). Cells are non-polarized and spindle-shaped, expressing myogenic markers such as myogenin and MyoD (Fukuzawa *et al.*, 2004; Miyagawa *et al.*, 1998). WT with stromal-predominant histology are often associated with *CTNNB1* mutations (Fukuzawa *et al.*, 2004)

Certain Wilms tumors may lack WT1 immunostaining although no alterations of the WT1 coding sequence can be identified (Satoh *et al.*, 2003). It is important, however, to mention that *WT1* may be inactivated by alterations that might not be detected by standard mutational analysis (Huff, 1998). An example of this phenomenon, Malik and colleagues showed that an antisense RNA (WT1-AS) transcribed from the *WT1* locus, can control WT1 protein levels (Malik *et al.*, 2000). The *WT1*-AS is imprinted and monoallelicaly expressed in the normal kidney. However, loss of imprinting results in biallelic expression of the WT1-AS in Wilms tumour tissues. Loss of imprinting is apparently due to loss of methylation within a regulatory region that *WT1*AS transcription (Hancock *et al.*, 2007; Moorwood *et al.*, 1998).

1.2.10.2 WT2 (Chromosome 11p15)

A second WT locus (WT2) was mapped to 11p15.5. Loss of heterozygosity (LOH) is observed in about 15% of WT cases. The significant bias towards the LOH for maternally derived alleles at 11p15, suggests the involvement of genomic imprinting (Williams *et al.*, 1989). The 11p15 region includes two known imprinted domains, *IGF2/H19* and *CDKN1C*^{KIP2}*/LIT1* (Mutter *et al.*, 1993; Rump *et al.*, 2005).

Insulin Growth Factor 2 (IGF2) is paternally expressed (maternal allele is silent) in the normal proliferating kidney during nephrogenesis (Hedborg *et al.*, 1994). Since IGF2 is a mitogenic growth factor, it is likely that its overexpression will lead to hyperplasia and contributes to Wilms tumorigenesis. IGF2 increased expression can be due to LOH of the maternal allele subsequently followed by duplication of the paternal. But a more frequent cause is the loss of imprinting (LOI) of the maternal allele yielding to biallelic expression IGF2 and a resultant increase of its level. One mechanism by which altered methylation leads to *IGF2* LOI involved a DMR that regulates both *IGF2* and *H19* gene expression. *IGF2* and *H19* are located approximately 90 kb apart and separated by the DMR that regulates their expression. Normally IGF2 is exclusively expressed from the paternal allele, whereas the adjacent paternal H19 allele is silenced (Frevel *et al.*, 1999; Zemel *et al.*, 1992). This DMR contains binding sites for the Zinc finger CCCTC-binding factor (CTCF), a chromatin insulator (enhancer blocking). The binding of CTCF to the unmethylated DMR on the maternal allele prevents IGF2 transcription and enables H19 transcription (Bell and Felsenfeld, 2000; Hark *et al.*, 2000). On the paternal allele, methylation of the DMR prevents CTCF binding, leading to *IGF2* transcription and *H19* silencing. IGF2 Loss of Imprinting (LOI) correlates with the *H19* DMR hypermethylation and occurs in 30-50% of Wilms tumors (Rainier *et al.*, 1993).

Another imprinted region involves CDKN1C^{KIP2}/LIT1. Demethylation of the DMR *LIT1*, a control region of the *KIP2/LIT1* domain, occurs in half of all patients with Beckwith–Wiedemann Syndrome (BWS). The *p57KIP2 (KIP2)/CDKN1C* gene within the KIP2/LIT1 domain, which is expressed predominantly from the maternal allele, encodes

a cyclin dependent kinase inhibitor and is a putative tumor suppressor. In several adult tumors, KIP2 expression is epigenetically reduced (Kikuchi *et al.*, 2002; Li *et al.*, 2002b; Soejima *et al.*, 2004).

IGF2 LOI must occur as an early event in Wilms tumorigenesis, because somatic mosaicism for IGF2 LOI is present in the normal renal kidney tissue adjacent in most Wilms tumors with IGF2 LOI (Okamoto *et al.*, 1997). As previously mentioned, a significant association between the presence of PLNR and IGF2 LOI in Wilms tumors has been described because somatic mosaicism in the tumor bearing kidney occurs more frequently for IGF2 LOI than 11p LOH (UPD) (Chao *et al.*, 1993), it is likely that IGF2 LOI is the predominant mechanism leading to PLNR formation. Presumably increased production of IGF2 arising from this epigenetic disturbance could lead to an imbalance in metanephric tissue growth and the persistence of these maturation delayed lesions.

Despite the identification of this imprinted domain, the 11p region remains complex. The fact that LOH of 11p15 is also seen in other cancers such as breast, lung and Leukemia, which indicates the presence of a tumor suppressor gene with a function that is not limited to Wilms tumor and kidney biology (Weston *et al.*, 1989).

1.2.10.3 CTNNB1 (chromosome 3p21)

Activating mutations of CTNNB1 coding beta-catenin is a relatively common somatic genetic lesion in Wilms tumor. Activating mutations occurs in the exon 3 of the β-catenin gene and disrupts its phosphorylation site. Phosphorylation of beta-catenin is regulated by CK1 (casein kinase 1) and GSK3 (glycogen synthase kinase 3) and normally facilitate its binding to a "destruction complex" containing APC (adenomatous polyposis coli) and AXIN (axis inhibition protein). In the absence of phosphorylation, β-catenin is not targeted for proteosomal degradation and enters the nucleus where it forms a transcriptional complex with TCF/LEF (T-cell specific transcription factor and lymphoid

enhancer factor) family members mimicking active WNT signaling (Moon *et al.*, 2004). Mutations in β-catenin are common in many different types of cancer and have been described in 10-15% of Wilms tumors (Koesters *et al.*, 1999). Beta-catenin mutations preferentially occurring in exon 3 at codon 45 indicate existence of an underlying mechanism causing such a tissue-specific mutational pattern (Kusafuka *et al.*, 2002).

Remarkably, there is a high degree of overlap between tumors that harbour mutations in β-catenin and in *WT1* genes; one report describes 19 out of 20 cases in which mutations in β-catenin occurred in tumors that also had mutations in *WT1* (Maiti *et al.*, 2000). *WT1* inactivation and β-catenin activation might therefore provide cooperative signals that drive renal tumorigenesis. It is conceivable that alterations in one pathway might actually trigger apoptotic signals that must be overcome by alterations in the second pathway before tumor formation can be initiated.

The sequence of mutational events in the *WT1* and *CTNNB1* genes have been studied by our collaborator in New Zealand who found that in ILNRs adjacent to the tumor with both alterations (*WT1* and *CTNNB1*) only *WT1* mutation was present suggesting that *CTNNB1* mutation occurs after the *WT1* mutational event (Fukuzawa *et al.*, 2007).

Even in the absence of mutations in CTNNB1 aberrant activation of the WNT signaling pathway can be observed in Wilms tumors (Koesters *et al.*, 2003). The recent identification of WTX and its ability to inhibit the beta-catenin pathway provide an explanation (Major *et al.*, 2007; Rivera *et al.*, 2007).

1.2.10.4 WTX (chromosome Xq11.1)

Recently Rivera and colleagues investigating the DNA copy-number changes in 51 primary WT using long-oligonucleotide array comparative genomic hybridization (array CGH) identified mutation and/or deletion at locus Xq11.1. The commonly deleted region

was found in about 30% of the tumors and was mapped within a single gene named WTX (Rivera *et al.*, 2007).

WTX protein is presumed to act as a tumor suppressor gene. Accordingly, introduction of WTX in Human Embryonic Kidney cells HEK293 significantly decreases colony formation in agar plate due to an increase of apoptosis after 48h (Rivera *et al.*, 2007). WTX is expressed in the developing kidney. Assessed by RNA in situ hybridization, the WTX expression profile closely resembles WT1 in terms of level and localization. Both WT1 and WTX are expressed in the condensing metanephric mesenchyme and in early epithelial structures that will form the glomerular podocytes (Rivera *et al.*, 2007).

The function of WTX during kidney development and Wilms tumorigenesis remains to be determined. Functional analyses in cultured cells, Xenopus and zebrafish demonstrate that WTX promotes beta-catenin ubiquitination and degradation, which antagonizes active WNT/beta-catenin signaling. Hence, inactivation of WTX enables beta-catenin translocation to the nucleus and subsequent up-regulation of WNT beta-catenin/tcf target genes upon WNT stimulation. This provides one possible mechanism for the tumor suppressor activity of WTX (Major *et al.*, 2007).

1.2.10.5 Other loci

Inactivating mutations in the *p53* gene are seen in about 5% of WT and are correlated with anaplastic histology (Malkin *et al.*, 1994; Takeuchi *et al.*, 1995). P53 can repress the *MDRR1* gene, which encodes a pump that prevents accumulation of drugs inside cells. Anaplastic cell lines carrying a *p53* mutation are resistant to chemotherapy and have been shown to overexpress P-glycoprotein, the product of the *MDR1* gene (Ramachandran *et al.*, 2000; Re *et al.*, 1997). Hence *p53* lesions determine chemoresistance in unfavorable anaplastic Wilms tumors (Bardeesy *et al.*, 1994; Lahoti *et al.*, 1996).

Tumor-specific LOH for both chromosomes 1p and 16q identifies a subset of Wilms tumor patients who have a significantly increased risk of relapse and death. LOH for these chromosomal regions can be used as an independent prognostic factor together with the disease stage, to determine intensity of treatment (Grundy *et al.*, 2005b). Chromosome 16q LOH has been observed in about 17% of Wilms tumors (Maw *et al.*, 1992).

Figure 1.8 Wilms tumor pathogenesis.

Wilms tumor pathogenesis can be classifed in 3 main setting:

1. Loss of *WT1* leading to intralobular nephrogenic rest (ILNR) followed by acquisition of activating mutation in the *CTNNB1* gene and resulting in a stromal histology tumor (earlier onset)
2. LOI of *IGF2* leading to perilobular nephrogenic rest (PLNR) followed by other genetic lesion causing a blatemal/epitheliela tumor (later onset).
3. Kidney develops normally and aquire genetic lesion in *WT1* and *WTX* or *WTX* and mutation/deletion or *IGF2* LOH that results in a typical triphasic histology Wilms tumor.

All of these tumors can aquire an anaplastic histology. Mutation in p53 and loss of chromosomes 1p and 16q are associated with the acquisition of this unfavorable histology.

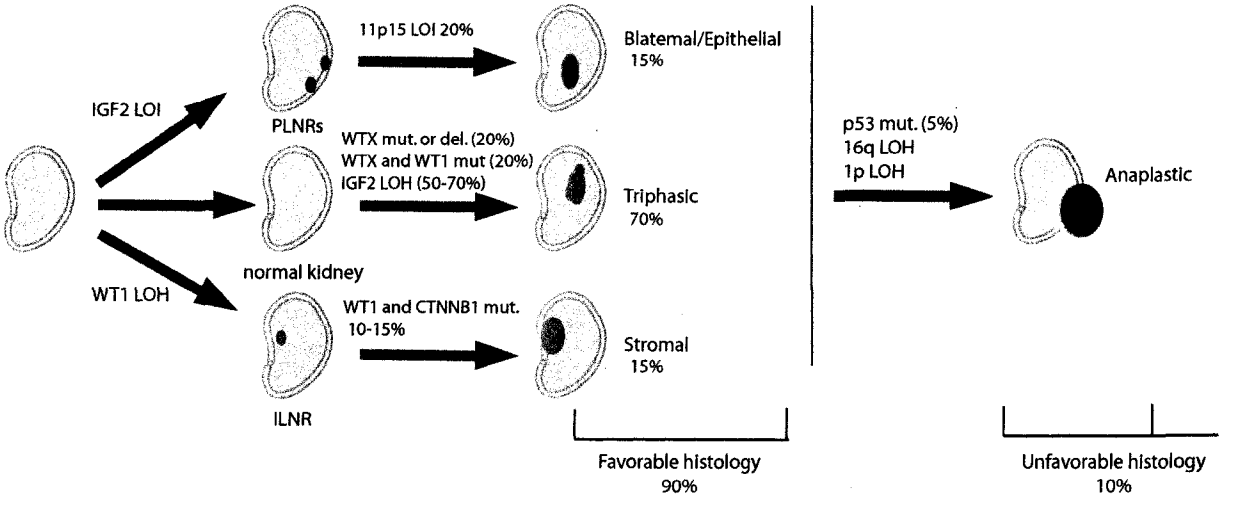
IGF2 LOI
PLNRs
11p15 LOI 20%
Blatemal/Epithelial
15%
WTX mut. or del. (20%)
WTX and WT1 mut (20%)
IGF2 LOH (50-70%)
Triphasic
70%
normal kidney
WT1 LOH
WT1 and CTNNB1 mut.
10-15%
Stromal
15%
ILNR
p53 mut. (5%)
16q LOH
1p LOH
Anaplastic
Favorable histology
90%
Unfavorable histology
10%

Fig.1.8

1.2.11 Nephrogenic rests

Wilms tumor is an embryonal tumor that originates from a progenitor cell lineage of the developing kidney. "Nephrogenic rests" refer to foci of persistent embryonal remnants that may be seen in normal newborns but are often seen in kidneys bearing Wilms tumours (Beckwith *et al.*, 1990). During normal kidney development, signals from the ureteric bud induce progenitor cells in the metanephric blastema to undergo mesenchyme-to-epithelium (MET) transition and form the epithelium of the nephron. Uninduced progenitor cells are committed to the alternative stromal cell fate. The pool of nephrogenic progenitor cells (metanephric blastema) is normally sustained throughout embryonic life but virtually disappears upon completion of renal development at 36 weeks of gestation. Nephrogenic rests appear to represent foci of progenitor cells that have not been appropriately committed to one differentiation pathway or the other (Beckwith *et al.*, 1990).

Beckwith and colleagues identified two distinct precursor lesions that distinguish WT subtypes according to pathogenesis; the perilobar Nephrogenic Rest (PLNR) that is located at the edge of the renal lobes and the Intralobar Nephrogenic Rest (ILNR) that are situated within the lobe. PLNRs, often found in multiplicity, are thought to arise relatively late in renal development and are associated with Wilms tumors in the Beckwith-Widemann syndrome. In contrast ILNRs are usually solitary, arise earlier and are associated with WAGR and DDS syndromes (Beckwith, 1998; Beckwith *et al.*, 1990). Intriguingly, perilobar nephrogenic rests may be seen in up to 1% of newborns otherwise considered clinically normal at postmortem examination but are rarely seen in adults, suggesting that PLNRs may involute with age. In contrast, intralobar rests are rarely seen in normal infants at postmortem examination. In any case, the presence of nephrogenic rests within a kidney resected for a Wilms tumor indicates the need for monitoring the contralateral kidney for tumor development, particularly in young infants.

A recent detailed analysis of 7500 nephrectomy specimens reveals that nephrogenic rests of one or the other type is present in the kidney in nearly 40% of the WT patients with

unilateral tumors and in virtually all cases associated with predisposition syndrome or bilateral tumor (Breslow *et al.*, 2006). In addition, ILNR is frequently associated with WT having stromal histology, younger age of onset and genomic *WT1* lesions. Conversely, WT associated with PLNR exhibits a blastemal/predominant histology and older age of onset. After adjusting for age of onset, no statistically significant difference in prognosis was found between the nephrogenic rest types associated with the tumor. Breslow and colleagues propose a refinement of Wilms tumor classification into three types according to nephrogenic rests: A) "ideal type I", accounting for about 20% of all WT, is characterized by early age of diagnostic, associated genito-urinary malformations and lesions in *WT1* and *CTNNB1* genes. B) "ideal type II" represents 20% of WT patients and is associated with PLNR, later age of onset and LOI at the IGF2 locus 11p15; C) the most common group comprises 60% of WT and is not associated with a specific type of nephrogenic rest (Breslow *et al.*, 2006). The specific link between Wilms tumor and nephrogenic rests remains unknown but underlines the connection between Wilms tumor and the pathways of embryonic kidney development.

1.2.12 Wilms tumor as an aberration of normal nephrogenesis

WT has long been considered a prototype for deranged cellular differentiation in cancer. The theory that WT arises from a pluripotent renal precusor cell is supported by its characteristic "triphasic" histology, which includes blastemal, epithelial and stromal components. In a triphasic tumor, the blastemal components are similar to the condensing nephrogenic mesenchyme; the epithelial components appear to recapitulate the mesenchyme-to-epithelium transition leading to nephrogenesis. Finally the stromal component of the triphasic tumor resembles the normal stromal renal cells but are thought to adopt an aberrant mesenchymal cell fate, giving rise to clusters of myogenic or adipose cells. Microarray gene-expression studies have shown that the gene expression profile of WT is similar to that of an 8-week human gestation developing kidney (Li *et al.*, 2002a; Li *et al.*, 2005a). Genes that are overexpressed in Wilms tumors include

PAX2, *IGF2* and genes of the WNT canonical pathway. Hence the molecular lesions that are involved Wilms tumorigenesis disrupt pathways that are important for renal development. For example WT1 (mutated in 10-15% of WT) has a key role in the induction of ureteric branching and survival of the metanephric mesenchyme. The WNT canonical signalling pathway (aberrantly active in nearly 50% of WT) is critical for the induction of epithelial differentiation in the metanephric mesenchyme. Although its role remains to be elucidated, WTX (mutated in 30% of WT) is highly expressed in the embryonic kidney.

1.3 Kidney development

1.3.1 Overview

The kidney develops in three distinctive stages: the pronephros (with no known function), the mesonephros (the excretory organ of the embryo) and the metanephros (which becomes the permanent kidney). The early development of the metanephros is a complex process that involves highly regulated interactions between two derivatives of the intermediate mesoderm, the Wolffian duct and the metanephric mesenchyme (MM) (**Figure 1.9**). At approximately embryonic day 35–37 in humans (10.5–11 in mice) a caudal outgrowth of the Wolffian duct, known as the ureteric bud (UB), invades the adjacent metanephric mesenchyme. The mesenchymal cells surrounding the ureteric bud (collectively known as the nephrogenic mesenchyme) then condenses to form caps of closely associated cells that undergo a mesenchyme-to-epithelium transition (MET) to form the anlage of renal tubules, the comma-shaped and S-shaped bodies. These transitional structures givre rise to the glomerular podocytes and epithelia of proximal tubules, loop of Henle and distal tubules. At its distal end, each nephron fuses to the branching ureteric bud which forms the collecting-duct system. Stromal cells arise within the nephrogenic zone, but migrate inward to intercalate between tubules. Although many different transcription factors orchestrate each stage of kidney embryogenenesis, the paired box family PAX2 and PAX8 and the zinc-finger protein, WT1, play a central role throughout renal development (Bouchard, 2004; Dziarmaga *et al.*, 2006). In addition, the canonical WNT pathway has an important function in nephrogenesis (Iglesias *et al.*, 2007).

1.3.2 PAX2/8 and WT1 in kidney development

PAX2 and PAX8 are highly expressed by the nephric duct cells during the caudal descent of the Wolffian duct (Bouchard *et al.*, 2000; Bouchard *et al.*, 2002). Although homozygous *Pax2* mutant mice initially form a mesonephric duct, its caudal decent is defective and rapidly degenerates and fails to reach the metanephric mesenchyme (Torres *et al.*, 1995). As a result, the animals are anephric and lack genital tracts (Favor *et al.*, 1996; Torres *et al.*, 1995). *Pax8* is the earliest known gene expressed during development of the pronephros ((Bouchard *et al.*, 2002; Dressler *et al.*, 1990). Interestingly, kidney development is unaffected in *Pax8* knockout mice, although these mice eventually die 3 weeks after birth due to thyroid defects (Mansouri *et al.*, 1998). Bouchard *et al* proved that there was significant functional redundancy between PAX2 and PAX8 (Bouchard *et al.*, 2002; Narlis *et al.*, 2007). At about 4 weeks fetal age in humans (and at E10.5 in the mouse), just before arriving at the cloaca, the nephric duct forms the ureteric bud. It grows laterally into the metanephric mesenchyme (MM) where it will induce the development of the metanephros by reciprocal interaction between the metanephric mesenchyme and the ureteric bud (UB). In the mouse *Pax2* and *Wt1* are essential for the invasion of the UB into the MM (Brophy *et al.*, 2001; Kreidberg *et al.*, 1993). Although WT1 is not expressed in the nephric duct itself, it is expressed in the intermediate mesoderm that surrounds the nephric duct (Armstrong *et al.*, 1993). *Wt1* knockout mice have no UB outgrowth and cells of the metanephric blastema undergo significant apoptosis (Kreidberg *et al.*, 1993). Furthermore, these mice do not express PAX2 in the metanephric blastema (Kreidberg *et al.*, 1993).

High levels of WT1 (but not PAX2) are seen in cells of the proximal S-shaped body destined to become podocytes; in contrast the distal portion of the S-shaped body expresses high level of PAX2 (but not WT1). This part of the S-shaped body gives rise to tubular segments of the nephron including proximal and distal convoluted tubules.

Figure 1.9 Stages of kidney development and nephrogenesis.

A) The invading UB in the MM, provides inductive signals that cause the mesenchymal cells in the proximity to condense around its tip, while others remain uninduced (blue).

B) The induced comitted cells undergo a mesenchymal to epithelial transition, initially forming a renal vesicle.

C) The renal vesicle progresses into a comma shaped-body.

D) Progressed form the comma-shaped, the S-shaped body consists of two distinct portions, the distal region that express WT1 (but no PAX2) and the proximal regions that express PAX2 (but not WT1). The distal portion will fuse to the collecting duct, while the proximal portion will form the epithelial portion (podocytes) of the glomerulus.

E) Tightly regulated proliferation and cellular differentiation continues until the final nephron structure is formed (Modified from (Cho EA, 2003).

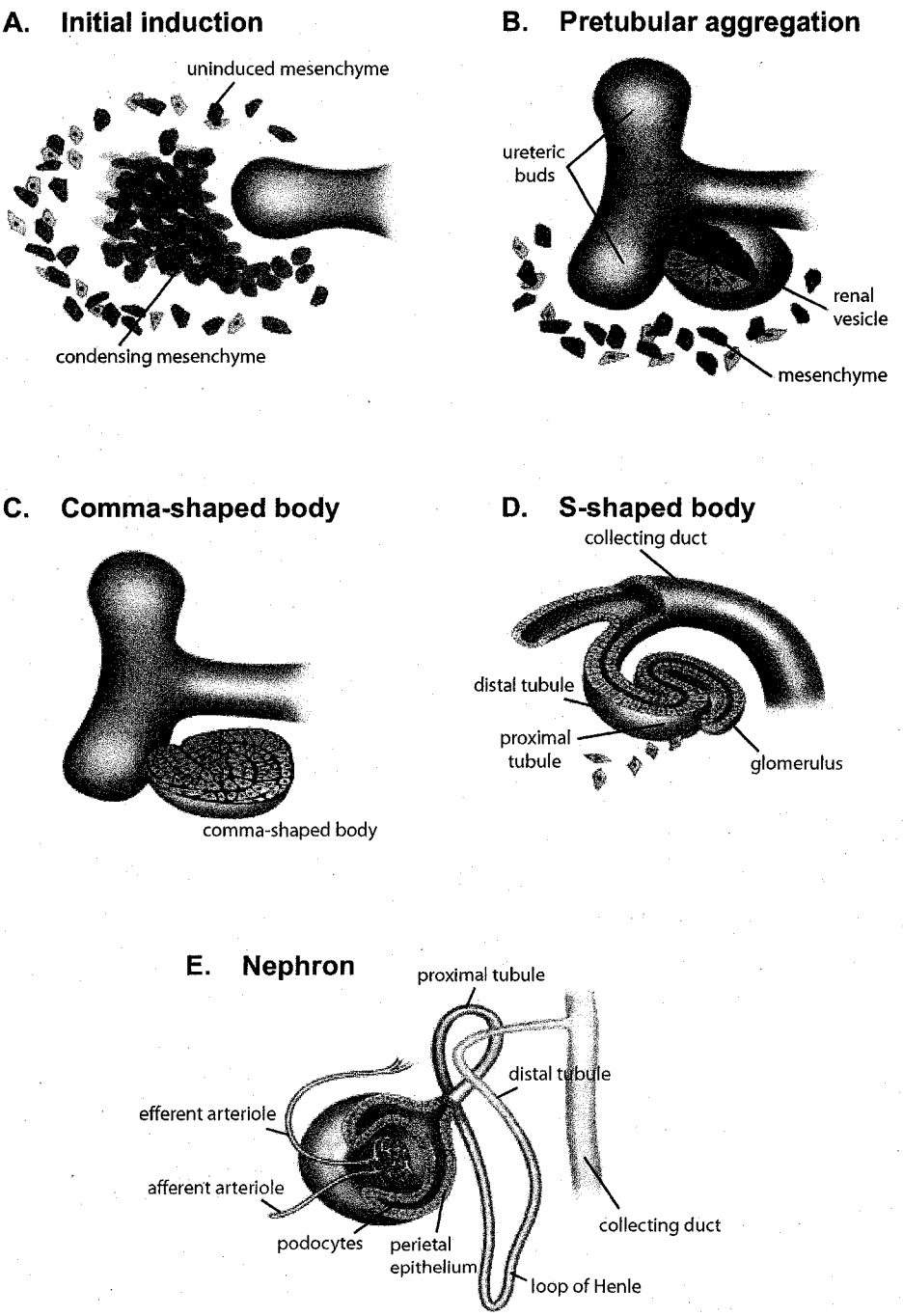
A. Initial induction
uninduced mesenchyme
condensing mesenchyme
B. Pretubular aggregation
ureteric buds
renal vesicle
mesenchyme
C. Comma-shaped body
comma-shaped body
D. S-shaped body
collecting duct
distal tubule
proximal tubule
glomerulus
E. Nephron
proximal tubule
distal tubule
efferent arteriole
afferent arteriole
podocytes
perietal epithelium
collecting duct
loop of Henle

Fig.1.9

1.3.3 The WNT canonical pathway in kidney development

The canonical signaling pathway is activated by WNT-family glycoproteins, which bind to cognate frizzled receptors. Activated receptors recruit dishevelled protein (Dvl) and inhibit degradation of cytoplasmic beta-catenin via the GSK3beta-axin-APC complex. When its degradation is blocked, cytoplasmic beta-catenin is available to translocate to the nucleus, dimerize with partners belonging to the T-cell factor (TCF) family and activate target genes. In general, canonical beta-catenin/TCF signaling is thought to activate gene targets involved in cell proliferation (cyclin D1, c-myc). In the metanephric kidney, intense canonical WNT signaling is present in epithelia of the branching ureteric bud and in nephrogenic mesenchyme during its transition into renal tubules (Iglesias *et al.*, 2007). WNT signaling activity is rapidly downregulated in maturing nephrons and becomes undetectable in the postnatal kidney (Iglesias *et al.*, 2007). Thus, it is likely that failure of mechanisms that normally suppress WNT signaling (or acquisition of constitutive activation of beta-catenin such as *CTNNB1* mutation in Wilms tumor) will result in incomplete epithelial differentiation and aberrant cellular proliferation.

1.3.4 Renal stem cells and cancer stem cell

Typically embryonic progenitor cells have the ability of self-renewal, unlimited proliferation and multipotent differenatiation potential. The identification of somatic cells with similar "embryonic" properties in adult tissues has established the concept of somatic stem cells. In fact, tissue-specific stem cells have been found in many organs, including bone marrow, gastrointestinal mucosa, liver, brain, prostate and skin (Blanpain *et al.*, 2007). These cells participate in the normal cell turnover of these organs and are a potential source of cells after organ injury. With regards to the kidney, stem cells exist in the metanephric mesenchyme during kidney development (Herzlinger *et al.*, 1992; Oliver *et al.*, 2002). During kidney development these mesenchymal stem/progenitor cells must be constantly renewed so that the kidney can continue to grow and induce additional

generations of nephrons. Once nephrogenesis is complete the stem cell population is significantly reduced and may be restricted to niches of dormant progenitors cells. Candidate stem cells have been identified in the adult kidney but the identity of the genes and mechanisms required to maintain this mesenchymal stem/progenitor cell population, remains to be clarified.

Putative renal stem cells have been isolated using CD133 as a surface marker which typically identifies progenitor cells in hematopoietic and neural tissues. Bussolati *et al.* reported that CD133-positive cells in the interstitium of the adult human kidney have characteristics of stem cells. Interestingly, these putative renal stem cells expressed PAX2, as well as several markers typical of bone marrow stromal cells, but were negative for hematopoietic cell markers such as CD34 or CD45. By using different culture conditions *in vitro*, the authors indicated that CD133+ renal cells have the capacity to differentiate into either type of tubular cells demonstrating their pluripotency (Bussolati *et al.*, 2005)

Recently the identification of cancer stem cell provides an additional link between embryogenesis and tumorigenesis (Reya *et al.*, 2001). Somatic stem cell are normally able to maintain their self proliferative capacity for the lifespan of the organism, without leading to the development of tumors. This probably might explain why these multipotent cells are typically sequestered in niches that to some extent insulate them from environmental stress susceptible to subvert their unlimited proliferative capacity towards the acquisition of a malignant phenotype (Pardal *et al.*, 2005; Spradling *et al.*, 2001). Nevertheless, since normal stem cells and cancer cells share the ability to selfrenew, it seems reasonable to predict that malignant growth might arise from the transformation of a stem cell (cancer stem cell theory). In is plausible that cancer cells utilize the gene machinery for self-renewing cell division that is normally expressed in stem cells. It follows that many of the molecular players involved in controlling developmental and stem cells self-renewal pathways are implicated in oncogenesis (Reya *et al.*, 2001).

PAX genes that are expressed both by embryonic cell during development by tissue-specific somatic stem in adult tissues; PAX gene aberrant expression have also been associated with the development of a variety of tumor thus providing a canonical illustration of this phenomenon (Robson *et al.*, 2006).

1.4 PAX genes in development and cancer

1.4.1 Overview

PAX (Paired Box) genes comprise a family of genes well conserved through evolution encoding for nine transcription factors that share the DNA binding paired-domain.
The PAX genes are classified into sub-groups I-IV (**Table 1.5**) according to which structural domain they can include (an octapeptide region and a homeodomain). During embryonic development, PAX genes expression is organ specific; PAX functions include cellular proliferation, cellular differentiation, migration and survival. Disrupting PAX gene function during embryonic development, results in abnormal development.
Once organogenesis is completed PAX gene expression progressively declines and is restricted to organ specific progenitor cells in which they confer a self-renewal property.
On the other hand, aberrant PAX gene expression is observed in a variety of cancers (summarized in **Table 1.6**) in which they have been associated with proliferation, resistance to apoptosis, metastasis and angiogenesis recapitulating all of the characteristics that define malignant growth (Robson *et al.*, 2006).

Table 1.5 PAX genes structure, chromosomal location and human syndromes:

The nine human *PAX* genes are organized according to groups (I to IV), based on their structural and functional homologies. All of these genes contain the "paired domain", while the octapeptide and the homeodomain are particular to specific groups. Both the human and mouse chromosomal locations are indicated, as are the human syndromes that have been associated with specific *PAX* gene mutations (Eccles *et al.*, 2002).

Table 1.5 PAX genes:

	Gene	Gene structure domains			Chromosomal locations		Human Syndrome
		Paired box	*Octapeptide*	*Homeodomain*	*Human*	*Mouse*	
Group I	PAX1				20p11	2	-
	PAX9				14q12-q13	12	Oligodontia
Group II	PAX2				10q24	19	Renal-Coloboma syndrome
	PAX5				9p13	4	-
	PAX8				2q12-14	2	Congenital hypothyroidism
Group III	PAX3				2q35	1	Waardenburg syndrome
	PAX7				1p36	4	-
Group IV	PAX4				7q32	6	-
	PAX6				11p13	2	Aniridia

Table 1.6 PAX genes expression and function in cancer:

PAX genes, representing subgroups II (*PAX2*, *PAX5* and *PAX8*) and III (*PAX3* and *PAX7*) are frequently expressed in a variety of cancer. Rearrangements implicating, *PAX3, PAX5, PAX7* and *PAX8*, are associated with characteristic chromosomal translocations that occur in specific tumors. *PAX* genes in subgroups II and III confer cell motility, cell survival and cell proliferation ability, which are often associated with tumour progression. On the other hand, *PAX* genes in subgroups I (*PAX1* and *PAX9*) and IV (*PAX4* and *PAX6*) are either less often involved in cancer or their expression is indicative of favourable prognosis, as observed for *PAX6*. (Robson *et al.*, 2006).

Table 1.6 PAX genes in Cancer:

Gene	Embryonic expression	Cancer	Function/prognosis
PAX1	Skeleton thymus and 3rd and 4th pharyngeal pouch	Not known to be associated with cancer	N.A.
PAX9	Skeleton, teeth and thymus	Oesophageal	Cell differentiation Neutral
PAX2	Kidney, eye and CNS	Breast, ovarian, prostate, renal carcinoma, Karposi sarcoma and Wilms tumor	Motility, survival Unfavorable
PAX5	B-cells and CNS	Lymphomas, leukemia, medulloblastoma, astrocytoma and neuroblastoma	Proliferation
PAX8	Kidney, thyroid and CNS	Thyroid, placenal, ovarian carcinoma and Wilms tumor	Survival Unfavorable
PAX3	Neural Crest, CNS and somites/muscles	Rhabdomysarcoma, Ewing sarcoma, neuroblastoma and melanoma	Motility, survival Unfavorable
PAX7	Neural Crest, CNS and somites/muscles	Rhabdomysarcoma, Ewing sarcoma, neuroblastoma and melanoma	Survival Unfavorable
PAX4	Pancreas and gut	Pancreas carcinoma	Cell survival Neutral
PAX6	Pancreas, gut, CNS and eye	Pancreas carcinoma, astrocytic glioma and glioblastoma	Tumor suppressor Favorable

1.4.2 PAX2

1.4.2.1 Overview

PAX2 is a transcription factor of the paired box family expressed throughout embryonic development in the central nervous system (CNS), the ear, the eye and the urogenital system. *Pax2* mouse knockouts have further emphasized the importance of PAX2 expression within these structures, since homozygous null mutants are lethal and fail to develop essential structures within the CNS, the ear and the urogenital system. *Pax2+/-* mutant mice exhibit increased apoptosis in various organs, including the kidney. Although PAX2 plays a role in differentiation and proliferation, its main function seem as an anti-apoptotic molecule.

1.4.2.2 Human Renal Coloboma Syndrome and the *Pax2^{1Neu}* mouse

Renal-Coloboma Syndrome (RCS, OMIM 120330) is a rare autosomal dominant condition, in which patients are affected by renal hypoplasia, ocular colobomas and vesico-ureteral reflux (Devriendt *et al.*, 1998; Sanyanusin *et al.*, 1995; Schimmenti *et al.*, 1997). Kidney hypoplasia is the principal feature of RCS and often leads to end stage renal failure, requiring a transplant (Cunliffe *et al.*, 1998; Devriendt *et al.*, 1998; Narahara *et al.*, 1997; Schimmenti *et al.*, 1997). RCS is associated with heterozygous *PAX2* inactivating mutations(Sanyanusin *et al.*, 1995). More than 10 different mutations have been identified but the most common mutation is an insertion of an extra guanine nucleotide in exon 2, causing a frame-shift and a nonfunctional truncated protein (Devriendt *et al.*, 1998).

Interestingly, this identical mutation occurs spontaneously in the (*Pax2^{1Neu}*) mouse (Favor *et al.*, 1996). *Pax2+/-* mice have a 50% reduction of PAX2 protein; this PAX2 deficit significantly diminishes branching morphogenesis during fetal kidney development

resulting in renal hypoplasia (Porteous *et al.*, 2000). Homozygous inactivation of the *Pax2* gene is lethal and mice exhibit complete renal agenesis (Favor *et al.*, 1996).

1.4.2.3 Genomic structure of *PAX2*

The *PAX* family of genes is classified into sub-groups according to homologies and *PAX2* is part of the *PAX2/5/8* sub-family (Dahl et al., 1997). In humans, *PAX2* is located on chromosome 10 within the boundaries of q24 and q25 (Narahara et al., 1997) and in mice it resides on chromosome 19. The Human PAX2 gene consists of 12 exons spanning over 70 Kb of genomic DNA (Sanyanusin et al., 1996). The *PAX2* gene encodes a 42k Da protein containing a paired domain, which mediates DNA binding, an octapeptide domain and a partial homeodomain. The first four exons code for the highly conserved paired box domain, while the fifth exon codes for the octapeptide domain (Sanyanusin et al., 1996). In humans and in mice, there are three exons that are alternately spliced; exons 6, 10 and 12 (Sanyanusin et al., 1996), resulting in alternatively spliced *PAX2* mRNAs. The function or the significance of these spliced isoforms remains to be determined.

1.4.2.4 PAX2 expression during development

During kidney development, PAX2 protein is one of the earliest transcription factors expressed. It is first seen in the pronephric duct and it is the first epithelial structure to form from the intermediate mesoderm. PAX2 expression continues in the mesonephric duct and tubules and finally in the Wolffian and Müllerian ducts. PAX2 is highly expressed in the metanephric kidney upon induction by the outgrowth and subsequent branching of the ureteric bud. Furthermore, PAX2 is expressed in the mesenchymal cells as they aggregate around the tips of the ureteric bud and it persists during formation of the comma and S-shaped bodies. During nephron formation, PAX2 is restricted to the

distal part of the S-shaped body, closest to the point of fusion with the ureteric bud, PAX2 is conspicuously absent in maturing WT1(+) podocytes of the glomerulus. Once nephrogenesis is complete, PAX2 is progressively attenuated to a relatively low level characteristic of adult kidneys (Eccles et al., 1992).

In the brain, PAX2 is expressed early, starting at embryonic day 7.5, within the organizing center at the midbrain-hindbrain boundary (MHB), (Rowitch & McMahon, 1995). As development proceeds, the PAX2 expression domain becomes restricted to a central narrow ring at the MHB (Rowitch & McMahon, 1995). This region specifies the posterior midbrain and cerebellum (Rowitch & McMahon, 1995). Absence of PAX2 results in an absence of the midbrain and cerebellum.

PAX2 is also expressed in both the developing eye and ear. During the development of the inner ear, PAX2 is first expressed in the optic placode and then becomes limited to the ventral region of the optic vesicle responsible for generating the structures of the saccule, the cochlea and spiral ganglia of the auditory nerve (Puschel et al., 1992) Homozygous mutant *Pax2* mice do not form any of these structures; massive apoptosis is observed in the spiral ganglion cells (Torres et al., 1995). During eye development, PAX2 is detected at embryonic day 9 in the optic vesicle. Later PAX2 marks the optic cup, the optic fissure and the optic stalk, which subsequently becomes the optic nerve (Puschel et al., 1992). In *Pax2* mutants, the optic fissure fails to close, resulting in a coloboma and there is an extension of the pigmented retina into the optic stalks.

1.4.2.5 PAX2 function during development

PAX2 is required for the development of the urogenital system. Although homozygous *Pax2* mutants initially form a nephric duct, the cells undergo apoptosis and no further urogenital structures are formed (Torres et al., 1995). PAX2 has been linked directly to

regulation of programmed cell death. Animals with heterozygous *Pax2* mutations have increased ureteric bud cell death with resultant renal hypoplasia (Porteous et al., 2000). Expression of the pro-apoptotic gene *Baxα*, under control of the *Pax2* promoter, increased apoptosis in the ureteric tree and markedly inhibited the extent of branching morphogenesis, reproducing the kidney phenotype of the *Pax2*+/- mouse and validating apoptosis as a mechanism underlying renal hypoplasia (Dziarmaga et al., 2003) . Reciprocally, the renal hypoplasia of the *Pax2*+/- mouse can be rescued either by suppressing apoptosis pharmacologicaslly with the caspase-inhibitor Z-vad-fmk or genetically by crossing *Pax2*+/- mutants with a mouse expressing the anti-apoptotic bcl2 within the PAX2 expression domain (Clark et al., 2004; Dziarmaga et al., 2006). Finally, NAIP (Neuronal Inhibitor of Apoptosis) has been identified as a direct downstream target of PAX2 in developing kidney (Dziarmaga et al., 2006). NAIP belongs to the IAP family and is an inhibitor of caspases-3 and 7, the final effectors of the apoptosis process. These observations provide one mechanism by which PAX2 exerts its anti-apoptotic function (Dziarmaga et al., 2006).

PAX2 has also been associated with abnormal cellular proliferation and renal cystic diseases (Winyard et al., 1996). Constitutive overexpression of *Pax2* in transgenic mice, leads to renal cyst formation, indicating that attenuation of *Pax2* expression is important for proper differentiation (Dressler et al., 1993). Reciprocally, in polycystic kidney mouse models, reduction of *Pax2* gene dosage resulted in a decrease in cyst size (Ostrom et al., 2000).

Although PAX2 is important for the mesenchyme-to-epithelial transtion during neophrogenesis, PAX2 must be downregulated for proper podocyte maturation (Wagner *et al.*, 2006). Ectopic PAX2 expression in the podocyte of transgenic mice leads to abnormal podocyte differentiation and glomerular dysplasia with end-stage renal failure soon after birth (Wagner *et al.*, 2006).

1.4.2.6 PAX2 expression in cancer

Expression of *PAX2* has been observed in kidney cancer including Wilms Tumor (WT) and Renal Cell Carcinoma (RCC) (Daniel *et al.*, 2001; Dressler and Douglass, 1992; Eccles *et al.*, 1992; Khoubehi *et al.*, 2001). PAX2 is also expressed in prostate (Khoubehi *et al.*, 2001), ovarian (Tong *et al.*, 2007), endometrial and bladder cancers (Muratovska *et al.*, 2003; Wu *et al.*, 2005). In addition, breast tumors, (Gibson *et al.*, 2007; Silberstein *et al.*, 2002), Kaposi sarcoma (Buttiglieri *et al.*, 2004) and leukemia (Siehl *et al.*, 2003) have also been shown to overexpress PAX2.

PAX2 expression has been detected in at least 25% of tumor samples in a large screening of over 400 primary tumors of all types (Muratovska *et al.*, 2003). More specific studies have observed expression of PAX2 in 40–53% of lobular or ductal breast carcinomas (Silberstein *et al.*, 2002). Similarly, PAX2 is expressed in 52% of primary prostatic cancers (Khoubehi *et al.*, 2001), but more strikingly, PAX2 is expressed in all histological renal tumor subtypes except transitional cell carcinomas. In particular PAX2 is expressed in 90% of clear cell RCC, the major histological subtype and virtually all papillary RCC. Moreover, PAX2 expression correlates with proliferation index and is significantly higher in patients with metastatic disease (Daniel *et al.*, 2001) PAX2 expression in renal tumors has been verified and validated by several studies as a reliable marker of renal neoplasms (Mazal *et al.*, 2005; Memeo *et al.*, 2007; Tong *et al.*, 2006).

The mechanism by which PAX2 is reactivated in neoplastic tissues is not well understood. However, a recent study suggests that this can occur through hypomethylation of the *PAX2* promoter (Wu *et al.*, 2005). The *PAX2* promoter is normally methylated and therefore silenced in normal adult endometrial cells, but loss of PAX2 promoter methylation is found in 75% of endometrial carcinomas (Wu *et al.*, 2005)

1.4.2.7 PAX2 function in cancer

Cell survival:

Mutatovska *et al.* used small interfering *PAX2* RNAs to silence PAX2 expression in bladder and ovarian cancer cells and showed that this caused inhibition of cell proliferation and increased apoptosis, confirming the previous finding by Gnarra *et al* (Gnarra and Dressler, 1995; Muratovska *et al.*, 2003). Similarly, inhibition of PAX2 in prostate cancer cell lines and Karposi sarcoma results in cancer cell apoptosis. Although PAX2 can repress *p53* expression the mechanism for PAX2-mediated protection from cell death in cancer cells is unknown (Stuart *et al.*, 1995). Inhibition of PAX2 in prostate cancer results in apoptosis that is not dependent on p53 (Gibson *et al.*, 2007).

Apoptosis:

Transfection of antisense *PAX2* into Kaposi sarcoma cells results in enhanced cell death following serum deprivation or vincristine treatment (Buttiglieri *et al.*, 2004). PAX2 expression has been associated with decreased levels of PTEN and increased levels of phosphrylated Akt in endothelial cells, but it is unclear whether this mechanism is applicable in other cancers (Fonsato *et al.*, 2006).

Metastasis:

PAX2 expression correlates with the presence of metastatic disease in RCC (Daniel *et al.*, 2001). In Karposi sarcoma PAX2 levels correlate with cellular motility and levels of the alphaVbeta3 integrin, known to be involved in tumor invasion (Buttiglieri *et al.*, 2004).

Angiogenesis: Introduction of PAX2 in normal endothelial cells conferred to these cells a proinvasive, proangiogenic phenotype similar to that of tumor-derived endothelial cells (Fonsato *et al.*, 2006). Conversely, the inhibition of PAX2 in tumor endothelial cells results in a decreased apoptosis resistance associated with reduced angiogenesis *in vivo* (Fonsato et al., 2006). The inhibition of PAX2 in tumor-derived endothelial cells increased the level of the tumor suppressor PTEN decreased AKT phosphorylation. This suggests that angiogenesis is associated with PAX2 expression which antagonizes PTEN,

thereby activating the Akt-survival pathway to promote angiogenesis (Fonsato *et al.*, 2006).

Tumorigenicity: Transfection of HEK293 cells with PAX2 enabling them to grow in xenograft transplants under the skin of nude mice, suggesting a transforming effect of PAX2 (Maulbecker & Gruss, 1993). Conversely, PAX2 knockdown in endometrial tumor cells result in decreased growth of tumor xenografts in nude mice (Wu *et al.*, 2005). Nevertheless, overexpression of PAX2 in transgenic mice results in cystic kidneys but not in renal cancer, suggesting that PAX2 by itself is not sufficient to transform renal cells.

1.4.3 PAX3

1.4.3.1 Overview

PAX3 is expressed in the developing embryo and is a critical factor for the proper formation of the mammalian nervous, cardiovascular and muscular systems. In the mouse, a spontaneous heterozygous mutation of *Pax3* results in a coat pigmentation (splotch) defect; in humans, haploinsufficiency of *PAX3* is associated with the Wardenburg syndrome (deafness, pigmentation defects, neural crest-related abnormalities and variable limb myopathy). In adult tissues, PAX3 expression is restricted to a pool of progenitor cells such as satellite muscle cells. Aberrant PAX3 expression can be observed in sarcomas and neural crest-derived tumors. Cellular proliferation, migration and apoptosis resistance have been attributed to PAX3 but the most well-established role for PAX3 involves its function in self-renewal of progenitor cells for myogenic and neural crest lineages.

1.4.3.2 The Splotch Mouse and the Waardenburg syndrome

A spontaneous murine *Pax3* mutation was first described by Auerbach in 1954 and was termed *splotch* because the mice exhibit a distinctive white belly spot (Goulding *et al.*, 1993). The *Pax3-/-* homozygous *splotch* mouse dies by day E14.5 due to cardiovascular defects. In addition, limb musculature is absent and numerous neural crest derivatives are abnormal, including dorsal root ganglia, melanocytes and enteric ganglia (Epstein *et al.*, 1993; Epstein *et al.*, 2000). Mutations leading to the *Splotch* phenotype affect the *PAX3* paired homeodomain, resulting in complete loss of PAX3 function (Epstein *et al.*, 1991).

In humans, *PAX3* mutations cause Waardenburg Syndrome (WS) type I and III (OMIM 193500 and 148820) (Baldwin *et al.*, 1992; Tassabehji *et al.*, 1992). WS is the most common cause of congenital sensorineural deafness and accounts for 2–3% of all congenital hearing disorders. First described by the Dutch ophthalmologist, Petrus Waardenburg, in 1951, affected patients also exhibit variable degrees of facial dysmorphology, myopathy and pigmentary abnormalities (Waardenburg, 1951). Dystopia canthorum, a lateral displacement of the eyes, is a feature of type III Waardenburg Syndrome and I. In addition, patients with type III WS or Klein-Waardenburg syndrome are characterized by muscle hypoplasia. Interestingly, type II Waardenburg Syndrome is not caused by PAX3 itself but by a mutation in a PAX3 target gene of the transcription factor MITF (Bondurand *et al.*, 2000). Hearing loss, pigmentation defects and heterochromia (different colored eyes irises) are related to neural-crest related defects. WS is inherited as an autosomal dominant trait. More than 50 different *PAX3* mutations have been identified in patients with Waardenburg Syndrome including missense, nonsense, frameshift, splicing and deletion mutations (Read & Newton, 1997).

1.4.3.3 Gene structure

PAX genes are clustered in sub-groups according to homologies and *PAX3* is part of the *PAX3/7* sub-family (Dahl *et al.*, 1997)]. In humans, *PAX3* is located on chromosome 2q and in mice it resides on chromosome 1 (Eccles *et al.*, 2002). PAX3 has two DNA binding domains, an amino-terminal 120 amino acid "paired" domain (PD) characteristic of the PAX family and a "paired-type" homeodomain (HD). In addition, PAX3 has a conserved octapeptide and a proline-serine-threonine rich C-terminal trans-activation domain, both of which are involved in protein-protein interactions (Apuzzo *et al.*, 2004; Apuzzo and Gros, 2006). The paired domain is encoded by exons 2-4, while exons 5 and 6 encode the octapeptide and homeodomain. Exons 7 and 8 encode a proline-serine-threonine-rich transactivation domain, while exons 8-10 encode the c-terminal domain. (Li *et al.*, 2007; Parker *et al.*, 2004; Wang *et al.*, 2007; Wang *et al.*, 2006; Wang *et al.*, 1998).

At least seven isoforms (PAX3a-h) resulting for alternative splicing have been identified (Li *et al.*, 2007; Parker *et al.*, 2004; Wang *et al.*, 2007; Wang *et al.*, 2006; Wang *et al.*, 1998). PAX3a and PAX3b are composed of exons 1 to 4 only and therefore lack the homeodomain and the carboxyl-terminal transactivation domain. In terms of distribution, PAX3b is almost ubiquitously expressed while most PAX3a expression is restricted to the cerebellum and skeletal muscle (Tsukamoto *et al.*, 1994). The *PAX3*c transcript extends to a secondary splice site within intron 8. *PAX3d* proceeds from the primary splice sites from exon 8 to exon 9. The functional DNA binding and transactivation properties of PAX3c and PAXd are comparable *in vitro* (Barber *et al.*, 1999). PAX3e contains exons 8, 9 and 10 but lacks introns 8 and 9. PAX3g and PAX3h are truncated isoforms of PAX3d and PAX3e, respectively, but also both lack part of the transactivation domain encoded by exon 8 (Parker *et al.*, 2004; Wang *et al.*, 2007; Wang *et al.*, 2006). Functional analysis further indicated that these isoforms have different activities in stably transfected mouse melanocytes *in vitro* (Wang et al., 2007; Wang et al., 2006).

There is very strong sequence conservation between mouse *Pax3* and human PAX3 (Goulding *et al.*, 1991). Mouse and human PAX3 protein are 98% homologous (Lalwani *et al.*, 1995; Macina *et al.*, 1995). The first cloned murine *Pax3* cDNA contained an open reading frame of 1437 bp over eight exons and was predicted to encode a protein of 479 amino acids with a molecular weight of 56 kDa (*Pax3c*) (Barber *et al.*, 1999; Goulding *et al.*, 1991) (Goulding et al 1991 and Barber et al). Alternatively spliced murine *Pax3* isoforms analogous to the human isoforms have been reported. Interestingly, Pritchard et al. identified isoform *Pax3*g (Pax3 Δ8) in murine myoblasts. PAX3g shows weak transcriptionally activity *in vitro* and inhibits PAX3d (PAX3 -8i) activity in myoblasts, presumably by competing for PAX3d binding sites (Pritchard *et al.*, 2003). In addition, murine *Pax3a and PAX3b* differ by the presence or absence of a glutamine residue in the linker region between the third and fourth alpha helix of the paired DNA-binding domain (Vogan *et al.*, 1996). These two isoforms have distinct DNA-binding properties (Vogan & Gros, 1997).

1.4.3.4 Expression during development

PAX3 is expressed in the developing hindbrain, mesencephalon and prosencephalon where it invariably remains confined to the ventricular zone of the developing central nervous system. PAX3 expression becomes restricted to the dorsal neural tube, where neural crest cells are specified (Goulding *et al.*, 1991). Neural crest cells represent a multipotent population of migratory cells that give rise to the entire peripheral nervous system; to melanocytes, enteric ganglia (a subpopulation of vascular smooth muscle), bone, cartilage of the face and to various other cell types. In the peripheral nervous system development, PAX3 is expressed in the dorsal root and sympathetic ganglia (Kioussi *et al.*, 1995). Accordingly the dorsal root ganglia are small or absent in *Splotch* embryos. *Pax3-/-* mice exhibit malformation of the trigeminal (Vth cranial nerve), superior (IX) and jugular (X) ganglia. (Tremblay *et al.*, 1995). Several reports suggested that PAX3 is required for proper neural crest migration(Conway et al., 1997), this may

involve survival of neural crest precursors as they move toward peripheral targets (Conway *et al.*, 2000; Epstein *et al.*, 2000).

Homozygous *Splotch* embryos display persistent truncus arteriosus. The vessel fails to divide into proximal aorta and the pulmonary artery (Conway *et al.*, 1997a).This failure of outflow tract septation in *Splotch* is almost certainly because of a defect in cardiac neural crest cell migration. Indeed neural crest cells normally contribute to the outflow tract and also differentiate into smooth muscle that contributes to the great vessels (Epstein *et al.*, 2000; Kirby *et al.*, 1983).

PAX3 plays a central role in developing skeletal muscle (Maroto *et al.*, 1997; Tajbakhsh *et al.*, 1997). PAX3-deficient embryos exhibit skeletal muscle defects and transgenic rescue experiments have demonstrated a requirement for PAX3 in development of the diaphragm and limb musculature (Li *et al.*, 1999). PAX3 is initially expressed widely in the presomitic mesoderm, but then its expression becomes restricted to the hypaxial domain of the somite. Myoblasts migrating from the lateral somites express PAX3 and take up residence in the ventral body wall, limbs and diaphragm (Ordahl & Le Douarin, 1992). As fetal muscles mature, PAX3 expression attenuates in parallel with the appearance of myogenic markers such as MYOD (Daston *et al.*, 1996; Tremblay *et al.*, 1998; Williams and Ordahl, 1994). However, PAX3 expression is maintained in a selective population of satellites cells (muscle progenitor cells) residing under a basal lamina that forms around the muscle fibers. (Relaix *et al.*, 2006; Relaix *et al.*, 2005).

1.4.3.4 PAX3 function during development

Cell survival:

A striking feature of *Pax3*-mutant embryos is the loss of the hypaxial dermomyotome, which is due to apoptosis (Borycki *et al.*, 1999). In addition, the introduction of dominant negative forms of PAX3 into cultured satellite cells increases cell death, demonstrating

that PAX3 is required for progenitor cell survival in postnatal muscle (Buckingham and Relaix, 2007; Relaix *et al.*, 2006).

Cell migration:

In myogenic precursors, PAX3 activates transcription of several target genes, among which are MyoD and c-Met (Birchmeier and Brohmann, 2000). The latter codes for a cell-surface receptor which mediates delamination of myoblast precursors from the epithelial dermomyotome and their migration in the limb bud. This occurs in response to hepatocyte growth factor/scatter factor (HGF/SF) ligand (Relaix *et al.*, 2003).

In neural crest derivatives, PAX3 also activates the c-*Ret* gene. This gene encodes a receptor that interacts with GDNF (glial cell–derived neurotrophic factor), which is secreted by mesenchymal cells that surround the enteric ganglia, thus determining their location (Lang *et al.*, 2000; Lang and Epstein, 2003; Lang *et al.*, 2005).

Cell fate:

PAX3 is required for the proper differentiation of neural crest and myogenic progenitor cells (Conway *et al.*, 1997b; Relaix *et al.*, 2004). PAX3 controls myogenic cell fate through the myogenic determination factors Myf5 and MyoD; for *Myf5*, in the embryo, this can involve direct transcriptional control (Bajard *et al.*, 2006; Maroto *et al.*, 1997) PAX3, when overexpressed in cultured neural tube explants, can induce ectopic MyoD expression (Maroto *et al.*, 1997). However, PAX3 protein expression seems to be associated with an intermediate precursor cell of the myogenic lineage. After the initial increased level of expression, PAX3 protein level is downregulated as the cells become committed myoblasts and this decline is necessary for terminal myogenic differentiation. This is why introduction of PAX3 can actually inhibit myogenic differentiation of myoblast cells (Epstein *et al.*, 1995).

In the skin, PAX3 is thought to function at a nodal point in melanocyte stem-cell differentiation (Lang *et al.*, 2005). PAX3 determines melanocyte stem-cell fate by triggering expression of microphthalmia-associated transcription factor (*Mitf*), essential

for initiation of melanogenesis. Meanwhile PAX3 simultaneously represses other melanogenic differentiation genes, such as dopachrome tautomerase (*Dct*), thereby maintaining melanoblasts in an early pre-differentiated state (Lang *et al.*, 2005). Similar to the process of myogenic stem cell differentiation, PAX3-expressing melanoblasts remain undifferentiated until PAX3-mediated repression is relieved by beta-catenin signaling that it permits melanocyte differentiation(Lang *et al.*, 2005).

It is important to emphasize that PAX3 expression is necessary for the initial commitment toward differentiation and that PAX3 downregulation is also necessary for terminal differentiation. Levels of PAX3 protein are regulated by ubiquitination and proteasomal degradation. Remarkably, one amino acid (lysine 475) at the C-terminal region of PAX3 appears to be critical, rendering PAX3 susceptible to ubiquitination and subsequent proteasomal degradation (Boutet *et al.*, 2007).

The *PAX3* gene has been termed the "Pan" gene (after the Greek god Pan - or the fictional character, Peter Pan) because of ability of *PAX3* to orchestrate cell fate commitment while simultaneously preventing differentiation (Lang *et al.*, 2005).

PAX3 contributes to stem cell properties:

Stem cells are defined by both their self-renewal properties and their ability to give rise to differentiated progeny. PAX3 expression is characteristic of at least two populations of progenitor cells. Skeletal muscle progenitor (satellite) cells have been isolated by flow cytometry from *Pax3GFP/+* mice (Montarras *et al.*, 2005). Satellite cells are the major myogenic progenitor cell population and can efficiently carry out skeletal muscle repair and also undergoes self-renewal (Montarras *et al.*, 2005). In addition, PAX3 is expressed by putative melanocyte stem cells within the hair follicle. These cells are pluripotent and exhibit self-renewal (Real *et al.*, 2006).

1.4.3.5 PAX3 expression in cancer

PAX3 expression has been reported in sarcomas such as embryonal rhabdomyosarcoma (ERMS) (Bernasconi *et al.*, 1996), alveolar rhabdomyosarcoma (ARMS)(Barr *et al.*, 1993), and Ewing sarcoma (Schulte *et al.*, 1997). In addition, PAX3 is expressed in some neural-crest-derived tumors including melanomas (Scholl *et al.*, 2001) and neuroblastomas (Barr *et al.*, 1999).

ARMSs are characterized by chromosomal translocations involving juxtaposition of *PAX3* (or PAX7*)* and the forkhead transcription factor gene, *FKHR*. These translocations are associated with t(2;13) and yield a chimeric *PAX3–FKHR* fusion protein in 55–73% of cases. However, ERMS may also show increased *PAX3* (or *PAX7*) expression in the absence of the PAX3–FKHR chimeric protein (Bernasconi *et al.*, 1996). PAX3 is expressed in primary melanomas (Scholl *et al.*, 2001). In addition, PAX3 expression in sentinel lymph nodes indicates poor prognosis in patients with melanoma (Takeuchi *et al.*, 2004).

It is important to mention that certain PAX3 isoforms are preferentially expressed in certain tumor cell types. For example PAX3c and PAX3d are predominantly expressed in melanoma and small-cell lung cancer. PAX3d protein was noted in some melanoma patients, indicating that PAX3d is a melanoma-specific isoform while PAX3g and PAX3h isoforms predominate in neuroblastomas (Kwang *et al.*, 2002). Incidentally, the expression of PAX3a, PAX3b and PAX3e are low or undetectable in these tumors (Wang *et al.*, 2007). Overall, the PAX3d protein is the predominant isoform expressed in cancer (Wang *et al.*, 2007).

1.4.3.6 Function in cancer

Cell survival:

Inhibition of PAX3 expression with antisense *PAX3* oligonucleotides, triggers apoptosis in either ERMS or melanoma cell lines (Bernasconi *et al.*, 1996; Scholl *et al.*, 2001), suggesting that PAX3 is required for canc(Wang *et al.*, 2006)er cell survival (He *et al.*, 2005). PAX3 and PAX3–FKHR proteins activate transcription of the anti-apoptotic gene, *BCL-XL* (Margue *et al.*, 2000). Like PAX2, PAX3 also activates the Akt pathway by inhibiting PTEN (Li *et al.*, 2007). In melanocytes, the isoforms PAX3c, PAX3d, PAX3g and PAX3h showed a protective effect against basal or etoposide induced apoptosis in vitro(Wang et al., 2006).

Cell proliferation:

Growth rate is increased growth rate in melanocytes transfected with PAX3c, PAX3d and PAX3h compared to control cells (Wang *et al.*, 2006). An interaction between PAX3 and the retinoblastoma tumor suppressor Rb have been suggested and could provide a molecular link between PAX3 and control of the cell cycle(Wang *et al.*, 2006; Wiggan *et al.*, 1998).

Cell migration:

PAX3 in sentinel lymphe node has been validated as a bad prognosis factor and metastatic disease (Takeuchi *et al.*, 2004). In vitro scratch assays showed that PAX3c, PAX3d and PAX3h increased melanocyte migration (Wang *et al.*, 2006). Activation of MET receptors by PAX3 may be responsible for increased cellular migration and metastasis.

Tumorigenicty:

In anchorage-independent growth assays, PAX3c, PAX3d, PAX3g or PAX3h expression in melanocytes confer the ability to grow in soft agar, whereas PAX3a-, PAX3b-, PAX3e-expressing melanocytes and vector control cells fail to form colonies. This suggests that PAX3 expression may transform cells. However, *in vivo* there is still no evidence that PAX3 is sufficient for tumorigenesis. It has been suggested that Pax3 overexpression might not be responsible tumorigensis itself but instead account for the acquisition of characteristics that define malignancy (Robson *et al.*, 2006).

1. 5 Research aims

The aim of my doctoral work has been to refine the understanding of PAX gene function during kidney development and to test the hypothesis that PAX genes may be used as potential therapeutic targets in renal cancer.

During normal kidney development, PAX2 exerts a powerful anti-apoptotic function in epithelial structures but its expression is strongly attenuated during the post-natal period. On the other hand, PAX2 expression is observed in all subtypes of renal cell carcinoma (RCC). I hypothesized that the anti-apoptotic function of PAX2 is highjacked by renal carcinoma cells and contributes to their resistance to chemotherapy. My specific aim is to demonstrate that PAX2 overexpression in renal cancer cells confers resistance to apoptosis induced by cisplatin and to show that inhibition of PAX2 sensitizes RCC cells to cisplatin-induced apoptosis. A second aim is to develop an *in vivo* model of subcutaneous RCC tumours in nude mice to test the proof of principal that PAX2 knockdown increases the effect of cisplatin therapy.

Until recently, *PAX2* and *PAX8* were considered to be the only *PAX* genes expressed in the developing kidney. However Englenka and colleagues unexpectedly identified transcriptional activity of the *Pax3* promoter in urogenital derivatives of the embryonic mouse. Although these observations suggest that *PAX3* is expressed during normal kidney development it could also be due to artificial reporter signal in the transgenic mice. Hence my third specific aim has been to characterize the pattern of PAX3 expression in fetal mouse kidney embryo and to determine whether it may be relevant to the fate of a specific cell lineage.

Since PAX3 is known to regulate cell fate of migrating myoblasts during normal muscle development, I hypothesized that it might play an important role in Wilms tumor with a myogenic phenotype. PAX3 has been implicated in other cancers such as rhabomyosarcoma but has never been investigated in Wilms tumors in the past. My final specific aim has been to examine PAX3 expression in a panel of Wilms tumor tissues and develop insight into how it might contribute to the tumor phenotype.

CHAPTER II: PAX2 as a therapeutic target for renal cancer

PAX2 as a therapeutic target for renal cancer

2.1 Overview:

All major subtypes of Renal Cell Carcinoma (RCC) express PAX2; the level of PAX2 protein correlates with aggressive tumour behaviour and increased proliferation index. For patients with RCC, an effective therapeutic strategy remains elusive due to the resistance of this cancer to current chemotherapeutic agents.

Part I: *PAX2* inactivation enhances cisplatin-induced apoptosis in renal carcinoma cells.

The first part of this work demonstrates that PAX2 expression confers apoptosis resistance of renal cell carcinoma cells to cisplatin. The central hypothesis is that PAX2 expression contributes to the resistance of Renal Cell Carcinoma to chemotherapy. We show that inhibition of *PAX2 in vitro* sensitized RCC cells to cisplatin-induced apoptosis. These findings have been published in Kidney International in April 2006.

Part II: *In Vivo* validation of *PAX2* as a target for renal cancer therapy.

Building on our *in vitro* finding we demonstrate *in vivo* that silencing of PAX2 gene expression in RCC cells enhances cisplatin-induced apoptosis and inhibits growth of subcutaneous RCC xenografts in nude mice. This last part of my work has been published in Cancer Letters in April 2008.

PAX2 inactivation enhances cisplatin-induced apoptosis in renal carcinoma cells

Pierre-Alain Hueber, Paula Waters, Patsy Clark, Michael Eccles and Paul Goodyer

Kidney International (2006) 69, 1139–1145

2.1.1 ABSTRACT

Human embryonic kidney 293 cells transfected with a *PAX2* expression vector and exposed to cisplatin (40 μM) exhibited 45+/-15% as much caspase-3 cleavage compared to control cells. Conversely, murine collecting duct cells stably transfected with *PAX2* antisense cDNA had twofold increase in cisplatin-induced apoptosis. Murine fetal (embryonic day 15) kidney explants from *Pax2*^{1Neu}+/- mice exposed to cisplatin (25 μM x24 h) had 50% increased apoptosis (terminal deoxynucleotidyl transferase-mediated dUTP nick-end labeling staining). We then show that RCC cells (CAKI-1 (human, Caucasian, kidney, carcinoma) and ACHN (human, Caucasian, kidney, adenocarcinoma)) express PAX2 protein. *PAX2*-small interfering RNA (100nM) reduces endogenous PAX2 protein (10% of baseline) and induces apoptosis (Annexin-V staining). PAX2 knockdown sensitized RCC cells to cisplatin-induced apoptosis, killing 50–60% of cisplatin-resistant ACHN and CAKI-1 cells. These findings suggest that PAX2 confers resistance to cisplatin-induced apoptosis in non-transformed kidney cells and fetal kidney explants. Similarly, PAX2 overexpression in RCC cells contributes to cisplatin resistance. Conceivably, a therapeutic strategy that inactivates PAX2 *in vivo* might enhance the efficacy of conventional cytotoxic drugs against RCC.

2.1.2 INTRODUCTION

It is estimated that over 30,000 people in the United States have renal cell carcinoma (RCC); over 10,000 RCC-related deaths occur each year [1]. Only 40% of patients have disease confined to the kidney at the time of diagnosis and nearly 25% of patients present with symptoms of metastatic lesions. With current therapy, the one-year survival of patient with metastatic RCC is less than 50% [2]. This resistance of RCC to conventional medical therapy remains the primary obstacle to survival and makes the development of new therapeutic strategies imperative.

Cisplatin is among the most widely used and most effective chemotherapeutic agents for many types of human cancer. Cisplatin is thought to act through direct binding to DNA causing cisplatin-DNA adducts. If cisplatin-DNA adducts are not efficiently processed by the cellular repair mechanism, the pathway of programmed cell death is initiated [3]. Molecular mechanisms, which subvert these pro-apoptotic signals, are thought to account for resistance of tumours to chemotherapy [4,5].

In some malignancies, resistance to apoptosis has been attributed to overexpression of genes encoding endogenous inhibitors of apoptosis (IAPs) [6-8], but the specific cause for the high resistance of RCC to therapy is unknown.

During normal kidney development, the transcription factor, *PAX2*, is expressed both in the ureteric bud and mesenchymal cell lineages. We have recently shown that *PAX2* functions to suppress programmed cell death during nephrogenesis; PAX2 gene mutations cause increased apoptosis of ureteric bud cells with resultant renal hypoplasia [9-12]. Once nephrogenesis is complete, however, renal PAX2 expression is rapidly downregulated and is barely detectable in the mature kidney. On the other hand, PAX2 is inappropriately re-expressed in a variety of cancers -- particularly in renal cell carcinoma [13-15].

Thus, the powerful anti-apoptotic function of PAX2 might contribute to the resistance of renal cell carcinoma cells to chemotherapy. If so, inhibitors of PAX2 expression might enhance programmed cell death in RCC, enhancing the efficacy of chemotherapeutic agents such as cisplatin.

In this report, we demonstrate that transfection of *PAX2* cDNA into a human fetal kidney cell (HEK293) line confers resistance to cisplatin-induced apoptosis. Conversely, we show that inhibition of PAX2 using antisense cDNA enhances cisplatin-induced apoptosis of a murine collecting duct cell (IMCD) and that cisplatin-induced apoptosis is increased in fetal kidney explants from heterozygous *PAX2*^{1Neu} mutant mice. Similarly, we show that small interfering RNAs (siRNA) can be used to inhibit PAX2 expression in two RCC cell lines (ACHN and Caki-1) derived from clear cell carcinomas and that *PAX2* siRNA enhances apoptosis and cell death of cisplatin-resistant RCC cells.

2.1.3 RESULTS

2.1.3.1 PAX2 confers resistant to cisplatin-induced apoptosis in non-transformed kidney cells

To evaluate whether PAX2 inhibits cisplatin-induced apoptosis in human fetal kidney cells, we stably transfected the HEK293 cell line with an expression vector containing full-length human *PAX2b* cDNA (or empty vector as control). Endogenous PAX2 protein was not detectable in HEK293 cells transfected with the empty expression vector or in the parental HEK293 cell line. However, as shown in **Figure 2.1.1A**, PAX2 protein was highly expressed in the HEK-293/PAX2 transfectants, providing an opportunity to examine the effects of aberrant PAX2 overexpression on cell survival.

HEK293/PAX2 and control HEK293 cells were exposed to cisplatin (40μM) and assayed for activation of caspase-3 at 24 hours. HEK293/PAX2 cells exhibited only 45% as much caspase-3 activation as controls in response to cisplatin **(Figure 2.1.1B).**

2.1.3.2 Reduced endogenous PAX2 expression increases susceptibility to cisplatin-induced apoptosis in renal collecting duct cells

To examine the effect of PAX2 inactivation on susceptibility to apoptosis, we utilized a cell line (IMCD) derived from murine renal collecting duct. IMCD cells were chosen because the collecting duct lineage is known to express high levels of endogenous PAX2 protein **(Figure 2A).** IMCD cells were stably transfected with a CMV-driven expression vector containing a full-length antisense *hPAX2b* cDNA. Stable transfectants (IMCD/PAX2-AS) showed significant reduction of Pax2 protein levels (30% of controls) **(Figure 2.1.2A**). These cells were cultured in the presence or absence of 40μM cisplatin and assayed for caspase-3 activation after 24 hours. In preliminary dose-response studies, we found that caspase-3 activation (cleavage) at 24 hours climbs with increasing cisplatin concentration, peaks at 40μM and then falls off at higher concentrations as cell necrosis

ensues (data not shown). In the absence of cisplatin, low basal levels of apoptosis were equivalent in IMCD/PAX2-AS and control IMCD cells. However, in the presence of cisplatin (40μM), activation (cleavage) of caspase-3 was twofold higher in IMCD/PAX2-AS transfectants compared to control IMCD cells **(Figure 2.1.2B).**

2.1.3.3 Reduced PAX2 expression in heterozygous mutant (Pax^{1Neu}) mice increases susceptibility of fetal kidney explants to cisplatin

To demonstrate that genetically reduced Pax2 expression increases apoptosis induced by cisplatin, whole fetal kidneys (E15) were isolated from wildtype and heterozygous mutant *PAX2*^{1Neu} mice and placed in explant culture as previously described [12]. Following exposure to cisplatin (25μM) for 24h, explants were processed for TUNEL immunohistochemistry. Untreated apoptosis in wildtype explants was only slightly lower than E15 *Pax2*^{1Neu} kidney explants (**Figure 2.1.3**). However, in the presence of cisplatin, the intensity of TUNEL staining per unit cross-sectional area was increased 9-fold above the untreated baseline in mutant explants, compared to an increase above baseline of only 5-fold in wildtype explants ($p<0.01$, mutant vs wildtype) (**Figure 2.1.3**).

Figure 2.1.1.PAX2 expression confers resistance to cisplatin-induced apoptosis.

Human embryonic kidney cells (HEK293) lacking endogenous PAX2 were stably transfected with hPAX2 cDNA to generate the HEK293/PAX2 cell line with elevated PAX2 protein expression (A). HEK293 control and HEK293/PAX2 cell lines were exposed to cisplatin (40μM) and assessed for caspase-3 activation (cleavage) at 24h (B). Bar graphs represent the mean and SD of three experiments (each experiment was performed in triplicate); HEK293/PAX2 versus HEK293 control, * $p < 0.01$.

A

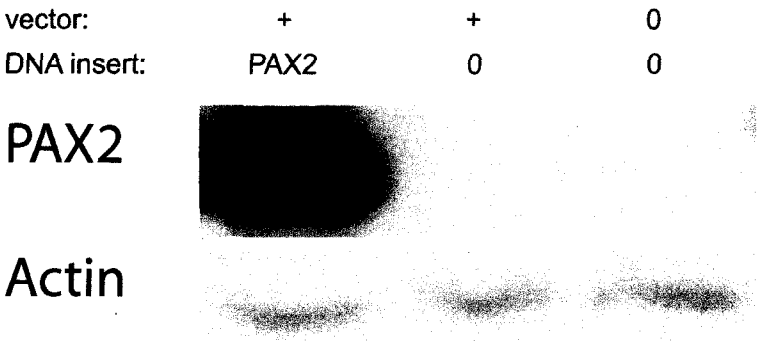
vector: + + 0
DNA insert: PAX2 0 0
PAX2
Actin

B

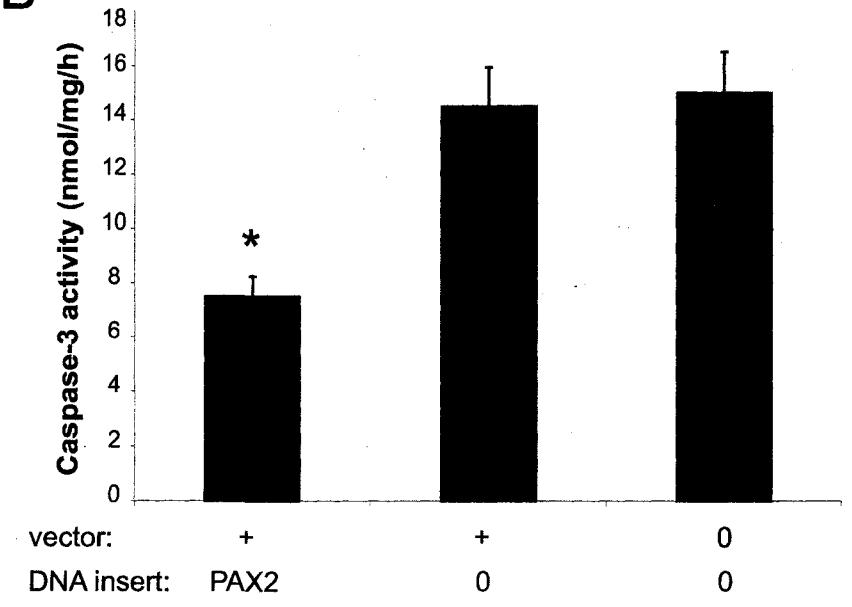
Caspase-3 activity (nmol/mg/h)
18
16
14
12
10
8
6
4
2
0
*
vector: + + 0
DNA insert: PAX2 0 0

Figure 2.1.2. Reduced PAX2 expression sensitizes IMCD cells to cisplatin.

IMCD cells were stably transfected with a vector containing a full-length antisense hPAX2b cDNA. Stable transfectants (IMCD/PAX2-AS) (third lane) had reduced levels of PAX2 protein compared to untransfected IMCD cells (first lane) or IMCD/empty vector cells (second lane) by Western immunoblotting (A). The cells were treated with cisplatin (40μM). The sensitivity to cisplatin-induced apoptosis was assessed by assay of caspase-3 activation (cleavage) at 24h (B). The bar graph represents the mean and SD of three experiments (each experiment was performed in triplicate); IMCD/PAX2-AS versus IMCD control, *$p < 0.01$.

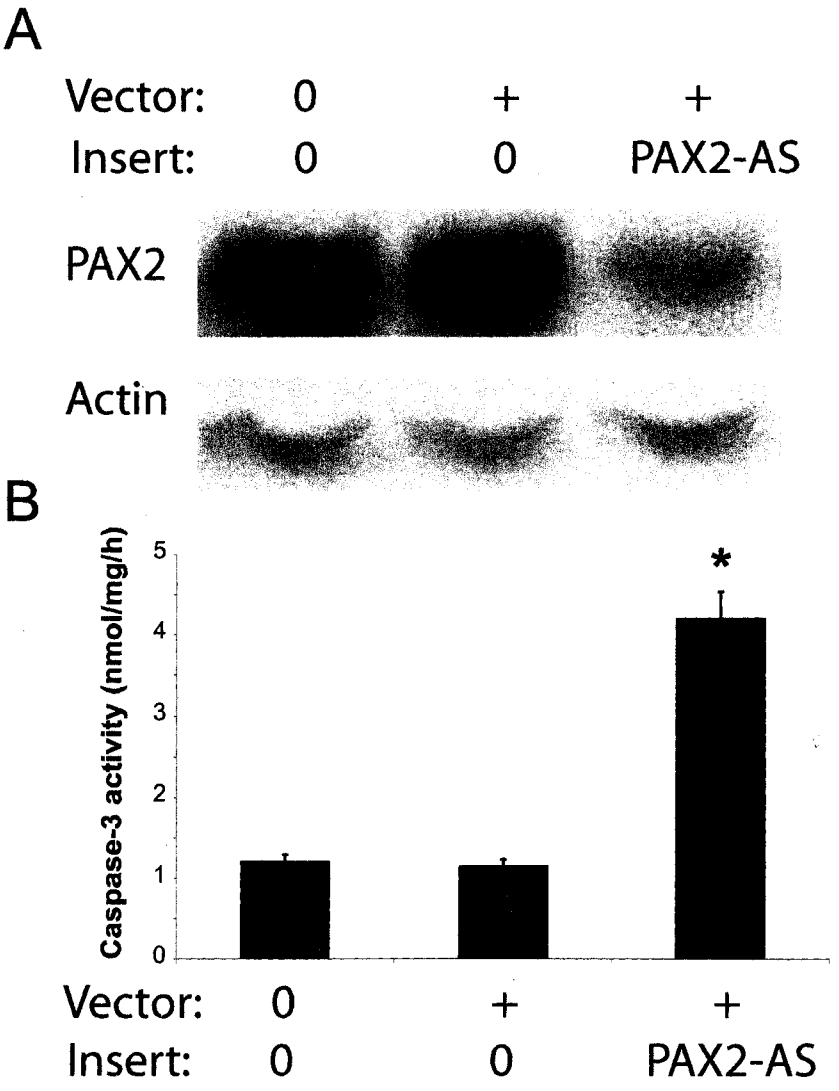
A
Vector: 0 + +
Insert: 0 0 PAX2-AS
PAX2
Actin
B
Caspase-3 activity (nmol/mg/h)
0
1
2
3
4
5
*
Vector: 0 + +
Insert: 0 0 PAX2-AS

Figure 2.1.3. Genetic reduction of PAX2 increases susceptibility to cisplatin-induced apoptosis.

Whole fetal kidneys were microdissected from E15 $Pax2^{1Neu}$ mutant (N=18 kidneys) and wildtype (N=10 kidneys) mice and cultured at 37°C for 30h. Half of the explants from each group were treated with cisplatin (25μM) in the culture medium for 24h. Apoptosis was measured by TUNEL-staining and quantified using Northern Eclipse software (staining intensity per mm^2). Cisplatin caused a 9-fold increase in apoptosis in the $Pax2^{1Neu}$ explants, but only a 5-fold increase in wildtype explants (*$p<0.01$).

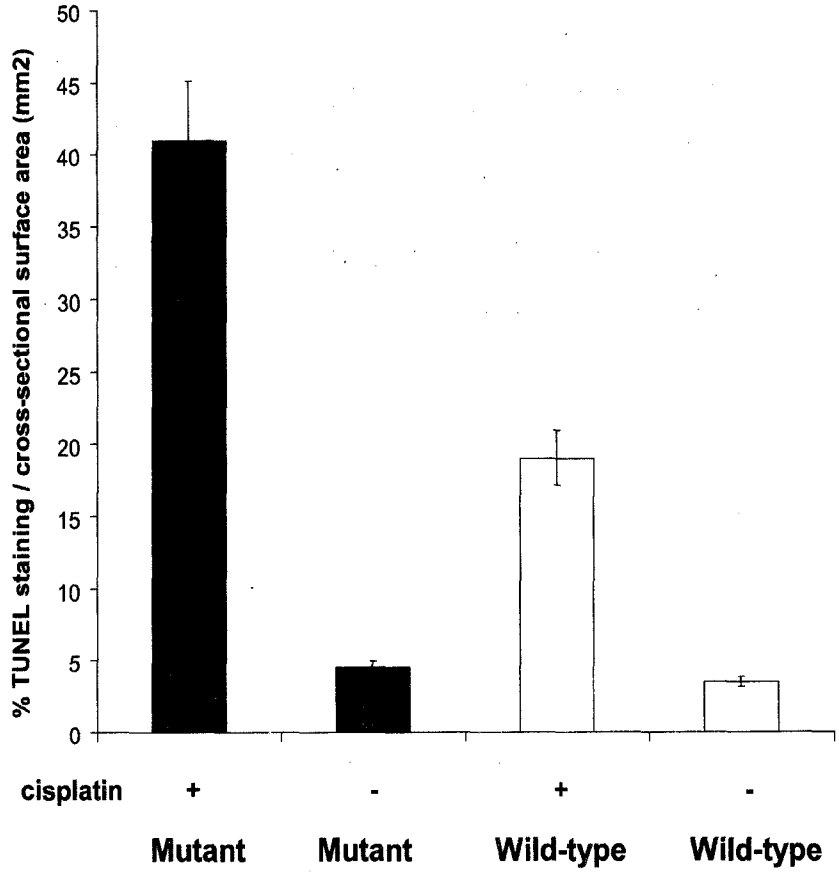
% TUNEL staining / cross-sectional surface area (mm2)
50
45
40
35
30
25
20
15
10
5
0
cisplatin
+
-
+
-
Mutant
Mutant
Wild-type
Wild-type

2.1.3.4 SiRNA-inactivation of endogenous PAX2 induces apoptosis in RCC cells

To demonstrate endogenous PAX2 expression in RCC cells, we assessed the 43-kDa PAX2 protein band intensity on Western immunoblots of ACHN and CAKi-1 cell lines derived from human clear cell carcinomas. Both cell lines exhibited high levels of endogenous PAX2 protein **(Figure 2.1.4A/B).**

In order to inhibit endogenous PAX2 protein expression, the cells were exposed to a pool of four *PAX2* siRNAs (25nM each) for 24h or 48h. PAX2 protein levels fell progressively with increased exposure time and by 48 hours were nearly undetectable in CAKI-1 cells and reduced to 15% of baseline in ACHN cells. (Fig.4A/B)

To assess whether PAX2 suppression induces apoptosis in RCC cells, ACHN and CAKI-1 cells were exposed to 100nM siRNAs or control medium for 24 hours and 48h. Cells undergoing apoptosis were then detected by fluorescent annexin-V staining *in situ* 24h and 48h post transfection **(Figure 2.1.5/6)**. For CAKI-1 cells, exposure to *PAX2* siRNAs resulted in 20.5 % and 38.6% annexin (+) cells after 48 hours compared to 6.8% annexin(+) cells exposed to nonspecific control siRNAs. Similarly, ACHN cells exposed to *PAX2* siRNAs showed 15% and 31.7% annexin(+) cells at 24 and 48 hours respectively vs 5% annexin(+) cells with nonspecific control-siRNAs ($p<0.001$) **(Figure 2.1.5/6)**.The effect of PAX2 siRNAs was specific to cells expressing endogenous PAX2 since the siRNAs had no effect on survival of HEK-293 cells (data not shown).

2.1.3.5 Effect of PAX2 siRNA and cisplatin on RCC cell survival and apoptosis is additive

We examined whether PAX2 inactivation might add to the cell death caused by cisplatin exposure *in vitro*. CAKI-1 and ACHN cells were treated with *PAX2* siRNAs or control-siRNAs for 24h, followed by exposure to various doses of cisplatin (10-160 μmol/L) for a further 24h. The effect of combined treatment on cell viability was assessed at 48h as

above and expressed as a percent of untreated cells. Addition of *PAX2* siRNAs to cisplatin-treated cells significantly reduced survival of CAKI-1 cells compared to control siRNA-treated cells: 62.2% v.s 37% (cisplatin = 10μmol/L); 42.21 v.s 26.8% (cisplatin = 20μmol/L); 25.2% v.s 15.5% (cisplatin = 40μmol/L), respectively (Fig 7). Similarly, exposure of ACHN cells to *PAX2* siRNAs killed 80% vs 42.8% (cisplatin = 10μmol/L); 61.4 v.s 34.7% (cisplatin = 20μm/L) and 45% v.s 22% (cisplatin = 40μmol/L) of cisplatin-resistant cells, respectively **(Figure 2.1.7A/B).** The level of apoptosis of RCC cells in response to the combined treatment was analyzed by annexin V staining *in situ*. Treatment with cisplatin (10-40uM) plus *PAX2* siRNAs (25nM each) resulted in a percentage of cells undergoing apoptosis equivalent to the sum of the individual treatments **(Figure 2.1.7C/D)**.

2.1.3.6 Therapeutic cell death of the combined treatment with PAX2-siRNA and cisplatin is caspases dependent

To demonstrate that the effects of *PAX2*-siRNA and cisplatin on RCC cell survival are mediated by the caspase pathways of programmed cell death, we analyzed the effect of a broad caspase (caspase 3,5,7) inhibitor (Z-VAD-fmk). The combined cytotoxicity of cisplatin and PAX2-siRNAs was >90% inhibited by concurrent exposure to 25μmol/L Z-VAD-fmk **(Figure 2.1.8)**.

Figure 2.1.4. Endogenous PAX2 protein expression by CAKI-1 and ACHN renal carcinoma cells is suppressed by PAX2-siRNA.

Endogenous expression of 42kDa PAX2 protein was confirmed by Western immunoblotting for both CAKi-1 (A) and ACHN (B) RCC cell lines from the NCI60 panel. Cells were seeded at 10^5 cells/ml in 24-well plates and exposed to PAX2 siRNAs or control siRNAs (100nM) added to media with lipofectamine-2000 according to the manufacturer's protocol. PAX2 protein level was assessed by Western immunoblotting after 24h and 48h treatment.

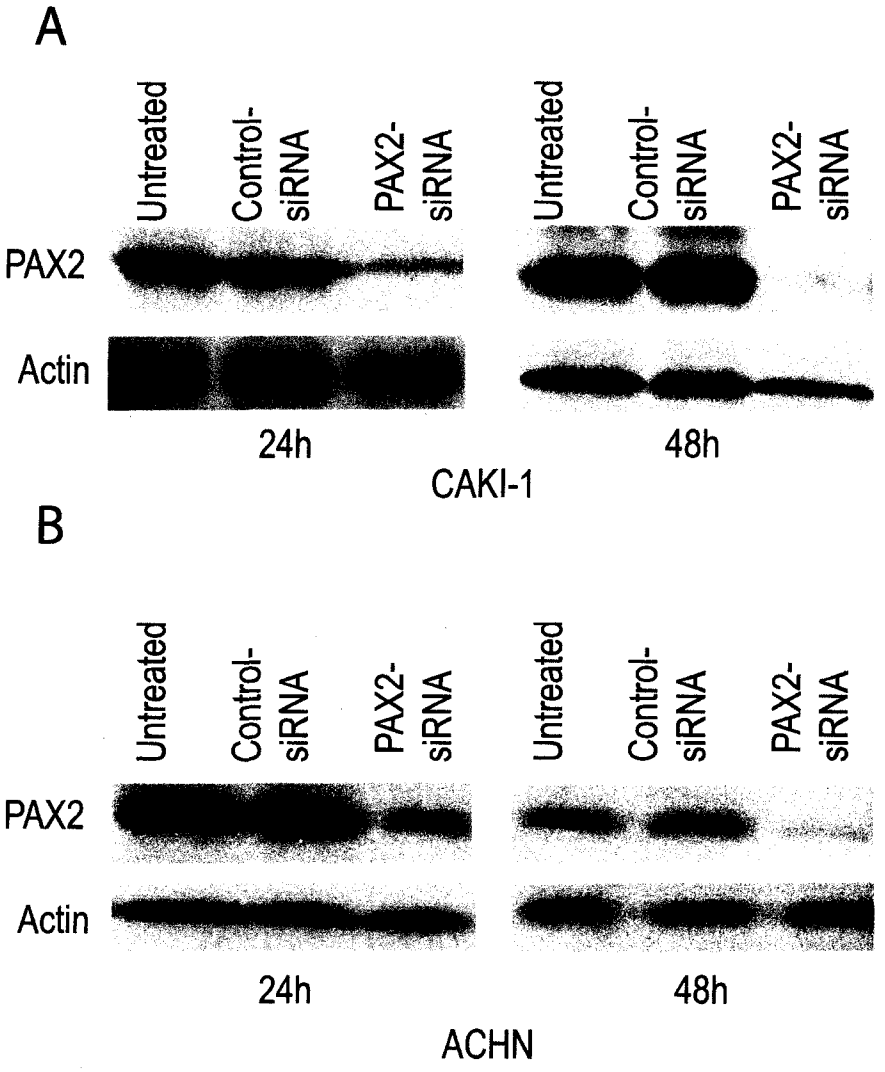
A
Untreated
Control-siRNA
PAX2-siRNA
Untreated
Control-siRNA
PAX2-siRNA
PAX2
Actin
24h
48h
CAKI-1
B
Untreated
Control-siRNA
PAX2-siRNA
Untreated
Control-siRNA
PAX2-siRNA
PAX2
Actin
24h
48h
ACHN

Figure 2.1.5. Inhibition of PAX2 induces apoptosis of Renal Cell Carcinoma cell lines.

CAKI-1 and ACHN cells were treated with 100nM *PAX2* siRNA or control siRNA (Dharmacon). Apoptosis was measured by counting the percentage of cells which were annexin-V positive after 24h and 48h. The bar graph represents the mean and SD for three experiments (each experiment was performed in triplicate); *PAX2*-siRNA versus siRNA-control, *$p < 0.01$.

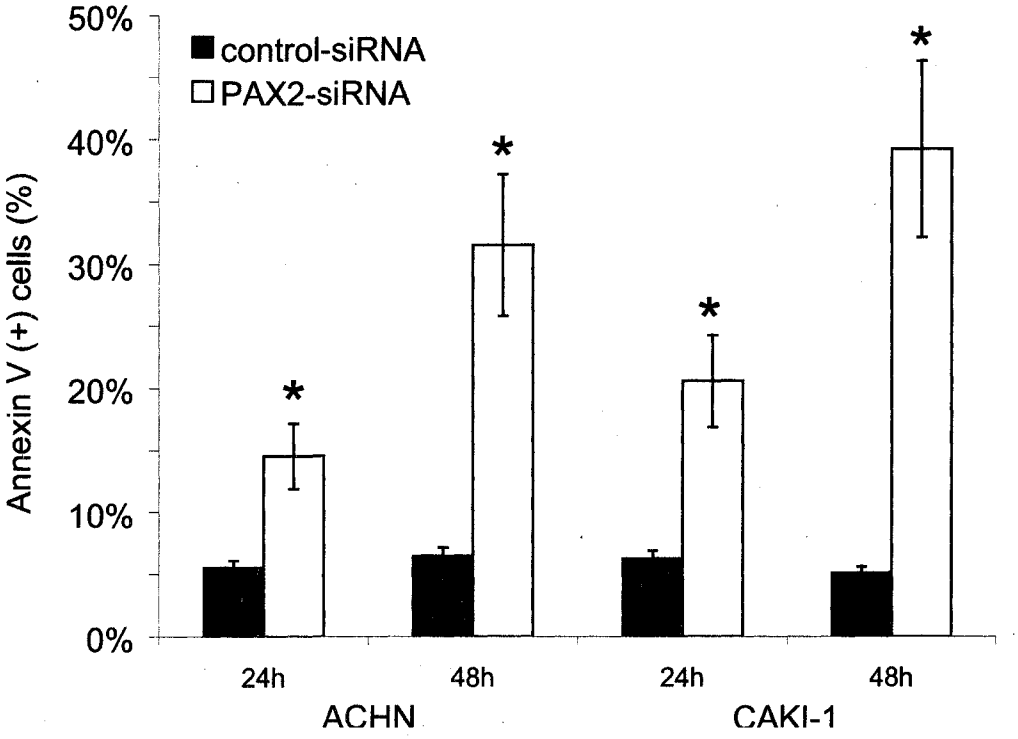
50%
40%
30%
20%
10%
0%
Annexin V (+) cells (%)
control-siRNA
PAX2-siRNA
*
*
*
*
24h
48h
24h
48h
ACHN
CAKI-1

Figure 2.1.6. Annexin V staining.

Immunocytochemical staining for annexin V in *PAX2*-siRNA treated cells vs Control-siRNA treated cells after 24h. ACHN (A) and CAKI-1 (B) were stained with anti-annexin V fluorescent (green) antibody, and with 4',6-diamidinophenylindole (DAPI) (blue).

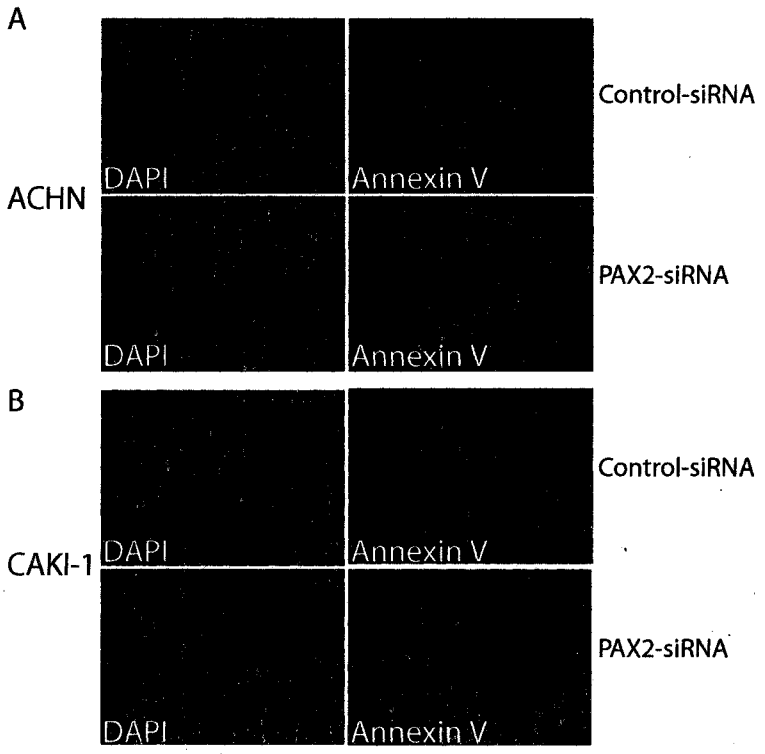
A
ACHN
DAPI
Annexin V
Control-siRNA
DAPI
Annexin V
PAX2-siRNA
B
CAKI-1
DAPI
Annexin V
Control-siRNA
DAPI
Annexin V
PAX2-siRNA

Figure 2.1.7. RCC cell death caused by PAX2 siRNA and cisplatin are additive.

The viability of CAKI-1 (A/C) and ACHN (B/D) cells was assessed after 24h of cisplatin exposure and 24h pre-treatment with *PAX2* siRNAs or control-siRNAs. Cell survival was measured by colorimetric assay of cellular dehydrogenase activity and expressed as a percentage of that in untreated cells. *PAX2*-siRNA versus siRNA-control, *$p < 0.01$.

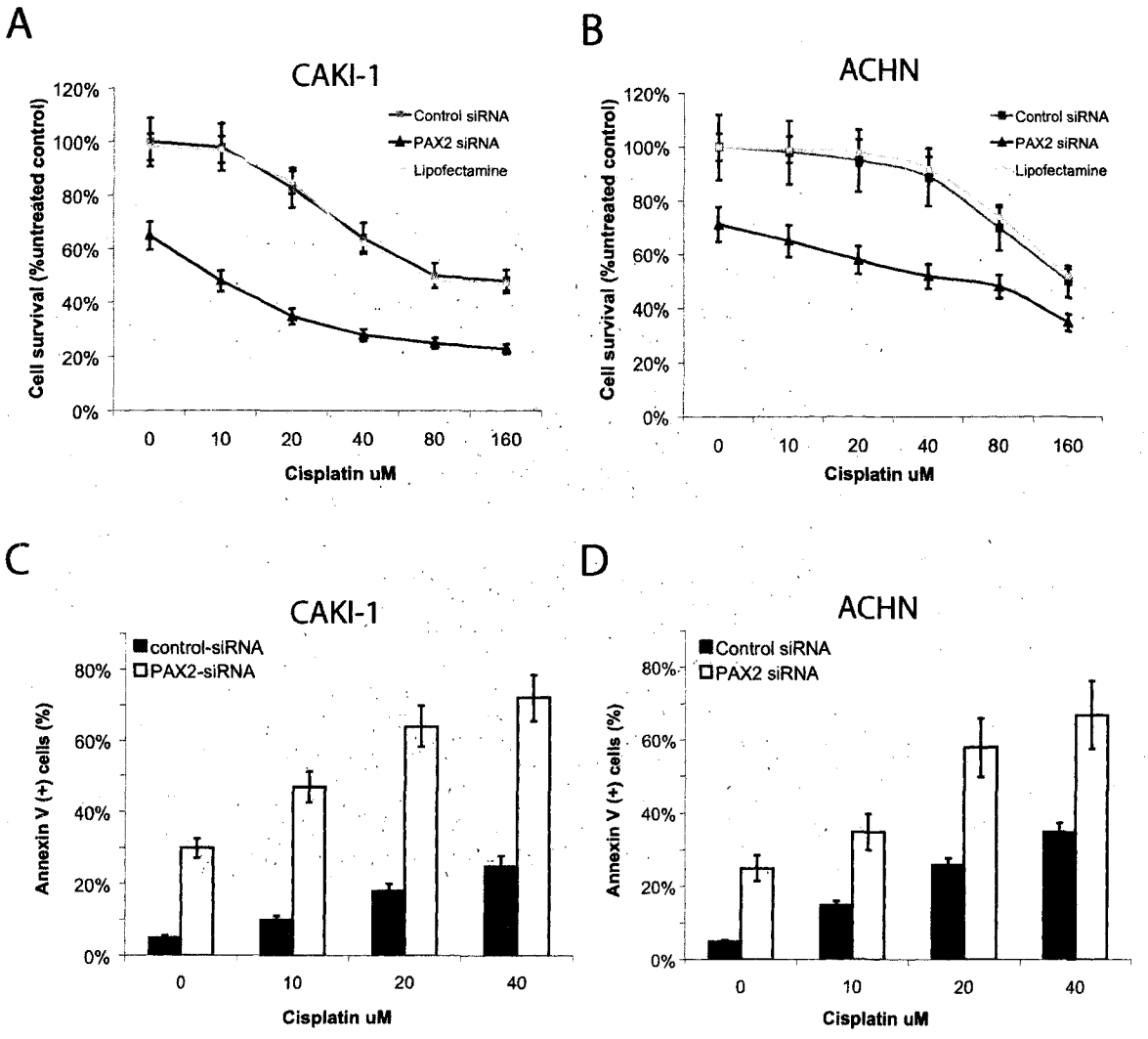
A
CAKI-1
Control siRNA
PAX2 siRNA
Lipofectamine
Cell survival (%untreated control)
120%
100%
80%
60%
40%
20%
0%
0
10
20
40
80
160
Cisplatin uM
B
ACHN
Control siRNA
PAX2 siRNA
Lipofectamine
Cell survival (%untreated control)
120%
100%
80%
60%
40%
20%
0%
0
10
20
40
80
160
Cisplatin uM
C
CAKI-1
control-siRNA
PAX2-siRNA
Annexin V (+) cells (%)
80%
60%
40%
20%
0%
0
10
20
40
Cisplatin uM
D
ACHN
Control siRNA
PAX2 siRNA
Annexin V (+) cells (%)
80%
60%
40%
20%
0%
0
10
20
40
Cisplatin uM

Figure 2.1.8. Combined killing induced by PAX2 inhibition plus cisplatin is caspase-dependent.

CAKI-1 and ACHN cells were treated with 25μM Z-VAD-fmk, a broad caspase inhibitor. After 4h, *PAX2* siRNAs or Control siRNAs were added to the media. At 24h, cells were exposed to cisplatin 30μmol/L. The effect of Z-VAD-fmk on the combined cytotoxicity of cisplatin and *PAX2*-siRNAs was measured by colorimetric assay of cellular dehydrogenase activity at 48h. For each cell line, *PAX2*-siRNA plus cisplatin significantly lowered cell survival versus siRNA-control (*$p < 0.01$) but cell survival was fully restored to control levels in the presence of Z-VAD-fmk (**$p<0.01$).

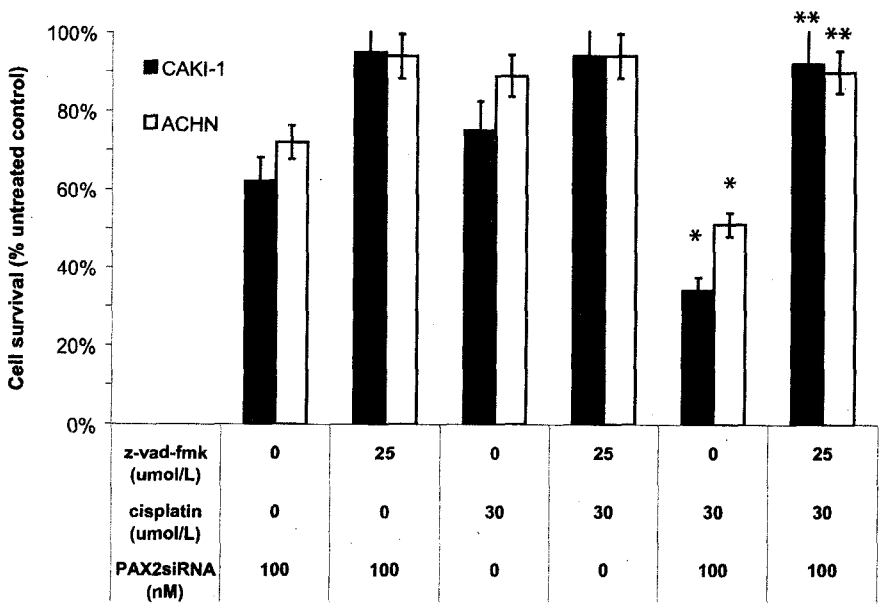
Cell survival (% untreated control)
100%
80%
60%
40%
20%
0%
CAKI-1
ACHN
*
*
*
**
**
z-vad-fmk (umol/L)
0
25
0
25
0
25
cisplatin (umol/L)
0
0
30
30
30
30
PAX2siRNA (nM)
100
100
0
0
100
100

2.1.4 DISCUSSION

We have recently shown that PAX2 suppresses apoptosis in the ureteric bud lineage during nephrogenesis [10]. By suppressing programmed cell death, PAX2 facilitates efficient branching of the ureteric bud and optimizes the final nephron number [9,12]. However, once nephrogenesis is complete, renal PAX2 expression is rapidly downregulated and is barely detectable in mature kidney [Cohen J T et al. Pediatric Academic Societies, annual meeting San-Francisco CA, abstract 3276, 2004]. In a variety of cancers - particularly in renal cell carcinomas - there is inappropriate re-expression of PAX2 [12,14,17].

Since PAX2 normally exerts a powerful anti-apoptotic function during development, we reasoned that it might have the same (but undesirable) effect on renal carcinoma cells, contributing to their relative resistance to chemotherapy (RCC).

Cisplatin has been used as an anticancer therapy for many years and its cytotoxic mode of action is primarily mediated by its interaction with DNA to form platinum-DNA adducts [5]. Cisplatin interaction with DNA induces several signal transduction pathways, including those involving p53, p73, caspases, cyclins, CDKs, pRb, PKC, MAPK and PI3K/Akt, and eventually results in the activation of apoptosis [3]. Possible mechanisms of resistance to cisplatin include reduced intracellular accumulation of cisplatin, enhanced drug inactivation and increased repair activity of DNA damage. However, since cisplatin cytotoxicity is mediated through the pathways of programmed cell death, mechanisms which block these pathways might also contribute to cisplatin resistance [3].

While PAX2 clearly suppresses basal apoptosis in developing kidney, the molecular mechanism underlying this phenomenon is not yet known. To determine whether the developmental effects of PAX2 can be generalized to cisplatin-induced apoptosis, we transfected human fetal kidney cells with a *PAX2* expression vector in the presence or absence of cisplatin. PAX2 was as effective in suppressing apoptosis associated with cisplatin exposure as it is in other settings [10]. Similarly, we were able to show a

protective effect of PAX2 on cisplatin-induced apoptosis in normal murine fetal kidney explants. Other investigators have reported that PAX2 enhances resistance of endothelial cells to vincristine-induced apoptosis [18]. Taken together, these observations suggest that PAX2 influences core components of the programmed cell death pathway in normal cells, independent of the pro-apoptotic stimulus.

We identified significant levels of Pax2 protein in RCC cell lines (CAKI-1 and ACHN). Initial efforts to inhibit *PAX2* with antisense oligonucleotides were met with limited success. However, we found that *PAX2* RNAi powerfully inhibited Pax2 protein expression and significantly increased basal apoptosis in RCC cells. Furthermore, 1/3 of RCC cells resistant to cisplatin were killed by exposure to the PAX2 siRNA. Our results extend previous observations suggesting that PAX2 affects basal RCC cell survival *in vitro* [17].

Recently, direct infusion of siRNA into the tail vein of mice selectively inhibited renal Fas protein and mRNA expression and Fas-mediated apoptosis following ischemic injury to the kidney [19]. Similarly it has been shown that injection of siRNA into the jugular vein could functionally silence vasopressin V2 receptors in the mouse kidney [20]. It is conceivable, therefore, that a *PAX2* siRNA could be delivered successfully into the kidney *in vivo*. Although PAX2 function is critical during embryogenesis, PAX2 levels fall to nearly undetectable levels in normal adult kidney. Thus, PAX2 inhibition should preferentially affect cancer cell viability with minimal or no effect on normal adult tissue.

RCC cells are relatively resistant to programmed cell death but the molecular mechanism is not well understood. Recent studies indicate that neither Bcl-2 nor Bax-α expression influence progression of RCC. On the other hand, the level of an endogenous caspase inhibitor, XIAP, correlates with decreased patient survival of patients with clear cell carcinoma, suggesting a possible role for this family of molecules [21-26]. Interestingly, preliminary observations by Dziarmaga *et al* suggest that PAX2 may activate transcription of another IAP, the neural apoptosis-inhibitory protein (NAIP) [Dziarmaga A et al. *Proceedings, International Pediatric Nephrology Association Workshop,*

Adelaide, p64, 2004], but the importance of NAIP in regulation of renal cell apoptosis has not been established.

PAX2 expression is aberrantly re-expressed in a variety of cancers including prostate, breast, leukemia and Wilms tumor [27-32]. In adults, all major subtypes of renal cell carcinoma express PAX2 and the level of PAX2 protein correlates with aggressive tumour behaviour and increased proliferation index [3,15]. This observation suggests PAX2 could also serve as a prominent tumor marker for patient with renal cell carcinoma and as a potential candidate for targeted molecular therapy for a variety of non-renal cancers.

For patients with renal cell carcinoma, an effective therapeutic strategy remains elusive. The overall response rate of RCC patients to current anticancer agents (including cisplatin) is only 10-20% [5]. Our findings suggest that strategies to inactivate aberrant PAX2 expression in tumour tissue might be used in combination with standard anticancer drugs to enhance therapy of RCC.

ACKNOWLEDGEMENTS

The authors would like to acknowledge the help of Dr. Massoud Dharma (McGill Department of Chemistry for synthesis of *PAX2* antisense oligodinucleotides. PA Hueber was supported by a Montreal Children's Hospital Research Institute Studentship; P Goodyer is a recipient of a James McGill Research Chair. The work was supported by MedTech Partners Inc., by the Canadian Institutes of Health Research (MOP 12954) and by the Kidney Foundation of Canada.

2.1.5 METHODS

Cell culture

The two human RCC cell lines (ACHN and CAKI-1 cells) selected from the NCI-60 cancer cell panel, were obtained from the American Type Culture Collection (Rockville, MD) and maintained as adherent monolayer cultures in RPMI culture medium (Life Technologies,Carlsbad CA), supplemented with 10% fetal bovine serum (Life Technologies).

SiRNA mediated inactivation of PAX2

RCC cells were transfected with a commercially available pool of 4 double-stranded small interfering RNAs (siRNAs) targeting PAX2 (siPAX2$^{smart\ pool}$ Dharmacon cat # M-003307-00-05) mRNA (Accession NM_000278) or a pool of control siRNAs (siControl Dharmacon cat # D-001206-13-20).All siRNAs were duplexed, desalted, 2' deprotected and purified (>80%) by Dharmacon Inc. (Dharmacon, CO, USA). Cells were seeded at 10^5 cells/ml in 24-well plates. PAX2 siRNAs or the control siRNAs (100nM) were added to media using a lipophilic transfection reagent according to the manufacturer's protocol (Lipofectamine 2000, Invitrogen Inc., Carlsbad, CA, USA).

Western Immunoblotting

A total of 30 μg of protein extracted from each transfected cell population was resolved on 10% sodium dodecyl sulfate-polyacrylamide gels 100V for 1.5 h at 4°C, and then transferred over 1 hour at 100V (4°C) onto polyvinylidene difluoride membranes (Bio-Rad,Mississauga ON). Blots were probed with polyclonal anti-PAX2 antibody (Zymed, San Francisco, CA) followed by anti-rabbit IgG secondary antibody and detected with an enhanced chemiluminescence detection system (Amersham, Piscataway, NJ). Membranes probed for PAX2 were reprobed for ß-actin (Oncogene Research Products, San Diego, CA) to normalize for loading differences and to allow comparisons between transfected and untransfected cell populations. Band intensities were quantified using an image acquisition system (Imaging Research, St. Catharines ON).

Stably transfected cell lines

HEK293/hPAX2 cells were stably co-transfected with a neomycin resistance vector and a CMV-driven expression plasmid containing the full-length human PAX2b cDNA as previously described [16]. IMCD cells, derived from the murine collecting duct lineage, were co-transfected with a neomycin resistance vector and a CMV-driven expression vector containing a full-length antisense human PAX2b cDNA. Stably transfected clones were selected in media containing neomycin.

Culture of whole fetal kidney explants

Kidneys were microdissected from wildtype and heterozygous mutant $PAX2^{1Neu}$ E15 embryos and cultured at 37°C as previously described [9,12]. These mice express about half the normal amount of Pax2 protein in fetal kidney [9,12]. At the end of the 30 hours culture period, explants were fixed in 4% formaldehyde for 1 hour and then transferred to 60% ethanol.

TUNEL staining

The *in situ* cell death detection POD kit (Roche Diagnostics, Laval, QC) was used to detect apoptosis by terminal deoxynucleotidyl transferase-mediated dUTP nick-end labelling (TUNEL) in serial sagital sections of paraffin-embedded wild-type and $PAX2^{1Neu}$ mutant kidneys as previously described [12]. TUNEL-stained sections of fetal mouse kidney were examined by light microscopy and Spot Advanced digital imaging software. The images obtained (magnification 40x) were analyzed using Northern Eclipse software to generate a value representing the percent of TUNEL (+) cells per cross-sectional surface area (mm^2) covered by a user-defined threshold of TUNEL staining intensity. All quantification of apoptosis was done blindly and without knowledge of the genotype or treatment status.

Caspase-3 assay

The caspase-3 substrate Ac-DEVD-AFC (BD Pharmingen San Jose, CA) was used in caspase-3 assays according to the manufacturer's instructions. 100 μg of cell lysate was added to the reaction buffer (20 mM HEPES, pH 7.4, 100 mM NaCl, 10 mM dithiothreitol, 0.1% CHAPS, 10% sucrose) containing 125 μM of Ac-DEVD-AFC in a 1ml cuvette. Fluorescence of the cleavage product was measured using a Luminescence Spectrometer LS50 (Perkin Elmer Fremont, CA).

Annexin-V staining

The percentage of cells undergoing programmed cell death was measured by double staining with fluorescein-conjugated annexin V and DAPI. Cells were washed and exposed to a solution containing 20 μl of Annexin-V-Fluos (Roche Diagnostic Systems, Mannheim Germany) according to the manufacturer's protocol. The cells were then washed and exposed to DAPI (1ug/ml) (Roche Diagnostic Systems, Mannheim, Germany) for 15 minutes at 37°C. The percentage of annexin(+) cells were determined with a fluorescence microscope (Axioscope; Zeiss, Jena, Germany).

Cell viability assay

The cell viability kit (CCK-8, Dojindo Molecular Technologies Inc, Gaithersburg, MD) was used according to the manufacturer's protocol. Z-VAD-fmk was obtained from Calbiochem (Darmstadt, Germany).

Statistical analysis

Each experiment has been repeated 3 times. Means and SD have been calculated for all the independent experiments. In each experiment, differences in means were tested for significance using the Student t-test.

REFERENCES:

1. Chow WH, Devesa SS, Warren JL, *et al.*: Rising incidence of renal cell cancer in the United States. *Jama* 281:1628-1631, 1999

2. Motzer RJ, Russo P: Systemic therapy for renal cell carcinoma. *J Urol* 163:408-417, 2000

3. Siddik ZH: Cisplatin: mode of cytotoxic action and molecular basis of resistance. *Oncogene* 22:7265-7279, 2003

4. Shiina H, Igawa M, Breault J, *et al.*: The human T-cell factor-4 gene splicing isoforms, Wnt signal pathway, and apoptosis in renal cell carcinoma. *Clin Cancer Res* 9:2121-2132, 2003

5. Eastman A (1999). *The mechanism of action of cisplatin: from adducts to apoptosis*, in *Cisplatin. Chemistery and Biochemistry of a Leading Anticancer Drug* (Bernhard Lippert ed). Wiley-VCH, Basel, pp 111-134.

5. Qi H, Ohh M: The von Hippel-Lindau tumor suppressor protein sensitizes renal cell carcinoma cells to tumor necrosis factor-induced cytotoxicity by suppressing the nuclear factor-kappaB-dependent antiapoptotic pathway. *Cancer Res* 63:7076-7080, 2003

6. Ramp U, Krieg T, Caliskan E, *et al.*: XIAP expression is an independent prognostic marker in clear-cell renal carcinomas. *Hum Pathol* 35:1022-1028, 2004

7. Marshall FF: XIAP expression is an independent prognostic marker in clear-cell renal carcinomas. *J Urol* 174:112, 2005

8. Porteous S, Torban E, Cho NP, *et al.*: Primary renal hypoplasia in humans and mice with PAX2 mutations: evidence of increased apoptosis in fetal kidneys of Pax2 (1Neu) +/- mutant mice. *Hum Mol Genet* 9:1-11, 2000

9. Torban E, Eccles MR, Favor J, *et al.*: PAX2 suppresses apoptosis in renal collecting duct cells. *Am J Pathol* 157:833-842, 2000

10. Dziarmaga A, Clark P, Stayner C, *et al.*: Ureteric bud apoptosis and renal hypoplasia in transgenic PAX2-Bax fetal mice mimics the renal-coloboma syndrome. *J Am Soc Nephrol* 14:2767-2774, 2003

11. Clark P, Dziarmaga A, Eccles M, *et al.*: Rescue of defective branching nephrogenesis in renal-coloboma syndrome by the caspase inhibitor, Z-VAD-fmk. *J Am Soc Nephrol* 15:299-305, 2004

12. Daniel L, Lechevallier E, Giorgi R, *et al.*: Pax-2 expression in adult renal tumors. *Hum Pathol* 32:282-287, 2001

13. Muratovska A, Zhou C, He S, *et al.*: Paired-Box genes are frequently expressed in cancer and often required for cancer cell survival. *Oncogene* 22:7989-7997, 2003

14. Mazal PR, Stichenwirth M, Koller A, *et al.*: Expression of aquaporins and PAX-2 compared to CD10 and cytokeratin 7 in renal neoplasms: a tissue microarray study. *Mod Pathol* 18:535-540, 2005

15. Torban E, Goodyer PR: Effects of PAX2 expression in a human fetal kidney (HEK293) cell line. *Biochim Biophys Acta* 1401:53-62, 1998

16. Gnarra JR, Dressler GR: Expression of Pax-2 in human renal cell carcinoma and growth inhibition by antisense oligonucleotides. *Cancer Res* 55:4092-4098, 1995

17. Buttiglieri S, Deregibus MC, Bravo S, *et al.*: Role of Pax2 in apoptosis resistance and proinvasive phenotype of Kaposi's sarcoma cells. *J Biol Chem* 279:4136-4143, 2004

18. Hamar P, Song E, Kokeny G, *et al.*: Small interfering RNA targeting Fas protects mice against renal ischemia-reperfusion injury. *Proc Natl Acad Sci U S A* 101:14883-14888, 2004

19. Hassan A, Tian Y, Zheng W, *et al.*: Small interfering RNA-mediated functional silencing of vasopressin V2 receptors in the mouse kidney. *Physiol Genomics* 21:382-388, 2005

20. Lipponen P, Eskelinen M, Syrjanen K: Expression of tumour-suppressor gene Rb, apoptosis-suppressing protein Bcl-2 and c-Myc have no independent prognostic value in renal adenocarcinoma. *Br J Cancer* 71:863-867, 1995

21. Hofmockel G, Wittmann A, Dammrich J, *et al.*: Expression of p53 and bcl-2 in primary locally confined renal cell carcinomas: no evidence for prognostic significance. *Anticancer Res* 16:3807-3811, 1996

22. Itoi T, Yamana K, Bilim V, *et al.*: Impact of frequent Bcl-2 expression on better prognosis in renal cell carcinoma patients. *Br J Cancer* 90:200-205, 2004

23. Sejima T, Miyagawa I: Expression of bcl-2, p53 oncoprotein, and proliferating cell nuclear antigen in renal cell carcinoma. *Eur Urol* 35:242-248, 1999

24. Vasavada SP, Novick AC, Williams BR: P53, bcl-2, and Bax expression in renal cell carcinoma. *Urology* 51:1057-1061, 1998

25. Yan Y, Mahotka C, Heikaus S, *et al.*: Disturbed balance of expression between XIAP and Smac/DIABLO during tumour progression in renal cell carcinomas. *Br J Cancer* 91:1349-1357, 2004

26. Eccles MR, Wallis LJ, Fidler AE, *et al.*: Expression of the PAX2 gene in human fetal kidney and Wilms' tumor. *Cell Growth Differ* 3:279-289, 1992

27. Dressler GR: Pax-2, kidney development, and oncogenesis. *Med Pediatr Oncol* 27:440-444, 1996

28. Tagge EP, Hanson P, Re GG, *et al.*: Paired box gene expression in Wilms' tumor. *J Pediatr Surg* 29:134-141, 1994

29. Eccles MR, Yun K, Reeve AE, *et al.*: Comparative in situ hybridization analysis of PAX2, PAX8, and WT1 gene transcription in human fetal kidney and Wilms' tumors. *Am J Pathol* 146:40-45, 1995

30. Khoubehi B, Kessling AM, Adshead JM, *et al.*: Expression of the developmental and oncogenic PAX2 gene in human prostate cancer. *J Urol* 165:2115-2120, 2001

31. Silberstein GB, Dressler GR, Van Horn K: Expression of the PAX2 oncogene in human breast cancer and its role in progesterone-dependent mammary growth. *Oncogene* 21:1009-1016, 2002

In Vivo validation of PAX2 as a target for renal cancer therapy

Pierre-Alain Hueber, Diana Iglesias, Lee Lee Chu, Michael Eccles and Paul Goodyer

Cancer Letters April 2008

2.2.1 ABSTRACT

PAX genes are frequently overexpressed in human cancer tissue and appear to contribute to the tumor phenotype, suggesting that they may be potential targets for cancer therapy. In particular, aberrant PAX2 expression has been reported in a high proportion of primary tumors, including the majority of Renal Cell Carcinomas (RCC). We recently demonstrated that PAX2 suppresses cisplatin-induced apoptosis in cultured RCC cells. We hypothesized that silencing of *PAX2* expression might partially overcome the notorious resistance of renal cell carcinomas to chemotherapy *in vivo*. In this report, we show that a *PAX2* shRNA successfully knocks down PAX2 mRNA and protein levels in an RCC cell line (ACHN). ACHN cells stably transfected with shRNAs targeted against the PAX2 homeodomain are 3-6-fold more susceptible to cisplatin-induced caspase-3 activation than control ACHN cells line. Furthermore, growth of subcutaneous ACHN/shPAX2 xenografts in nude mice is significantly more responsive to cisplatin therapy than control ACHN cell tumors. Our observations validate *PAX2* as a potential therapeutic gene target in renal cancer and suggest that adjunctive PAX2 knockdown may enhance the efficacy of other chemotherapeutic agents.

2.2.2 INTRODUCTION

Paired box (PAX) transcription factors are critical regulators of normal embryogenesis but generally exhibit oncogenic properties when aberrantly expressed in adult tissues. The aberrant re-expression of PAX proteins is observed in a variety of cancers including leukemia, breast, prostate, kidney and bladder carcinoma [2, 3]. As a result, PAX proteins have become a hallmark of malignant cells, suggesting that they might be potential therapeutic targets for cancer gene therapy.

During normal kidney development PAX2 is highly expressed in cells of both the condensing mesenchyme and the ureteric bud lineages but expression is sharply suppressed in the perinatal period as new nephron formation comes to an end [4]. Heterozygous *PAX2+/-* mutations cause renal hypoplasia (Renal-Coloboma Syndrome) and increased apoptosis of the ureteric bud, suggesting an anti-apoptotic function of PAX2 during nephrogenesis [5]. PAX2 expression is observed in 90% of clear cell Renal Cell Carcinomas (RCC); this is the most common subtype of RCC and PAX2 expression is associated with a metastatic phenotype [6-8].

RCC accounts for approximately 3% of all cancer cases worldwide [9]. Metastatic disease is present at the time of diagnosis in one third of patients and, since RCC cells are notoriously resistant to chemotherapy, the prognosis is poor. The one-year survival in patients with advanced metastatic RCC is less than 50%[9]. Thus, the development of novel therapeutic strategies bypassing resistance is imperative.

We have recently shown that the anti-apoptotic function of PAX2 contributes to the resistance of RCC cells to chemotherapy *in vitro*; inhibition of *PAX2* expression by small interfering RNAs (siRNAs) in cultured RCC cells enhances programmed cell death induced by cisplatin [10]. In this report, we provide *in vivo* proof of principle that *PAX2* knockdown sensitizes RCC tumours to cisplatin. RCC cells, stably transfected with an shRNA expression vector targeting PAX2, were tested in a nude mouse xenograft model.

2.2.3 RESULTS

2.2.3.1 Stable knockdown of PAX2 mRNA and protein in ACHN cells

Knockdown of PAX2 expression in ACHN cells was achieved using a vector-based small hairpin RNA (shRNA) strategy. shRNA constructs targeted against *PAX2* mRNA were inserted into pRNATin-H1.2 expression vector bearing a GFP marker (**Figure 2.2.1A/B**). shRNA constructs were stably transfected into ACHN cells and selected with neomycin for 4 weeks. Individual neomycin-resistant, GFP-positive clones were expanded for characterization. Out of 5 constructs that were initially screened, two *PAX2* shRNA constructs (shPAX2-1 and shPAX2-2) were able to inhibit PAX2 expression efficiently (**Figure 2.2.1A/B**).

To identify clones with efficient *PAX2* knockdown, the *PAX2* transcript was measured by QRT/PCR in pooled clones generated from each construct (**Figure 2.2.2A**). ACHN/sh*PAX2* clones expressing sh*PAX2*-1 and sh*PAX2*-2 reduced *PAX2* mRNA levels to 40% and 20%, respectively, in comparison to control ACHN cells stably transfected with empty vector (ACHN/shvector) (**Figure 2.2.2A**). None of the control clones derived from the ACHN cell line (ACHN/shvector) differed from the parental cell line in terms of *PAX2* mRNA expression level (**Figure 2.2.2B**).

To confirm that PAX2 mRNA knockdown correlates with reduced PAX2 protein levels, Western immunoblotting was performed on the individual clones derived from each construct. Control (ACHN/shvector) clones showed no reduction of PAX2 protein compared to the parental ACHN cell line. Individual clones transfected with either shPAX2-1 or shPAX2-2 showed a significant reduction in PAX2 protein (**Figure 2.2.2 C/D**). In half (3/6) of the ACHN/sh*PAX2*-1 clones, PAX2 protein levels were reduced to <20% of controls (**Figure 2.2.2C**). More than 70% (5/7) of the clones generated with the shPAX2-2 construct showed nearly complete knockdown of PAX2 protein. The remaining 2 clones showed an intermediate but significant decrease of PAX2 protein levels.

Figure 2.2.1 Diagram of Pax2 shRNA construct.

A) Pax2 shRNA sequences targeting the human Pax2 mRNA (Accession number NM_00278) were selected using GeneScript software; B) two shRNAs were inserted into pRNATin-H1.2 plasmids.

A

PAX2 shRNA insert

sequence	sense	loop	antisense
shPAX2-1	**TCATTGGAGGCGCTGGAAACA**	*TTGATATCCG*	**TGTTTCCAGCGCCTCCAATGA**
shPAX2-2	**TAACCAGGCAGAGTGGTGCTC**	*TTGATATCCG*	**GAGCACCACTCTGCCTGGTTA**

B

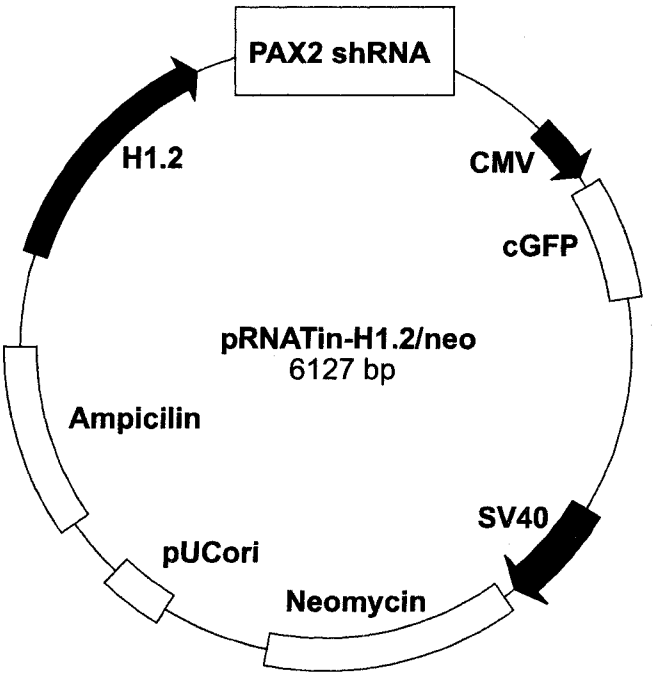

Figure 2.2.2 Stable knockdown of PAX2 mRNA and protein in ACHN cells expressing shRNA constructs.

A) Quantitative RT-PCR demonstrates that clones expressing shPAX2-1 and shPAX2-2 reduced mRNA level to 40% and 20% respectively of control ACHN cells stably transfected with empty vector, respectively. B) Western immunoblots show no reduction of PAX2 protein compared to parental cell line in ACHN cells stably transfected with empty vector. C/D) Individual clones transfected with shPAX2-1 or shPAX2-2 show significant reduction in PAX2 protein

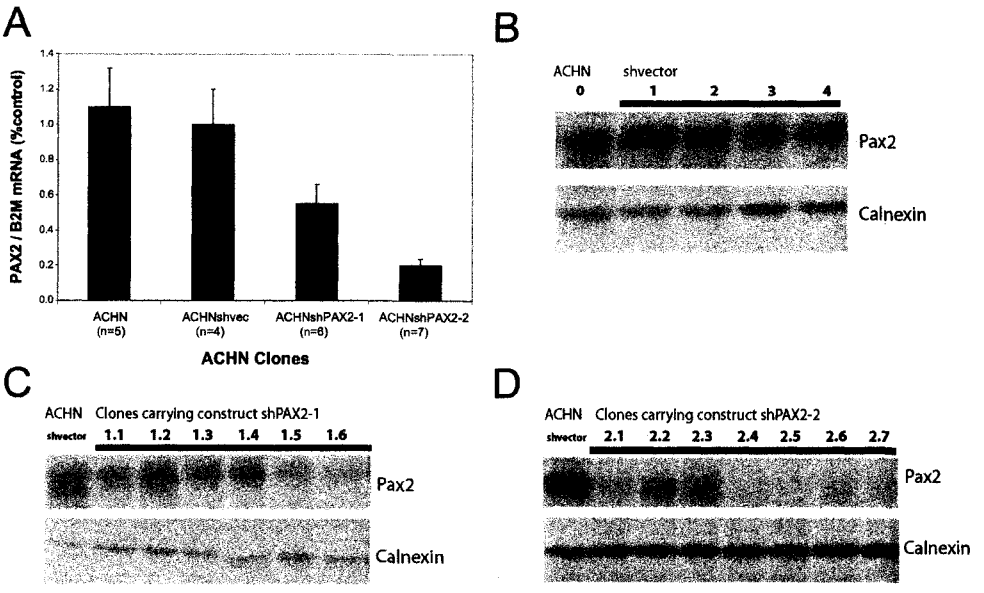
A
PAX2 / B2M mRNA (%control)
1.4
1.2
1.0
0.8
0.6
0.4
0.2
0.0
ACHN (n=5)
ACHNshvec (n=4)
ACHNshPAX2-1 (n=6)
ACHNshPAX2-2 (n=7)
ACHN Clones
B
ACHN
shvector
0
1
2
3
4
Pax2
Calnexin
C
ACHN Clones carrying construct shPAX2-1
shvector
1.1
1.2
1.3
1.4
1.5
1.6
Pax2
Calnexin
D
ACHN Clones carrying construct shPAX2-2
shvector
2.1
2.2
2.3
2.4
2.5
2.6
2.7
Pax2
Calnexin

2.2.3.2 Stable knockdown of PAX2 sensitizes ACHN cells to cisplatin-induced caspase-3 activation.

To determine whether PAX2 inhibition confers increased susceptibility to cisplatin–induced apoptosis, two ACHN/sh*PAX2* clones (sh*PAX2*-2.3 and sh*PAX2*-2.1) with reduced PAX2 expression (**Figure 2.2.2C/D**) were selected. *PAX2* mRNA knockdown was confirmed in these two clones by RT-PCR (**Figure 2.2.3A**). Apoptosis was measured by assessing caspase-3 activation compared to control ACHN shvector and ACHN parental cell lines. After exposure to cisplatin (50μM) for 24 hours, the sh*PAX2*-2.3 and sh*PAX2*-2.1 clones exhibited 3-6 fold greater activation of caspase-3 compared to control cell lines (**Figure 2.2.3B**).

Figure 2.2.3: Stable knockdown of PAX2 sensitizes ACHN cells to Caspase-3 induced by treatment with cisplatin.

A) Two ACHN clones (shPAX2-2.3 and shPAX2-2.1), selected after Western immunoblot screening, were analyzed by RT-PCR to confirm significant PAX2 mRNA knockdown. B) After exposure to cisplatin (50μM for 24 hours), these clones exhibited 3-6 fold greater activation of caspase-3 compared to control cell lines.

A

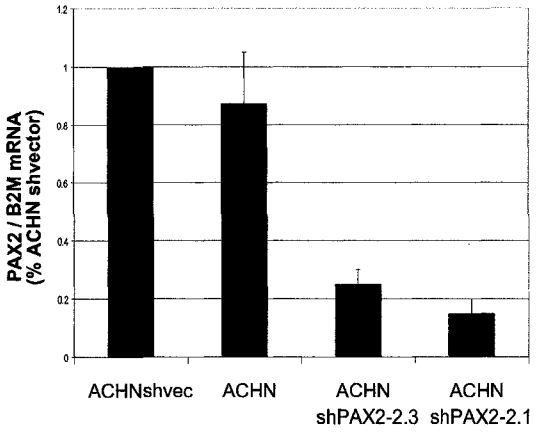
PAX2 / B2M mRNA
(% ACHN shvector)
1.2
1
0.8
0.6
0.4
0.2
0
ACHNshvec
ACHN
ACHN shPAX2-2.3
ACHN shPAX2-2.1
Cell lines

B

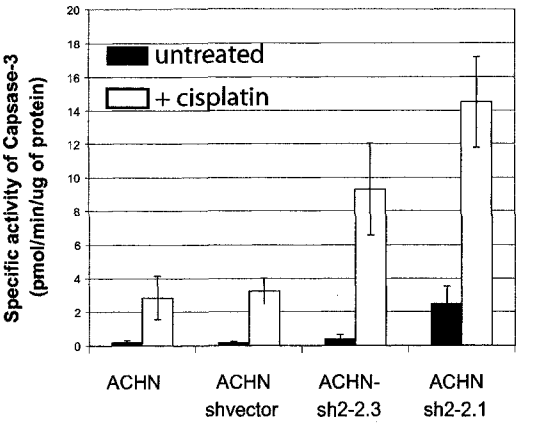
Specific activity of Capsase-3
(pmol/min/ug of protein)
20
18
16
14
12
10
8
6
4
2
0
untreated
+ cisplatin
ACHN
ACHN shvector
ACHN-sh2-2.3
ACHN sh2-2.1
Cell lines exposed to Cisplatin (50uM x24h)

2.2.3.3 PAX2 knockdown in ACHN tumor xenografts enhances the anti-tumor growth effect of cisplatin in nude mice.

To validate *PAX2* as a potential therapeutic target *in vivo*, we examined subcutaneous tumor growth of ACHN/sh*PAX2* xenografts in a nude mouse model. Nude mice were injected subcutaneously with control (ACHN/shvector) or ACHN/sh*PAX2*-2.1 clones (5 million cells) and monitored for external tumor volume every 2 days (**Figure 2.2.4A**). Measurable tumors appeared after a lag period of 15 days. At 21 days, ACHN/sh*PAX2* and ACHN/shvector tumor volumes were not significantly different ($p > 0.05$). Similarly, ACHN/shvector tumor growth was comparable to tumours arising from ACHN parental cell lines (data not shown). On day 21, mice were injected intra-peritoneally (i.p.) with PBS or cisplatin (2 mg/kg). This cisplatin dose was determined in preliminary studies to achieve a measurable effect on tumor volume.

Over the subsequent week, untreated tumors arising from ACHN/sh*PAX2* cells and control ACHN/shvector cells grew rapidly and, by day 27, were not significantly different in size (tumor volume = + 200% and 186% of baseline at day 21, respectively) ($p>0.05$) (**Figure 2.2.4A**). Cisplatin treatment of control ACHN/shvector tumors slowed growth rate somewhat from day 21 to 27 compared to the untreated mice (tumor volume = 140% of baseline), but did not induce tumor regression. In contrast, cisplatin treatment of mice with ACHN/sh*PAX2*-2.1 tumors showed a striking reduction in tumor growth rate; tumor volume fell by 10% from day 21 to 25 (**Figure 2.2.4A**). The effect of cisplatin treatment was also expressed as a ratio of treated (T) to untreated (C) tumor volumes (%) (**Figure 2.2.4B**). The therapeutic effect of cisplatin measured by T/C was significantly enhanced in shPAX2-2.1 cells compared to empty shvector controls ($p=0.008$, paired t-test), suggesting a synergistic effect of PAX2 inhibition and cisplatin chemotherapy.

Figure 2.2.4 Effect of PAX2 knockdown on the growth of ACHN tumor xenografts in nude mice treated with cisplatin.

A) Nude mice were injected subcutaneously with control (empty vector) or shPAX2-2.1 ACHN clones (5 million cells) and monitored for external tumour volume every 2 days. Each point represents the mean tumor volume (+/- standard deviation) in each experimental group (n=6 mice). Measurable tumour appeared after a lag period of 15 days. On day 21, mice were injected with cisplatin (2 mg/kg). Over the subsequent week, tumours from the ACHN shPAX2-2.1 clone showed a significant reduction in growth (-10% of baseline) compared to tumours arising from control ACHN cells transfected with empty shvector (+ 180% of baseline) or compared to untreated tumours.

B) Effect of cisplatin was also expressed as the ratio of treated (T) to untreated (C) tumour volume (%). The therapeutic effect of cisplatin was significantly enhanced in shPAX2-2.1 cells compared to empty shvector controls (p=0.008, paired t-test).

A

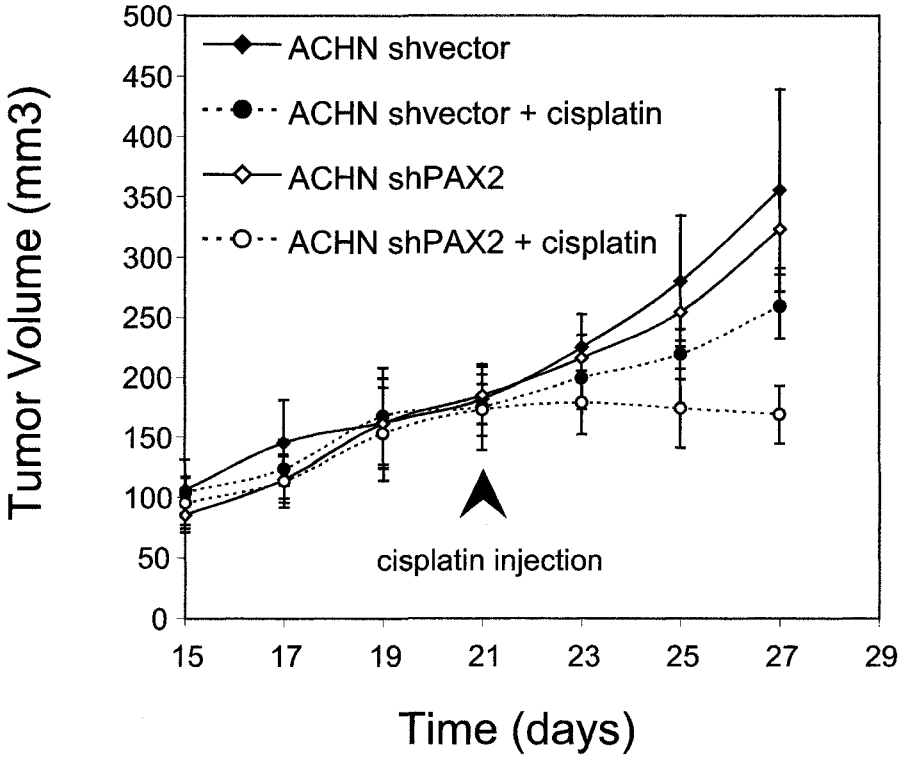
ACHN shvector
ACHN shvector + cisplatin
ACHN shPAX2
ACHN shPAX2 + cisplatin
Tumor Volume (mm3)
500
450
400
350
300
250
200
150
100
50
0
15
17
19
21
23
25
27
29
cisplatin injection
Time (days)

B

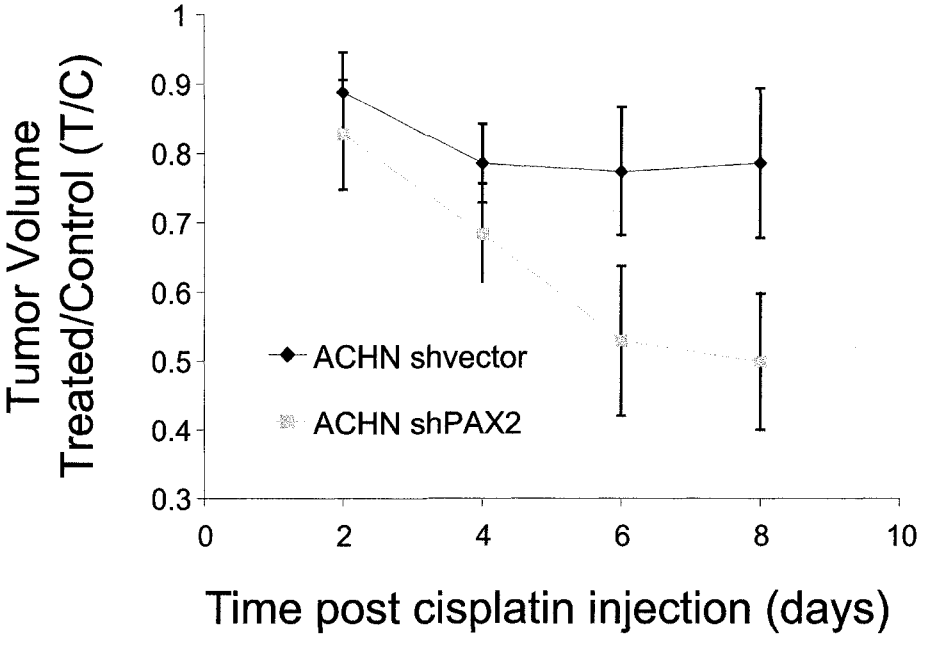
Tumor Volume
Treated/Control (T/C)
1
0.9
0.8
0.7
0.6
0.5
0.4
0.3
ACHN shvector
ACHN shPAX2
0
2
4
6
8
10
Time post cisplatin injection (days)

2.2.4 DISCUSSION

Renal cell carcinoma (RCC) is the most common cancer of the kidney. Recurrent tumours develop in almost 50% of patients treated for localized disease. The striking resistance of RCC to chemotherapy is, to a large extent, attributable to suppression of programmed cell death pathways normally activated by chemotherapeutic agents [9]. Renal cancer cells escape apoptosis by a number of mechanisms including the overexpression of anti-apoptotic genes such as *XIAP* [12-14]. Thus, adjunctive therapies, which inactivate the anti-apoptotic responses of tumour cells, might enhance the efficacy of primary chemotherapeutic agents.

Over 90% of RCC cells express the developmental transcription factor PAX2. We previously reported that knockdown of PAX2 in RCC cells by transient transfection of pooled siRNAs enhances basal and cisplatin-induced apoptosis *in vitro*. In this study, we developed shRNAs to achieve stable knockdown of PAX2 in subcutaneous tumours derived from RCC cells. Our aim was to provide *in vivo* proof of principle that this strategy sensitizes RCC tumours to chemotherapeutic agents such as cisplatin. In initial experiments, we screened a panel of potential shRNA sequences for efficient PAX2 knockdown; two shRNAs targeting the *PAX2* homeodomain were found to reduce *PAX2* mRNA and protein significantly when stably transfected into RCC cells. Since the ACHN/sh*PAX2*.1 clone showed the greatest reduction of *PAX2* mRNA and increased both basal and cisplatin-induced apoptosis, it was chosen for our *in vivo* studies.

Interestingly, RCC cells transfected with sh*PAX2*.1 were able to form subcutaneous tumours in nude mice, despite substantial knockdown of PAX2. This contrasts somewhat with the observation that PAX2 overexpression promotes tumorigenicity of endometrial cancer cells in nude mice compared to the parental ECC-1 cell line that was unable to form subcutaneous tumors [15]. Conceivably, PAX2 is necessary to permit the initial oncogenic program in endometrial cancer, but once transformation has occurred, its suppression does not restore the normal phenotype. However, the primary transforming event in renal cell carcinoma is likely to be independent of PAX2. Indeed, loss of the *VHL*

gene function is evident in about 50–70% of sporadic cases of RCC [16]. *VHL* encodes an E3 ligase that promotes ubiquitination of hypoxia-inducible transcription factors HIF1, HIF2 and HIF3, leading to their degradation [16]. Unregulated expression of HIF is sufficient to drive the primary transforming event in this large subset of renal cell carcinomas [17, 18]. The *VHL* gene is intact in some renal cell carcinomas and this is the case in the ACHN cell line. The primary transforming event in ACHN tumors might be loss of the tumor repressor, JADE-1, barely detectable in ACHN cells. However, The effect of JADE-1 on ACHN cell tumorigenicity has not been demonstrated directly [19]. Nevertheless, it seems that molecular pathways independent of PAX2 drive primary oncogenic transformation of renal tubular cells in renal cell carcinoma.

It is conceivable that the widespread expression of PAX2 in renal cell carcinomas may represent a characteristic response of renal cells to stress. We have shown that renal PAX2 expression is normally down-regulated in the postnatal period but is re-activated to fetal levels in response to urinary tract obstruction [4]. Reappearance of PAX2 in the obstructed kidney is associated with partial protection from apoptosis [4]. Similarly, others have shown that PAX2 expression is induced by osmotic stress and protects renal medullary cell from apoptosis following exposure to high salt concentrations *in vitro* [20]. Also, PAX2 directly interacts with a BRCT-domain protein (PAX2 Interacting Protein, PTIP), which is activated by cellular stress and promotes resistance to ionizing radiation [21-23].

During normal kidney development, PAX2 exerts a powerful anti-apoptotic effect in cells of the collecting duct lineage through direct transcriptional activation of the neural apoptosis inhibitory protein (NAIP) gene [11]. NAIP was originally identified as an endogenous suppressor of caspase-3 and caspase-7 activities in neuronal cells. We identified NAIP expression in the normal fetal kidney and showed that NAIP suppresses the apoptotic pathway in renal tubular cells[11]. However, the resistance of RCC cells to programmed cell death is likely to be more complex. At least one other member of the inhibitor of apopotosis (IAP) gene family, XIAP, is overexpressed in renal cell carcinomas [24] and high XIAP expression is associated with a worse clinical prognosis

[13, 24]. The relationship between PAX2 and other members of the IAP gene family remains to be clarified. Additionally, there is evidence that PAX2 may inhibit programmed cell death by regulating BID/BAD (in prostate cancer) or PTEN/AKT (in renal endothelial cells), though these pathways may be context specific [1, 25].

Cisplatin binds to DNA causing chromosomal damage, which may be repaired or may activate the apoptotic pathway [26]. In this study, we found that shRNA knockdown of *PAX2* expression increased susceptibility to cisplatin-induced caspase activation *in vitro* and enhanced the effect of cisplatin on subcutaneous tumor growth in nude mice. PAX2 has also been implicated in resistance to chemotherapy of prostate cancer cells and Kaposi's sarcoma [25] [1]. While growth of ACHN/sh*PAX2*.1 tumors was sharply suppressed by cisplatin, tumor growth recovered once the effect of the single cisplatin dose had worn off after 5-6 days. It should be noted that our ACHN/sh*PAX2* transfectants were initially selected in culture medium with neomycin, possibly selecting for additional resistance mechanisms that could compensate for loss of anti-apoptotic effects of PAX2. For example, PAX2 may be partially compensated for by PAX8, which is commonly expressed in RCC cells. Heterozygous inactivation of *Pax8* in $Pax2^{+/-}$ mutant mice increases ureteric bud cell apoptosis during branching morphogenesis of the kidney and causes exaggerated renal hypoplasia [27]. Thus, an shRNA targeting conserved domains of both *PAX* genes might heighten the response to cisplatin compared to *PAX2* knockdown alone.

Following intravenous injection in mice, siRNA accumulates spontaneously in the kidney and has been shown to selectively suppress gene function in the proximal tubules [28]. Most renal cell carcinomas are thought to arise from the renal proximal tubule, raising the possibility that *PAX2* siRNAs might be used as adjunctive therapy for chemotherapy of RCC. In preliminary studies, nanoparticles have been used to deliver modified siRNAs safely to monkey tissues [29] and tumor-targeted nanoparticles have been shown to deliver siRNA to metastatic tumors in a murine pancreatic cancer model [30]. Although protracted *PAX2* knockdown is not expected from a synthetic siRNA, the effect might be sustained long enough to enhance bolus cisplatin therapy, as in our subcutaneous RCC

tumor model. PAX2 is expressed at high levels in fetal brain, kidney and retina during development, but is sharply down-regulated in mature adult organs [2, 4]. Thus, *PAX2* siRNAs are expected to enhance cytotoxicity of chemotherapeutic drugs in renal tumours rather than in normal tissues. While the delivery systems for siRNAs *in vivo* are not yet fully developed, our observations suggest that reagents to silence *PAX2* warrant consideration as adjunctive therapy for renal cell carcinoma.

ACKNOWLEDGEMENTS

This work was supported by an operating grant from the Kidney Foundation of Canada. Pierre-Alain Hueber was the recipient of a Graduate Studentship award from the Montreal Children's Hospital Research Institute. Paul Goodyer is the recipient of a James McGill Research Chair.

2.2.5 METHODS

Vector construction

ShRNA constructs targeting *PAX2* mRNA (NM_NM_000278) were designed using Genescript software guidelines (Genescript, Piscataway, NJ, USA). The two 21-base oligonucleotides (sense and antisense) linked by a loop sequence were cloned into the pRNATin-H1.2 vector. Stably expressing cell lines were selected using 1mg/ml neomycin. After 4 weeks, resistant clones that were positive for GFP expression by fluorescent microscopy were chosen and amplified.

Cell culture

A human RCC cell line (ACHN) was selected from the NCI-60 cancer cell panel and obtained from the American Type Culture Collection (Rockville, MD, USA). ACHN cells were maintained as adherent monolayer cultures in MEM culture medium (Invitrogen, Burlington, Ontario, Canada) supplemented with 10% fetal bovine serum.

Quantatitative RT-PCR

RNA was isolated from cells with RNeasy® Plus columns (Qiagen Laboratories, Valencia, CA, USA) according o the manufacturer's directions. Quantitative real-time reverse transcription/polymerase chain reaction (RT-PCR) was carried out using the Qiagen QuantiTect SYBR® Green RT-PCR method (Qiagen Laboratories, Valencia, CA). Each 25μl PCR reaction contained 100ng RNA, forward and reverses primers, and the passive reference dye (ROX) to normalize the SYBR Green/double-stranded DNA complex signal during analysis to correct for well-to-well variations. Triplicate reactions were performed for each template amount. As a control, DNA standard template was replaced with water. Primers were as follows:

PAX2 Forward primer: 5'-CCCAGCGTCTCTTCCATCA-3'

PAX2 Reverse primer: 5'-GGCGTTGGGTGGAAAGG -3',

B2M Forward primer: 5'-AGATGAGTATGCCTGCCGTGT-3'

B2M Reverse primer: 5'-GCTTACATGTCTCGATCCCACTTA-3'.

PCR cycling conditions (N=40 cycles) were as follows: initial denaturation at 95°C for 15 min, followed by annealing for 30 seconds at 55 °C and 30 seconds/kb extension at 72°C. We performed simulatenous real-time RT-PCR with beta-2-microglobulin (*B2M*) and all resulting values were normalized with this houskeeping gene. These conditions yielded a single-band amplicon by agarose gel electrophoresis; the identity of the PCR product was confirmed by melting curve analysis on the Mx4000 (Stratagene, Cedar Creek, TX, USA). Estimates of *PAX2/B2M* transcript levels were quantified by the CT method as previously described[11].

Western immunoblotting

A total of 50μg of protein extracted from each cell population was resolved on 10% sodium dodecyl sulphate-polyacrylamide gels at 100V for 1.5 h at 4°C, and then transferred over 1 h at 100 V (4°C) onto polyvinylidene difluoride membranes (Bio-Rad, Mississauga, ON, Canada). Blots were probed with polyclonal anti-PAX2 antibody (Zymed, San Francisco, CA, USA), followed by anti-rabbit IgG secondary antibody and detected with an enhanced chemiluminescence detection system (Amersham, Piscataway, NJ, USA). Membranes probed for PAX2 were reprobed for Calnexin (Calbiochem, EMD Chemicals Inc, San Diego, CA, USA) to normalize for loading differences. Antibody was detected by a chemiluminescence system (ECL Plus) Amersham Biosciences, NJ USA) . Analysis was performed using ImageQuant TL on a Storm® phosphoImager (Amersham Biosciences, NJ, USA)

Caspase-3 assay

The caspase-3 substrate *N*-acetyl-Asp-Glu-Val-Asp-7-amino-4-trifluoromethylcoumarin (BD Pharmingen San Jose, CA, USA) was used in caspase-3 assays according to the manufacturer's instructions. Cell lysate (100μg) was added to the reaction buffer (20 mM *N*-2-hydroxyethylpiperazine-*N*'-2-ethanesulphonic acid, pH 7.4, 100 mM sodium chloride, 10 mM dithiothreitol, 0.1% 3-[(3-cholamydopropyl)-dimethylammonio]-2-hydroxy-1-propanesulphonic acid, 10% sucrose) containing 125 μM of N-acetyl-Asp-Glu-Val-Asp-7-amino-4-trifluoromethylcoumarin in a 1 ml cuvette. Fluorescence of the

cleavage product was measured using a Luminescence Spectrometer LS50 (Perkin–Elmer, Fremont, CA, USA).

Subcutaneous xenograft in nude mice

ACHN cells were trypsinized, washed twice with PBS, pelleted and resuspended in PBS; the viability of collected cells was confirmed by staining with trypan blue. To establish ACHN tumor xenografts in mice, 6-week-old SCID mice were injected subcutaneously in the right flank with 5 million ACHN cells in 200 µl of PBS. When tumor volume reached $150mm^3$, mice were randomized for therapy in two experimental groups (+/- cisplatin). Tumor volume was determined every 2 days by external measurements with a caliper and calculated as $V=L\times l^2 \times 0.5$, where L and l represent the larger and the smaller tumor diameters. Animal care was provided according to institutional guidelines. Cisplatin was injected intra-peritoneally (i.p.) at day 21.

Statistical analysis

Each experiment was repeated three times. Means and standard deviations have been calculated for each independent experiment. In each experiment, differences in means were tested for significance using the Student's *t*-test. Statistical significance was defined as $p < 0.05$.

REFERENCES:

1. Buttiglieri S, Deregibus MC, Bravo S, *et al.*: Role of Pax2 in apoptosis resistance and proinvasive phenotype of Kaposi's sarcoma cells. *J Biol Chem* 279:4136-4143, 2004

2. Muratovska A, Zhou C, He S, *et al.*: Paired-Box genes are frequently expressed in cancer and often required for cancer cell survival. *Oncogene* 22:7989-7997, 2003

3. Robson EJ, He SJ, Eccles MR: A PANorama of PAX genes in cancer and development. *Nat Rev Cancer* 6:52-62, 2006

4. Cohen T, Loutochin O, Amin M, *et al.*: PAX2 is reactivated in urinary tract obstruction and partially protects collecting duct cells from programmed cell death. *Am J Physiol Renal Physiol* 292:F1267-1273, 2007

5. Torban E, Eccles MR, Favor J, *et al.*: PAX2 suppresses apoptosis in renal collecting duct cells. *Am J Pathol* 157:833-842, 2000

6. Daniel L, Lechevallier E, Giorgi R, *et al.*: Pax-2 expression in adult renal tumors. *Hum Pathol* 32:282-287, 2001

7. Mazal PR, Stichenwirth M, Koller A, *et al.*: Expression of aquaporins and PAX-2 compared to CD10 and cytokeratin 7 in renal neoplasms: a tissue microarray study. *Mod Pathol* 18:535-540, 2005

8. Memeo L, Jhang J, Assaad AM, *et al.*: Immunohistochemical analysis for cytokeratin 7, KIT, and PAX2: value in the differential diagnosis of chromophobe cell carcinoma. *Am J Clin Pathol* 127:225-229, 2007

9. Cohen HT, McGovern FJ: Renal-cell carcinoma. *N Engl J Med* 353:2477-2490, 2005

10. Hueber PA, Waters P, Clark P, *et al.*: PAX2 inactivation enhances cisplatin-induced apoptosis in renal carcinoma cells. *Kidney Int* 69:1139-1145, 2006

11. Dziarmaga A, Hueber PA, Iglesias D, *et al.*: Neuronal apoptosis inhibitory protein is expressed in developing kidney and is regulated by PAX2. *Am J Physiol Renal Physiol* 291:F913-920, 2006

12. Yan Y, Mahotka C, Heikaus S, *et al.*: Disturbed balance of expression between XIAP and Smac/DIABLO during tumour progression in renal cell carcinomas. *Br J Cancer* 91:1349-1357, 2004

13. Mizutani Y, Nakanishi H, Li YN, *et al.*: Overexpression of XIAP expression in renal cell carcinoma predicts a worse prognosis. *Int J Oncol* 30:919-925, 2007

14. Byun SS, Yeo WG, Lee SE, *et al.*: Expression of survivin in renal cell carcinomas: association with pathologic features and clinical outcome. *Urology* 69:34-37, 2007

15. Wu H, Chen Y, Liang J, *et al.*: Hypomethylation-linked activation of PAX2 mediates tamoxifen-stimulated endometrial carcinogenesis. *Nature* 438:981-987, 2005

16. Kim WY, Kaelin WG: Role of VHL gene mutation in human cancer. *J Clin Oncol* 22:4991-5004, 2004

17. Kondo K, Klco J, Nakamura E, *et al.*: Inhibition of HIF is necessary for tumor suppression by the von Hippel-Lindau protein. *Cancer Cell* 1:237-246, 2002

18. Maranchie JK, Vasselli JR, Riss J, *et al.*: The contribution of VHL substrate binding and HIF1-alpha to the phenotype of VHL loss in renal cell carcinoma. *Cancer Cell* 1:247-255, 2002

19. Zhou MI, Foy RL, Chitalia VC, *et al.*: Jade-1, a candidate renal tumor suppressor that promotes apoptosis. *Proc Natl Acad Sci U S A* 102:11035-11040, 2005

20. Cai Q, Dmitrieva NI, Ferraris JD, *et al.*: Pax2 expression occurs in renal medullary epithelial cells in vivo and in cell culture, is osmoregulated, and promotes osmotic tolerance. *Proc Natl Acad Sci U S A* 102:503-508, 2005

21. Kim D, Wang M, Cai Q, *et al.*: Pax transactivation-domain interacting protein is required for urine concentration and osmotolerance in collecting duct epithelia. *J Am Soc Nephrol* 18:1458-1465, 2007

22. Lechner MS, Levitan I, Dressler GR: PTIP, a novel BRCT domain-containing protein interacts with Pax2 and is associated with active chromatin. *Nucleic Acids Res* 28:2741-2751, 2000

23. Hoffmeister A, Ropolo A, Vasseur S, *et al.*: The HMG-I/Y-related protein p8 binds to p300 and Pax2 trans-activation domain-interacting protein to regulate the trans-activation activity of the Pax2A and Pax2B transcription factors on the glucagon gene promoter. *J Biol Chem* 277:22314-22319, 2002

24. Ramp U, Krieg T, Caliskan E, *et al.*: XIAP expression is an independent prognostic marker in clear-cell renal carcinomas. *Hum Pathol* 35:1022-1028, 2004

25. Gibson W, Green A, Bullard RS, *et al.*: Inhibition of PAX2 expression results in alternate cell death pathways in prostate cancer cells differing in p53 status. *Cancer Lett* 248:251-261, 2007

26. Siddik ZH: Cisplatin: mode of cytotoxic action and molecular basis of resistance. *Oncogene* 22:7265-7279, 2003

27. Narlis M, Grote D, Gaitan Y, *et al.*: Pax2 and pax8 regulate branching morphogenesis and nephron differentiation in the developing kidney. *J Am Soc Nephrol* 18:1121-1129, 2007

28. van de Water FM, Boerman OC, Wouterse AC, *et al.*: Intravenously administered short interfering RNA accumulates in the kidney and selectively suppresses gene function in renal proximal tubules. *Drug Metab Dispos* 34:1393-1397, 2006

29. Heidel JD, Yu Z, Liu JY, *et al.*: Administration in non-human primates of escalating intravenous doses of targeted nanoparticles containing ribonucleotide reductase subunit M2 siRNA. *Proc Natl Acad Sci U S A* 104:5715-5721, 2007

30. Pirollo KF, Zon G, Rait A, *et al.*: Tumor-targeting nanoimmunoliposome complex for short interfering RNA delivery. *Hum Gene Ther* 17:117-124, 2006

Connecting Chapter II and III:

The work presented in chapter II illustrates the proof of principle that therapeutic strategies which suppress PAX2 have potential as adjunctive agents in treatment of renal cancer. Most importantly, our findings establish the connection between normal kidney development and renal cancer.

Wilms' tumor (WT) is the most common pediatric kidney cancer and is thought to arise from multipotent embryonic renal precursors of the metanephric blastema, which fail to terminally differentiate and continue to proliferate. Accordinly the Wilms tumors typically include blastemal, epithelial and stromal cells (triphasic histology). Furthermore, the presence of heterologous elements such as muscle, cartilage and fat reflects the pluripotential ability of the renal progenitor cells from which the tumor originates. Due to its embryonic features, Wilms Tumor has served as canonical model to study developmental pathways leading to cancer.

During normal kidney development, renal progenitor cells of the metanephric blastema can give rise to all the cell types of the nephron. A dichotomy that delineates two main distinct cellular programs of differentiation can be established: The nephrogenic program gives rise to the epithelial cell lineages while the mesenchymal program produce the stromal cell lineages. Upon inductive signal from the invading UB, metanephric progenitor cells adjacent to the UB tip will condense and form a cap. This cap of induced mesenchyme undergoes mesenchymal to epithelial transition to form the polarized epithelial cells lining the lumen of an S-shaped tubular structure that will give rise to the all epithelials cells of the nephron including the renal tubule and the podocytes. While inductive signals from the ureteric bud drives contiguous mesenchymal cells toward a nephrogenic fate, the remaining satellite mesenchymal cells are induced to adopt an alternative differentiation program marked by the expression of a different set of transcription factors. These cells retain a non-polarized mesenchymal phenotype, migrate between the emerging tubules and form a stromal component of the renal medulla.

PAX2 is initially expressed in the nephric duct epithelium and high levels of PAX2 protein are seen throughout the branching ureteric bud as well as in the distal portion of the S-shaped body. In the S-shaped body it activates WNT4 expression and genes involved in the mesenchyme to epithelial transition. In the previous chapter we showed that aberrant PAX2 expression in renal cell carcinoma, may account for the characteristic resistance of tumor cells to apoptosis induced by chemotherapeutic agents (Hueber *et al.*, 2006). Aberrant PAX2 expression is seen in a subset of triphasic Wilms tumors, but PAX2 is conspicuously absent in Wilms tumours with a prominent stromal phenotype. Until recently, PAX2 and PAX8 were the only members of the PAX gene family described to be expressed in the fetal kidney (Dziarmaga et al., 2006). However, recent studies characterizing PAX3 expression in a transgenic mouse expressing β-galactosidase induced by Cre recombinase under the control of a 6.4kb region located upstream the PAX3 genomic found beta-galactosidase activity in the urogenital derivative of the mouse embryo indirectly suggesting the potential presence of PAX3+ cells in the kidney (Engleka *et al.*, 2005). Here, I show for the first time, that PAX3 is expressed in developing kidney and in Wilms tumors.

CHAPTER III: PAX3: from kidney development to Wilms tumor

PAX3 is expressed in the stromal developing kidney and in Wilms tumor with myogenic phenotype.

Pierre-Alain Hueber, Ryuji Fukuzawa, LeeLee Chu, Reyhan Elkares, Shu-Jie He, Matthew Anaka, Anthony Reeve, Michael Eccles Myriam Blumentkrantz, Nada Jabado, Diana Iglesias and Paul Goodyer.

Manuscript submitted to Pediatric Developmental Pathology.

3.1 ABSTRACT

Wilms tumour (WT) is the most frequent renal neoplasm of childhood; a myogenic component is observed in 5-10% of tumours. We demonstrate for the first time that myogenic Wilms tumors are associated with expression of PAX3, a transcription factor known to specify myoblast cell fate during muscle development. In a panel of 20 Wilms tumors, PAX3 was identified in 13/13 tumour samples with myogenic histopathology, but was absent in 7/7 tumours lacking a myogenic component. Furthermore, we show that PAX3 is expressed in the metanephric mesenchyme and stromal compartment of developing mouse kidney; a specific pattern of Pax3 isoforms was identified in fetal vs adult kidney. Modulation of endogenous PAX3 expression in human embryonic kidney (HEK293) cells influenced cell migration in *in vitro* assays.

Mutations of WT1 were consistently associated with PAX3 expression in Wilms tumors and modulation of WT1 expression in HEK293 cells was inversely correlated with the level of endogenous PAX3 protein. We demonstrate abundant PAX3 and absence of PAX2 expression in a novel cell line (WitP3) isolated from the stromal portion of a Wilms tumor, bearing a homozygous deletion of the WT1 gene. In contrast, PAX2 was strongly expressed and PAX3 was absent in a Wilms tumor cell line (Wit49) with epithelial phenotype and intact WT1 gene.

We hypothesize that PAX3 sets stromal cell fate in developing kidney but is normally suppressed by WT1 during the mesenchyme-to-epithelium transition leading to nephrogenesis. Loss of WT1 permits aberrant PAX3 expression in a subset of Wilms tumors with myogenic phenotype.

3.2 INTRODUCTION

Wilms Tumor (WT) is the most common pediatric solid tumor, arising in 1/10000 children. This malignancy was first described by Max Wilms in 1899, as a "mischgeschwulste der niere"; composed of mixed stromal, epithelial and undifferentiated mesenchymal cells. This triphasic histology is thought to reflect the derivation of Wilms tumor from stem cells of the metanephric mesenchyme, capable of differentiating toward either a stromal or an epithelial cell fate (1). It follows that genes controlling the divergence of these cell lineages from a pluripotent precursor must be central to the pathogenesis of WT (2, 3).

During normal kidney development, signals from each branch of the arborizing ureteric bud induce adjacent mesenchymal cells to cluster and express specific transcription factors, including the paired box gene, *PAX2*. This cap of induced mesenchyme is rapidly transformed into polarized epithelial cells lining the lumen of an S-shaped tubular structure. At its distal end, PAX2-positive cells of the S-shaped body generate the various segments of the renal tubule and fuse to the arborizing ureteric bud. At its proximal end, PAX2 expression is suppressed as cells undergo further differentiation into podocytes and elicit the ingrowth of capillaries to form the glomerulus of each nephron.

While inductive signals from the ureteric bud propel many mesenchymal cells toward a nephrogenic fate, other mesenchymal cells are induced to express alternative transcription factors, such as retinoic acid receptor-β (4). These cells retain a non-polarized mesenchymal phenotype, migrate between the emerging tubules and form a substantial component of the renal medulla (5).

Until recently, it was generally agreed that, of the nine PAX family members, only PAX2 and PAX8 are expressed in mammalian fetal kidney. However, in the course of their studies of neuromuscular development, Engleka et al. created a novel murine *PAX3* allele by inserting Cre downstream of the *Pax3* promoter (6). In Cre-dependent R26R reporter mice, the allele was used to track Pax3 promoter activity during development. Beta-

galactosidase reporter activity was noted in expected sites such as dorsal neural tube, somites and cardiac neural crest cells, but was unexpectedly seen in mesenchymal compartments of newborn mouse kidney (6). This observation suggests that PAX3 could be involved in renal development.

In this study we demonstrate that PAX3 is expressed in metanephric mesenchyme and stromal cells of normal embryonic mouse kidney but is progressively down-regulated in the perinatal period. Aberrant PAX3 expression was seen in a subset of Wilms tumor with myogenic phenotype and loss of *WT1*. PAX3 was noted in a novel Wilms tumor cell line bearing a homozygous deletion of WT1 but not in a Wilms tumor cell line with intact WT1. Our observations suggest a new model of Wilms tumor pathogenesis in which loss of WT1 permits PAX3 expression, accounting for the myogenic phenotype.

3.3 RESULTS

3.3.1 PAX3 mRNA and protein is detected in the mouse embryonic kidney and in renal cell lines

To determine whether *PAX3* is expressed in the developing mouse kidney, we first isolated RNA from E15 and E18 and adult kidneys and amplified a portion of the *Pax3* transcript (RT-PCR), which allowed us to distinguish three known murine *Pax3* isoforms. These are formed by alternative splicing of the eighth exon and/or intron (7). The primary *Pax3c* transcript (lacking intron 8) was evident at all stages (Fig.3.1A). However, fetal kidney samples also exhibited expression of the *Pax3d* (+ intron 8), lacking in the adult (Fig 1A). At E18, the putative inhibitory transcript, *Pax3g*, was also identified. PAX3 protein was also detected by Western immunoblotting at various stages. The 56kDa PAX3 protein was detectable at E12.5, peaked between E15-E18 and was down-regulated thereafter to relatively low levels in adult kidney (Fig.3.1B).

To clarify whether *Pax3* expression is characteristic of mesenchymal vs ureteric bud lineage, we assessed PAX3 protein and mRNA in an established mouse embryonic

mesenchymal (MK4) cell line (8) and in an epithelial cell line (IMCD) derived from murine collecting duct (9). As seen in Figure 3.1C/1D, both PAX3 mRNA and protein are detected in MK4 cells but are undetectable in the IMCD line (Fig.3.1C&D). MK4 cells express both the Pax3c (-8i) and *Pax3*g (Δ8e) transcript identified in whole E18 mouse kidney (Fig.3.1).

3.3.2 PAX3 protein expression is restricted to the mesenchymal compartment of embryonic kidney

We performed PAX3 immunohistochemistry on fetal and adult mice. As the ureteric bud emerges from the nephric duct at E11, PAX3 protein is evident in the somites (Som), brain and the neural tube (NT) (Fig.3.2), but is absent from the uninduced metanephric mesenchyme. As the ureteric bud arborizes and initiates nephrogenesis, strong PAX3 nuclear staining appears in cells of stromal compartment and metanephric blastema (MB) (Fig.3.2). Between E14 and E18, this pattern of PAX3 expression intensifies, but fades as committed cells undergo the mesenchyme-to-epithelium transition to form the S-shaped body (S). PAX3 is faintly seen in maturing proximal tubules (PT) at P1, but is absent in epithelium of mature glomeruli (G) and collecting duct (CD) (Fig.3.2). From E18 onward, PAX3 expression progressively declines, to reach relatively low adult level by 3-weeks of age. Control E17 kidney stained without primary antibody is negative for PAX3 staining (Fig.3.2).

Figure 3.1. *PAX3* mRNA and PAX3 protein are expressed in mouse embryonic kidney and in renal cell lines.

A) Whole murine kidney RNA was amplified by RT-PCR with primers spanning exons 8-9. Three *Pax3* isoforms were detected: *Pax3*(+8i) containing exon 8 and intron 8 (1007bp); *Pax3* (-8i) with exon 8 but intron 8 deleted (516bp); and *Pax3*(Δ8e), the inactive form of *Pax3*, with both intron 8 and exon 8 deleted (267bp).

B) Renal PAX3 protein was assessed by Western immunoblotting normalized for beta-actin. Each bar represents the mean of three independent experiments at embryonic day E12.5 through 6 weeks postnatal age (adult). Insert shows representative Western immunoblot. C) PAX3(+8i) and Pax3(-8i) transcripts were identified by RT-PCR in MK4 cells derived from induced metanephric mesenchyme but not in IMCD cells derived from the inner medullary collecting duct. (D) PAX3 protein was identified by Western immunoblotting in MK4 but not mIMCD cells.

A

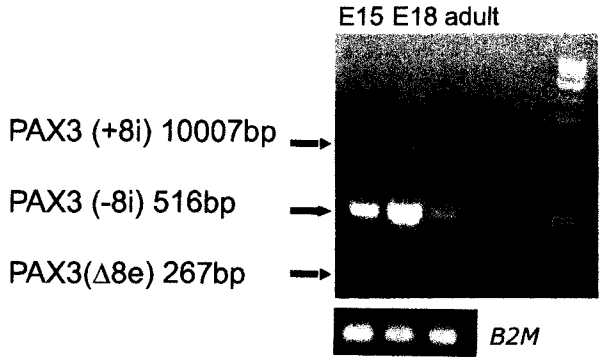
E15 E18 adult
PAX3 (+8i) 10007bp
PAX3 (-8i) 516bp
PAX3(Δ8e) 267bp
B2M

B

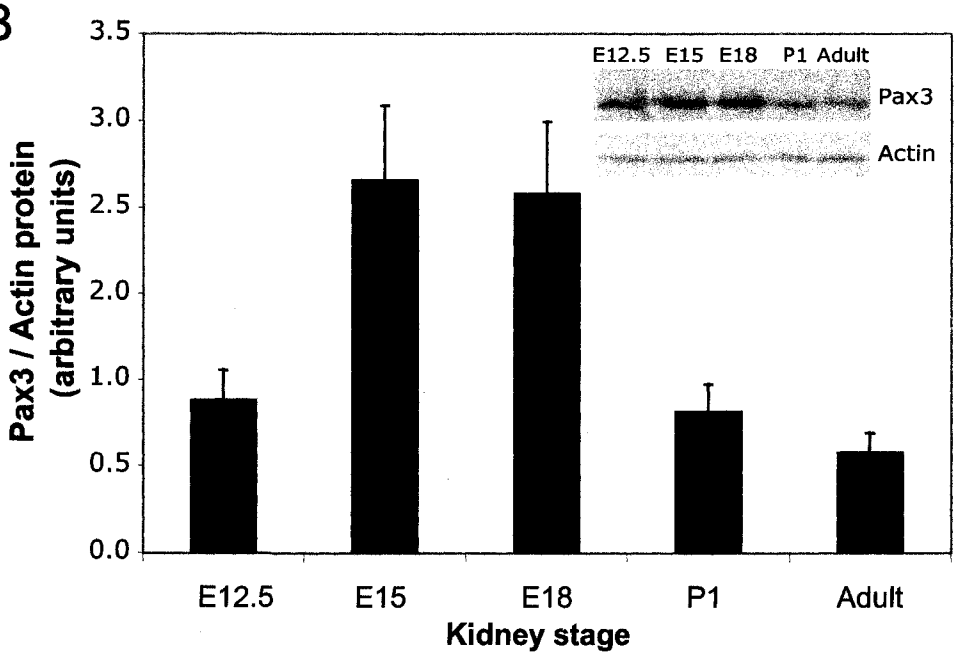
E12.5 E15 E18 P1 Adult
Pax3
Actin
Pax3 / Actin protein (arbitrary units)
3.5
3.0
2.5
2.0
1.0
0.5
0.0
E12.5
E15
E18
P1
Adult
Kidney stage

C

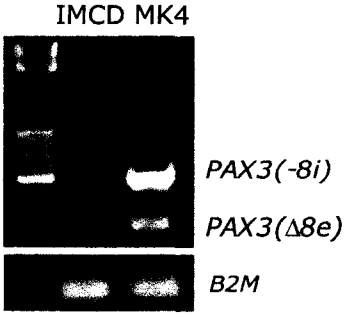
IMCD MK4
PAX3(-8i)
PAX3(Δ8e)
B2M

D

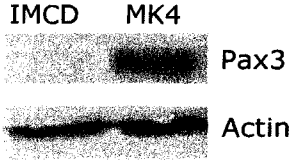
IMCD MK4
Pax3
Actin

Figure 3.2 PAX3 protein localizes in the stromal and the mesenchymal compartments of developing mouse kidney.

PAX3 immunostaining at various stages of development. At E11, PAX3 is not detected in the ureteric bud (UB) or uninduced metanephric mesenchyme, but a strong signal is seen in the neural tube (NT), somites (Som), mandibule (M), lateral and medial nasal process (mnp & lnp); PAX3 is absent from the gut (G), heart (H) and liver (L). From E12.5 onward, PAX3 immunostaining appears in the stromal (Str) and the mesenchymal lineage of the kidney, but is absent from epithelial cells of the S-shaped body (S), glomerulus (G) and collecting duct (CD). From E18 to 6 weeks of age, PAX3 staining is progressively attenuated to a relatively low level in mature kidney.

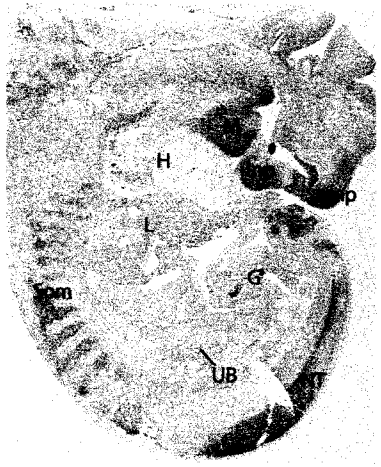

E11

E12.5

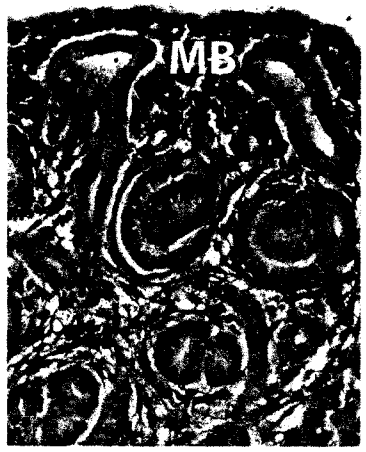

E15

E17

P1

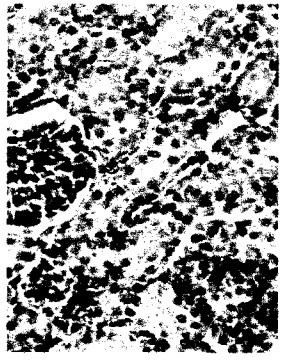

Adult

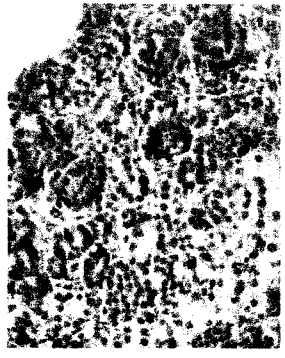

Control (E17)

3.3.3 PAX3 is expressed in a subset of myogenic Wilms Tumor

Since Wilms tumors (WT) are thought to arise from progenitor cells of the metanephric blastema, we considered the possibility that PAX3 might be sustained in tumor tissue, contributing to its phenotype. In preliminary studies, we observed that PAX3 staining was associated with the stromal component of myogenic Wilms tumors; this was especially evident in tumors bearing WT1 mutations (Fig.3.3 A/B). Since PAX3 has a well-known role in setting myoblast fate during normal muscle differentiation, we systematically examined *PAX3* mRNA (qRT-PCR) and PAX3 protein (immunohistochemistry) in a panel of twenty primary Wilms tumors, chosen to include 13 tumors with myogenic characteristics (based on histopathology and gene expression array studies) and 7 tumors without evidence of myogenic markers (21 and unpublished). Nuclear PAX3 mRNA and protein were identified in all myogenic WT (Fig.3.3C). In contrast, PAX3 expression was absent in Wilms tumors devoid of myogenic differentiation (Fig.3.3 B/C). The correlation between myogenic phenotype and PAX3 expression was confirmed by *PAX3* RT-PCR whenever RNA was available (Fig 3.3C). Interestingly, many (8/13) of the myogenic tumors had previously been shown to have *WT1* coding mutations (Fig.3.3 C)

3.3.4 PAX3 is regulated by WT1(-/+KTS) in human embryonic kidney (HEK293) cells

Since WT1 mutations were identified in many of the PAX3-expressing myogenic Wilms' tumors gene, we investigated whether one of the WT1 isoforms could suppress PAX3 expression *in vitro*. First, we tested this hypothesis by overexpressing the four WT1 isoforms in HEK293 cells; PAX3 band intensity was quantified relative to calnexin by Western immunoblotting and compared to the endogenous level in untransfected HEK293 cells. At 48 hours, WT1(+ KTS) suppressed PAX3 protein level to 60% of

baseline (Fig.3.4 A). The other WT1 isoforms had no significant effect on PAX3 protein level (Fig.3.4 A).

Since HEK293 cells express endogenous WT1 protein, we also examined the effect of WT1 inactivation, in transient transfection assays with a WT1 siRNA. By 48 hours WT1 protein level was reduced to 25-50% of baseline 48 hours after siRNA transfection; PAX3/calnexin band intensity rose to about 200% of baseline (Fig.3.4 C).

Figure 3.3 PAX3 mRNA transcript and protein is up regulated in a panel of Wilms Tumor with myogenesis.

A) PAX3 immunostaining of triphasic Wilms tumor tissues. Strong PAX3 expression (arrow) is seen in the stromal component but not in epithelial cells (epith) or blastemal cells (blast). Note that, in the left hand panel, a nest of PAX3(+) stromal cells underlies an area of PAX3(-) cells undergoing myogenic differentiation (Myo).

B) PAX3 immunostaining (arrow) in a stromal-predominant Wilms tumor with proven WT1 mutation. PAX3(-) blastemal cells (blast) lie adjacent to a region of PAX3(+) stromal cells (Str); an epithelial component to the tumor is typically lacking.

C) Summary of the PAX3 immunohistochemistry results in a panel of 13 Wilms tumors with myogenic components and 7 Wilms tumors lacking myogenic features. *PAX3* expression was characterized by quantitative RT-PCR and immunostaining. The coding sequence for *WT1* and *CTNNB1* genes were analyzed by RT-PCR amplification of each exon followed by direct sequencing.

A

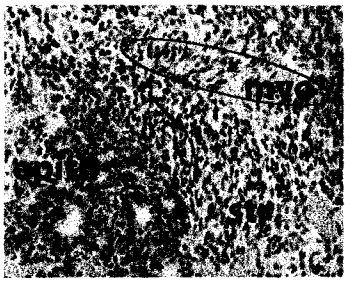

Triphasic

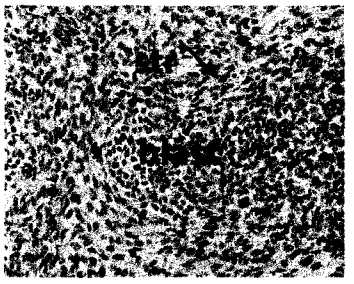

Triphasic

B

WT1 mutant

C

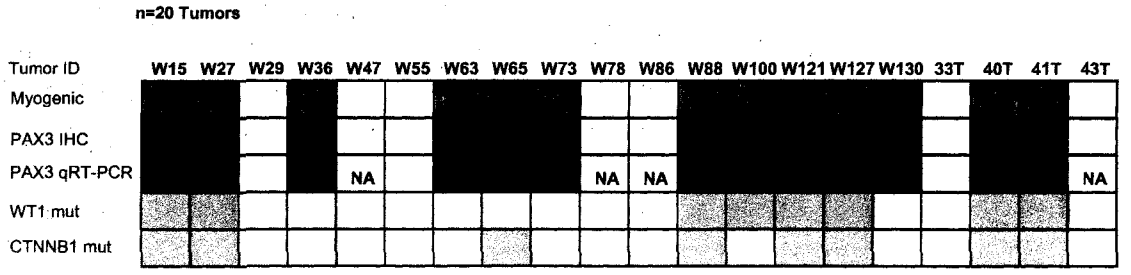

Figure 3.4 WT1 inhibits PAX3 promoter transcriptional activity in human embryonic kidney (HEK293) cells.

A) Representative Western immunoblot showing endogenous PAX3 protein expression in HEK293 cells transiently transfected with various WT1 isoforms. PAX3 band intensity was normalized for calnexin and expressed as a percent of empty vector control. Each bar represents the mean of 3 experiments +/- s.d. *p <0.01.

B) Representative Western immunoblot showing endogenous PAX3 protein expression in HEK293 cells after transient transfection with an siRNA targeting WT1. WT1 and PAX3 band intensities were normalized for calnexin; each bar represents the mean and s.d. as a percentage of standard siRNA control. * p<0.05.

A

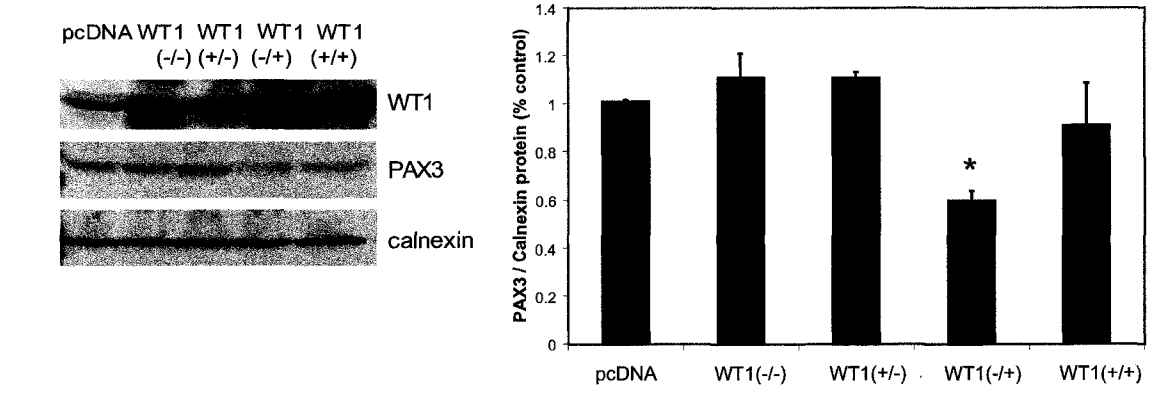
HE293 48h
pcDNA WT1 (-/-) WT1 (+/-) WT1 (-/+) WT1 (+/+)
WT1
PAX3
calnexin
PAX3 / Calnexin protein (% control)
1.4
1.2
1
0.8
0.6
0.4
0.2
0
*
pcDNA
WT1(-/-)
WT1(+/-)
WT1(-/+)
WT1(+/+)

B

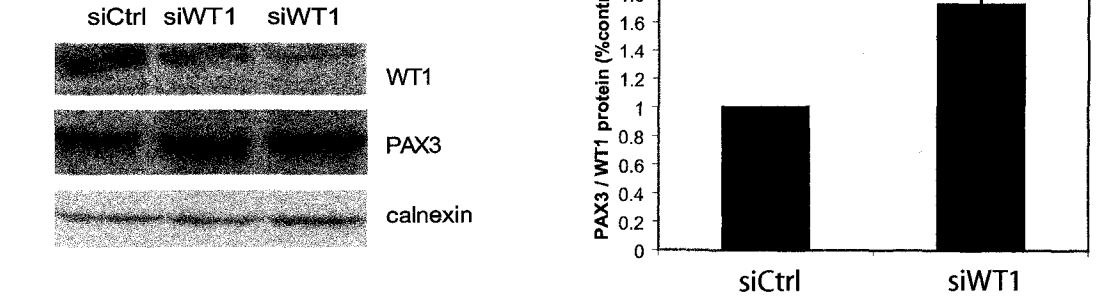
HE293 48h
siCtrl siWT1 siWT1
WT1
PAX3
calnexin
PAX3 / WT1 protein (%control)
2
1.8
1.6
1.4
1.2
1
0.8
0.6
0.4
0.2
0
*
siCtrl
siWT1

3.3.5 PAX3 enhances proliferation and migration of HEK293 cells

Aberrant *PAX3* gene expression has been observed in a variety of cancers, enhancing cell survival by suppressing apoptosis and stimulating cell migration (10). We examined the effect of PAX3 overexpression on the phenotype of HEK293 cells. This human embryonic kidney cell line is derived from the metanephric mesenchyme, expressing low levels of WT1 and PAX2 (13). HEK293 cells were stably transfected with the full-length *PAX3* cDNA and isolated in neomycin selection medium. A clone with high PAX3 protein expression and the parental cell line were used for further study (Fig. 3.5A).

In previous work, we identified a strong anti-apoptotic effect of PAX2 during kidney development (12, 13). To determine whether PAX3 also suppresses apoptosis, we measured caspase-3 activity in the parental HEK293 cell line and the HEK293/PAX3 cells 24 hours after exposure to cisplatin (50uM). There was no protective effect of PAX3 on cisplatin-induced caspase-3 activation (data not shown). In the absence of cisplatin, PAX3 had no effect on proliferation/survival of subconfluent HEK293 cells (assessed by change in total lactate dehydrogenase activity in the monolayer) after 24 hours but a modest but significant increase was noticed after 72h (Fig. 3.5B).

During embryonic development, Pax3 is expressed in myoblasts as they migrate toward the limb bud (14). In a scratch assay, we compared the migration of HEK293 cells after suppression or enhancement of endogenous PAX3 expression. Twenty-four hours after transient transfection with a *PAX3* expression vector or empty vector control (about 75% transfection efficiency), the monolayer was scratched; change in scratch width measured from baseline to 48 hours was used as an index of cell migration. PAX3 overexpression had no apparent effect on cell migration (FIG 3.5E). On the other hand, when we used a PAX3 siRNA to knock down PAX3 expression after 48 hours (Fig. 3.5D), cell migration was significantly reduced (65% of empty vector controls) compared to control cells transfected with a standard siRNA (95% of empty vector controls) (Fig 3.5C).

3.3.6 PAX3 is expressed in a primary cell line derived from the stromal portion of a triphasic Wilms tumor

To further assess the relationship between WT1 and expression of PAX3 or PAX2, we compared a WT1(-) Wilms tumor cell line cell line (WiTP3) to a previously described WT1(+) Wilms tumor cell line (Wit49) {Alami, 2003 #54}. We isolated the novel WitP3 from a stromal nodule protruding through the renal capsule in a triphasic Wilms tumour from a 5-month-old boy (Fig. 6A). *WT1* genomic status was assessed by RT-PCR and direct sequencing. WiTP3 cells exhibited a *de novo* homozygous deletion of the *WT1* gene and WT1 protein was undetectable (Fig. 6B/C). Conversely, WT1 sequence was intact in Wit49 cells (data not shown) and WT1 protein was easily detected (Fig. 6C).

PAX3 protein was abundant in WiTP3 cells as assessed by Western immunoblotting, but PAX2 protein was undetectable (Fig. 6C). In contrast, Wit49 cells expressed high levels of PAX2 protein but no endogenous PAX3 (Fig. 6C).

Figure 3.5 Function of PAX3 in HEK293 cells.

A) Western immunoblot showing low endogenous PAX3 expression in parental HEK293 cells and high PAX3 expression in HEK293 cells stably transfected with *PAX3* cDNA expression vector.

B) Proliferation of HEK293/PAX3 cells compared to parental cell line HEK293 in culture (MTT assay). Bars represent mean cell number of three independent experiments +/- standard deviation (SD).

C) Western immunoblot showing PAX3 knockdown in HEK293 transfected with *PAX3* siRNA compared to siRNA control.

D) Effects of PAX3 overexpression or knockdown on HEK293 cell migration as assessed by scratch wound assay. Cell movement into the wound is shown 48 hours after scratching. Bars represent mean migratory distance normalized to empty vector controls in three independent experiments +/- SD.

A

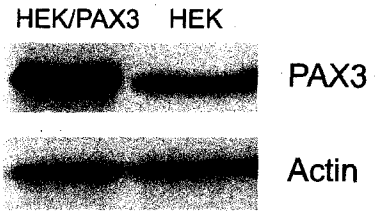
HEK/PAX3
HEK
PAX3
Actin

B

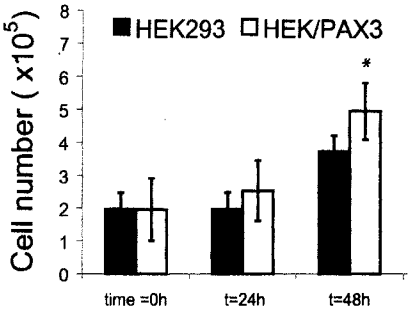
HEK293
HEK/PAX3
Cell number (x10^5)
time =0h
t=24h
t=48h
*

C

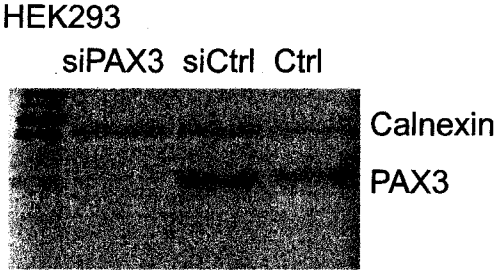
HEK293
siPAX3
siCtrl
Ctrl
Calnexin
PAX3

D

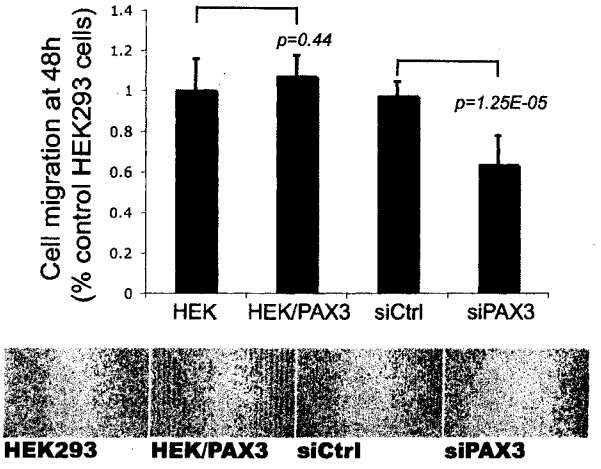
Cell migration at 48h
(% control HEK293 cells)
p=0.44
p=1.25E-05
HEK
HEK/PAX3
siCtrl
siPAX3
HEK293
HEK/PAX3
siCtrl
siPAX3

Figure 3,6 Characterization of a primary Wilms tumor cell line (WiTP3).

A) H&E staining and WT1 immunostaining (left panels) of a triphasic Wilms tumor showing a WT1(-) nodule (Str nod) protruding through the renal capsule. The right-hand panel shows the stromal phenotype of WiTP3 cells in monolayer culture.

B) PCR of *WT1* exons demonstrates homozygous deletion of spanning exons 3-9 in WiTP3 cells; DNA extracted from the patient's peripheral leukocytes shows an intact *WT1* coding sequence.

C) Western immunoblot showing strong PAX3 (but weak PAX2 and absent WT1) expression in WiTP3 cells (lane 2). Conversely, WiT49 cells show strong PAX2 and WT1 protein bands but no PAX3 (lane 3). All three proteins are detected at low levels in control human embryonic kidney HEK293 cells (lane 1).

A

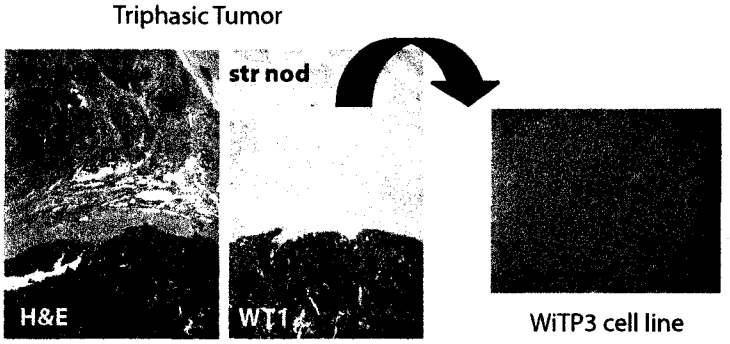
Triphasic Tumor
str nod
H&E
WT1
WiTP3 cell line

B

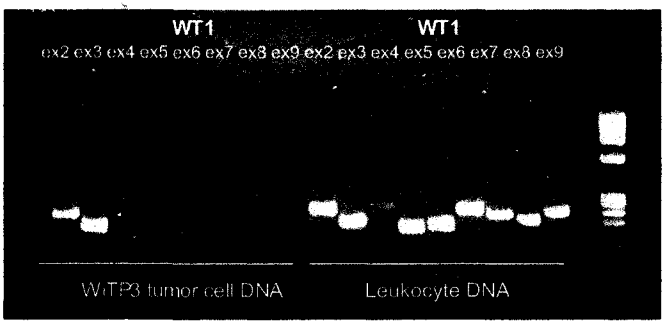
WT1
WT1
ex2 ex3 ex4 ex5 ex6 ex7 ex8 ex9 ex2 ex3 ex4 ex5 ex6 ex7 ex8 ex9
WiTP3 tumor cell DNA
Leukocyte DNA

C

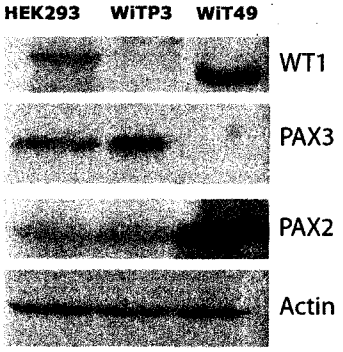
HEK293
WiTP3
WiT49
WT1
PAX3
PAX2
Actin

Figure 3.7 Development model of Wilms tumor molecular pathogenesis.

During normal kidney development, signals from the ureteric bud commit progenitor cells in the metanephric mesenchyme to differentiate toward the nephrogenic lineage (transition to the epithelial phenotype of cells which will form renal tubules) vs the stromal lineage (non-polarized cells which migrate to peritubular zones). Loss of WT1 prevents mesenchyme-to-epithelium transition (MET), sustaining PAX3 expression and stromal phenotype; second genetic hits (eg activating mutations of CTNNB1) are required for Wilms tumorigenesis. When WT1 is intact, progenitor cells can undergo MET, lose PAX3 expression and commit toward nephrogenesis; genetic lesions such as loss of WTX cause Wilms tumors exhibiting triphasic histology with partially-committed blastemal cells that may progress toward PAX2(+) epithelium or regress toward the PAX3(+) stromal phenotype.

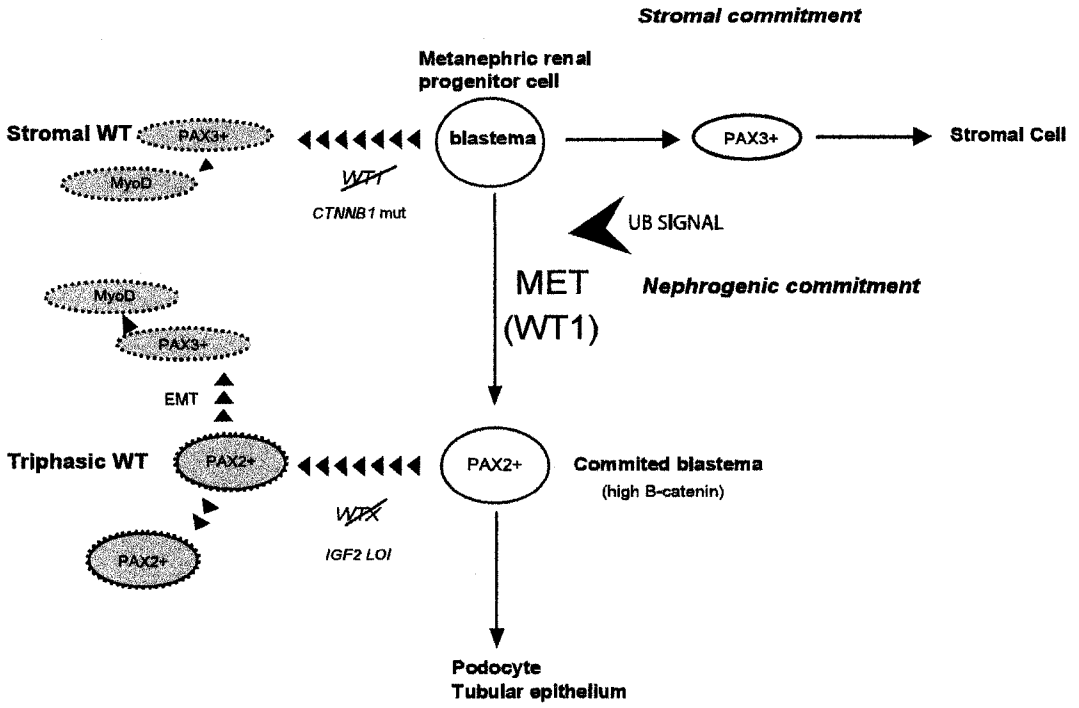
Stromal commitment
Metanephric renal progenitor cell
Stromal WT
PAX3+
MyoD
WT1
CTNNB1 mut
blastema
PAX3+
Stromal Cell
UB SIGNAL
MET
(WT1)
Nephrogenic commitment
MyoD
PAX3+
EMT
Triphasic WT
PAX2+
WTX
IGF2 LOI
PAX2+
PAX2+
Commited blastema
(high B-catenin)
Podocyte
Tubular epithelium

3.4 DISCUSSION

In embryonic kidney, the transcriptions factors PAX2 and PAX8 cooperate in setting cell fate of nephric duct epithelia and in regulation of nephrogenesis. However, no other members of the PAX family were suspected to play a role in renal development until Engleka reported that a 5' flanking sequence of *Pax3* was able to target gene expression to the renal mesenchyme (6). The expression pattern of reporter genes targeted by isolated promoter fragments do not always mirror events in vivo, but here, we demonstrate that robust PAX3 protein is evident in metanephric mesenchyme and throughout the stromal compartment of fetal kidney. Renal PAX3 expression is significantly down-regulated after E18 to the relatively low levels characteristic of adult mice. Accordingly, PAX3 is expressed in the MK4 cell line derived from metanephric mesenchyme, but not in IMCD cells derived from epithelial cells of the renal collecting duct. These observations strongly suggest a developmental role for PAX3 in the renal stromal lineage during organogenesis.

Interestingly, we identified the well-described primary *Pax3* (-8i) transcript in murine kidney and in the MK4 cell line (derived from metanephric mesenchyme). According to Pritchard *et al* this isoform is abundant in myoblasts of developing muscle and exerts the most powerful transcriptional effect on a Pax3-responsive reporter gene *in vitro* (7). However, in both (E15 and E18) fetal mouse kidney samples, we also noted the presence of the *Pax3* (+8i) transcript. The human homolog of this isoform (PAX3D) has been identified in melanoma cells and appears to have similar effect on transcriptional activity of target genes when compared to the human homolog (PAX3C) of murine *Pax3*(-8i) (16). However, since the *Pax3*(+8i) isoform is restricted to fetal kidney, it is conceivable that there is a need for specific fetal regulation of *Pax3* during development involving sequence information within the eighth Pax3 intron.

At E18 (and in MK4 cells) we noted a third *Pax3* transcript, *Pax3*(-8e). Pritchard previously showed that this isoform is present in fetal myoblasts and has very weak

capacity to activate transcriptional activity of a *Pax3*-responsive reporter *in vitro* (7). This suggests that expression of the PAX3(Δ8e) isoform, lacking exon 8, might normally attenuate the transcriptional activity of the predominant PAX3 isoform. In developing kidney, PAX3 protein begins to fall at E18. Conceivably, the transient appearance of an inhibitory isoform could reflect the need to downregulate PAX3 function at that stage.

During normal muscle development, PAX3 is thought to determine cell fate in myoblasts and neural crest cells as they migrate toward peripheral sites within the embryo (14). PAX3 activates a set of genes critical for the myogenic pathway, but PAX3 is downregulated in myoblasts as they take up residence in the limb buds and undergo terminal differentiation (14). During kidney development, signals from the ureteric bud induce adjacent metanephric progenitor cells to undergo mesenchyme to epithelial transition and form the epithelial component of individual nephrons. A second subset of the metanephric progenitor cells acquires markers of the stromal lineage such as RARβ and FOXB (17, 18). These cells migrate inward from the nephrogenic zone to form the stromal compartment surrounding renal glomeruli and tubules. Our "scratch" assays showed that PAX3 knockdown blunts migration of human embryonic kidney (HEK293) cells *in vitro*. It is therefore plausible that PAX3 regulates molecular pathways involved in stromal cell movement during normal kidney development.

Although many Wilms tumors show "triphasic" histology, comprised of mixed blastemal, epithelial and stromal components (23), a discrete subset of tumors (5-10%) exhibit a predominantly "stromal" phenotype with elements showing myogenic differentiation (19-22). This subset of Wilms tumors is further defined by genomic lesions of *WT1* and associated missense mutations of the beta-catenin gene (*CTNNB1*) exon 3, causing constitutive activation of the canonical WNT signaling pathway (21, 23, 24). Since, we identified strong PAX3 expression in stromal cells of the developing kidney, we hypothesized that PAX3 might be characteristic of Wilms tumors with predominance of mesenchymal cells. We used a panel of myogenic (N=13) vs non-myogenic (N=7) Wilms tumors to determine whether aberrant PAX3 expression was associated with the myogenic phenotype (2). We noted that PAX3 mRNA and protein was expressed in all

myogenic tumor samples, but were never seen among the non-myogenic tumors. This observation strongly suggests that PAX3 expression underlies the myogenic phenotype of this Wilms tumor subset. Interestingly, gene rearrangements which fuse the PAX3 DNA binding domain to a truncated 3' portion of the forkhead gene (*FKHR*) cause aggressive rhabdomyosarcomas in humans (25)

Since aberrant PAX3 expression was highly associated with *WT1* mutations in our Wilms tumor panel, we examined the effect of WT1 on PAX3 expression in HEK293 cells in vitro. When the cells were transiently transfected with WT1 (-/+ KTS), PAX3 protein levels were reduced to 60% of control after 48 hours. Conversely, when siRNAs were used to knock down endogenous WT1 expression to about 50% of control, we observed a corresponding increase in PAX3 protein of about 30%. Taken together, these studies support the hypothesis that *PAX3* is normally regulated by WT1 during renal development. This idea is consistent with our observation that PAX3 is excluded from WT1-expressing cells such as the glomerular podocyte and with the report that transient transfection of *WT1* into murine C2C12 myoblasts inhibits the myogenic program (3) However, we noted Pax3 expression in three myogenic tumors apparently lacking a mutation of the *WT1* coding sequence. Furthermore, the effects of WT1 on *in vitro* expression of PAX3 were modest, suggesting that other factors may be important for PAX3 regulation. Alternatively, WT1 could affect PAX3 in an indirect manner, simply by promoting the mesenchyme-to-epithelium transition of progenitor cells.

We isolated a primary stromal cell line (WiTP3) from a patient with a large stromal nodule arising within a triphasic Wilms Tumor. Although WT1 immunostaining was strong in blastemal and epithelial compartments of the tumor, the stromal nodule lacked WT1 immunostaining and the stromal cell line was found to have deletion of both WT1 alleles. Relatively high levels of PAX3 mRNA and protein were evident in WiTP3 cells, whereas PAX2 protein was barely detectable. This contrasts with the WT1-positive WiT49 Wilms tumor cell line isolated by Alami et al., (15) which expresses abundant PAX2 but no PAX3. The contrasting gene expression patterns in these two cell lines

further support the dichotomy between the PAX3-positive and PAX3-negative subtypes of Wilms tumors.

We propose a model of normal renal development in which progenitor cells of the metanephric blastema express PAX3 when targeted toward the stromal cell fate. PAX3 expression may contribute to the phenotype of migrating stromal cells, but does not appear to have a major influence on cell division or control of apoptotic pathways. Suppression of PAX3 is integral to the mesenchyme-to-epithelium transition, which defines the nephrogenic cell fate and may be accomplished, in part, by WT1. Conversely, failure to suppress PAX3 may account for the myogenic phenotype in a subset of WT1-negative Wilms tumors.

ACKNOWLEDGEMENTS

PAX3 antibody was obtained from hybridoma culture media. (Developmental Studies Hybridoma Bank, Iowa City, IA). The WiT49 cell line was a gift from Dr H Yeger (Hospital for Sick Children Toronto, Canada). This work was supported by an operating grant from the Kidney Foundation of Canada. Pierre-Alain Hueber was the recipient of a Graduate Studentship award from the Montreal Children's Hospital Research Institute. Paul Goodyer is the recipient of a James McGill Research Chair.

3.5 METHODS

Western Immunoblotting

Cells or embryonic kidney were lysed in radioimmunoprecipitation assay (RIPA) buffer [50 mmol/L Tris-Cl (pH 8.0), 150 mmol/L NaCl, 1% NP40, 0.5% sodium deoxycholate, 0.1% SDS, 1 mmol/L phenylmethylsulfonyl fluoride, 1 mmol/L sodium orthovanadate]. Subsequently, protein concentrations were determined using the protein assay reagent kit (Pierce, Rockford, IL) with bovine serum albumin as a standard. Equivalent amounts of protein were loaded in each lane of a 10% SDS polyacrylamide gel and electrophoresed followed by blotting onto a polyvinylidene difluoride membrane. After blocking with 5% (w/v) fat-free milk powder, 0.1% Tween 20 in PBS, the membrane was incubated for 1 hour at room temperature with anti-PAX3 antibody (1:1000) (Hybridoma bank, University of Iowa), anti-WT1 antibody (Santa-Cruz, CA); anti-PAX2 1/250 antibody (Zymed, Santa-Cruz, CA) or anti-actin antibody (Sigma, St. Louis, MO) diluted into 3% (w/v) fat-free milk powder, 0.1% Tween 20 in PBS, washed and incubated with secondary antibody (Sigma). The membrane was then washed and incubated with ECLplus reagents according to the manufacturer's directions (Amersham, GE Healthcare Buckinghamshire UK). The signals were then detected using a Phosphoimager (Amersham, GE Healthcare Buckinghamshire UK)

Immunohistochemistry on embryonic mouse kidney

PAX3 staining was carried out as previously described. Briefly, sections were deparaffinized and re-hydrated using xylene and graded alcohol series, then rinsed in tap water. Microwave antigen retrieval using 0.01 M citrate buffer (pH 7.0 and pH 2.0, respectively) was performed twice for 30 min. Sections were incubated with primary mouse monoclonal anti-quail PAX3 antibody (Hybridoma bank, Iowa, USA) (1:100) overnight at 4°C. Slides were then incubated with secondary biotinylated horse anti-mouse IgG at room temperature for 30 min, followed by avidin-biotinylated horseradish peroxidase (HRP) for 30 min according to the manufacturer's instructions (Vector Laboratories). Peroxidase activity was developed for 2 min at RT using

diaminobenzidene tetrachloride (DAB; Zymed) as the chromogen, with hematoxylin as the counterstain, and then rinsed in Scott's water for 5 minutes.

Patient samples

20 Wilms tumors samples were selected from a collection of tumors obtained with informed consent from North Health Ethics Committee Auckland, New Zealand. For all tumors, each WT1 exon was amplified by PCR and sequenced {Fukuzawa, 2004 #2}. The cell line WiTP3 was obtained with informed consent from a Wilms tumor ressected at the Montreal Children's Hospital under a Children Oncology Group (COG) protocol, approved by the Institutional Review Board.

Immunohistochemistry on Wilms Tumor tissue

WT1 (6F-H2, DAKO, CA, USA), PAX3 (Hybridoma bank, Iowa, USA) were used as primary antibodies, and the DAKO Envision horseradish peroxidase system (K4001, DAKO Cytomation, CA, USA) was used to detect the primary antibodies

RNA Extraction

RNA was extracted from cells using RNeasy plus kit (Qiagen, Valencia, CA) as per manufacturer's recommendations. RNA quantities and quality were assessed by spectrophotometry. (NanoDrop ND-1000, Wilmington, DE, USA

***PAX3* RT-PCR**

Mouse *Pax3* transcripts were amplified from RNA isolated from whole embryonic kidney using the primers spanning exon 7-9 as described by Pritchard and colleagues {Pritchard, 2003 #49}

5' GTGTCAGATCCCAGTAGCACCG 3'

5' TCCAAGTGGACAGTTCACTTATGC 3'.

Quantitative PAX3 RT-PCR

PAX3 mRNA expression was quantified in relationship to the mRNA level for a housekeeping gene, ubiquitin-conjugating enzyme *E2G2* according to the formula: PAX3/E2G $2=(E_{Pax3})^{\Delta CTPax3\ (mean\ control\ -\ mean\ sample)} / (E_{E2g2})^{\Delta CTE2g\ 2(mean\ control-\ mean\ sample)}$, using Relative Expression Software Tool (REST© – Pffafl *et al.*, 2002) and average efficiencies calculated by LinRegPCR.

Human PAX3 primers were as follows:

Forward primer (exon2): 5' TCCATACGTCCTGGTGCCAT 3'

Reverse primer (exon3): 5' TTCTCCACGTCAGGCGTTG 3'

WT1 *PCR*

Primers for each *WT1* exon are summarized below (annealing temperature = 58°C)

WT1 exon	Forward primers 5'-3'	Reverse primer 5'-3'	amplicon (bp)
exon 1A	CAGCAAATGGGCTCCGACGTG	CGGGCGCTTCGGCTTAC	150
exon 1B	CCGGTGCTGGACTTTGCG	CCTGAATTCCCGGCCTACTTACCC	351
exon 2	GTGGCTGGTTCAGACCCA	GAGGATAGCACGGAAGAAG	250
exon 3	CAGCCTCGCACCCCGAGC	CAAGGACCCAGACGCAGA	199
exon 4	TGTGGAGGCTTGCACTTTC	TCTTCATAAGTTCTAAGCACC	271
exon 5	CCATGCATGCTCC	AGTCCTAACTCCTGCATTGC	179
exon 6	GATAAGCATTTCCAAATGGCG	GCTGGGGCCTGTCTGTG	185
exon 7	CAAGACCTACGTGAATGTTC	TGTTTGCCCAAGACTGGAC	249
exon 8	AGGAGAGGTTGCCTTTAATGA	AAGAGAATCATGAAATCAACCC	230
exon 9	GGCCGAGGCTAGACCTTC	TCCATCCCTCTCATCACAAT	211
exon 10	GACTTCACTCGGGCCTTG	GCCTGGGACACTGAACGG	236

Cell lines

HEK293 cells were purchased from ATCC and grown in DMEM media (Invitrogen, Carlsbad, CA, USA) supplemented with 10% fetal calf serum and 10% Pen/Strep (Invitrogen, Carlsbad, CA, USA). The WiT49 cell line (derived from a primary lung metastasis of an aggressive Wilms tumor) {Alami, 2003 #54} was generously provided by Dr H Yeger (The Hospital for Sick Children, Toronto, Canada). WiT49 cells were maintained in 1:1 high glucose DMEM:F12 Nutrient Mix, 10% fetal calf serum, 100

U/ml penicillin, 100 μg/ml streptomycin. The HEK293/PAX3 cell line was generated by transfecting HEK293 with a PAX3 cDNA expression vector; stably transfected clones were selected and maintained in media containing neomycin. PAX3 expression was confirmed by Western immunoblotting. Primary WiTP3 cells were isolated from a stromal nodule arising from within a triphasic Wilms tumor resected from a 5 month-old patient at the Montreal Children's Hospital. A sample of the stromal nodule was microdissected and cultured in DMEM (Invitrogen, Carlsbad, CA, USA) with 10% fetal calf serum.

RNA interference

Short interfering RNA (siRNA) duplexes specific for human WT1 were obtained from Santa Cruz Biotechnology Inc. (Santa Cruz, CA, USA). The PAX3 silencer, pre-designed human PAX3 siRNA ID# 215907, and a standard negative siRNA control were obtained from Ambion (Austin, TX, USA). HEK293 cells were transfected with 10nM of siRNA using lipofectamine 2000 (Invitrogen, Carlsbad, CA, USA) according to the manufacturer's protocol.

REFERENCES:

1. Rivera MN, Haber DA. Wilms' tumour: connecting tumorigenesis and organ development in the kidney. *Nat Rev Cancer* 2005; **5:** 699-712.

2. Kim HS, Kim MS, Hancock AL, Harper JC, *et al.* Identification of novel Wilms' tumor suppressor gene target genes implicated in kidney development. *J Biol Chem* 2007; **282:** 16278-16287.

3. Li CM, Guo M, Borczuk A, Powell CA, *et al.* Gene expression in Wilms' tumor mimics the earliest committed stage in the metanephric mesenchymal-epithelial transition. *Am J Pathol* 2002; **160:** 2181-2190.

4. Mendelsohn C, Batourina E, Fung S, Gilbert T, *et al.* Stromal cells mediate retinoid-dependent functions essential for renal development. *Development* 1999; **126:** 1139-1148.

5. Schmidt-Ott KM, Chen X, Paragas N, Levinson RS, *et al.* c-kit delineates a distinct domain of progenitors in the developing kidney. *Dev Biol* 2006; **299:** 238-249.

6. Engleka KA, Gitler AD, Zhang M, Zhou DD, *et al.* Insertion of Cre into the Pax3 locus creates a new allele of Splotch and identifies unexpected Pax3 derivatives. *Dev Biol* 2005; **280:** 396-406.

7. Pritchard C, Grosveld G, Hollenbach AD. Alternative splicing of Pax3 produces a transcriptionally inactive protein. *Gene* 2003; **305:** 61-69.

8. Valerius MT, Patterson LT, Witte DP, Potter SS. Microarray analysis of novel cell lines representing two stages of metanephric mesenchyme differentiation. *Mech Dev* 2002; **112:** 219-232.

9. Stoos BA, Naray-Fejes-Toth A, Carretero OA, Ito S, *et al.* Characterization of a mouse cortical collecting duct cell line. *Kidney Int* 1991; **39:** 1168-1175.

10. Robson EJ, He SJ, Eccles MR. A PANorama of PAX genes in cancer and development. *Nat Rev Cancer* 2006; **6:** 52-62.

11. Torban E, Goodyer PR. Effects of PAX2 expression in a human fetal kidney (HEK293) cell line. *Biochim Biophys Acta* 1998; **1401:** 53-62.

12. Dziarmaga A, Hueber PA, Iglesias D, Hache N, *et al.* Neuronal apoptosis inhibitory protein is expressed in developing kidney and is regulated by PAX2. *Am J Physiol Renal Physiol* 2006; **291:** F913-920.

13. Torban E, Eccles MR, Favor J, Goodyer PR. PAX2 suppresses apoptosis in renal collecting duct cells. *Am J Pathol* 2000; **157:** 833-842.

14. Buckingham M, Relaix F. The Role of Pax Genes in the Development of Tissues and Organs: Pax3 and Pax7 Regulate Muscle Progenitor Cell Functions. *Annu Rev Cell Dev Biol* 2006.

15. Alami J, Williams BR, Yeger H. Derivation and characterization of a Wilms' tumour cell line, WiT 49. *Int J Cancer* 2003; **107:** 365-374.

16. Wang Q, Kumar S, Slevin M, Kumar P. Functional analysis of alternative isoforms of the transcription factor PAX3 in melanocytes in vitro. *Cancer Res* 2006; **66:** 8574-8580.

17. Hatini V, Huh SO, Herzlinger D, Soares VC, *et al.* Essential role of stromal mesenchyme in kidney morphogenesis revealed by targeted disruption of Winged Helix transcription factor BF-2. *Genes Dev* 1996; **10:** 1467-1478.

18. Dolle P, Ruberte E, Leroy P, Morriss-Kay G, *et al.* Retinoic acid receptors and cellular retinoid binding proteins. I. A systematic study of their differential pattern of transcription during mouse organogenesis. *Development* 1990; **110:** 1133-1151.

19. Schumacher V, Schneider S, Figge A, Wildhardt G, *et al.* Correlation of germ-line mutations and two-hit inactivation of the WT1 gene with Wilms tumors of stromal-predominant histology. *Proc Natl Acad Sci U S A* 1997; **94:** 3972-3977.

20. Fukuzawa R, Heathcott RW, More HE, Reeve AE. Sequential WT1 and CTNNB1 mutations and alterations of {beta}-catenin localisation in intralobar nephrogenic rests and associated Wilms tumours. *J Clin Pathol* 2006.

21. Fukuzawa R, Heathcott RW, Sano M, Morison IM, *et al.* Myogenesis in Wilms' tumors is associated with mutations of the WT1 gene and activation of Bcl-2 and the Wnt signaling pathway. *Pediatr Dev Pathol* 2004; **7:** 125-137.

22. Miyagawa K, Kent J, Moore A, Charlieu JP, *et al.* Loss of WT1 function leads to ectopic myogenesis in Wilms' tumour. *Nat Genet* 1998; **18:** 15-17.

23. Schumacher V, Schuhen S, Sonner S, Weirich A, *et al.* Two molecular subgroups of Wilms' tumors with or without WT1 mutations. *Clin Cancer Res* 2003; **9:** 2005-2014.

24. Maiti S, Alam R, Amos CI, Huff V. Frequent association of beta-catenin and WT1 mutations in Wilms tumors. *Cancer Res* 2000; **60:** 6288-6292.

25. Davis RJ, Barr FG. Fusion genes resulting from alternative chromosomal translocations are overexpressed by gene-specific mechanisms in alveolar rhabdomyosarcoma. *Proc Natl Acad Sci U S A* 1997; **94:** 8047-8051.

CHAPTER IV: DISCUSSION AND FUTURE DIRECTIONS

4.1 DISCUSSION

4.1.1 Paradigm

Embryonic and tumor cells share similar features as they both have potential for rapid proliferation, migration and dedifferentiation. Accordingly the same genetic programs that are active during embryogenesis are often re-activated during tumorigenesis (Monk & Holding, 2001). Furthermore embryonic genes expressed in human tumors are typically not expressed in normal adult tissues and thereby have the potential of being specific targets for cancer therapy (Dressler and Woolf, 1999; Monk and Holding, 2001). The transcription factor PAX2 is essential and abundantly expressed during normal kidney development but is downregulated once organogenesis is completed. On the other hand, PAX2 is estimated to be aberrantly expressed in 25% of cancers, including breast, brain, lymphoma and ovarian (Muratovska *et al.*, 2003). In particular PAX2 expression is considered a reliable and specific marker for renal cell carcinoma (RCC) tumors; about 90% of clear cell carcinomas exhibits nuclear PAX2-postive immunostaining (Daniel *et al.*, 2001; Mazal *et al.*, 2005).

During normal kidney development PAX2 functions as an anti-apoptotic gene (Dziarmaga *et al.*, 2006a; Torban *et al.*, 2000). Apoptosis is a genetically controlled process that plays an important role in both embryonic development and adult tissues homeostasis, by which cells can initiate their own death in response to specific stimuli (Kerr *et al.*, 1972). Cells undergoing apoptosis or programmed cell death are typically (Kerr *et al.*, 1972) characterized by the activation of the caspase-enzyme family.

Apoptosis can be triggered by chemotherapeutic drugs and is considered an important mechanism by which chemotherapy exerts its anti-tumoral therapeutic effect. For example, platinum-compounds such as cisplatin used in clinical oncology for more than 30 years, control tumor growth by causing cellular DNA damage resulting in cancer cells apoptosis (Kelland, 2007). On the other hand, apoptosis resistance can hamper the sensitivity of cancer cells to chemotherapy; renal cancer has a notorious resistance to chemotherapy, which is thought to be the primary cause of its poor prognosis (Motzer *et*

al., 1997). Various mechanisms can underlie the resistance of cancer cells to cisplatin-induced apoptosis among which is the overexpression of anti-apoptotic genes (Kelland, 2007).

Building on the well-established anti-apoptotic function of PAX2 in development we hypothesize that PAX2 expression in RCC contributes to its resistance to cisplatin-induced cell death. Hence targeted inhibition of PAX2 should selectively sensitize RCC cells to cisplatin therapy whereas it should have minimal influence on normal tissues in which PAX2 has been appropriately downregulated. Thus the first objective was to determine whether the anti-apoptotic function of PAX2 played a significant role in the response to chemotherapy.

4.1.2 PAX2 confers resistance to cisplatin-induced apoptosis

Our first aim was to show that the role of PAX2 in protecting embryonic cells from apoptosis could be extended to normal kidney cells that are challenged with a pro-apoptotic agent such as a chemotherapeutic drug. To address this issue we generated cell lines expressing different levels of PAX2 and examined their susceptibility to apoptosis when treated with cisplatin. The human embryonic kidney (HEK293) cell line was chosen as a model of a human renal cell lineage; aberrant PAX2 expression in this cell line was produced by stable transfection with a *PAX2* expression vector. We chose cisplatin as a representative of the chemotherapeutic drugs that typically causes cancer cell death via induction of apoptosis (Eastman, 1990; Lee *et al.*, 2001; Park *et al.*, 2002). Cisplatin induces apoptosis of renal cells; indeed this accounts for the well-known nephrotoxicity of cisplatin. Cisplatin is effective in other tumors of the genitourinary tract might be a useful agent in RCC if the resistance to apoptosis could be overcome (Servais *et al.*, 2007).

Activation of the apoptotic pathway by chemotherapy eventually converges on caspase-3,

leading to the morphological changes associated with programmed cell death. Since caspase-3 is considered the central effector of apoptosis, we assessed caspase-3 activity as a measure of apoptosis pathway activity. We showed that cisplatin treatment activates capase-3 in HEK293 cells but that PAX2 overexpression diminishes cisplatin-induced caspase-3 activation. Conversely suppressing endogenous PAX2 in a murine inner medullary collecting duct cell line sensitizes the cells to caspase-3 activation following cisplatin treatment.

These experiments establish that PAX2 expression in normal cells is protective against cisplatin treatment and suggests that the PAX2 level in renal cells correlates with their susceptibility to cisplatin-induced apoptosis. Our findings are consistent with other studies which have shown that the level of PAX2 protein in endothelial cells is correlated with sensitivity to vincristine-induced apoptosis (Fonsato *et al.*, 2006).

4.1.3 Suppression of PAX2 enhances cisplatin-induced apoptosis in RCC cells

We predicted that the role of PAX2 in protecting normal embryonic cells from apoptosis could be extended to renal tumor cells that express endogenous PAX2 and exhibit a chemoresistant phenotype. We supposed that by inhibiting PAX2 the cellular apoptotic machinery balance would be shifted towards cell death and enhance sensitivity to chemotherapy.

Although PAX2 expression is well established in primary renal tumors, we had to find a PAX2 expressing renal cancer cell line that could serve as an *in vitro* model. We screened all the renal cancer cell lines of the NCI-60 panel which includes 60 human cancer cell lines used by the Developmental Therapeutic Program of the National Cancer Institute (NCI) to screen compounds for anticancer activity (Grever *et al.*, 1992; Weinstein *et al.*, 1997). Using Western immunoblotting to measure PAX2 protein expression we found that A498, CAKI-1 and ACHN cells express significant levels of PAX2 protein. On the

other hand, some other renal cancer cell lines such as 786-0 did not express PAX2 protein. CAKI-1 and ACHN are both cell lines derived from metastatic clear cell carcinoma found in the pleural effusion of patients and therefore are representative of chemo-resistant metastatic aggressive RCC tumors.

In order to inhibit PAX2 expression, we initially used *PAX2* oligonucelotide antisenses (AS-ODN). We had mixed success with AS-ODNs because of nonspecific toxicity and this led us to an alternative approach using small inhibitory RNAs (siRNA). These molecules had just emerged as the state-of-the-art strategy for targeted knockdown of genes in mammalian cell lines (Couzin, 2002). Treatment with *PAX2*-siRNA successfully inhibited the expression of PAX2 protein in RCC cells ACHN and CAKI-1.

The reduction of PAX2 expression in RCC cells results in an increase in the level of basal apoptosis. In addition, RCC cells with reduced levels of PAX2 were more sensitive to the therapeutic effect of cisplatin treatment both in terms of apoptosis measured by annexin V and cell survival measured by a dehydrogenase enzymatic assay. Although PAX2 has been previously shown to be important for RCC cell survival (Gnarra & Dressler, 1995), our studies demonstrate for the first time that inhibition of PAX2 results in caspases-dependent apoptosis in RCC cells. This was conclusively shown by the observation that pre-treatment of of RCC cells with the drug Z-Vad-Fmk (a pan caspases inhibitor) was able to prevent the cell death induced by the combined effect of PAX2 inhibition and cisplatin treatment.

Since the publication of our results, several studies have shown that PAX2 inhibition causes apoptosis in a variety of cancer cell types including ovarian, prostate carcinoma and Karposi sarcoma (KS). Our collaborator from the Eccles group in New Zealand showed that PAX2 expression is required for ovarian cancer cell survival; *PAX2*-siRNA treatment causes a 50% decrease in cell survival (Muratovska *et al.*, 2003). In KS cells, Buttiglieri and colleagues observed that inhibition of PAX2, using stable transfection of *PAX2* antisense, significantly increased the number of apoptotic KS cells measured by TUNNEL assay under basal conditions. It also enhanced the sensitivity of KS cells to

apoptosis induced by serum deprivation or vincristine treatment (Buttiglieri *et al.*, 2004). Similarly, inhibition of PAX2 using *PAX2*-siRNA in prostate cancer cells results in significant cellular death (Gibson *et al.*, 2007). Thus, our observations have been broadened by other to additional forms of cancer and have clearly established a role for PAX2 in setting susceptibility of cancer cell to apoptosis.

However, the molecular mechanism by which PAX2 acts on the apoptosis pathway remains rather unclear. In endothelial cells, PAX2 expression was associated with a reduction of expression of the tumor suppressor gene PTEN and concomitant activation of the AKT-survival pathway. Interestingly the PTEN/AKT pathway is often deregulated in RCC (Hara *et al.*, 2005) and its aberrant activation has been demonstrated as a molecular mechanism of cisplatin resistance (Stewart, 2007). In addition, AKT expression significantly decreases in p53 wildtype LNCaP and DU145 prostate cancer cells following PAX2 knockdown. Yet the AKT levels were unchanged in p53 mutant PC3 cells (Gibson *et al.*, 2007). These observations suggest that PAX2 perhaps interacts with the AKT pathway at least when p53 is intact.

P53 acts on the apoptotic pathway via activation of mitochondrial pro-apoptotic genes including BAX and PUMA (Jiang *et al.*, 2006) and is involved in cisplatin-induced apoptosis of renal cells (Wei *et al.*, 2007a; Wei *et al.*, 2007b). Furthermore p53 can contribute to resistance of cancer cells to cisplatin (Lin and Howell, 2006), and has been suggested as a PAX2 target gene (Stuart *et al.*, 1995). However studies in prostate cancer show that apoptosis induced by PAX2 knockdown is independent of p53 function (Gibson *et al.*, 2007). This latter observation is consistent with our results in which PAX2 inhibition causes apoptosis both in an RCC cell line (ACHN) with wild-type p53 and in a RCC cell line (CAKI) with a null mutation of p53.

The anti-apoptotic function of PAX2 was first discovered in normal embryonic mouse kidney cells. This anti-apoptotic activity appears to involve activation of NAIP (Neuronal Inhibitor of Apoptosis), a gene belonging to the "inhibitor of apoptosis" (IAP) family. IAP proteins are major regulators of apoptosis primarily due to their ability to inhibit

cellular caspases enzymes (Deveraux *et al.*, 1998; Deveraux *et al.*, 1999). NAIP was shown to be downstream target gene of PAX2 in normal embryonic kidney. The NAIP anti-apoptotic function was confirmed in renal collecting duct cells, in which inhibition of NAIP enhances caspases activation upon apoptotic stimulus induced by transfection with the mitochondrial pro-apoptotic *BAX-α* (Dziarmaga *et al.*, 2006a).

Nevertheless when we looked for differences in NAIP expression in ACHN cells with PAX2 knockdown compared to ACHN parental cells, the NAIP protein levels were not affected, suggesting that PAX2 suppresses apoptosis in RCC cells via some other mechanism.

Although expression of the eight members of the IAP family have been described in cancer cells, XIAP is considered to be the most potent member in terms of its ability to inhibit caspase activity. Interestingly high levels of XIAP expression are observed in RCC tumors (Mizutani *et al.*, 2005; Ramp *et al.*, 2004; Yan *et al.*, 2004) and correlates with a bad prognosis. Moreover inhibition of XIAP expression with siRNA induced apoptosis and sensitized renal cancer cells to TRAIL-induced apoptosis (Chawla-Sarkar *et al.*, 2004). However, XIAP mRNA level was unchanged in cisplatin-resistant HEK293/PAX2 cells compared to cisplatin-sensitive HEK293 cells as assessed in an expression gene array (Dziarmaga *et al.*, 2006a). To date there is no evidence that PAX2 interacts with XIAP in renal cells.

In summary, although the molecular mechanism by which PAX2 interacts with the apoptotic pathway appears complex and perhaps context-specific, our studies clearly demonstrate that PAX2 inhibition causes caspase-dependent RCC cell death and enhances *in vitro* the potential of cisplatin to reduce renal cancer cell survival. Our findings suggest that strategies inactivating aberrant PAX2 expression in renal tumor tissue might be used in combination with classic chemotherapy protocol to enhance the response to therapy.

4.1.4 Suppression of PAX2 enhances *in vivo* response of renal tumor to cisplatin

The second major objective of my research project was to develop an *in vivo* model of renal tumors that allows us to test the therapeutic potential of PAX2 inhibition in combination with cisplatin treatment. Subcutaneous injection (s.c) of human cancer cells in nude mice forms xenografts and has been used as a standard tumor model for testing drugs in a pre-clinical setting. By injecting ACHN cells under the skin of nude mice, we generated an *in vivo* model to test the effect of PAX2 inhibition on cisplatin response.

Although synthetic *PAX2* siRNAs were useful to establish proof of principle *in vitro*, in vivo delivery of siRNAs remain highly challenging and are extremely costly. For these reasons, we decided to establish proof-of-principle in vivo, by using a plasmid-based expression system that allows a stable expression of siRNAs in the RCC cells. Transfection of cells with shRNA-producing plasmids has the advantage of a more pronounced and long-lived knockdown compared to transient transfection with siRNA (Yu *et al.*, 2002).

Our strategy was to engineer an RCC cell line that constitutively expresses a PAX2 shRNA to achieve a lasting and efficient knockdown of PAX2 expression in 100% of the cells. We constructed various *PAX2* shRNA expression vectors and screened them individually for PAX2 knockdown in ACHN cell lines. Clones with PAX2 inhibition and sensitization to cisplatin *in vitro* were injected under the skin of nude mice and tumor growth was compared to ACHN/empty vector controls. PAX2 inhibition clearly enhanced the suppression of tumor growth in response to cisplatin over a five-day observation period.

An interesting observation is that PAX2 knockdown in the absence of cisplatin treatment ACHN cells did not affect basal growth of subcutaneous tumor xenografts. Thus, PAX2 appears to modify susceptibvility to cisplatin but is not required for malignant growth of RCC cells. In contrast, Wu et al. observed that PAX2 knockdown in endometrial cancer cells results in a significant decrease in tumor xenograft growth (Wu *et al.*, 2005).

Conceivably, other genes exert a partially redundant function for PAX2 in RCC. Interestingly, PAX8 has is expressed in ACHN cells and has been shown by Bouchard to have overlapping function with PAX2 during normal kidney development.

Following the discovery of the RNA interference (RNAi) pathway (Fire *et al.*, 1998), it was demonstrated that small-interfering RNAs (siRNA) could be exploited for gene silencing in mammalian cells (Elbashir *et al.*, 2001). VEGF siRNA has recently been shown to be safe and well tolerated in clinical phase I trials as treatment for age-related macular degeneration (AMD) (Kim & Rossi, 2007). Our observations establish proof-of-principle that PAX2 siRNA knockdown might have potential as adjunctive therapy in renal cell carcinoma.

Despite the promising results in terms of the safety of RNAi based therapeutics, the principal challenge is the actual delivery of these agents (de Fougerolles *et al.*, 2007). Providentially, the kidney appears to be an organ where siRNA tends to accumulate spontaneously following systemic injection (van de Water *et al.*, 2006). Therefore renal cancer might be a reasonable candidate for the use of RNAi-based therapeutics (van de Water *et al.*, 2006). Van de Water and colleagues demonstrated that siRNA accumulates spontaneously in the kidney after i.v. injection, where it selectively suppresses gene function in the proximal tubules (van de Water *et al.*, 2006). Interestingly, clear cell RCC, the major subtype of renal cancer, is thought to arise from a proximat tubule cell. Conceivably, PAX2 constitute a therapeutic target in other forms of cancer as well. For example, both prostate (Khoubehi *et al.*, 2001) and breast cancer (Silberstein *et al.*, 2002), the two most common cancers amongst men and women respectively, express aberrant PAX2.

4.1.5 Other PAX genes in cancer

The reappearance of embryonic genes expression in tumors suggests that the transformed cells can be understood by reference to the properties of normal embryonic cells (Monk & Holding, 2001). Our finding also illustrates how developmental biology studies can lead to the identification of essential genes function in tumors and can help to identify novel candidate genes for therapeutic strategies. Developmental genetic programs are typically active during embryogenesis and are shut off once organogenesis is completed. The latter aspect (i.e. developmental genes are usually expressed at low level in adult tissues), predicts that therapies targeted against these genes will have a limited toxicity in patients and thereby may offer greater potential for specific tumor targeting in cancer treatment.

Recently, a report by Englenka from the J. Epstein group mentioned an indirect observation that a *PAX3* gene regulatory region was transcriptionally active within the urogenital derivative. This prompted us to examine whether PAX3 was also expressed during renal development (Engleka et al., 2005). If so, we reasoned that PAX3 might also be expressed in renal neoplasia. PAX3 is expressed in melanoma and alveolar rhabdomyosarcoma and has been suggested as a therapeutic target in both (Bernasconi et al., 1996; Scholl et al., 2001). Thus, PAX3 might have a novel role in the pathogenesis of renal cancer and perhaps serve as a potential target for renal cancer therapy.

4.1.6 *PAX3* is expressed in the developing kidney

For the first time, we demonstrate that the *PAX3* gene mRNA and protein are expressed in the developing kidney. Until recently, PAX2 and PAX8 were the only PAX gene family members thought to be involved in the renal development (Dziarmaga et al. 2006). We demonstrate PAX3 immunostaining in the mesenchymal and stromal compartment of the kidney. This is consistent with the observation of PAX3 expression in MK4 cells

derived from the metanephric mesenchyme in contrast with the absence of PAX3 in the epithelial cell line IMCD derived from the collecting duct.

During normal kidney development multipotent blastmal cells residing in the metanephric mesenchyme can differentiate along two main distinct cell lineages: nephrogenic vs stromal. Signals from the invading ureteric bud induce the metanephric mesenchyme to cluster into a cap that is composed of cells committed towards the nephrogenic lineages.

In contrast, the metanephric cells that are located further from the UB tip are directed toward the stromal cell lineage. Stromal progenitor cells expresse specific transcription factors including RAR-beta, FoxD (BF-2) and Pod-1 (Hatini *et al.*, 1996; Quaggin *et al.*, 1999). These stromal cells further differentiate and migrate in peritubular position to form the interstitial cells of the cortex and medulla. It is thought that they may also give rise to glomerular mesengial cells in response to VEGF signals from podocytes (Cullen-McEwen *et al.*, 2005).

Our observations indicate that PAX3 is a novel marker of the stromal lineage in the developing kidney. Interestingly kidney-targeted knockout of mesenchymal markers, such as FoxD1 or retinoic acid receptor-beta, typically leads to renal hypoplasia and fewer nephrons. This renal hypoplastic phenotype has been associated with a reduction of the pool of progenitor metanephric blastemal cells available to undergo MET to form the nephrons (Hatini *et al.*, 1996; Mendelsohn *et al.*, 1999; Schmidt-Ott *et al.*, 2006).

The Pax3-/- knockout mouse undergoes early embryonic death due to cardiac malformation and the Pax3+/- heterozygous mouse has a relatively mild phenotype. Thus a possible role for PAX3 in kidney development has not been explored. If we assume that Pax3 is important for renal progenitor cells, it is conceivable that Pax3 knockdown targeted in the renal tissue will result in renal hypoplasia or reduced nephrogenesis.

In conclusion, PAX3 is for the first time directly characterized in the developing kidney. PAX3 expression defines the renal mesenchymal and the stromal compartment suggesting that PAX3 has a specific function during kidney development.

4.1.7 PAX3 expression is identified in myogenic Wilms tumors

Wilms tumor is thought to arise from progenitor cells residing in the metanephric mesenchyme. Accordingly, genes expressed during kidney development in the metanephric mesenchyme are often expressed in Wilms tumors and might play a role in tumorigenesis or contribute to the tumor phenotype (Davies *et al.*, 1999; Jones *et al.*, 2007; Li *et al.*, 2002). Reflecting its progenitor cells origin, Wilms tumor recapitulates all the cellular lineages of the embryonic kidney including blastemal, stromal and epithelial components. In addition, 10-15% of Wilms tumors exhibit a myogenic differentiation (Fukuzawa *et al.*, 2007).

Although PAX3 is a transcription factor well-characterized in muscle development and rhabdomyosarcomas, we are the first to identify PAX3 expression in Wilms tumor. Our finding designates PAX3 as the missing piece of the puzzle that accounts for the potential of renal cells to differentiate into skeletal muscle in Wilms tumor. Indeed PAX3 was observed in 13/13 Wilms tumors that contain myogenic elements; PAX3 was not expressed in Wilms tumors lacking myogenesis (7/7). Interestingly we did not find PAX3 expression in RCC cells (ACHN and CAKI-1) that are assumed to have derived from the renal proximal tubules epithelium.

Aberrant PAX3 expression has been observed in a variety of cancers including melanoma and rhabdomyosarcoma (Barr *et al.*, 1993; Scholl *et al.*, 2001). Alveolar rhabdomyosarcoma (RMS), an aggressive skeletal muscle cancer, carries a unique t(2;13) chromosomal translocation resulting in the formation of a chimeric transcription factor PAX3-FKHR. This fusion protein contains the intact DNA-binding domains (PD: paired

box binding domain; HD: paired-type homeodomain) of Pax3 fused to the activation domain of FKHR (Zhang & Wang, 2007). The expression of the resulting fused oncoprotein PAX3-FKH is associated with increased metastasis and myogenic differentiation of the tumor (Sorensen *et al.*, 2002; Zhang and Wang, 2007).

4.1.8 PAX3 is regulated by WT1 during renal development

Our results suggest an association between *WT1* loss and the presence of PAX3 expression in Wilms tumors. In addition, we provide evidence *in vitro* for WT1 as a potential regulator of PAX3 expression in the renal context of HEK293 cells. Interestingly, the association of *WT1* loss and ectopic myogenesis in Wilms tumor has already been established by Hastie et al.(Fukuzawa *et al.*, 2004; Miyagawa *et al.*, 1998). Our observation that WT1 is able to regulate PAX3 expression fits perfectly in this model. The effect of WT1 on PAX3 is relatively modest, however. Thus, WT1 may affect PAX3 expression indirectly, for example by influencing the process of stromal cell commitment.

4.1.9 PAX3 function

Aberrant PAX3 expression in melanoma contributes to cell survival and migratory ability (Scholl *et al.*, 2001). Similarly, in normal myoblasts, PAX3 is required for proper cell migration from the neural tube to the limb bud (Buckingham & Relaix, 2007). By overexpressing and knocking down endogenous PAX3 in human embryonic kidney HEK293 cells, we show that PAX3 can influence cellular proliferation and cellular migration potential. By inference, PAX3 may function during in kidney development to enhance the migratory ability of the stromal progenitor cells. Similarly we can hypothesize that PAX3 expression in Wilms tumor may contribute to metastasis.

Although stromal-predominant myogenic tumors generally have a good prognosis they respond poorly to chemotherapy (Maes *et al.*, 1999). Since we previously showed that

PAX2 contributes to chemotherapy resistance of RCC, we also examined the effect of PAX3 aberrant expression on apoptosis susceptibility. However PAX3 expression had no significant effect on cisplatin-induced apoptosis in HEK293 cells.

Our work demonstrates PAX3 expression in a subset of Wilms tumors and suggests PAX3 as a marker of Wilms tumor with myogenic differentiation.

4.1.10 A novel WT1(-) primary Wilms tumor cell line

We isolated a novel WT1(-) Wilms tumor cell line (WiTP3) derived from the stromal portion of a triphasic Wilms tumor. WiTP3 cells were shown to express abundant PAX3 protein but very low levels of PAX2. In addition, WiTP3 cells were shown to harbor a *de novo* genomic WT1 deletion.

In contrast the WT1(+) WiT49 cell line derived from the epithelial compartment of a Wilms tumor (Alami *et al.*, 2003) expresses high levels of WT1 and PAX2. Other investigators have noticed PAX2 expression in Wilms tumors but did not associate this with a specific tumor subtype (Dressler and Douglass, 1992; Eccles *et al.*, 1992). Our observations suggest that PAX2 expression marks progression toward an epithelial lineage (MET) (Rothenpieler & Dressler, 1993) and is characteristic of the epithelial component of triphasic Wilms tumors. In contrast, the expression of Pax3 in WT1(-) cells allow us to propose a dichotomy between cell fates marked by PAX3 vs PAX2 in stromal vs epithelial Wilms tumors.

4.1.11 A novel model of renal development and Wilms tumor

Our finding of PAX3 expression in the stromal compartment of the developing kidney and our observation that PAX3 expression is suppressed by WT1 prompt us to propose a novel model of kidney development. We suggest that WT1 participates in the control of MET which leads to PAX2 expression in the nephrogenic lineage. Conversely, cells

directed toward the stromal lineage lose WT1 and express alternative transcription factors, including PAX3. These cells retain a non-polarized mesenchymal phenotype and migrating inwardly between emerging tubules to form the stromal component of the renal medulla. We hypothesize that PAX3 is implicated in this process.

In Wilms tumors associated with loss of WT1, cells fail to undergo EMT and are pushed toward the stromal cell fate. Expression of PAX3 contributes to the potential for myogenic differentiation. However, loss of WT1 and expression of PAX3 do not appear to be sufficient for malignant transformation, since most WT1(-) tumors acquire activating mutations of CTNNB1.

In other forms of Wilms tumors where WT1 is intact, metanephric progenitor cells can undergo EMT, express CTNNB1 and PAX2. These cells are partially committed and may differentiate into epithelial lineages even after transforming events such as loss of WTX or loss of IGF2 inhibition. This subset of Wilms tumors exhibits triphasic histology. While some cells can undergo epithelial differentiation, the majority appears as undifferentiated blastemal cells; neither expresses PAX3. Presumably, a small fraction of the partially committed blastemal cells can revert (EMT) toward the PAX3(+) stromal component.

4.2 SUMMARY

1) PAX2 contributes to the resistance of Renal Cell Carcinoma cells to apoptosis *in vitro.* SiRNA inhibiton of endogenous PAX2 sensitizes cultured RCC cells to cisplatin-induced cell death.

2) I*n vivo* observations provide proof-of-principle for the hypothesis that PAX2 may be a potential therapeutic target in renal cancer. Growth of subcutaneous RCC tumor xenografts in nude mice is relatively resistant to intraperitoneal cisplatin administration. However, growth of tumors from RCC cells stably transfected with PAX2 shRNA ceases after cisplatin treatment.

3) PAX3 is expressed in the stromal compartment in the developing kidney but is downregulated postnatally. Specific embryonic Pax3 transcripts are identified from E15-E18.

4) PAX3 is expressed in a subset of Wilms tumors with mutations of WT1, absence of PAX2 expression and evidence of myogenic differentiation. This suggests that a novel approach to classification of Wilms tumors.

5) WT1 suppresses PAX3 in vitro. Taken together with observations in a novel WT1(-), Pax3(+) primary cell line, we suggest that WT1 participates in the mesenchyme-to-epithelium transition during normal kidney development and that loss of WT1 accounts for the migratory stromal phenotype of some Wilms tumors.

4.3 FUTURE DIRECTIONS

As previously mentioned, PAX2 RNAi based therapeutics should be developed and tested in an *in vivo* model of renal cancer. Orthotopic injection of RCC xenograft cells in the renal capsule of nude mice could provide such a model to test the efficacy and the delivery of the RNAi therapeutics to the renal tumor site. Alternatively, it may be possible to develop small molecule inhibitors which either block PAX2 expression or activation of PAX2 gene targets.

The Angiotensin II receptor activation has been shown to have an effect on PAX2 mRNA and protein in the embryonic kidney (Zhang *et al.*, 2004a; Zhang *et al.*, 2004b). Similarly, Angiotensin II stimulates PAX2 in rat kidney proximal tubular cells (Zhang *et al.*, 2004a; Zhang *et al.*, 2004b). Since, RCC is thought to arise from proximal tubule cells, it would be of interest to examine the effects of angiotensin receptor blockers (routinely used for the treatment of hypertension) for effects on PAX2 expression in renal cancer cells. Conceivably, these agents might sensitize RCC to chemotherapeutic agents as did Pax2 knockdown in our studies.

Small peptides could be synthesized and tested for their potential interaction with PAX2 and disruption of its function. The protein Grg4 of the Groucho/TLE family has been described as a normal endogenous inhibitor of PAX2 transcriptional activity and its interaction with PAX2 prevents its phosphorylation by c-Jun N-terminal kinase (JNK) and thereby inhibits PAX2 transcriptional activity (Cai *et al.*, 2003; Cai *et al.*, 2002). Therefore molecules with an analogue structure to Groucho may have potential as a protein PAX2 inhibitor.

In addition, the expression of specific embryonic PAX3 isoforms in the kidney remains to be clarified. Furthermore, it would be interesting to determine whether targeted renal Pax3 knockout further reveals PAX3 function during renal development. A targeted Cre-loxP system, inactivating Pax3 in embryonic mesenchymal cells, would be an appropriate tool to examine these issues.

It would be interesting to know whether PAX3 inhibition has a significant effect on the PAX3+ Wilms tumor phenotype. Also the precise frequency of PAX3 expression and its association with tumor histology should be confirmed in a large panel of tumor samples. From a clinical perspective, myogenic tumors are resistant to chemotherapy and therefore PAX3 could constitute a reliable histological marker that will identify such tumors.

Other approaches should not be ignored. Recently, a "PAX3" experimental vaccine has been developed. Although PAX3 acts as a nuclear transcription factor, PAX3 cleavage products are expressed at the cell surface in conjunction with HLA class I peptides and can serve as epitopes which trigger specific cytotoxic T-cell recognition. Rodeneberg and colleagues successfully synthesized an immunogenic PAX3 peptide that induced specific CTL recognition of PAX3-containing tumors (Rodeberg *et al.*, 2006). Intravenous administration of anti-PAX3 T-cells caused regression of established PAX3+ tumors in mice, indicating a promising clinical application for anti-PAX3 immunotherapy (Himoudi *et al.*, 2007).

Concluding remarks

Our work illustrates how the study of kidney embryogenesis can provide insight into the molecular pathogenesis of renal cancer. We are now witnessing the emergence of the first generation of targeted molecular therapies for cancer. Along with this comes a great optimism that through the understanding of the basic molecular biology of the tumor, we are indeed on the road towards developing successful therapies for the treatment of cancer.

4.4 ORIGINAL CONTRIBUTIONS

1. I showed that the *PAX2* expression confers resistance to cisplatin-apoptosis in HEK293 cells *in vitro*.

2. Treatment of ACHN and CAKI-1 with PAX2 siRNA results in a significant reduction of PAX2 protein expression and a concomitant increase of basal cellular apoptosis.

3. I showed that PAX2 inhibition in ACHN and CAKI-1 cells sensitizes RCC cells to cisplatin-induced apoptosis.

4. I showed that ACHN cells injected subcutaneously can serve as an *in vivo* model of renal tumors.

5. I showed that *Pax2*-shRNAs are able to successfully inhibit PAX2 in ACHN cells.

6. I demonstrated that ACHN-shPAX2 tumors were more responsive to caspase-3 induced cisplain *in vitro* and to the growth inhibition caused by cisplatin treatment in vivo.

7. I showed that PAX3 is expressed in the murine developing kidney where it marks the stromal and mesenchymal compartment.

8. I showed that the PAX3 level is regulated by WT1 in HEK293 cells.

9. I showed that HEK293 cells overexpressing PAX3 have enhanced cell proliferation and migration *in vitro*.

10. I showed that the WiTP3 WT1(-) cell line expresses high levels of PAX3, low levels of PAX2 and no WT1.

11. I proposed a novel model of renal development and Wilms tumorigeneis based on PAX2 vs. PAX3 expression dichotomy.

CITED REFERENCES:

(1991). *J Clin Oncol*, **9,** 877-87.

AJCC. (2002). *AJCC Cancer Staging Manual New York: Springer*, **6th edition,** 323-325.

Al-Qudah HS, Rodriguez AR and Sexton WJ. (2007). *Cancer Control*, **14,** 218-30.

Anderson J, Slater O, McHugh K, Duffy P and Pritchard J. (2002). *J Pediatr Hematol Oncol*, **24,** 31-4.

Armstrong JF, Pritchard-Jones K, Bickmore WA, Hastie ND and Bard JB. (1993). *Mech Dev*, **40,** 85-97.

Barr FG, Galili N, Holick J, Biegel JA, Rovera G and Emanuel BS. (1993). *Nat Genet*, **3,** 113-7.

Beckwith JB. (1997). *Cancer Invest*, **15,** 153-62.

Beckwith JB, Kiviat NB and Bonadio JF. (1990). *Pediatr Pathol*, **10,** 1-36.

Bergstrom A, Hsieh CC, Lindblad P, Lu CM, Cook NR and Wolk A. (2001). *Br J Cancer*, **85,** 984-90.

Blanpain C, Horsley V and Fuchs E. (2007). *Cell*, **128,** 445-58.

Borycki AG, Li J, Jin F, Emerson CP and Epstein JA. (1999). *Development*, **126,** 1665-74.

Boss A, Clasen S, Kuczyk M, Schick F and Pereira PL. (2007). *Eur Radiol*, **17,** 725-33.

Breslow N, Olshan A, Beckwith JB and Green DM. (1993). *Med Pediatr Oncol*, **21,** 172-81.

Breslow N, Olshan A, Beckwith JB, Moksness J, Feigl P and Green D. (1994). *J Natl Cancer Inst*, **86,** 49-51.

Breslow NE, Beckwith JB, Perlman EJ and Reeve AE. (2006). *Pediatr Blood Cancer*, **47,** 260-7.

Bruening W, Bardeesy N, Silverman BL, Cohn RA, Machin GA, Aronson AJ, Housman D and Pelletier J. (1992). *Nat Genet*, **1,** 144-8.

Brugarolas J. (2007). *N Engl J Med*, **356,** 185-7.

Buckingham M and Relaix F. (2007). *Annu Rev Cell Dev Biol*, **23,** 645-73.

Calle EE and Kaaks R. (2004). *Nat Rev Cancer*, **4,** 579-91.

Chao LY, Huff V, Tomlinson G, Riccardi VM, Strong LC and Saunders GF. (1993). *Nat Genet*, **3,** 127-31.

Cho D, Signoretti S, Regan M, Mier JW and Atkins MB. (2007). *Clin Cancer Res*, **13,** 758s-763s.

Cho EA DG. (2003). *The Kidney: From Developmental to Congenitcal Disease.* Academic press: London.

Chow WH, Devesa SS, Warren JL and Fraumeni JF, Jr. (1999). *JAMA*, **281,** 1628-31.

Chow WH, Gridley G, Fraumeni JF, Jr. and Jarvholm B. (2000). *N Engl J Med*, **343,** 1305-11.

Cohen HT and McGovern FJ. (2005). *N Engl J Med*, **353,** 2477-90.

Conway SJ, Henderson DJ and Copp AJ. (1997). *Development*, **124,** 505-14.

Couzin J. (2002). *Science*, **298,** 2296-7.

Cullen-McEwen LA, Caruana G and Bertram JF. (2005). *Nephron Exp Nephrol*, **99,** e1-8.

Curado. M. P. E, B., Shin. H.R., Storm. H., Ferlay. J., Heanue. M. and Boyle. P. (2007). *IARC Scientific Publications*, **160.**

Dahl E, Koseki H and Balling R. (1997). *Bioessays*, **19,** 755-65.
de Fougerolles A, Vornlocher HP, Maraganore J and Lieberman J. (2007). *Nat Rev Drug Discov*, **6,** 443-53.
Diller L, Ghahremani M, Morgan J, Grundy P, Reeves C, Breslow N, Green D, Neuberg D, Pelletier J and Li FP. (1998). *J Clin Oncol*, **16,** 3634-40.
Dziarmaga A, Clark P, Stayner C, Julien JP, Torban E, Goodyer P and Eccles M. (2003). *J Am Soc Nephrol*, **14,** 2767-74.
Dziarmaga A, Quinlan J and Goodyer P. (2006). *Pediatr Nephrol*, **21,** 26-31.
Eccles MR, Wallis LJ, Fidler AE, Spurr NK, Goodfellow PJ and Reeve AE. (1992). *Cell Growth Differ*, **3,** 279-89.
Epstein DJ, Vekemans M and Gros P. (1991). *Cell*, **67,** 767-74.
Ficarra V, Galfano A, Mancini M, Martignoni G and Artibani W. (2007). *Lancet Oncol*, **8,** 554-8.
Fire A, Xu S, Montgomery MK, Kostas SA, Driver SE and Mello CC. (1998). *Nature*, **391,** 806-11.
Fleming S and O'Donnell M. (2000). *Histopathology*, **36,** 195-202.
Fuhrman SA, Lasky LC and Limas C. (1982). *Am J Surg Pathol*, **6,** 655-63.
Fukuzawa R, Heathcott RW, More HE and Reeve AE. (2007). *J Clin Pathol*, **60,** 1013-6.
Fyfe G, Fisher RI, Rosenberg SA, Sznol M, Parkinson DR and Louie AC. (1995). *J Clin Oncol*, **13,** 688-96.
Gibson W, Green A, Bullard RS, Eaddy AC and Donald CD. (2007). *Cancer Lett*, **248,** 251-61.
Gnarra JR and Dressler GR. (1995). *Cancer Res*, **55,** 4092-8.
Goulding MD, Chalepakis G, Deutsch U, Erselius JR and Gruss P. (1991). *EMBO J*, **10,** 1135-47.
Green DM. (2007). *Eur J Cancer*, **43,** 2453-6.
Grundy P, Perlman E, Rosen NS, Warwick AB, Bender JG, Ehrlich P, Hoffer FA and Lee ND. (2005). *Curr Probl Cancer*, **29,** 221-60.
Habib R, Loirat C, Gubler MC, Niaudet P, Bensman A, Levy M and Broyer M. (1985). *Clin Nephrol*, **24,** 269-78.
Hartley AL, Birch JM, Tricker K, Wallace SA, Kelsey AM, Harris M and Jones PH. (1993). *Cancer Genet Cytogenet*, **67,** 133-5.
Hedborg F, Holmgren L, Sandstedt B and Ohlsson R. (1994). *Am J Pathol*, **145,** 802-17.
Hueber PA, Waters P, Clark P, Eccles M and Goodyer P. (2006). *Kidney Int*, **69,** 1139-45.
Huff V. (1998). *Am J Med Genet*, **79,** 260-7.
Hunt JD, van der Hel OL, McMillan GP, Boffetta P and Brennan P. (2005). *Int J Cancer*, **114,** 101-8.
Kaelin WG, Jr. (2002). *Nat Rev Cancer*, **2,** 673-82.
Kaelin WG, Jr. (2007). *Clin Cancer Res*, **13,** 680s-684s.
Kalapurakal JA, Dome JS, Perlman EJ, Malogolowkin M, Haase GM, Grundy P and Coppes MJ. (2004). *Lancet Oncol*, **5,** 37-46.
Kelland L. (2007). *Nat Rev Cancer*, **7,** 573-84.
Kerr JF, Wyllie AH and Currie AR. (1972). *Br J Cancer*, **26,** 239-57.
Khoubehi B, Kessling AM, Adshead JM, Smith GL, Smith RD and Ogden CW. (2001). *J Urol*, **165,** 2115-20.

Kim DH and Rossi JJ. (2007). *Nat Rev Genet*, **8,** 173-84.
Klatte T, Pantuck AJ, Kleid MD and Belldegrun AS. (2007). *Rev Urol*, **9,** 47-56.
Knauth K, Bex C, Jemth P and Buchberger A. (2006). *Oncogene*, **25,** 370-7.
Knudson AG. (1997). *Ann N Y Acad Sci*, **833,** 58-67.
Knudson AG, Jr. and Strong LC. (1972). *J Natl Cancer Inst*, **48,** 313-24.
Koesters R, Ridder R, Kopp-Schneider A, Betts D, Adams V, Niggli F, Briner J and von Knebel Doeberitz M. (1999). *Cancer Res*, **59,** 3880-2.
Kusafuka T, Miao J, Kuroda S, Udatsu Y and Yoneda A. (2002). *Int J Mol Med*, **10,** 395-9.
Larkin JM, Chowdhury S and Gore ME. (2007). *Nat Clin Pract Oncol*, **4,** 470-9.
Lendvay TS and Marshall FF. (2003). *J Urol*, **169,** 1635-42.
Linet MS, Ries LA, Smith MA, Tarone RE and Devesa SS. (1999). *J Natl Cancer Inst*, **91,** 1051-8.
Little M and Wells C. (1997). *Hum Mutat*, **9,** 209-25.
Maes P, Delemarre J, de Kraker J and Ninane J. (1999). *Eur J Cancer*, **35,** 1356-60.
Maher ER and Reik W. (2000). *J Clin Invest*, **105,** 247-52.
Mansouri A, Chowdhury K and Gruss P. (1998). *Nat Genet*, **19,** 87-90.
Margue CM, Bernasconi M, Barr FG and Schafer BW. (2000). *Oncogene*, **19,** 2921-9.
Maulbecker CC and Gruss P. (1993). *EMBO J*, **12,** 2361-7.
Maw MA, Grundy PE, Millow LJ, Eccles MR, Dunn RS, Smith PJ, Feinberg AP, Law DJ, Paterson MC, Telzerow PE and et al. (1992). *Cancer Res*, **52,** 3094-8.
McCredie M, Pommer W, McLaughlin JK, Stewart JH, Lindblad P, Mandel JS, Mellemgaard A, Schlehofer B and Niwa S. (1995). *Int J Cancer*, **60,** 345-9.
McDonald JM, Douglass EC, Fisher R, Geiser CF, Krill CE, Strong LC, Virshup D and Huff V. (1998). *Cancer Res*, **58,** 1387-90.
McLaughlin JK, Lindblad P, Mellemgaard A, McCredie M, Mandel JS, Schlehofer B, Pommer W and Adami HO. (1995). *Int J Cancer*, **60,** 194-8.
Metzger ML and Dome JS. (2005). *Oncologist*, **10,** 815-26.
Mickisch GH. (1994). *World J Urol*, **12,** 214-23.
Minasian LM, Motzer RJ, Gluck L, Mazumdar M, Vlamis V and Krown SE. (1993). *J Clin Oncol*, **11,** 1368-75.
Miyata Y, Kanetake H and Kanda S. (2006). *Clin Cancer Res*, **12,** 4876-81.
Monk M and Holding C. (2001). *Oncogene*, **20,** 8085-91.
Moon RT, Kohn AD, De Ferrari GV and Kaykas A. (2004). *Nat Rev Genet*, **5,** 691-701.
Motzer RJ, Russo P, Nanus DM and Berg WJ. (1997). *Curr Probl Cancer*, **21,** 185-232.
Narod SA and Lenoir GM. (1991). *Int J Epidemiol*, **20,** 346-8.
Oken MM, Creech RH, Tormey DC, Horton J, Davis TE, McFadden ET and Carbone PP. (1982). *Am J Clin Oncol*, **5,** 649-55.
Oliver RT, Nethersell AB and Bottomley JM. (1989). *Br J Urol*, **63,** 128-31.
Ordahl CP and Le Douarin NM. (1992). *Development*, **114,** 339-53.
Ostrom L, Tang MJ, Gruss P and Dressler GR. (2000). *Dev Biol*, **219,** 250-8.
Pastan I and Gottesman M. (1987). *N Engl J Med*, **316,** 1388-93.
Pavlovich CP and Schmidt LS. (2004). *Nat Rev Cancer*, **4,** 381-93.
Pelletier J, Bruening W, Li FP, Haber DA, Glaser T and Housman DE. (1991). *Nature*, **353,** 431-4.

Permpongkosol S, Bagga HS, Romero FR, Solomon SB and Kavoussi LR. (2006). *BJU Int*, **98,** 751-5.
Petrella BL and Brinckerhoff CE. (2006). *Mol Cancer*, **5,** 66.
Phillips E and Messing EM. (1993). *Urology*, **41,** 9-15.
Puschel AW, Westerfield M and Dressler GR. (1992). *Mech Dev*, **38,** 197-208.
Rainier S, Johnson LA, Dobry CJ, Ping AJ, Grundy PE and Feinberg AP. (1993). *Nature*, **362,** 747-9.
Rashidkhani B, Lindblad P and Wolk A. (2005). *Int J Cancer*, **113,** 451-5.
Read AP and Newton VE. (1997). *J Med Genet*, **34,** 656-65.
Real C, Glavieux-Pardanaud C, Le Douarin NM and Dupin E. (2006). *Dev Biol*, **300,** 656-69.
Reed WB, Walker R and Horowitz R. (1973). *Acta Derm Venereol*, **53,** 409-16.
Refae MA, Wong N, Patenaude F, Begin LR and Foulkes WD. (2007). *Nat Clin Pract Oncol*, **4,** 256-61.
Reya T, Morrison SJ, Clarke MF and Weissman IL. (2001). *Nature*, **414,** 105-11.
Richard S, Lidereau R and Giraud S. (2004). *Nephrol Dial Transplant*, **19,** 2954-8.
Ritchey ML, Green DM, Thomas PR, Smith GR, Haase G, Shochat S, Moksness J and Breslow NE. (1996). *Med Pediatr Oncol*, **26,** 75-80.
Robson EJ, He SJ and Eccles MR. (2006). *Nat Rev Cancer*, **6,** 52-62.
Rodeberg DA, Nuss RA, Elsawa SF, Erskine CL and Celis E. (2006). *Int J Cancer*, **119,** 126-32.
Rosenberg SA. (2007). *Nat Clin Pract Oncol*, **4,** 497.
Rothenpieler UW and Dressler GR. (1993). *Development*, **119,** 711-20.
Rowitch DH and McMahon AP. (1995). *Mech Dev*, **52,** 3-8.
Ruteshouser EC and Huff V. (2004). *Am J Med Genet C Semin Med Genet*, **129,** 29-34.
Sanyanusin P, McNoe LA, Sullivan MJ, Weaver RG and Eccles MR. (1995). *Hum Mol Genet*, **4,** 2183-4.
Sanyanusin P, Norrish JH, Ward TA, Nebel A, McNoe LA and Eccles MR. (1996). *Genomics*, **35,** 258-61.
Satoh Y, Nakagawachi T, Nakadate H, Kaneko Y, Masaki Z, Mukai T and Soejima H. (2003). *J Biochem (Tokyo)*, **133,** 303-8.
Scelo G and Brennan P. (2007). *Nat Clin Pract Urol*, **4,** 205-17.
Scholl FA, Kamarashev J, Murmann OV, Geertsen R, Dummer R and Schafer BW. (2001). *Cancer Res*, **61,** 823-6.
Schulte TW, Toretsky JA, Ress E, Helman L and Neckers LM. (1997). *Biochem Mol Med*, **60,** 121-6.
Servais H, Ortiz A, Devuyst O, Denamur S, Tulkens PM and Mingeot-Leclercq MP. (2007). *Apoptosis*.
Shamberger RC, Guthrie KA, Ritchey ML, Haase GM, Takashima J, Beckwith JB, D'Angio GJ, Green DM and Breslow NE. (1999). *Ann Surg*, **229,** 292-7.
Stewart DJ. (2007). *Crit Rev Oncol Hematol*, **63,** 12-31.
Stiller CA and Parkin DM. (1990). *Br J Cancer*, **62,** 1026-30.
Storkel S and van den Berg E. (1995). *World J Urol*, **13,** 153-8.
Teh BT, Giraud S, Sari NF, Hii SI, Bergerat JP, Larsson C, Limacher JM and Nicol D. (1997). *Lancet*, **349,** 848-9.

Torres M, Gomez-Pardo E, Dressler GR and Gruss P. (1995). *Development*, **121,** 4057-65.
Tremblay P, Kessel M and Gruss P. (1995). *Dev Biol*, **171,** 317-29.
Tsukamoto K, Nakamura Y and Niikawa N. (1994). *Hum Genet*, **93,** 270-4.
van Dijk BA, Schouten LJ, Oosterwijk E, Hulsbergen-van de Kaa CA, Kiemeney LA, Goldbohm RA, Schalken JA and van den Brandt PA. (2006). *Br J Cancer*, **95,** 374-7.
Vogan KJ and Gros P. (1997). *J Biol Chem*, **272,** 28289-95.
Vogan KJ, Underhill DA and Gros P. (1996). *Mol Cell Biol*, **16,** 6677-86.
Waardenburg PJ. (1951). *Am J Hum Genet*, **3,** 195-253.
Wagner KD, Wagner N, Guo JK, Elger M, Dallman MJ, Bugeon L and Schedl A. (2006). *Curr Biol*, **16,** 793-800.
Wang Q, Kumar S, Mitsios N, Slevin M and Kumar P. (2007). *Int J Cancer*, **120,** 1223-31.
Wang Q, Kumar S, Slevin M and Kumar P. (2006). *Cancer Res*, **66,** 8574-80.
Williams JC, Brown KW, Mott MG and Maitland NJ. (1989). *Lancet*, **1,** 283-4.
Willins AFaB. (2003). *Wilms Tumor as a Model for Cancer biology*: Totowa, NJ, USA.
Wilms M. (1899). *Die Mischgeschwulste der Niere*: Leipzig, Germany.
Yagoda A, Abi-Rached B and Petrylak D. (1995). *Semin Oncol*, **22,** 42-60.
Zhang L and Wang C. (2007). *Oncogene*, **26,** 1595-605.
Zucchi A, Mearini L, Mearini E, Costantini E, Vivacqua C and Porena M. (2003). *J Urol*, **169,** 905-8.

APPENDIX I

PUBLICATIONS

LIST OF PUBLICATIONS

Published articles:

Hueber PA et al. *In vivo* validation of PAX2 as a target for cancer gene therapy (Cancer Letters April 2008)

Hueber PA, Waters P, Clark P, Eccles M, Goodyer P. Pax2 inactivation enhances cisplatin-induced apoptosis in renal carcinoma cells. (Kidney International, April 2006)

Dziarmaga A, **Hueber PA** et al. Neuronal apoptosis inhibitory protein is expressed in developing kidney and is regulated by PAX2. (Am J Physiol Renal Physiol. October 2006)

Iglesias M. D., **Hueber PA** et al. Canonical wnt signaling in kidney development (American Journal of Physiology, May 2007)

Zhang Z, Quinlan J, Lemire M, Hudson T, **Hueber PA,** Chu L, Benjamin A, Rpy A, Pascuet E, Foodyer M, Raju C, Houghton F and Goodyer P. A common RET variant is associated with reduced kidney size and function in normal newborns. (Journal of American Society of Nephrology 2008)

Manuscripts submitted:

Hueber PA et al. PAX3 is expressed in myogenic Wilms Tumor and is associated with loss of WT1. ***Submitted to Pediatric Developmental Pathology.***

Published abstracts:

First Annual Canadian Human Genetics Conference April 2008. Wilms tumor arising in a child with congenital nephrogeic diabetes insipidus El-Kares R, **Hueber PA**, Blumenkrantz M, Kim M, Jabado N, Bichet D.G and Paul Goodyer

6th International Conference on the Biology of Childhood Renal Tumours Chamonix, Mont-Blanc France March 12-15, 2008 **Hueber PA** et al. PAX3 expression characterizes the stromal component of myogenic Wilms tumours

American Society of Nephrology (ASN) Renal Week November 2007 San Francisco, USA **Hueber PA** et al. PAX3 is expressed in the developing kidney and in Wilms tumors with myogenic differentiation

Pediatric Academic Societies' Annual Meeting May 2007 Toronto, Canada **Hueber PA** et al. PAX3 is expressed in the developing kidney and in Wilms tumors

World Congress of Nephrology April 2007 Rio de Janeiro, Brazil **Hueber PA** et al. Validation of PAX2 as a target for renal cancer therapy

Montreal Children's Hospital (December 2004) **Hueber PA** et al. Sensitization of Renal Cancer to Chemotherapy-Induced Apoptosis

5th Annual McGill Biomedical Graduate Conference (February 2005) **Hueber PA** et al. PAX2 Novel Gene Therapy for Renal Cancer

Pediatric Academic Societies' Annual Meeting May 2004 San Francisco, CA **Hueber PA** et al. Chemo-sensitization of Human Cancer to Cisplatin using RNAi targeting PAX2

Am J Physiol Renal Physiol 293: F494–F500, 2007.
First published May 9, 2007; doi:10.1152/ajprenal.00416.2006.

Canonical WNT signaling during kidney development

Diana M. Iglesias,[1] Pierre-Alain Hueber,[2] LeeLee Chu,[3] Robert Campbell,[3] Anne-Marie Patenaude,[3] Alison J. Dziarmaga,[1] Jacklyn Quinlan,[1] Othman Mohamed,[4] Daniel Dufort,[4] and Paul R. Goodyer[1,2,3]

[1]*Department of Human Genetics,* [2]*Department of Experimental Medicine,* [3]*Department of Pediatrics, McGill University-Montreal Children's Hospital Research Institute,* [4]*Department of Obstetrics and Gynecology, McGill University Health Centre Research Institute and McGill University, Montreal, Quebec, Canada*

Submitted 20 October 2006; accepted in final form 3 May 2007

Iglesias DM, Hueber P-A, Chu LL, Campbell R, Patenaude A-M, Dziarmaga AJ, Quinlan J, Mohamed O, Dufort D, Goodyer PR. Canonical WNT signaling during kidney development. *Am J Physiol Renal Physiol* 293: F494–F500, 2007. First published May 9, 2007; doi:10.1152/ajprenal.00416.2006.—The canonical WNT signaling pathway plays a crucial role in patterning of the embryo during development, but little is known about the specific developmental events which are under WNT control. To understand more about how the WNT pathway orchestrates mammalian organogenesis, we studied the canonical β-catenin-mediated WNT signaling pathway in kidneys of mice bearing a β-catenin-responsive *TCF/βGal* reporter transgene. In metanephric kidney, intense canonical WNT signaling was evident in epithelia of the branching ureteric bud and in nephrogenic mesenchyme during its transition into renal tubules. WNT signaling activity is rapidly downregulated in maturing nephrons and becomes undetectable in postnatal kidney. Sites of *TCF/βGal* activity are in proximity to the known sites of renal WNT2b and WNT4 expression, and these WNTs stimulate TCF reporter activity in kidney cell lines derived from ureteric bud and metanephric mesenchyme lineages. When fetal kidney explants from *HoxB7/GFP* mice were exposed to the canonical WNT signaling pathway inhibitor, Dickkopf-1, arborization of the ureteric bud was significantly reduced. We conclude that restricted zones of intense canonical WNT signaling drive branching nephrogenesis in fetal kidney.

nephrogenesis; β-catenin; branching morphogenesis

THE WNT FAMILY is comprised of 19 secreted glycoproteins which act as short-range intercellular signaling molecules, recognizing one of the 10 frizzled receptors expressed at the surface of nearby target cells. The canonical signaling pathway is activated by WNTs which bind to cognate frizzled receptors heterodimerized with LRP5 or LRP6 coreceptors (2). Activated receptors recruit dishevelled protein (Dvl) and inhibit degradation of cytoplasmic β-catenin via the GSK3β-axin-APC complex (11). When its degradation is blocked, cytoplasmic β-catenin is available to translocate to the nucleus, dimerize with partners belonging to the T-cell factor (TCF) family, and activate target genes. TCF recognition motifs have been well-studied, allowing design of vectors (e.g., TOPFlash) which drive transcription of reporter genes in response to canonical WNT signaling activity (32). In general, canonical β-catenin/TCF signaling is thought to activate gene targets (e.g., *c-myc*) involved in cell proliferation (3, 27).

More than 35 years ago, Unsworth and Grobstein (33) reported that tissue from spinal cord could induce formation of renal tubules when cocultured with isolated metanephric mesenchyme. In 1994, Herzlinger et al. (12) found that WNT1-expressing NIH3T3 cells were also able to induce tubule formation in the coculture assay, suggesting that the canonical (β-catenin-mediated) WNT signaling pathway is essential for mammalian nephrogenesis. However, the precise function of canonical WNT signaling in renal development is unknown.

Surprisingly, WNT1 is not present in the developing kidney, but numerous other WNTs are transiently expressed in specific cell lineages (34). Several of these are able to activate the canonical signaling pathway in other contexts; these include WNT4 (19), WNT2b (15), and WNT7b (35). Additional WNTs (WNT6, WNT9, and WNT11) are expressed in fetal kidney (4, 13, 16) but have not been shown to activate the canonical signaling pathway. Little is known about the expression patterns of the many FRZ and LRP5/6 receptors in fetal kidney. Thus it has been difficult to decipher the function of canonical *Wnt* and/or *Fz* genes during renal development. Furthermore, there is insufficient information about the specific sites of canonical signaling activity to predict the precise role of this pathway in nephrogenesis.

In this study, we report the detailed spatio-temporal pattern of canonical WNT signaling activity in developing kidney from a β-catenin-responsive *TCF/βGal* transgenic reporter mouse. We found that the renal *TCF* signal is initially evident throughout the nephric duct and ureteric bud (UB) but becomes progressively focused at two sites: branching ureteric bud tips and in distal portions of the S-shaped body. In the perinatal period, it is sharply downregulated as nephrogenesis comes to an end. Several WNTs expressed in close proximity to the sites of canonical β-catenin/TCF pathway activity were found to activate the canonical pathway in cultured MK4 (derived from nephrogenic mesenchyme) cells and inner medullary collecting duct (IMCD, derived from renal collecting duct epithelium) cells. We also show that when fetal kidney explants are exposed to the canonical pathway inhibitor, Dickkopf-1, branching morphogenesis of the UB is significantly suppressed.

MATERIALS AND METHODS

Cell culture. MK4 cells (kindly provided by Dr. S. Potter) and IMCD-3 (mouse collecting duct) cells (ATCC number CRL-2123) were all cultured in DMEM (Invitrogen, Carlsbad, CA) supplemented with 10% FBS and 1% penicillin-streptomycin.

Transient transfection assays. Expression plasmids used for transient transfection assays include: empty expression plasmid pCDNA3.1 (as a control), full-length human DKK1 cDNA (kindly provided Dr. X. He), mouse WNT4 cDNA (Upstate Biotech, Char-

Address for reprint requests and other correspondence: P. Goodyer, Montreal Children's Hospital Research Institute, 4060 St. Catherine West, Montreal, QC, Canada H3Z 2Z3 (e-mail: Paul.Goodyer@mcgill.ca).

The costs of publication of this article were defrayed in part by the payment of page charges. The article must therefore be hereby marked "*advertisement*" in accordance with 18 U.S.C. Section 1734 solely to indicate this fact.

lottesville, VI), mouse WNT7b cDNA (kindly provided by E. Morrisey), mouse WNT2b cDNA (kindly provided by I. Drummond), TOPFLASH and FOPFLASH reporter vectors (Upstate Biotech), and pGL2 basic (Promega, Madison, WI; as a control). All transfections included the renilla luciferase expression vector, pRL-SV40 (Promega), as a control for sample-to-sample variation in transfection. Transfections were performed in triplicate in 24-well plates; each experiment was performed three times. At 60% confluency, cells were transfected with 200 ng of the various plasmids using FuGENE 6 Transfection Reagent (Roche, Penzberg, Germany) according to the protocol recommended by the manufacturer. Firefly luciferase and renilla luciferase reporter activities were determined using Dual Luciferase Assay System reagents (Promega) and quantified in a Microlumat Plus Luminometer (EG&G Berthold). Reporter activity was expressed as the ratio of luciferase to renilla values. Statistical analysis was performed using Student's *t*-test.

For study of the canonical signaling inhibitor, DKK1, cells were plated at 60% confluency in a 24-well plate; recombinant mouse DKK1 protein (R&D Systems, Minneapolis, MN) was added (0 or 500 ng/ml) to the wells. After 24 h, the cells were transfected with either TOPFLASH or control vector and pRL-SV40 renilla as a transfection efficency control. Fresh DKK1 was added to the media 1 h after the transfection was performed. Firefly luciferase and renilla luciferase reporter activities were determined after 24 h. The experiment was performed two times in triplicate.

Reporter mice. Animal procedures followed the guidelines established by the Canadian Council of Animal Care and were approved by the Animal Care Committee from McGill University. CD1 mice bearing a β-catenin-responsive *lacZ* reporter gene have been previously described (22). Briefly, this transgene contains six *TCF/LEF* response elements cloned upstream of a minimal Hsp68 promoter driving the *lacZ* reporter gene. C3H mice (provided by F. Costantini) bearing a GFP transgene under the control of the HoxB7 promoter have been described elsewhere (30).

Immunohistochemistry. Paraffin-embedded sections (7 μm) of embryonic kidneys were incubated in 5% H_2O_2 to quench endogenous peroxidase activity, followed by a 30-min incubation with normal horse serum. Tissue sections were then incubated with anti-nonphosphorylated β-catenin antibody (Upstate, Lake Placid, NY), washed, and incubated with a universal biotinylated secondary antibody (Vector Laboratory, Burlingame, CA). Staining was developed using DAB (Vector Laboratory) and counterstained with Gill's hematoxylin.

Analysis of LacZ activity in transgenic mice. The protocol for β-galactosidase staining has been described elsewhere (23). Kidneys from mice bearing the *TCF-lacZ* transgene and wild-type mice were removed and fixed in PBS containing 2 mM $MgCl_2$, 0.02% NP-40, 0.01% deoxycholate, 1% formaldehyde, and 0.2% glutaraldehyde, rinsed in washing buffer (PBS with 2 mM $MgCl_2$, 0.02% NP-40, 0.01% deoxycholate), and stained in the dark overnight in washing buffer supplemented with 1 mg/ml X-gal, 5 mM potassium ferricyanide, and 5 mM potassium ferrocyanide. After being stained, kidneys were washed in PBS and visualized directly or embedded in paraffin for sectioning and standard counterstaining with hematoxylin and eosin.

Immunofluorescent microscopy. Frozen sections of embryonic kidneys (10 μm) from transgenic mice were blocked in normal serum and incubated with rabbit anti-β-galactosidase antibody (1:250, Chemicon International, Temecula, CA). Sections were washed and incubated with rhodamine-tagged secondary anti-rabbit IgG antibody (1:50, Chemicon International), washed, and incubated with fluorescein-tagged *dolichos biflorus* lectin (1:200, Vector Laboratory) before microscopic examination under fluorescent light.

For WT1 staining of GFP explants, kidneys were fixed for 10 min in methanol, washed in PBS 0.1% Tween 20 (PBST), and incubated overnight at 4°C with rabbit polyclonal anti WT1 antibody (C19, Santa Cruz Biotechnology, Santa Cruz, CA) diluted 1:200 in PBST/2% BSA. After washes in PBST, kidneys were incubated with anti-rabbit Alexa Fluor 594 (Invitrogen) 1:400 at 22°C for dual immunofluorescent microscopy.

Kidney explant culture. Kidneys from *HoxB7/GFP* mice were dissected from embryonic *day 13.5* (*E13.5*) embryos and placed on a filter in six-well plates in DMEM with 10% BSA (control) or medium containing 2 μg/ml recombinant mouse DKK1 protein (R&D Systems). The explants were cultured in a humidified 37°C incubator under 5% CO_2. Kidneys were supplemented every 24 h with fresh medium (control) or medium containing DKK1. Pictures were taken every 24 h under fluorescent light. UB tips were counted using Image J software. Statistical analysis was performed using Student's *t*-test.

RESULTS

Canonical β-catenin signaling activity is progressively restricted to UB tips and newly formed S-shaped bodies in developing kidney. To examine the pattern of canonical β-catenin pathway signaling activity, *E11.5* embryos (*E11.5*) or microdissected kidneys (*E14-P21*) from *TCF/β-galactosidase* mice were assessed for transgene activity. The *TCF* signal is first seen in the nephric duct at *E11.5* (Fig. 1, *A* and *B*). By *E13-E15*, the *TCF* reporter signal is seen throughout the arborizing UB but is somewhat stronger in UB tips than in its trunk (Fig. 1, *C*, *D*, *E*). By *E16.5* the *TCF* signal is highly restricted to the UB tips and distal S-shaped body but is suppressed in UB trunks (Fig. 1*F*).

To confirm that transgene expression reflects endogenous canonical WNT signaling activity, sections from X-gal-stained E15 transgenic kidney (Fig. 2*A*) were compared with sections from *E15* wild-types stained with an antibody against active (nonphosphorylated) β-catenin (Fig. 2*B*). Active β-catenin staining is, like the *TCF* signal, intense at the tips of the UB and in distal portions of the S-shaped body. To confirm that canonical WNT signaling becomes restricted to the tips (vs. trunks) of the UB, cryosections of *E16.5* kidney were costained with antibody for β-galactosidase (red) and a UB marker *dolichos biflorus agglutinin* (green). At this stage, the fused image shows restricted *TCF* signaling at UB tip but is disappearing in the UB trunk (Fig. 2, *C–E*).

As kidney development proceeds, the *TCF* signal is sustained only in the nephrogenic zone (Fig. 3, *A* and *B*). All canonical signaling activity is extinguished as nephrogenesis comes to an end in the early postnatal period (Fig. 3, *C* and *D*).

WNT2b, WNT4, and WNT7b stimulate canonical β-catenin signaling. Since our observations in the *TCF/LacZ* mouse indicate intense activity of the canonical WNT pathway at the UB tips and in the distal S-shaped bodies, we used cell lines derived from these two lineages, MK4 (murine nephrogenic mesenchyme) and IMCD (murine collecting duct), to screen various WNTs for canonical activity. Six WNTs have been reported in developing kidney, but only four of these (WNT2b, WNT4, WNT7b, and WNT11) are expressed in sustained fashion near the branching UB tips and emerging S-shaped bodies. Cells were grown to 60% confluence and transiently transfected with pcDNA expression vectors containing various full-length murine WNT cDNAs (or empty vector) in the presence of either TOPFLASH or FOPFLASH (mutant) reporter vectors. Cotransfection with SV40/renilla vector was used as a control for transfection efficiency. In the absence of any WNT vectors, TOPFLASH had significant basal activity above a promoterless luciferase vector in both cell lines. TOPFLASH activity reflects β-catenin/TCF signaling in these

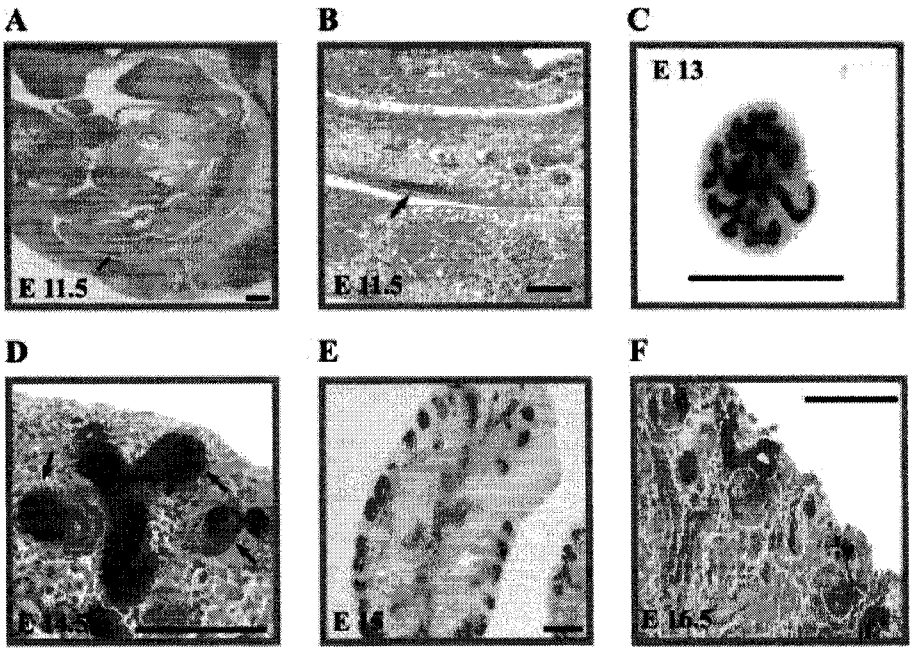

Fig. 1. Ontogeny of β-catenin signaling during early development in *TCF/lacZ* reporter transgenic mouse kidney. Mouse embryonic (*A* and *B*) and kidney (*C*, *D*, *E*) sections were stained for β-galactosidase activity. At embryonic *day 11.5* (*E11.5*), β-galactosidase is seen in the nephric duct (arrows; *A* and *B*). At *E13*, strong signal is observed throughout the arborizing ureteric bud (UB; *C*). At *E14.5*, strong staining is seen in the branching UB, particularly at its tips, and in distal segments of S-shaped bodies (arrows; *D*). Low-power view of *E15.5* kidney shows strong β-galactosidase staining in UBs, whereas maturing collecting ducts show reduced staining (*E*). At *E16.5*, the β-galactosidase signal is restricted to the tips of the branching UBs (*F*). Scale bar = 100 μm for *A*, *B*, *D*, *E*, and *F* and 1 mm for *C*.

cells, since mutation of one of the three sense TCF response elements (FOPFLASH) reduced activity by 40%. TOPFLASH activity was unaffected by cotransfection with a (noncanonical) WNT11 expression vector (data not shown). In the presence of WNT2b, basal TOPFLASH activity was stimulated 5.6-fold in MK4 cells ($P = 0.03$) and 6.6-fold ($P < 0.05$) in IMCD cells above the empty expression vector controls (Fig. 4, *A* and *B*). WNT7b stimulated TOPFLASH 7.4-fold ($P = 0.09$) and 4.3-

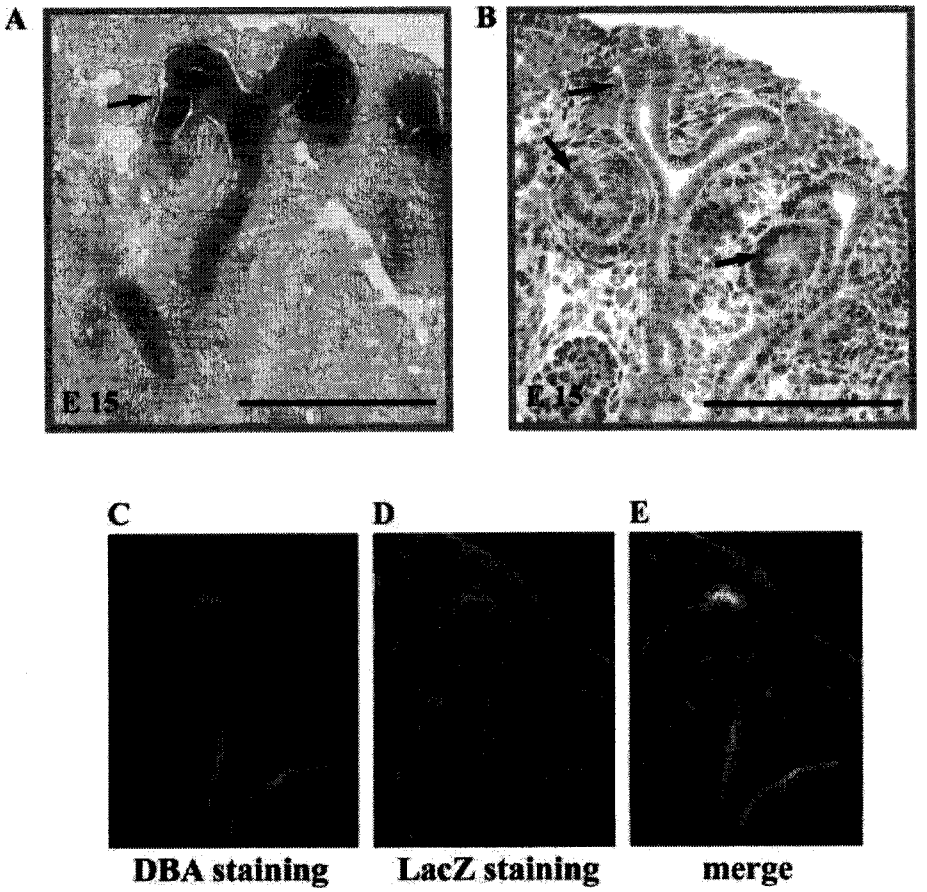

Fig. 2. β-Catenin signaling is restricted to the UB tips at later stages in development. Higher-power view of *E15* kidney shows β-galactosidase staining at the tips of the UB and in the distal portion of S-shaped bodies (arrow); there is reduced β-galactosidase staining in the maturing trunk of the collecting duct (*A*). *E15* wild-type mouse kidney probed with anti-unphosphorylated β-catenin antibody shows active β-catenin (arrows) at the tips of the branching UB and in the S-shaped bodies (*B*). Cryosections from *E16.5* kidneys were stained with the fluorescent UB marker *dolichos biflorus agglutinin* (green; *C*) and a rhodamine-labeled antibody raised against β-galactosidase (red; *D*); the merged image demonstrates colocalization at the UB tip (*E*). Scale bar = 100 μm.

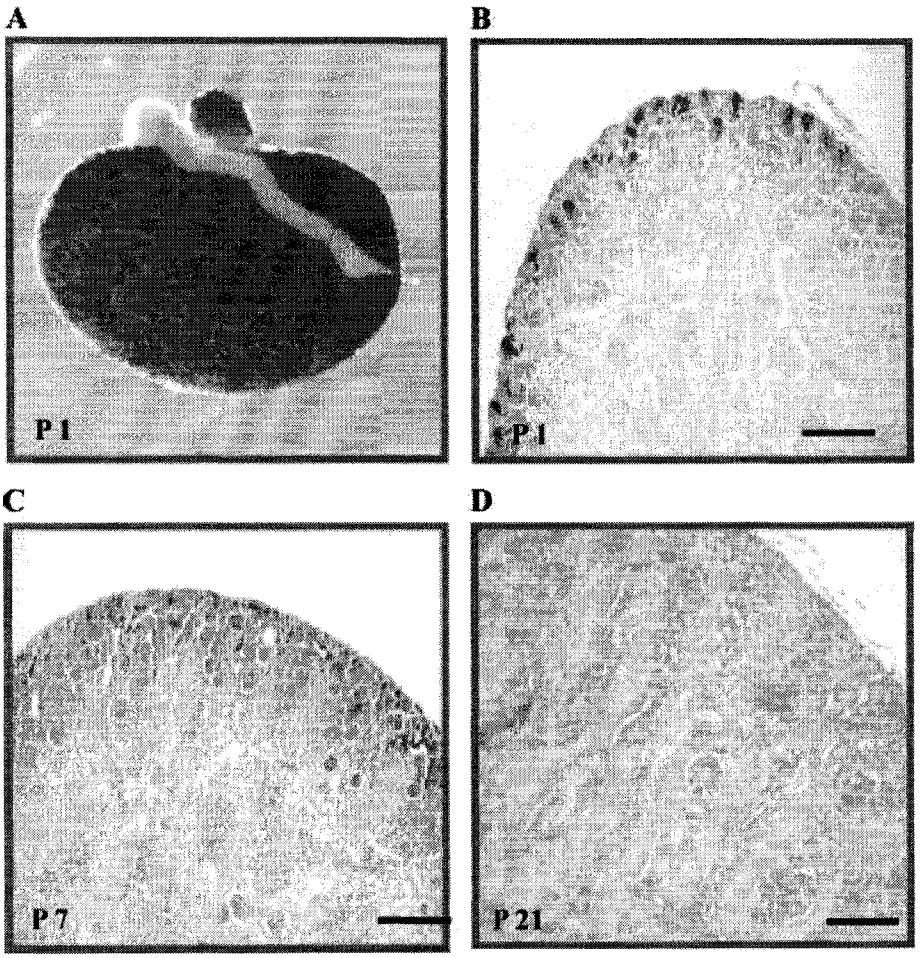

Fig. 3. β-Catenin signaling disappears after kidney development is completed. From *E18.5* through 3 wk of age, the β-galactosidase signal fades progressively: P1 [whole kidney (*A*), kidney section (*B*)], 1 wk (*C*), 3 wk (*D*). Scale bar = 100 μm.

fold ($P < 0.01$), in the two cell lines, respectively. Although WNT4 had no effect on MK4 cells, it stimulated TOPFLASH 2.7-fold ($P < 0.01$) in IMCD cells (Fig. 4, *A* and *B*).

DKK1 inhibition of the canonical β-catenin pathway suppresses branching nephrogenesis. Since β-catenin/TCF signaling was associated with UB tips, we considered the possibility that the canonical WNT pathway might be involved in branching nephrogenesis. To first confirm that DKK1 inhibits the canonical WNT signaling pathway in cells derived from the UB, as it does in other cell types (1), we transiently cotransfected IMCD cells with TOPFLASH and an expression vector containing the full-length murine DKK1 cDNA or an empty vector control. Cells were harvested after 48 h and assayed for luciferase activity. Luciferase activity was reduced to 23% of control in the presence of DKK1 plasmid ($P < 0.05$; Fig. 5*A*). IMCD cells were also exposed to recombinant murine DKK1 protein (0 or 500 ng/ml) for 24 h and then transiently transfected with TOPFLASH reporter vector. Fresh DKK1 was added 1 h after transfection and luciferase was measured 24 h later. As seen in Fig. 5*B*, recombinant DKK1 suppressed TOPFLASH activity by ~40% ($P < 0.01$).

To examine the effect of DKK1 on branching morphogenesis, *E13.5* kidneys were isolated from *HoxB7/GFP* mice and placed in explant culture for 24–48 h. From each embryo ($n = 4$), one kidney was cultured in the presence of recombinant DKK1 protein (2 μg/ml) to inhibit the canonical pathway, while the contralateral kidney served as a control. At 0, 24, and 48 h, explants were photographed under fluorescent light to assess the number of terminal UB tips; the extent of arborization was expressed as the percent increase in UB tip number compared with baseline for each kidney. At 24 h, UB tip number increased by 40% in controls but by only 18% in kidneys exposed to DKK1 ($P < 0.005$; Fig. 6, *A* and *B*). At 48 h, UB tip number had increased by 70% of baseline in controls vs. 40% of baseline in the presence of DKK1 ($P < 0.01$; Fig. 6, *A* and *B*).

To ascertain whether DKK1 blockade of canonical signaling affects structure of individual nephrons derived from induced mesenchyme, we visualized the expression pattern of Wilms Tumour protein (WT1) in *E13* kidney explants isolated from *HoxB7/GFP* mice after 24-h exposure to DKK1. In normal explants, WT1 protein is seen in condensing mesenchyme capping UB tips and in podocyte layers of emerging glomeruli; this pattern is well-preserved in DKK1-treated explants (Fig. 6*C*).

DISCUSSION

In this study, β-catenin/TCF signaling activity was first noted at *E11.5* in cells of the nephric duct cells during its caudal descent. This was also noted by Maretto et al. (20) in *E13.5* kidney of a similar β-catenin/TCF reporter mouse. The

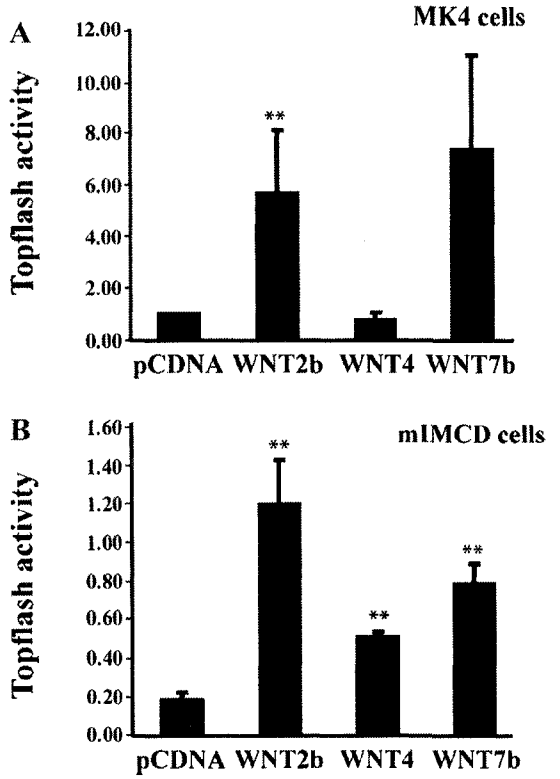

Fig. 4. Effect of WNTs on canonical signaling activity. MK4 (murine mesenchyme; *A*) and IMCD (murine collecting duct; *B*) cell lines were transfected with WNT2b, WNT4, WNT7b expression vectors, or empty vector to test their effect on the cotransfected canonical WNT pathway reporter vector, TOPFLASH. In both cell lines, WNT2b activated TOPFLASH (**$P < 0.05$) compared with empty vector controls. WNT4 had no effect on TOPFLASH in MK4 cells but had a significant effect in IMCD cells ($P < 0.01$). WNT7b also had a significant stimulatory effect in IMCD cells (**$P < 0.01$).

nephric duct lineage expresses a unique panel of genes such as *Lim-1*, *c-Ret*, *Pax2*, *Pax8*, and *Gata3*. Conceivably, canonical WNT signaling may specify nephric duct cell fate as it does in a variety of other developmental settings. In zebrafish, the canonical effects of WNT2b in lateral plate mesoderm are required for liver specification; liver organogenesis fails in *prt*(−/−) mutants bearing *Wnt2b* null alleles (25). Canonical WNT signals propel differentiation of bone cell precursors along the osteoblast pathway (10). In the inner ear, canonical WNT signals drive precursor cells toward the otic placode fate (26). Canonical WNT signaling is important for organogenesis of lung, pancreas, and mammary gland as well (5, 7, 24).

In developing metanephric kidney, we noted that β-catenin signaling activity becomes progressively focused at the tips of UB branches and gradually disappears from maturing UB trunks. Costantini has shown that UB tip cells express a unique panel of genes such as *Ret* and *Wnt11*, distinguishing them from sister cells which comprise the UB trunk (28). Davies and Michael (21) have also drawn attention to the fact that cell division at UB tips is especially intense at UB tips compared with the UB trunk. The β-catenin/TCF pathway activates transcription of specific gene targets including *Myc* and cyclin D1 (9) and can negatively regulate transcription of the potent cell cycle inhibitor, p21, in HEK293 cells (14). It seems plausible therefore that the β-catenin pathway could be involved in cell fate specification and proliferation of UB tip cells.

Strong β-catenin/TCF signaling activity was observed in the mesenchymal clusters capping each UB tip. As mesenchymal condensates progressed to the S-shaped body stage, β-catenin/TCF signaling was restricted to the distal portion of the structure, comprising the anlage of renal proximal and distal tubules; WNT signaling was conspicuously absent in the emerging glomerulus. This could suggest an additional role for canonical WNT signaling in cell fate specification and rapid growth of the nephron's tubular segments derived from mesenchyme. Interestingly, mice with a conditional knockout of β-catenin in lung epithelial cells exhibit fairly normal proximal airways but lack the distal portions of the pulmonary tree (24).

Since β-catenin/TCF signaling was especially intense in the nephrogenic zone of developing kidney, we considered the possibility that the pathway might be required for branching morphogenesis. To test this hypothesis, we blocked the canonical WNT signaling in kidney explants using recombinant DKK1. DKK1 specifically blocks the canonical pathway by binding to the frizzled coreceptor, LRP5/6, and interfering with WNT ligand binding (1). When *E13.5* kidney explants from *HoxB7/GFP* fetal mice were exposed to DKK1, we found that the number of UB branch tips was significantly reduced (40% of controls) within 24 h. If we take into account that UB branching is reiterated many times before nephrogenesis comes to an end, the impact of a moderate inhibition of branching is amplified many times over. The effect of DKK1 is comparable to the effect of Pax2 haploinsufficiency which produces renal insufficiency in mutant mice (8). This is the first demonstration

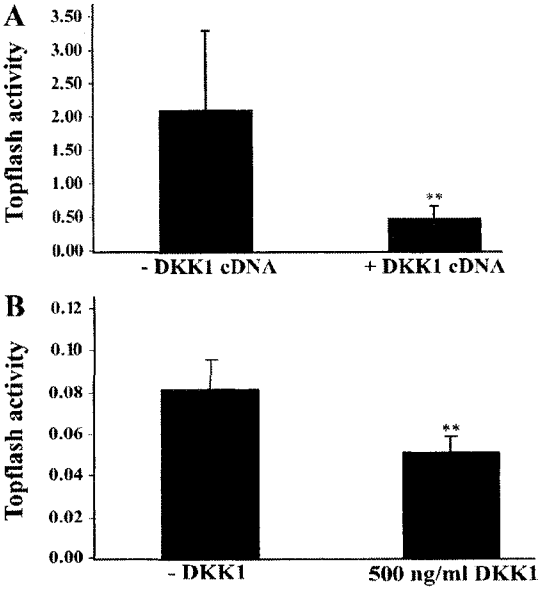

Fig. 5. DKK1 suppresses canonical WNT signaling activity in cell culture. Inner medullary collecting duct (IMCD) cells were transiently cotransfected with TOPFLASH and an expression vector containing full-length DKK1 cDNA or empty vector control (*A*). After 48 h, luciferase activity was significantly reduced (23% of control, **$P < 0.05$) by DKK1. To test the ability of recombinant mouse DKK1 protein to inhibit canonical signaling, IMCD cells were transiently cotransfected with TOPFLASH and a control vector in the presence (500 ng/ml) or absence (0 ng/ml) of DKK1 protein (*B*). After 24 h, luciferase activity was reduced to 40% of the control (**$P < 0.01$).

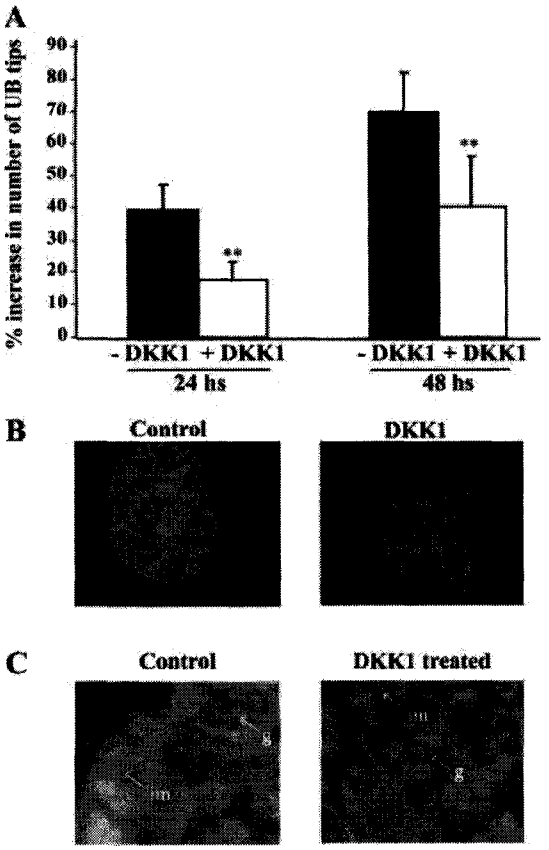

Fig. 6. DKK1 reduces UB branching in *E13.5* mouse kidney explants. *E13.5* kidneys from *Hoxb7/GFP* mice were cultured in the presence or absence of recombinant murine DKK1 protein. UB tip number was counted under fluorescent light at 0, 24, and 48 h and expressed as the percent increase above baseline (*A*). After 24 h, control kidney UB tips had increased by 40%, while kidneys exposed to DKK1 inhibitor showed an increase of only 18% in UB tip number (**$P < 0.005$). After 48 h, control kidney UB tip number had increased to 70% of baseline, whereas UB tip number had increased to only 40% of baseline in kidneys exposed to DKK1 (**$P = 0.01$). Representative images (*B*) of control and DKK1 explants at 48 h (×40) demonstrate the decrease in UB branching. Immunofluorescent staining of WT1 in *E13* HoxB7/GFP kidney explants shows similar WT1 expression pattern in induced mesenchyme (im) and podocyte layers of emerging glomeruli (g) in both control and DKK1-treated tissue (*C*).

that canonical WNT signaling is required for branching morphogenesis in the kidney. De Langhe et al. (6) observed similar inhibition of pulmonary branching in murine fetal lung explants exposed to DKK1.

Our studies identify the primary sites of canonical β-catenin/TCF pathway activity during kidney development. This begs the question as to which WNT ligands might be driving this focused pathway activity. Several canonical WNTs (WNT7b, WNT6, and WNT9b) are expressed in the nephric duct and the early UB. However, WNT7b is evident in the UB stalk by *E13.5* (16) but is not evident at UB tips or in S-shaped bodies. WNT6 is expressed in the UB at early stages but is downregulated after *E14.5* (13). WNT6 can induce tubulogenesis in tissue culture assays but was unable to support UB branching in vitro. Similarly, WNT9b is expressed in the nephric duct and UB stalk from *E9.5* to *E14.5*, but is downregulated thereafter (4). While each of these three WNTs could contribute to canonical signaling in early stages, none could account for the intense TCF signaling activity associated with UB tips or S-shaped bodies during later stages of nephrogenesis.

WNT11, WNT2b, and WNT4 are all expressed at sites that might account for the observed TCF signaling activity. However, WNT11 has been consistently associated with noncanonical signaling pathway activity in other reports and had no effect on TOPFLASH in our assays. On the other hand, WNT2b is expressed as early as *E11.5* in metanephric mesenchyme (18) and has been shown to activate the β-catenin pathway in other settings (17). Lin et al. (30) showed that WNT2b supported growth of isolated mouse UB. In our studies, WNT2b activated the canonical pathway in both MK4 (mesenchymal) and IMCD (UB lineage) cells.

WNT4 is expressed in the condensing mesenchyme and in the S-shaped bodies as they differentiate (31) and can activate the canonical pathway in Madin-Darby canine kidney cells derived from the renal collecting duct (19). Similarly, in our assays, WNT4 activated the canonical TOPFLASH reporter in IMCD cells. However, there was no apparent effect on mesenchymally derived MK4 cells. Furthermore, we found no apparent effect of DKK1 on WT1 expression in glomeruli of fetal kidney explants. Thus the restricted canonical signaling activity at the distal end of the S-shaped body may reflect stimulation by mesenchymal WNT2b. WNT4 derived from the condensing mesenchyme might contribute to other canonical ligands affecting the UB tip, but the profound effects of WNT4 on progression of condensing mesenchyme to the S-shaped body stage must involve its capacity to activate noncanonical signaling pathways (19).

As murine kidney development progresses, canonical WNT signaling activity disappears from maturing segments of the nephron and is restricted to the nephrogenic zone. In the perinatal period, as nephrogenesis comes to an end, WNT signaling activity is completely extinguished. The inhibitory mechanism is not entirely clear, but Simons et al. (29) proposed that onset of tubular flow through mature nephron segments induces signals from luminal cilia which may suppress the canonical WNT pathway. When IMCD cells were exposed to laminar flow in vitro, expression of the cilial protein, inversin, increased and cytoplasmic levels of β-catenin fell. Inversin appears to suppress TOPFLASH activity by inducing degradation of the key signal transduction pathway molecule, dishevelled.

In summary, intense canonical WNT signaling pathway activity is evident throughout the nephric duct and early UB, where it is required for normal branching morphogenesis. When canonical WNT activity is blocked by exogenous Dickkopf-1 protein, arborisation of the UB is diminshed. As development proceeds, WNT signaling is progressively restricted to UB tips and distal portions of the S-shaped body but is suppressed in the emerging glomerulus and in maturing trunks of the UB and is globally downregulated as nephrogenesis comes to an end. We hypothesize that suboptimal WNT signaling could result in renal hypoplasia, whereas failure of mechanisms that normally suppress WNT signaling might contribute to aberrant budding growth of tubular cells in polycystic kidney disease.

GRANTS

This work was supported by a grant from the Canadian Institutes of Health Research (CIHR; MOP 12954). D. M. Iglesias is the recipient of a research

fellowship award from the Kidney Foundation of Canada. P. R. Goodyer is the recipient of a CIHR/James McGill Research Chair. P.-A. Hueber was the recipient of a Montreal Children's Hospital Research studentship and A. Dziarmaga held a CIHR studentship award.

REFERENCES

1. **Bafico A, Liu G, Yaniv A, Gazit A, Aaronson SA.** Novel mechanism of Wnt signaling inhibition mediated by Dickkopf-1 interaction with LRP6/Arrow. *Nat Cell Biol* 3: 683–686, 2001.
2. **Brennan K, Gonzalez-Sancho JM, Castelo-Soccio LA, Howe LR, Brown AM.** Truncated mutants of the putative Wnt receptor LRP6/Arrow can stabilize beta-catenin independently of Frizzled proteins. *Oncogene* 23: 4873–4884, 2004.
3. **Cadoret A, Ovejero C, Saadi-Kheddouci S, Souil E, Fabre M, Romagnolo B, Kahn A, Perret C.** Hepatomegaly in transgenic mice expressing an oncogenic form of beta-catenin. *Cancer Res* 61: 3245–3249, 2001.
4. **Carroll TJ, Park JS, Hayashi S, Majumdar A, McMahon AP.** Wnt9b plays a central role in the regulation of mesenchymal to epithelial transitions underlying organogenesis of the mammalian urogenital system. *Dev Cell* 9: 283–292, 2005.
5. **Chu EY, Hens J, Andl T, Kairo A, Yamaguchi TP, Brisken C, Glick A, Wysolmerski JJ, Millar SE.** Canonical WNT signaling promotes mammary placode development and is essential for initiation of mammary gland morphogenesis. *Development* 131: 4819–4829, 2004.
6. **De Langhe SP, Sala FG, Del Moral PM, Fairbanks TJ, Yamada KM, Warburton D, Burns RC, Bellusci S.** Dickkopf-1 (DKK1) reveals that fibronectin is a major target of Wnt signaling in branching morphogenesis of the mouse embryonic lung. *Dev Biol* 277: 316–331, 2005.
7. **Dessimoz J, Bonnard C, Huelsken J, Grapin-Botton A.** Pancreas-specific deletion of beta-catenin reveals Wnt-dependent and Wnt-independent functions during development. *Curr Biol* 15: 1677–1683, 2005.
8. **Dziarmaga A, Eccles M, Goodyer P.** Suppression of ureteric bud apoptosis rescues nephron endowment and adult renal function in Pax2 mutant mice. *J Am Soc Nephrol* 17: 1568–1575, 2006.
9. **Giles RH, van Es JH, Clevers H.** Caught up in a Wnt storm: Wnt signaling in cancer. *Biochim Biophys Acta* 1653: 1–24, 2003.
10. **Glass DA, 2nd Bialek P, Ahn JD, Starbuck M, Patel MS, Clevers H, Taketo MM, Long F, McMahon AP, Lang RA, Karsenty G.** Canonical Wnt signaling in differentiated osteoblasts controls osteoclast differentiation. *Dev Cell* 8: 751–764, 2005.
11. **He X, Semenov M, Tamai K, Zeng X.** LDL receptor-related proteins 5 and 6 in Wnt/beta-catenin signaling: arrows point the way. *Development* 131: 1663–1677, 2004.
12. **Herzlinger D, Qiao J, Cohen D, Ramakrishna N, Brown AM.** Induction of kidney epithelial morphogenesis by cells expressing Wnt-1. *Dev Biol* 166: 815–818, 1994.
13. **Itaranta P, Lin Y, Perasaari J, Roel G, Destree O, Vainio S.** Wnt-6 is expressed in the ureter bud and induces kidney tubule development in vitro. *Genesis* 32: 259–268, 2002.
14. **Kamei J, Toyofuku T, Hori M.** Negative regulation of p21 by beta-catenin/TCF signaling: a novel mechanism by which cell adhesion molecules regulate cell proliferation. *Biochem Biophys Res Commun* 312: 380–387, 2003.
15. **Katoh M, Kirikoshi H, Terasaki H, Shiokawa K.** WNT2B2 mRNA, upregulated in primary gastric cancer, is a positive regulator of the WNT-beta-catenin-TCF signaling pathway. *Biochem Biophys Res Commun* 289: 1093–1098, 2001.
16. **Kispert A, Vainio S, Shen L, Rowitch DH, McMahon AP.** Proteoglycans are required for maintenance of Wnt-11 expression in the ureter tips. *Development* 122: 3627–3637, 1996.
17. **Landesman Y, Sokol SY.** Xwnt-2b is a novel axis-inducing *Xenopus* Wnt, which is expressed in embryonic brain. *Mech Dev* 63: 199–209, 1997.
18. **Lin Y, Liu A, Zhang S, Ruusunen T, Kreidberg JA, Peltoketo H, Drummond I, Vainio S.** Induction of ureter branching as a response to Wnt-2b signaling during early kidney organogenesis. *Dev Dyn* 222: 26–39, 2001.
19. **Lyons JP, Mueller UW, Ji H, Everett C, Fang X, Hsieh JC, Barth AM, McCrea PD.** Wnt-4 activates the canonical beta-catenin-mediated Wnt pathway and binds Frizzled-6 CRD: functional implications of Wnt/beta-catenin activity in kidney epithelial cells. *Exp Cell Res* 298: 369–387, 2004.
20. **Maretto S, Cordenonsi M, Dupont S, Braghetta P, Broccoli V, Hassan AB, Volpin D, Bressan GM, Piccolo S.** Mapping Wnt/beta-catenin signaling during mouse development and in colorectal tumors. *Proc Natl Acad Sci USA* 100: 3299–3304, 2003.
21. **Michael L, Davies JA.** Pattern and regulation of cell proliferation during murine ureteric bud development. *J Anat* 204: 241–255, 2004.
22. **Mohamed OA, Clarke HJ, Dufort D.** Beta-catenin signaling marks the prospective site of primitive streak formation in the mouse embryo. *Dev Dyn* 231: 416–424, 2004.
23. **Mohamed OA, Jonnaert M, Labelle-Dumais C, Kuroda K, Clarke HJ, Dufort D.** Uterine Wnt/beta-catenin signaling is required for implantation. *Proc Natl Acad Sci USA* 102: 8579–8584, 2005.
24. **Mucenski ML, Wert SE, Nation JM, Loudy DE, Huelsken J, Birchmeier W, Morrisey EE, Whitsett JA.** β-Catenin is required for specification of proximal/distal cell fate during lung morphogenesis. *J Biol Chem* 278: 40231–40238, 2003.
25. **Ober EA, Verkade H, Field HA, Stainier DY.** Mesodermal Wnt2b signaling positively regulates liver specification. *Nature* 442: 688–691, 2006.
26. **Ohyama T, Mohamed OA, Taketo MM, Dufort D, Groves AK.** Wnt signals mediate a fate decision between otic placode and epidermis. *Development* 133: 865–875, 2006.
27. **Omer CA, Miller PJ, Diehl RE, Kral AM.** Identification of Tcf4 residues involved in high-affinity beta-catenin binding. *Biochem Biophys Res Commun* 256: 584–590, 1999.
28. **Shakya R, Watanabe T, Costantini F.** The role of GDNF/Ret signaling in ureteric bud cell fate and branching morphogenesis. *Dev Cell* 8: 65–74, 2005.
29. **Simons M, Gloy J, Ganner A, Bullerkotte A, Bashkurov M, Kronig C, Schermer B, Benzing T, Cabello OA, Jenny A, Mlodzik M, Polok B, Driever W, Obara T, Walz G.** Inversin, the gene product mutated in nephronophthisis type II, functions as a molecular switch between Wnt signaling pathways. *Nat Genet* 37: 537–543, 2005.
30. **Srinivas S, Goldberg MR, Watanabe T, D'Agati V, al-Awqati Q, Costantini F.** Expression of green fluorescent protein in the ureteric bud of transgenic mice: a new tool for the analysis of ureteric bud morphogenesis. *Dev Genet* 24: 241–251, 1999.
31. **Stark K, Vainio S, Vassileva G, McMahon AP.** Epithelial transformation of metanephric mesenchyme in the developing kidney regulated by Wnt-4. *Nature* 372: 679–683, 1994.
32. **Steel MD, Puddicombe SM, Hamilton LM, Powell RM, Holloway JW, Holgate ST, Davies DE, Collins JE.** Beta-catenin/T-cell factor-mediated transcription is modulated by cell density in human bronchial epithelial cells. *Int J Biochem Cell Biol* 37: 1281–1295, 2005.
33. **Unsworth B, Grobstein C.** Induction of kidney tubules in mouse metanephrogenic mesenchyme by various embryonic mesenchymal tissues. *Dev Biol* 21: 547–556, 1970.
34. **Vainio SJ.** Nephrogenesis regulated by Wnt signaling. *J Nephrol* 16: 279–285, 2003.
35. **Wang Z, Shu W, Lu MM, Morrisey EE.** Wnt7b activates canonical signaling in epithelial and vascular smooth muscle cells through interactions with Fzd1, Fzd10, and LRP5. *Mol Cell Biol* 25: 5022–5030, 2005.

Am J Physiol Renal Physiol 291: F913–F920, 2006.
First published May 30, 2006; doi:10.1152/ajprenal.00004.2006.

Neuronal apoptosis inhibitory protein is expressed in developing kidney and is regulated by PAX2

Alison Dziarmaga,[1] Pierre-Alain Hueber,[2] Diana Iglesias,[1] Nancy Hache,[1] Aaron Jeffs,[3] Nathalie Gendron,[4] Alex MacKenzie,[4] Michael Eccles,[3] and Paul Goodyer[1,2]

[1]*Department of Human Genetics, McGill University, Montreal Children's Hospital Research Institute, Montreal, Quebec;* [2]*Department of Pediatrics, McGill University, Montreal Children's Hospital 2300 Tupper, Montreal, Quebec;* [4]*Department of Pediatrics, University of Ottawa, Ottawa, Ontario, Canada; and* [3]*Department of Pathology, University of Otago, Hercus Building, Dunedin, New Zealand*

Submitted 5 January 2006; accepted in final form 9 May 2006

Dziarmaga, Alison, Pierre-Alain Hueber, Diana Iglesias, Nancy Hache, Aaron Jeffs, Nathalie Gendron, Alex MacKenzie, Michael Eccles, and Paul Goodyer. Neuronal apoptosis inhibitory protein is expressed in developing kidney and is regulated by PAX2. *Am J Physiol Renal Physiol* 291: F913–F920, 2006. First published May 30, 2006; doi:10.1152/ajprenal.00004.2006.—During fetal kidney development, the extent of ureteric bud (UB) branching will determine final nephron endowment for life. Nephron number varies widely among normal humans and those who are born at the low end of the nephron number spectrum may be at risk for essential hypertension in adulthood. Little is known about how nephron number is set. However, we previously showed that the transcription factor, *Pax2*, suppresses apoptosis in UB cells during kidney development and optimizes branching morphogenesis. Here, we report that PAX2 directly binds to a specific recognition motif in the human neuronal apoptosis inhibitory protein (*NAIP*) gene promoter. NAIP is an endogenous inhibitor of apoptosis, inactivating caspase-3 and caspase-7 in neuronal tissues. PAX2 activates *NAIP* gene transcription (7-fold) in vitro and *NAIP* transcript level is increased fourfold in HEK293 cells stably transfected with *PAX2*. We show that *Naip* is expressed in embryonic *day 15* (*E15*) fetal kidney tissue (RT-PCR) and NAIP protein is demonstrated by immunohistochemistry in *E15* mouse kidney collecting ducts and P1 proximal tubules. *Naip* mRNA is significantly reduced (50%) in heterozygous *Pax2* mutant mice. Finally, we show that an antisense *Naip1* cDNA transfected into murine collecting duct cells doubles caspase-3/7 activity induced by *Baxα*. These observations suggest that the powerful effects of PAX2 on renal branching morphogenesis and final nephron number may be mediated by activation of *Naip* which then suppresses apoptosis in UB cells.

Naip (*Birc1*); kidney development; renal hypoplasia

DEVELOPMENT OF THE METANEPHRIC kidneys begins when the ureteric bud (UB) emerges from the wall of the nephric duct and grows laterally into the adjacent mesenchyme and begins to arborize. Signals from the tip of each UB branch induce formation of individual nephrons. When nephrogenesis finally comes to an end (~1 mo before birth in humans), the number of UB branching events by that time will determine nephron number for life. Although there are multiple genes required for branching morphogenesis, the molecular mechanism by which nephron number is set remains unknown.

When congenital nephron number is severely reduced, renal functional capacity is insufficient for postnatal life and children develop progressive renal failure as they grow. About 40% of pediatric end-stage renal disease is due to some form of congenital hypoplasia (2). Even in the "normal" population, however, nephron number varies widely, ranging from 300,000 to over one million per kidney (7). This was once dismissed as a benign reflection of human diversity but recent evidence suggests that subtle renal hypoplasia may be of considerable clinical importance. Mice with heterozygous *Gdnf* mutations have a significant decrease (30%) in total nephron number. These mice develop glomerular hypertrophy and hypertension as adults (9). This observation is remarkably similar to the report of Keller et al. (22) who found that patients with essential hypertension have roughly 50% fewer nephrons than age-matched controls.

In 1995, Sanyanusin et al. (42, 43) reported that a rare form of autosomal dominant renal hypoplasia, Renal-Coloboma Syndrome (RCS), is caused by mutations of the developmental transcription factor, *PAX2*. In this syndrome, renal hypoplasia is associated with defects of the optic nerve (36). Some patients lacking obvious eye findings were initially assigned the diagnosis of "oligomeganephronia," based on renal biopsies showing an absolute reduction in nephron number associated with striking hypertrophy of glomeruli (40). Subsequently, the patients were also found to have heterozygous *PAX2* mutations (40), suggesting that *PAX2* is centrally involved in setting nephron number.

PAX2 is one of the nine members of the "paired-box" family of transcription factor genes and is normally expressed in fetal midbrain-hindbrain region, the eye, the ear, and the kidney (11). During kidney development, *Pax2* is first expressed in the nephric duct during its caudal descent and then in the branching UB (4, 11). Fetal mice with heterozygous *Pax2* mutations exhibit a striking increase in apoptosis of UB cells (36). *Pax2* inactivation also enhances apoptosis in mIMCD-3 cells derived from murine collecting duct (46). Targeted expression of a proapoptotic gene (*Baxα*) to the fetal UB increases apoptosis and reduces the number of branching events by embryonic *day 15* (*E15.5*), mimicking RCS (12). Furthermore, the renal branching deficit in *Pax2* mutants can be reversed in vitro and in vivo by the caspase inhibitor z-VAD-fmk (8). Thus PAX2 appears to suppress programmed cell death in the UB lineage during branching morphogenesis of the kidney. This effect is critical to achieve optimal nephron number at birth (12).

Address for reprint requests and other correspondence: P. Goodyer, Montreal Children's Hospital Research Institute, 4060 Ste-Catherine St. West, #413–1, Montreal, Quebec, Canada H3Z 2Z3 (e-mail: Paul.Goodyer@muhc.mcgill.ca).

The costs of publication of this article were defrayed in part by the payment of page charges. The article must therefore be hereby marked "*advertisement*" in accordance with 18 U.S.C. Section 1734 solely to indicate this fact.

The mechanism by which PAX2 suppresses the pathways of programmed cell death is unknown. We examined expression of apoptosis-related genes in HEK293 cells stably transfected with *PAX2*. This focused our attention on the neuronal apoptosis inhibitory protein (*NAIP*) gene, also known as *BIRC1*, encoding an endogenous caspase inhibitor. Although *NAIP* was initially discovered during positional cloning of the spinal muscular atrophy gene and NAIP protein was subsequently shown to inhibit caspases-3 and -7 in neural tissue (27), we show that NAIP is also expressed in fetal kidney UB. PAX2 directly binds to a motif in the *NAIP* promoter and stimulates transcriptional activity in vitro. *Naip* transcript levels are decreased in $Pax2^{1Neu}$ mutant mice. Unlike humans who have a single functional NAIP gene, mice have multiple copies. However, we show that the *Naip1* transcript is abundant in fetal kidney and an anti-sense *Naip1* cDNA enhances apoptosis in cultured murine kidney collecting duct cells.

MATERIALS AND METHODS

RNA isolation. Total RNA was isolated from mouse kidneys at fetal stages *E15.5* and *E18.5*, at postnatal *day 1*, and adult kidney of wild-type and $Pax2^{1Neu}$ mice. Briefly, tissues were microdissected and placed in RNAlater (Ambion, Austin, TX) at 4°C. Each kidney was homogenized in TRIzol (Invitrogen, Carlsbad, CA) for 5 min and then mixed with 0.2 volumes of chloroform and incubated at room temperature for 10 min. Samples were centrifuged at 12,000 rpm for 15 min at 4°C. The aqueous layer was removed and equal volume of 70% ethanol was added. Samples were then processed with the RNeasy kit (Qiagen, Valencia, CA) as per manufacturer's recommendations and total RNA was eluted in 30 μl of RNase-free water. Total RNA was also isolated from cultured cells with TRIzol (Invitrogen) as above or with phenol/chloroform extraction followed by DNaseI treatment (Promega, Madison, WI).

Real-time RT-PCR of IAPs. Human fetal kidney (HEK293) cells were stably cotransfected with a hygromycin resistance vector and a pUHD mammalian expression vector containing a CMV-driven full length human *PAX2b* cDNA or an empty vector control (46). Transfectants were selected in hygromycin and cloned. PAX2 expression was confirmed by Western immunoblotting. RNA samples from cells ± *PAX2* were analyzed for the following inhibitors of apoptosis (IAPs): *XIAP*, *NAIP*, *HIAP1*, *HIAP2*, and *Survivin*, by real-time RT-PCR (with *GAPDH* as internal standard) as previously described (30). The comparative C_T method was used for relative quantification between HEK293/*PAX2*(+) and HEK293/*PAX2*(−) cells (26).

RT-PCR of total Naip transcripts in mIMCD-3 cells. Total RNA (200 ng or 1 μg) was reverse transcribed by using a one-step RT-PCR kit (Qiagen) with gene-specific primers as per manufacturer's recommendations. Mouse *Naip* primers were designed for a 487-bp fragment of the coding region spanning exons 2–9. The primers contained conserved sequences common to all mouse *Naip* isoforms (21). *Naip* forward: 5′-GGGACATCACCACGTGTACTC-3′; *Naip* reverse: 5′-TTGTTGTGCTCTTGTATTGGG-3′; *Gapdh* forward: 5′-AAGGGCTCATGACCACAGTC-3′; and *Gapdh* reverse: 5′-CATACTTGGCAGGTTTCTCCA-3′. RT-PCR conditions were as follows; a 30-min reverse transcription step at 50°C proceeded by an incubation at 95°C for 15 min. A total of 35 cycles were performed at 94°C for 1 min, 58°C for 1 min, 72°C for 1 min, followed by 72°C for 10 min. Samples were run on a 1% agarose gel. The product sizes for *Naip* and *Gapdh* were 487 and 252 bp, respectively.

Real-time RT-PCR assay of total Naip transcripts in $Pax2^{1Neu}$ (+/−) mutant mice. cDNA was synthesized from 500 ng of mouse kidney total RNA using random hexamer primers (Promega) and Superscript III (Invitrogen) as per the manufacturer's recommendation. One microliter of cDNA was used for Sybr Green-based quantitative real-time RT-PCR by using a Prism 7000 Sequence Detection System (ABI). PCR conditions were as follows: 2-min incubation at 95°C, followed by 40 cycles of 95°C for 30 s, 60°C for 30 s, and 72°C for 30 s. Results were standardized with a housekeeping gene, beta 2 microglobulin (*B2m*), and the comparative C_T method was used for relative quantification (3, 26). Duplicate samples from four different litters of *E15.5* fetuses (wild-type, $n = 12$ and $Pax2^{1Neu}$, $n = 16$) and two different litters of postnatal *day 1* animals (wild-type, $n = 13$ and $Pax2^{1Neu}$, $n = 5$) were studied. Intron-spanning primers were designed for mouse *Naip* and *B2m* as follows: *Naip* forward primer: 5′-GCCAGGTACCATGAAGAGGA-3′; *Naip* reverse primer: 5′-CCACAGGAAAAACACTGCAC-3′; *B2m* forward primer: 5′-TGCAGAGTTAAGCATGCCAGTATGG-3′; and *B2m* reverse primer: 5′-TGATGCTTGATCACATGTCTCG-3′. Amplicons for *Naip* and *B2m* were 143 and 75 bp, respectively.

Real-time RT-PCR of Naip1 transcript in mouse kidney. For real-time quantitative RT-PCR of *Naip1*, 100 ng of total RNA for each sample were assayed in triplicate for expression of *Naip1* RNA simultaneously with mouse *Gapdh* mRNA. RT-PCR reactions were performed in the ABI Prism 7700 Sequence Detection System (Perkin Elmer Applied Biosystems, Foster City, CA) with the *Taq*Man EZ RT-PCR kit (Perkin Elmer Applied Biosystems) and *Taq*Man Rodent *Gapdh* control reagent (Perkin Elmer Applied Biosystems). Reactions were performed according to manufacturer's recommendations. Briefly, 25-μl RT-PCR reactions contained: 1× *Taq*Man EZ Buffer, 3 mM Mn(OAc), 300 μM deoxy-ATP, -CTP, -GTP, 600 μM deoxyUTP, 100 nM rodent *Gapdh* primers and probe, 600 nM mouse *Naip1* primers, 200 nM mouse *Naip1* probe, 0.25 μl AmpErase UNG, and 2.5 U rTth DNA Polymerase. RT-PCR conditions were: 2 min at 50°C, 30 min at 60°C, 5 min at 95°C, followed by 40 cycles of 15 s at 94°C and 1 min at 60°C. Samples were normalized for *Gapdh* mRNA content and expressed as fold induction. Primers and probes use for *Naip1* were: forward primer: 5′-TTCCTGTGGCGGAAGCTT-3′; reverse primer: 5′-TGGGCAATTTCCTCTGAAGATT-3′; and probe: 5′-AGCATGCCAAGTGGTTCCCCAAATG-3′.

Western immunoblotting. Stably transfected HEK293 cells (+/− PAX2) were incubated on ice for 15 min in 10 mM HEPES, pH 7.9, 10 mM KCl, 0.1 mM EDTA, 0.1 mM EGTA, 1 mM dithiothreitol, 0.5 mM PMSF, and proteinase inhibitory cocktail (Roche Diagnostics, Mannheim, Germany). NP-40 was then added (0.3%) and the mix was vortexed, incubated on ice for 1 min, and centrifuged at 13,000 rpm for 5 min. The supernatant was discarded and the pellet was resuspended in lysis buffer containing 20 mM HEPES, pH 7.9, 400 mM NaCl, 1 mM EDTA, 1 mM EGTA, 1 mM dithiothreitol, 1 mM PMSF, proteinase inhibitory cocktail (Roche Diagnostics) and glycerol (25%). Following a 1-h incubation on ice, the lysate was centrifuged at 13,000 rpm for 5 min and the supernatant was removed and stored at −70°C until ready to use.

Cytoplasmic protein was extracted from whole postnatal *day −1* mouse kidney tissue. Briefly, kidneys were homogenized in 500 μl of RIPA buffer (50 mM Tris·HCl, pH 7.4, 150 mM NaCl, 1 mM PMSF, 1 mM EDTA, 5 μg/ml aprotinin, 5 μg/ml leupeptin, 1% Triton X-100, 1% Na Deoxycholate, 0.1% SDS), incubated on ice for 20 min, centrifuged at 13,500 rmp for 25 min at 4°C, and the supernatant was removed and stored at −70°C until ready to use.

Extracts containing 30 μg of protein (Pierce Biotechnology, Rockford, IL) were resolved on a 10% SDS-polyacrylamide gel and transferred to a nitrocellulose membrane (Bio-Rad, Mississauga, Ontario). Blots were probed with a 1:200 dilution of polyclonal anti-hNAIP antibody (AbCam) or a 1:250 dilution of polyclonal anti-mPAX2 antibody (Zymed, San Francisco, CA) followed by a 1:1,000 dilution of anti-rabbit IgG secondary antibody (Perkin Elmer Life Sciences, Boston, MA), detected with an enhanced chemiluminescence detection system (Amersham, Picataway, NJ) and exposed to autoradiography film (Kodak Biomax MR Film). Membranes probed for PAX2 were reprobed for β-actin (Oncogene Research Products, San Diego, CA) to normalize for loading differences.

Immunofluorescent staining. Kidneys from wild-type CD1 animals were microdissected at fetal age *day 15.5* and postnatal *day 1* and fixed in 4% paraformaldehyde (Sigma, St. Louis, MO) for 4 h at 4°C. Kidneys were rinsed briefly and then kept overnight in cold PBS. Tissues were placed in 15% sucrose/PBS until they sank, followed by 30% sucrose/PBS incubation and then placed in Tissue-Tek OCT (Sakura, Torrance, CA) at room temperature for 2 h before freezing on dry ice. Fourteen-micrometer sections were washed in PBS for 5–10 min, dried at room temperature for 10 min, and fixed in cold acetone for 10 min at room temperature. Sections were incubated in universal blocking horse serum in PBS for 1 h at room temperature, followed by an overnight incubation at 4°C with a 1:25 dilution of a polyclonal IgG rabbit anti-hNAIP antibody (Abcam, Cambridge, MA). Sections were then incubated with a 1:200 dilution of goat IgG anti-rabbit Texas Red (Vector Laboratories, Burlingame, CA) in a 0.1 M sodium bicarbonate, 0.15 M sodium chloride buffer, pH 8.5, for 1 h at room temperature in the dark. For double labeling, sections were also incubated overnight at 4°C with fluorescein-labeled lectins, *Dolichos Biflorus Agglutinin* (DBA), to identify collecting duct tubules and *Lotus Tetragonolobus* Lectin (LTL) to identify proximal tubules (Vector Laboratories), mounted with fluoromount (Sigma), and visualized with a Zeiss microscope. This antibody did not work on paraffin-embedded sections.

Vector construction and assay of promoter activity in vitro. A 780-bp *Sma*I and an end-filled *Age*I fragment containing the 5′ flanking sequence of the human *NAIP* gene (−780 to +1) was ligated into pGL2-basic upstream of the luciferase reporter using *Sma*I sites. NIH3T3 cells were cultured in monolayer and transiently transfected with the reporter vector using FuGene (Roche, Laval, QC) in the presence and absence of a full-length human PAX2b cDNA in pcDNA3. Cells at 60–70% confluency were transfected with 0.5 μg of human NAIP-Luciferase, 0.5 μg of human PAX2b cDNA or empty vector control, and 5 ng of *renilla* luciferase as a standard control. Cells were harvested after 48 h posttransfection and lysed in a 1× passive lysis buffer (Promega) and assayed for firefly and *renilla* luciferase using the Dual Luciferase Kit (Promega) as per the maufacturer's recommendations. Transfections were performed (6 replicates) on three separate occasions.

EMSA. Initial screening of the 780-bp human *NAIP* promoter sequence was done by MatInspector software. Putative PAX2 binding sites were identified and 40-bp oligos were synthesized, annealed, and labeled with [α-^{32}P]dCTP via the Klenow fill in reaction. Binding reactions containing buffer and purified human PAX2b protein were incubated on ice for 15 min, after which hot probe was added, and reactions were further incubated on ice for 30 min in a total volume of 20 μl. Samples were resolved at room temperature on a 6% nondenaturing polyacrylamide mini gel in 0.25× TBE at 90 V. Gels were then dried at 80°C for 30 min in a vacuum and exposed to film at room temperature overnight. To confirm specificity of DNA/protein complexes, reactions were also incubated with rabbit anti-PAX2 antibody (Zymed) or with mutated oligonucleotides. Competitive binding assays were performed with cold unlabeled probe at 50× and 100× excess. Full-length human *PAX2b* cDNA cloned into pcDNA3 was used to synthesize purified protein by a coupled in vitro transcription-translation system (TNT/T7, Promega) as per the manufacturer's recommendations and run on a 4% SDS-PAGE gel to confirm specificity: *NAIP* oligo: 5′-TGCCAGTGATTTAGCCAATCATGCCTAAGTGATGGCACCT; *NAIP* mut: 5′-TGCCAGTGATTTAGCCAATAATGTCTAAGTGATGGCACCT.

Naip1 knockdown in vitro in cultured cells. To study the effects of *Naip1* knockdown, murine inner medullary collecting duct (mIMCD-3) cells were cultured in DMEM medium supplemented with 10% fetal bovine serum and with 1% penicillin/streptomycin in six-well plates. Cells that were 50–60% confluent were transiently cotransfected with *Bax* cDNA and mouse *Naip1* anti-sense cDNA. The *Naip1* anti-sense construct is a 566-bp fragment of the first coding exon (exon 2) of the mouse *NAIP* gene cloned into the pCI plasmid (20). One microgram of total DNA (0.5 μg of *Bax* and 0.5 μg of either *Naip* anti-sense or empty pCI control) using FuGene (Roche) reagents as per the manufacturer's recommendations. Cells were harvested after 48 h of transfection in 1.0 ml of PBS by scraping and centrifugation at 4,000 rpm for 4 min. After several PBS washes, cell pellets were lysed in 1% NP-40, 0.1% SDS lysis buffer in PBS and incubated on ice for 20 min, followed by a 20-min centrifugation at 14,000 rpm at 4°C. The supernatant was removed and stored at −70°C until ready for analysis of caspase-3 activity (Promega). Total protein was measured (Pierce) and 10 μg were used in a volume of 50 μl and combined with 50 μl of caspase 3/7 substrate with buffer and incubated at room temperature for 1 h in the dark. Samples were assayed for caspase 3/7 activity by measure of firefly luciferase activity according to the manufacturer (Promega). Experiments were repeated on three separate occasions in duplicate.

RESULTS

PAX2 selectively activates endogenous NAIP in HEK293 cells. The HEK293 human embryonic kidney cell line expresses low levels of PAX2 protein. To determine whether PAX2 has an effect on the transcriptional activation of IAP genes, HEK293 cells were stably transfected with a CMV-driven expression vector containing the full-length human *PAX2b* cDNA. Stably transfected HEK293/*PAX2* cells exhibited high levels of PAX2 protein by Western immunoblotting compared with control cells transfected with empty plasmid (Fig. 1*A*). Total RNA was extracted from the cells and analyzed by real-time RT-PCR for changes in transcript levels of various IAP family members (*HAIP1*, *HAIP2*, *XIAP*, *Survivin*, and *NAIP*). Of these, only *NAIP* showed a significant increase (4-fold ±0.20 SE) in transcript level compared with control cells transfected with an empty plasmid ($P < 0.01$; Fig. 1*B*).

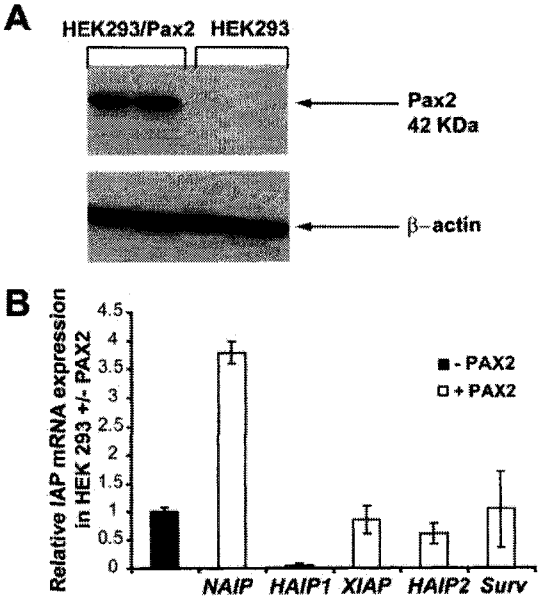

Fig. 1. Increased *NAIP* expression in HEK293 cells transfected with *PAX2*. HEK293 cells transiently transfected with full-length human *PAX2* cDNA had increased PAX2 protein compared with HEK293 cells transfected with an empty plasmid as a control (*A*). HEK293 cells ± *PAX2* were analyzed by real-time RT-PCR for changes in inhibitors of apoptosis (IAP) mRNA expression normalized to *GAPDH*. In the presence of *PAX2*, *NAIP* mRNA was increased 4-fold ($P < 0.01$; *B*). No other IAP was significantly stimulated by *PAX2*.

Naip is expressed in developing mouse kidney. Unlike humans who bear only one functional copy of the *NAIP* gene (51), mice have undergone gene duplication events resulting in six separate but highly homologous *Naip* genes (13, 52). To determine whether one or more *Naip* genes is expressed in the developing mouse kidney, we first assessed total *Naip* transcripts in RNA from *E15.5*, *E18.5*, P1 mouse kidney tissues, and mIMCD-3 cells (derived from murine collecting duct) by qualitative RT-PCR using primers for a completely conserved region spanning exons 2–8. *Naip* transcripts were evident in all samples (Fig. 2*A*), although earlier time points were not examined.

To demonstrate NAIP protein expression in the developing mouse kidney, we performed Western immunoblotting on whole P1 kidneys and immunofluorescent microscopy on frozen sections of normal *E15.5* mouse kidney, using a rabbit polyclonal antibody raised against human NAIP. Earlier time points were not studied. NAIP protein was identified as a single 140-kDa band by Western immunoblotting, confirming specificity of our antibody (Fig. 2*B*). As a marker for fetal collecting ducts, sections were costained with FITC-labeled DBA. As a marker for proximal tubules, the sections were costained with LTL. NAIP expression, detected with an anti-hNAIP primary antibody and Texas Red-tagged secondary antibody, was strong in all collecting duct structures (Fig. 2, *C*, *D*, *E*). By postnatal *day 1*, NAIP staining was also evident in proximal tubules (Fig. 2, *F*, *G*, *H*). Subcellular NAIP staining pattern is broader than that of DBA or LTL luminal markers (implying cytoplasmic and/or basolateral localization) but also seems to involve some NAIP protein at the luminal membrane. These expression patterns show some overlap with those of PAX2, which is strongly expressed in both collecting ducts and proximal tubules of fetal kidney (4, 36). Sections stained with secondary antibody alone showed no signal.

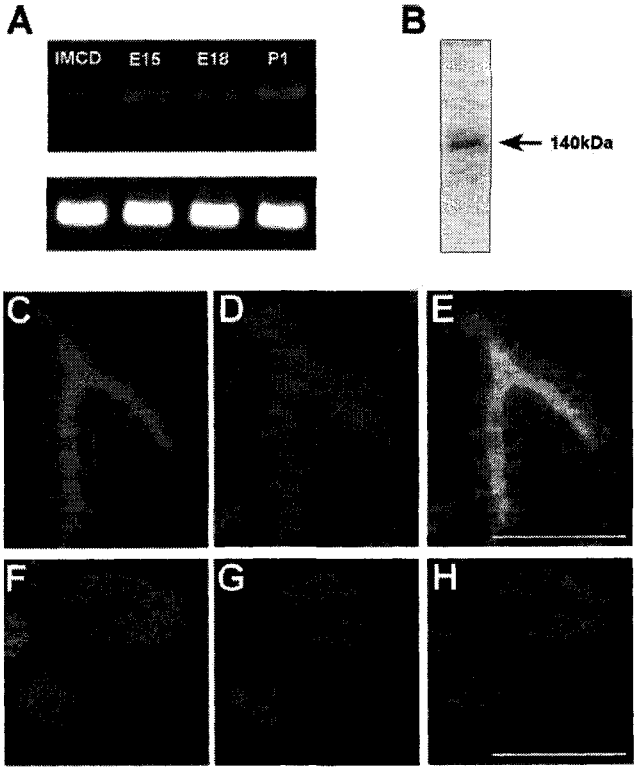

Fig. 2. *Naip* expression in fetal mouse kidney. *Naip* mRNA was detected in RNA from murine mIMCD-3 cells by RT-PCR (*A*). *Naip* mRNA was also detected in fetal (*E15.5*, *E18.5*) and newborn (P1) mouse kidney tissues (*A*). NAIP protein is seen as a 140-kDa band in extracts of whole P1 kidney (*B*). In frozen sections of *E15.5* mouse kidney, collecting duct cells stained by FITC-labeled *dolichos biflorus agglutinin* (DBA; *C*) also expressed NAIP protein (*D*). Coexpression of NAIP and DBA in collecting ducts is clearly demonstrated in the merged image (*E*). Newborn proximal tubular cells staining with *lotus tetragonolobus* lectin (LTL; *F*) also expressed NAIP protein (*G*). The coexpression of NAIP in proximal tubule cells is also demonstrated in a merged image (*H*).

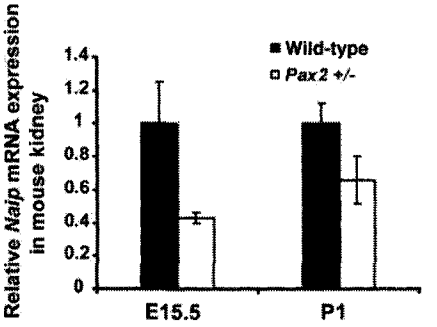

Fig. 3. Decreased *Naip* expression in heterozygous $Pax2^{1Neu}$ mutant mice. Real-time RT-PCR was used to assess levels of *Naip* mRNA (normalized to beta 2 microglobulin mRNA) in both fetal (*E15.5*) and newborn (P1) mouse kidneys. In *E15.5* $Pax2^{1Neu}$ heterozygous mutant kidneys, *Naip* mRNA was significantly reduced (50%) compared with wild-type controls ($P < 0.005$). *Naip* mRNA was similarly decreased in newborn *Pax2* mutants ($P < 0.05$).

Naip mRNA expression is reduced in fetal kidney of $Pax2^{1Neu}$ *(+/−) mutant mice.* Total RNA was isolated from wild-type and heterozygous $Pax2^{1Neu}$ mutant mouse kidney tissues at *E15.5* and postnatal *day −1* (P1). Quantitative real-time RT-PCR was used to assess *Naip* mRNA transcript levels normalized for beta 2 microglobulin. Kidneys from *E15.5* $Pax2^{1Neu}$ (+/−) mice showed a significant reduction (43 ± 3.4% SE of wild-type littermate controls) in the level of *Naip* transcript ($P < 0.005$). In P1 mutant kidneys, the decrease in *Naip* transcript expression was slightly less prominent (66 ± 16% SE of wild-type littermates; $P < 0.05$; Fig. 3).

PAX2 activates the NAIP promoter in vitro. Initial screening of the 780-bp 5′ flanking sequence of the human *NAIP* gene revealed a site homologous to the published core consensus sequence for PAX2 recognition motifs (Fig. 4*A*). This motif was located 140 bp upstream of the transcriptional start site. To determine whether *PAX2* activates the human *NAIP* promoter, a 780-bp fragment of the human *NAIP* 5′ flanking sequence was cloned into a luciferase reporter vector (Fig. 4*B*). NIH3T3 cells were transiently cotransfected with the *NAIP* promoter reporter and an expression vector containing the full-length *PAX2b* cDNA. Luciferase activity was increased 6.7-fold (±0.05 SD) in the presence of *PAX2b* compared with empty vector controls (1.0 ± 0.17 SD; $P < 0.001$; Fig. 4*C*).

PAX2 protein binds directly to the NAIP promoter. EMSA were used to demonstrate direct binding of human PAX2 protein to the human *NAIP* promoter. PAX2b protein was synthesized in vitro; presence of PAX2 protein in the translation mix was confirmed by Western immunoblotting (Fig. 5*A*). For EMSA, a 40-bp oligonucleotide containing the putative PAX2 binding motif was radiolabeled and incubated with PAX2b protein. A DNA/protein complex was observed that

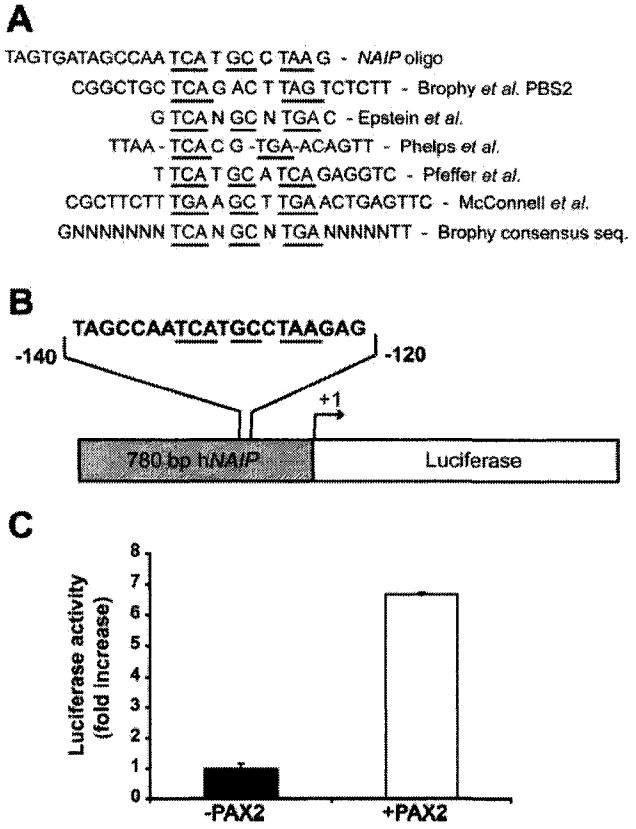

Fig. 4. Putative PAX2 binding sites in the *NAIP* promoter. A unique motif was identified in the 780-bp 5′ flanking sequence of the human *NAIP* gene which was highly homologous to published PAX2 binding sites (*A*). This putative PAX2 recognition motif was in close proximity to the *NAIP* transcriptional start site (*B*). To assess the promoter activity of this sequence in vitro, the whole 780-bp fragment was cloned into a luciferase reporter vector. The *NAIP*-luciferase construct was transiently cotransfected into NIH3T3 cells with or without a full-length PAX2 expression vector. In the presence of PAX2, *NAIP* promoter activity was significantly increased (6.7-fold) compared with an empty vector control ($P < 0.001$; *C*).

disappeared in the presence of PAX2 antibody (Fig. 5*B*). To confirm the specificity of the putative PAX2 binding motif, we performed competitive assays, incubating the protein and hot probe with 50× and 100× excess cold probe. Incubation with cold probe resulted in the disappearance of the DNA/protein complex (Fig. 5*C*). Furthermore, we mutated 2 bp in the conserved region of the published consensus sequence (Fig. 5*E*) and repeated the EMSA. When mutated oligos were incubated with PAX2b protein, a band shift was no longer observed (Fig. 5*D*).

Naip1 is expressed in fetal mouse kidney. In preliminary experiments using gene-specific primers for quantitative RT-PCR, we found that multiple *Naip* isoforms are expressed in mouse kidney (data not shown). However, *Naip1* (the most homologous to human *NAIP*) was a dominant transcript. *Naip1* levels in *E15* normal fetal mouse kidney were 7.4-fold higher (±1.87 SE) than in adult kidney (1.0 ± 0.138 SE; $P < 0.0001$; Fig. 6).

Naip1 antisense cDNA enhances apoptosis induced by Baxα in IMCD cells. In previous studies, we showed that mice expressing a *Baxα* transgene in renal collecting ducts caused increased apoptosis of those cells, mimicking the effects of *Pax2* haploinsufficiency (12). To ascertain whether *Naip1* inactivation affects susceptibility of murine collecting duct cells to apoptosis, we transiently transfected mIMCD-3 cells with an expression vector containing the full-length murine *Bax-α* cDNA to initiate the caspase cascade (Fig. 7). Cells were cotransfected with control (empty pCI vector) or a *Naip1* antisense cDNA expression vector previously shown to inactivate *Naip1* expression in neuronal cells (19). This antisense vector contains a 566-bp sequence complementary to the first

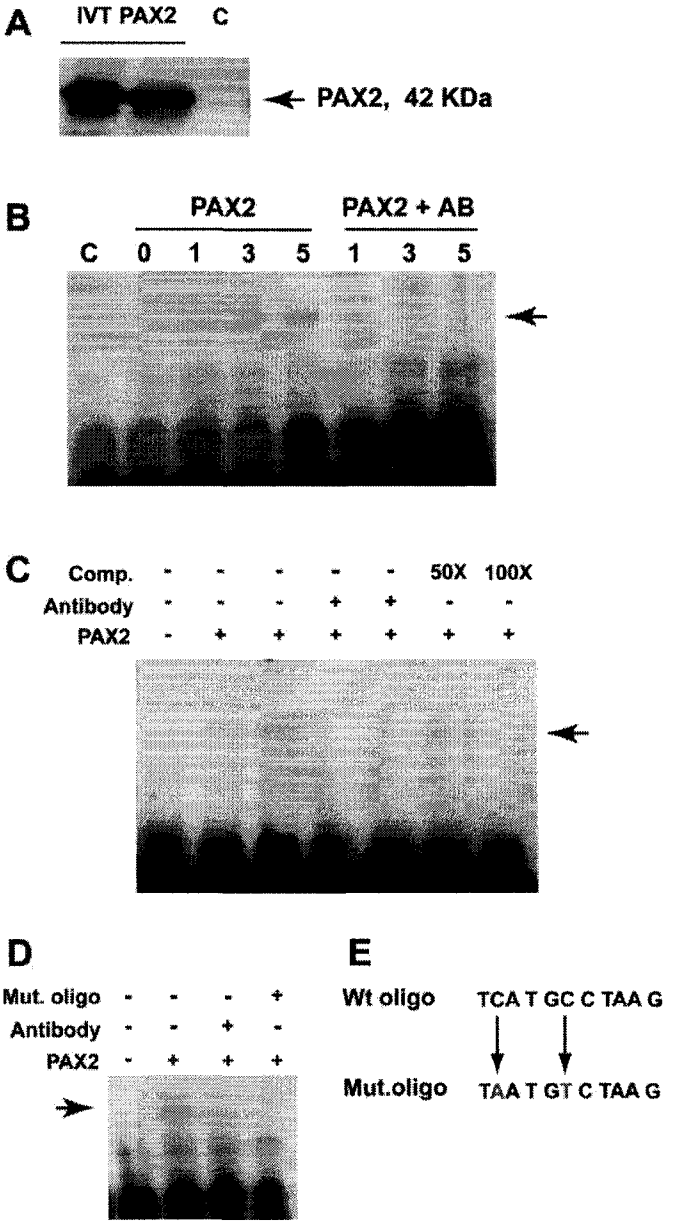

Fig. 5. Direct binding of PAX2 to human *NAIP* promoter. PAX2 protein was synthesized in a cell-free system and confirmed by immunoblotting (*A*). In EMSA experiments, PAX2 protein formed a high-molecular-weight complex with a radiolabeled 40-bp oligonucleotide containing the putative *NAIP* binding site (*B*). The band shift disappeared when the PAX2 protein was first incubated with anti-PAX2 antibody (*B* and *C*). The band shift was progressively competed out by increasing concentrations of cold *NAIP* probe (*C*). *NAIP* oligonucleotides containing mutations of 2 core nucleotides in the putative PAX2 recognition motif (*E*) abrogated PAX2 binding (*D*).

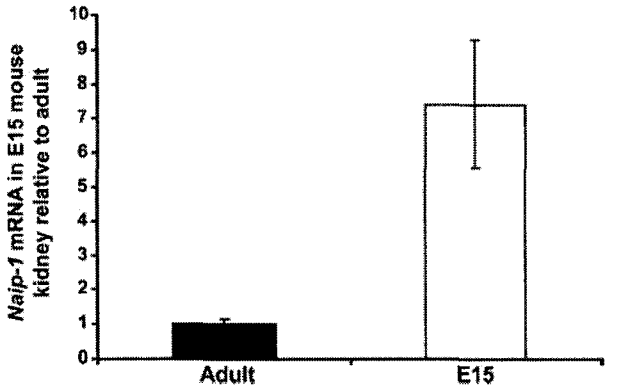

Fig. 6. *Naip-1* mRNA expression in fetal (*E15*) mouse kidney relative to that in adult mouse kidney. *Naip-1* mRNA was quantified by transcript-specific RT-PCR (normalized to *Gapdh*) in total RNA extracted from whole kidney isolated from 3 *E15* and 5 adult (4 mo) wild-type CD1 mice. *Naip-1* mRNA level in *E15* kidney was 7.4-fold greater than in adult kidney ($P < 0.0001$).

coding exon of *Naip1* (20). mIMCD-3 cells cotransfected with anti-sense *Naip1* showed a twofold (192 ± 35% SE) increase in *Baxα*-induced caspase 3/7 activity ($P < 0.05$).

DISCUSSION

Studies of mice and humans with RCS clearly implicate PAX2 in the regulation of final nephron number (36, 42, 43). During normal branching morphogenesis, UB cells rarely undergo programmed cell death but in mice with heterozygous *Pax2* mutations there is a dramatic increase in the fraction of UB cells undergoing apoptosis. This phenomenon was primarily seen in the elongating trunks of the UB rather than at UB tips in the nephrogenic zone (36). Our previous studies show that there is a direct relationship between the susceptibility of UB cells to programmed cell death, the extent of UB branching during development, and congenital nephron number (36).

The effects of PAX2 on programmed cell death have been confirmed in a variety of settings. In cancers where PAX2 is aberrantly overexpressed, *PAX2* inactivation with siRNAs was shown to sensitize the cells to apoptosis induced by chemotherapeutic agents (29). PAX2 promotes survival of cultured HEK293 cells overexpressing caspase genes (46) or renal collecting duct cells exposed to high-salt concentrations (6). Increased PAX2 expression has also been observed in renal cystic epithelium (49). Heterozygosity for a null *Pax2* mutation increased cyst cell apoptosis and reduced cyst size in the *cpk* mouse (33).

Although it is now clear that PAX2 suppresses apoptosis during organogenesis, the mechanism by which it promotes cell survival is currently unknown. Here, we show that PAX2 directly binds to specific recognition motifs in the human *NAIP* gene promoter and specifically activates its transcription. In our studies, addition of polyclonal PAX2 antibody eliminated the complex formed by PAX2b protein and an oligonucleotide containing the putative PAX2 recognition motif. Presumably, this antibody interferes with interactions between the binding domain of PAX2b protein and the recognition motif. Numerous other reports show that specific antibodies do not always cause a supershift but can often eliminate complex formation (15, 37). The sevenfold activation of *NAIP* transcription by PAX2 demonstrated in vitro appears to be physiologically relevant as total *Naip* transcript levels were significantly reduced in heterozygous *Pax2* mutant mice.

The *NAIP* gene encodes a member of a family of endogenous caspase inhibitors called IAPs. Eight human IAPs have been identified (24). These show a certain degree of tissue specificity and are frequently overexpressed in cancer cells (45). Specifically, NAIP inhibits caspases-3 and -7 (27) and has been shown to suppress apoptosis in neural tissues (16, 20, 25, 34, 50). *NAIP* was initially discovered during positional cloning of the causative gene for spinal muscular atrophy (SMA) (39). It was later confirmed that mutation of the survivor motor neuron (*SMN*) gene adjacent to *NAIP* is responsible for SMA (23). However, patients with deletions spanning both genes present with a significantly more severe form of SMA (1, 39).

Although only one functional *NAIP* has been identified thus far in humans (39, 51), six highly homologous but separate *Naip* genes have been identified in the mouse (16, 52). Thus knockout of the murine *Naip1* homolog did not cause a developmental abnormality of the brain, although neurons exhibited increased susceptibility to kainic acid-induced injury compared with controls (18). Presumably, this reflects the functional redundancy of *Naip* genes in mice, making them suboptimal models for study of *NAIP* function in humans. The renal status of humans with SMA and homozygous *NAIP* deletions is unknown, but our observations predict that increased susceptibility to apoptosis during kidney development should reduce congenital nephron number (36). It is of interest that the *Naip1* transcript is 7.4-fold higher in fetal than in adult kidney. This parallels the ontogeny of PAX2 expression during murine kidney development (10, 47). In mouse kidney, the effects of PAX2 may reflect its regulation of the *Naip1* gene. However, we cannot rule out similar transcriptional regulation of the other murine *Naip* homologs.

Developmental pathways regulated by PAX2 in the kidney may also be important for brain development. Homozygous null *Pax2* mutant mice are anephric, but also exhibit a massive defect in the fetal midbrain/hindbrain region (14). PAX2 has been shown to activate the glial cell-derived neurotrophic factor (*Gdnf*) gene in the kidney (5). In developing kidney,

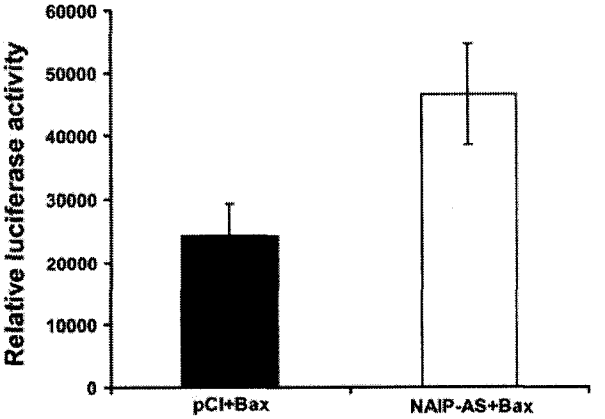

Fig. 7. Inhibition of *Naip* in renal collecting duct cells causes increased apoptosis. Mouse mIMCD-3 cells derived from renal collecting duct cells were transiently transfected with a *Bax* expression vector (to stimulate apoptosis) in the presence or absence of a *Naip* antisense cDNA expression vector. After 48 h, Bax-stimulated caspase-3/7 activity was significantly higher in the cells cotransfected with the *Naip* antisense vector than with an empty vector control ($P < 0.05$).

GDNF is essential for outgrowth and arborization of the UB (28, 35, 41) and promotes survival of UB cells (48). GDNF is also expressed in the brain where it is an important trophic signal for neural differentiation and neuronal cell survival (44). However, it is unknown whether PAX2 directly activates *Gdnf* in brain as it does in kidney. PAX2 activates fibroblast growth factor 8 (*Fgf8*) at the midbrain-hindbrain boundary, a central organizer during neuronal development which is also expressed in the developing kidney (17, 53).

Similar to the neuroprotective role of NAIP in brain tissues, we show that NAIP also has an anti-apoptotic function in kidney cells. Inner medullary collecting ducts cells were more sensitive to *Baxα*-induced apoptosis, as measured by caspase 3/7 activity, when cotransfected with a *Naip* antisense cDNA. Previous in situ hybridization experiments show that *Naip* expression colocalizes with *Pax2* in the midbrain/hindbrain region, the otic vesicle, and the retina during fetal mouse development (21, 31, 38). Similarly, NAIP is expressed in the collecting ducts and emerging proximal tubules, paralleling the known expression pattern of *Pax2* (4, 47).

Final nephron number ranges widely in humans (0.3 and 1.3 million nephrons/kidney) (19, 32). Recent evidence suggests that subtle renal hypoplasia may have far-reaching clinical implications. Humans born into the lower percentiles of the nephron number spectrum have reduced renal reserve and appear to be at risk for essential hypertension later in life (22). Our previous work suggests that PAX2 is centrally involved in regulating final nephron number by suppressing programmed cell death in the UB lineage. Here, we show that the powerful anti-apoptotic effects of PAX2 may be mediated by activation of the endogenous caspase inhibitor, *NAIP*. We hypothesize that *NAIP* activation by PAX2 transiently confers resistance of UB cells to programmed cell death during branching morphogenesis in fetal kidney, thereby optimizing final nephron number. Conceivably, *NAIP* could also play a role in the phenotype of cancer cells and cystic epithelium where PAX2 is inappropriately overexpressed.

GRANTS

This study was supported by an operating grant from the Canadian Institutes of Health Research (CIHR; MOP 12954). A. Dziarmaga is a recipient of a CIHR doctoral studentship award. Dr. P. Goodyer is the recipient of a James McGill Research Chair.

REFERENCES

1. **Akutsu T, Nishio H, Sumino K, Takeshima Y, Tsuneishi S, Wada H, Takada S, Matsuo M, and Nakamura H.** Molecular genetics of spinal muscular atrophy: contribution of the NAIP gene to clinical severity. *Kobe J Med Sci* 48: 25–31, 2002.
2. **Ardissino G, Dacco V, Testa S, Bonaudo R, Claris-Appiani A, Taioli E, Marra G, Edefonti A, and Sereni F.** Epidemiology of chronic renal failure in children: data from the ItalKid project. *Pediatrics* 111: e382–e387, 2003.
3. **Biosystems A.** User Bulletin #2. ABI Prism 7700 Sequence Detection System, 2001, p. 36.
4. **Bouchard M, Souabni A, Mandler M, Neubuser A, and Busslinger M.** Nephric lineage specification by Pax2 and Pax8. *Genes Dev* 16: 2958–2970, 2002.
5. **Brophy PD, Ostrom L, Lang KM, and Dressler GR.** Regulation of ureteric bud outgrowth by Pax2-dependent activation of the glial derived neurotrophic factor gene. *Development* 128: 4747–4756, 2001.
6. **Cai Q, Dmitrieva NI, Ferraris JD, Brooks HL, van Balkom BW, and Burg M.** Pax2 expression occurs in renal medullary epithelial cells in vivo and in cell culture, is osmoregulated, and promotes osmotic tolerance. *Proc Natl Acad Sci USA* 102: 503–508, 2005.
7. **Clark AT and Bertram JF.** Molecular regulation of nephron endowment. *Am J Physiol Renal Physiol* 276: F485–F497, 1999.
8. **Clark P, Dziarmaga A, Eccles M, and Goodyer P.** Rescue of defective branching nephrogenesis in renal-coloboma syndrome by the caspase inhibitor, Z-VAD-fmk. *J Am Soc Nephrol* 15: 299–305, 2004.
9. **Cullen-McEwen LA, Kett MM, Dowling J, Anderson WP, and Bertram JF.** Nephron number, renal function, and arterial pressure in aged GDNF heterozygous mice. *Hypertension* 41: 335–340, 2003.
10. **Dressler GR, Deutsch U, Chowdhury K, Nornes HO, and Gruss P.** Pax2, a new murine paired-box-containing gene and its expression in the developing excretory system. *Development* 109: 787–795, 1990.
11. **Dressler GR, Wilkinson JE, Rothenpieler UW, Patterson LT, Williams-Simons L, and Westphal H.** Deregulation of Pax-2 expression in transgenic mice generates severe kidney abnormalities. *Nature* 362: 65–67, 1993.
12. **Dziarmaga A, Clark P, Stayner C, Julien JP, Torban E, Goodyer P, and Eccles M.** Ureteric bud apoptosis and renal hypoplasia in transgenic PAX2-Bax fetal mice mimics the renal-coloboma syndrome. *J Am Soc Nephrol* 14: 2767–2774, 2003.
13. **Endrizzi MG, Hadinoto V, Growney JD, Miller W, and Dietrich WF.** Genomic sequence analysis of the mouse Naip gene array. *Genome Res* 10: 1095–1102, 2000.
14. **Favor J, Sandulache R, Neuhauser-Klaus A, Pretsch W, Chatterjee B, Senft E, Wurst W, Blanquet V, Grimes P, Sporle R, and Schughart K.** The mouse Pax2(1Neu) mutation is identical to a human PAX2 mutation in a family with renal-coloboma syndrome and results in developmental defects of the brain, ear, eye, and kidney. *Proc Natl Acad Sci USA* 93: 13870–13875, 1996.
15. **Flock G and Drucker DJ.** Pax-2 activates the proglucagon gene promoter but is not essential for proglucagon gene expression or development of proglucagon-producing cell lineages in the murine pancreas or intestine. *Mol Endocrinol* 16: 2349–2359, 2002.
16. **Gotz R, Karch C, Digby MR, Troppmair J, Rapp UR, and Sendtner M.** The neuronal apoptosis inhibitory protein suppresses neuronal differentiation and apoptosis in PC12 cells. *Hum Mol Genet* 9: 2479–2489, 2000.
17. **Grieshammer U, Cebrian C, Ilagan R, Meyers E, Herzlinger D, and Martin GR.** FGF8 is required for cell survival at distinct stages of nephrogenesis and for regulation of gene expression in nascent nephrons. *Development* 132: 3847–3857, 2005.
18. **Holcik M, Thompson CS, Yaraghi Z, Lefebvre CA, MacKenzie AE, and Korneluk RG.** The hippocampal neurons of neuronal apoptosis inhibitory protein 1 (NAIP1)-deleted mice display increased vulnerability to kainic acid-induced injury. *Proc Natl Acad Sci USA* 97: 2286–2290, 2000.
19. **Hoy WE, Douglas-Denton RN, Hughson MD, Cass A, Johnson K, and Bertram JF.** A stereological study of glomerular number and volume: preliminary findings in a multiracial study of kidneys at autopsy. *Kidney Int Suppl* 83: S31–S37, 2003.
20. **Hutchison JS, Derrane RE, Johnston DL, Gendron N, Barnes D, Fliss H, King WJ, Rasquinha I, MacManus J, Robertson GS, and MacKenzie AE.** Neuronal apoptosis inhibitory protein expression after traumatic brain injury in the mouse. *J Neurotrauma* 18: 1333–1347, 2001.
21. **Ingram-Crooks J, Holcik M, Drmanic S, and MacKenzie AE.** Distinct expression of neuronal apoptosis inhibitory protein (NAIP) during murine development. *Neuroreport* 13: 397–402, 2002.
22. **Keller G, Zimmer G, Mall G, Ritz E, and Amann K.** Nephron number in patients with primary hypertension. *N Engl J Med* 348: 101–108, 2003.
23. **Lefebvre S, Burglen L, Reboullet S, Clermont O, Burlet P, Viollet L, Benichou B, Cruaud C, Millasseau P, Zeviani M, LePaslier D, Frézal J, Cohen D, Weissenback J, Munnich A, and Melki J.** Identification and characterization of a spinal muscular atrophy-determining gene. *Cell* 80: 155–165, 1995.
24. **Liston P, Fong WG, and Korneluk RG.** The inhibitors of apoptosis: there is more to life than Bcl2. *Oncogene* 22: 8568–8580, 2003.
25. **Liston P, Roy N, Tamai K, Lefebvre C, Baird S, Cherton-Horvat G, Farahani R, McLean M, Ikeda JE, MacKenzie A, and Korneluk RG.** Suppression of apoptosis in mammalian cells by NAIP and a related family of IAP genes. *Nature* 379: 349–353, 1996.
26. **Livak KJ and Schmittgen TD.** Analysis of relative gene expression data using real-time quantitative PCR and the $2^{-\Delta\Delta C_T}$ method. *Methods* 25: 402–408, 2001.
27. **Maier JK, Lahoua Z, Gendron NH, Fetni R, Johnston A, Davoodi J, Rasper D, Roy S, Slack RS, Nicholson DW, and MacKenzie AE.** The

neuronal apoptosis inhibitory protein is a direct inhibitor of caspases 3 and 7. *J Neurosci* 22: 2035–2043, 2002.

28. **Moore MW, Klein RD, Farinas I, Sauer H, Armanini M, Phillips H, Reichardt LF, Ryan AM, Carver-Moore K, and Rosenthal A.** Renal and neuronal abnormalities in mice lacking GDNF. *Nature* 382: 76–79, 1996.
29. **Muratovska A, Zhou C, He S, Goodyer P, and Eccles MR.** Paired-box genes are frequently expressed in cancer and often required for cancer cell survival. *Oncogene* 22: 7989–7997, 2003.
30. **Nemoto T, Kitagawa M, Hasegawa M, Ikeda S, Akashi T, Takizawa T, Hirokawa K, and Koike M.** Expression of IAP family proteins in esophageal cancer. *Exp Mol Pathol* 76: 253–259, 2004.
31. **Nornes HO, Dressler GR, Knapik EW, Deutsch U, and Gruss P.** Spatially and temporally restricted expression of Pax2 during murine neurogenesis. *Development* 109: 797–809, 1990.
32. **Nyengaard JR and Bendtsen TF.** Glomerular number and size in relation to age, kidney weight, and body surface in normal man. *Anat Rec* 232: 194–201, 1992.
33. **Ostrom L, Tang MJ, Gruss P, and Dressler GR.** Reduced Pax2 gene dosage increases apoptosis and slows the progression of renal cystic disease. *Dev Biol* 219: 250–258, 2000.
34. **Perrelet D, Ferri A, MacKenzie AE, Smith GM, Korneluk RG, Liston P, Sagot Y, Terrado J, Monnier D, and Kato AC.** IAP family proteins delay motoneuron cell death in vivo. *Eur J Neurosci* 12: 2059–2067, 2000.
35. **Pichel JG, Shen L, Sheng HZ, Granholm AC, Drago J, Grinberg A, Lee EJ, Huang SP, Saarma M, Hoffer BJ, Sariola H, and Westphal H.** Defects in enteric innervation and kidney development in mice lacking GDNF. *Nature* 382: 73–76, 1996.
36. **Porteous S, Torban E, Cho NP, Cunliffe H, Chua L, McNoe L, Ward T, Souza C, Gus P, Giugliani R, Sato T, Yun K, Favor J, Sicotte M, Goodyer P, and Eccles M.** Primary renal hypoplasia in humans and mice with PAX2 mutations: evidence of increased apoptosis in fetal kidneys of Pax2(1Neu) +/− mutant mice. *Hum Mol Genet* 9: 1–11, 2000.
37. **Ramchandran R, Bengra C, Whitney B, Lanclos K, and Tuan D.** A (GATA)(7) motif located in the 5′ boundary area of the human beta-globin locus control region exhibits silencer activity in erythroid cells. *Am J Hematol* 65: 14–24, 2000.
38. **Rowitch DH and McMahon AP.** Pax-2 expression in the murine neural plate precedes and encompasses the expression domains of Wnt-1 and En-1. *Mech Dev* 52: 3–8, 1995.
39. **Roy N, Mahadevan MS, McLean M, Shutler G, Yaraghi Z, Farahani R, Baird S, Besner-Johnston A, Lefebvre C, Kang X, Salih M, Aubrey H, Tamai K, Guan X, Ioannu P, Crawford TO, de Jong PJ, Surh L, Ikeda J-E, Korneluk RG, and Mackenzie A.** The gene for neuronal apoptosis inhibitory protein is partially deleted in individuals with spinal muscular atrophy. *Cell* 80: 167–178, 1995.
40. **Salomon R, Tellier AL, Attie-Bitach T, Amiel J, Vekemans M, Lyonnet S, Dureau P, Niaudet P, Gubler MC, and Broyer M.** PAX2 mutations in oligomeganephronia. *Kidney Int* 59: 457–462, 2001.
41. **Sanchez MP, Silos-Santiago I, Frisen J, He B, Lira SA, and Barbacid M.** Renal agenesis and the absence of enteric neurons in mice lacking GDNF. *Nature* 382: 70–73, 1996.
42. **Sanyanusin P, McNoe LA, Sullivan MJ, Weaver RG, and Eccles MR.** Mutation of PAX2 in two siblings with renal-coloboma syndrome. *Hum Mol Genet* 4: 2183–2184, 1995.
43. **Sanyanusin P, Schimmenti LA, McNoe LA, Ward TA, Pierpont ME, Sullivan MJ, Dobyns WB, and Eccles MR.** Mutation of the PAX2 gene in a family with optic nerve colobomas, renal anomalies and vesicoureteral reflux. *Nat Genet* 9: 358–364, 1995.
44. **Sariola H and Saarma M.** Novel functions and signalling pathways for GDNF. *J Cell Sci* 116: 3855–3862, 2003.
45. **Tamm I, Kornblau SM, Segall H, Krajewski S, Welsh K, Kitada S, Scudiero DA, Tudor G, Qui YH, Monks A, Andreeff M, and Reed JC.** Expression and prognostic significance of IAP-family genes in human cancers and myeloid leukemias. *Clin Cancer Res* 6: 1796–1803, 2000.
46. **Torban E, Eccles MR, Favor J, and Goodyer PR.** PAX2 suppresses apoptosis in renal collecting duct cells. *Am J Pathol* 157: 833–842, 2000.
47. **Torres M, Gomez-Pardo E, Dressler GR, and Gruss P.** Pax-2 controls multiple steps of urogenital development. *Development* 121: 4057–4065, 1995.
48. **Towers PR, Woolf AS, and Hardman P.** Glial cell line-derived neurotrophic factor stimulates ureteric bud outgrowth and enhances survival of ureteric bud cells in vitro. *Exp Nephrol* 6: 337–351, 1998.
49. **Winyard PJ, Risdon RA, Sams VR, Dressler GR, and Woolf AS.** The PAX2 tanscription factor is expressed in cystic and hyperproliferative dysplastic epithelia in human kidney malformations. *J Clin Invest* 98: 451–459, 1996.
50. **Xu DG, Crocker SJ, Doucet JP, St-Jean M, Tamai K, Hakim AM, Ikeda JE, Liston P, Thompson CS, Korneluk RG, MacKenzie A, and Robertson GS.** Elevation of neuronal expression of NAIP reduces ischemic damage in the rat hippocampus. *Nat Med* 3: 997–1004, 1997.
51. **Xu M, Okada T, Sakai H, Miyamoto N, Yanagisawa Y, MacKenzie AE, Hadano S, and Ikeda JE.** Functional human NAIP promoter transcription regulatory elements for the NAIP and PsiNAIP genes. *Biochim Biophys Acta* 1574: 35–50, 2002.
52. **Yaraghi Z, Korneluk RG, and MacKenzie A.** Cloning and characterization of the multiple murine homologues of NAIP (neuronal apoptosis inhibitory protein). *Genomics* 51: 107–113, 1998.
53. **Ye W, Bouchard M, Stone D, Liu X, Vella F, Lee J, Nakamura H, Ang SL, Busslinger M, and Rosenthal A.** Distinct regulators control the expression of the mid-hindbrain organizer signal FGF8. *Nat Neurosci* 4: 1175–1181, 2001.

APPENDIX II

Compliance forms

The American Physiological Society

9650 Rockville Pike, Bethesda, MD 20814-3991, USA
Phone: (301) 634-7070
Fax: (301) 634-7243

March 27, 2008

Pierre-Alain Hueber
Montreal Children's Hospital- McGill University
4060 Ste Catherine West
H2X2B4 Montreal Canada

Dear Mr. Hueber:

The American Physiological Society grants you permission to use the following *American Journal of Physiology Renal Physiology* articles in your doctoral thesis appendix for McGill University:

Alison Dziarmaga, Pierre-Alain Hueber, Diana Iglesias, Nancy Hache, Aaron Jeffs, Nathalie Gendron, Alex MacKenzie, Michael Eccles, and Paul Goodyer, **Neuronal apoptosis inhibitory protein is expressed in developing kidney and is regulated by PAX2,***Am J Physiol Renal Physiol* 291: F913-F920, 2006,

and

Diana M. Iglesias, Pierre-Alain Hueber, LeeLee Chu, Robert Campbell, Anne-Marie Patenaude, Alison J. Dziarmaga, Jacklyn Quinlan, Othman Mohamed, Daniel Dufort, and Paul R. Goodyer **Canonical WNT signaling during kidney development,** *Am J Physiol Renal Physiol* 293: F494-F500, 2007.

McGill University may provide single copies of the dissertation on demand, but may not make the appendix available for free internet download.

The American Physiological Society publication must be credited as the source with the words "used with permission" added when referencing the *AJP Renal* articles.

Sincerely,

Margaret Reich

Ms. Margaret Reich
Director of Publications
The American Physiological Society

MR/pr

MMS Reference Number: PS - 2008 - 3499
MMS Invoice Number: RY - 2008 - 3499

April 08, 2008

BASIC PROVISIONS of GRANT OF PERMISSION

- This permission applies only to copyrighted material that the Massachusetts Medical Society ("MMS") owns, and not to copyrighted text or illustrations from other sources. If material appears in our work with credit to another source, you must also obtain permission from the original source cited in our work.

- All content reproduced from copyrighted material owned by the MMS remains the sole and exclusive property of the MMS. The right to grant permission to a third party is reserved solely by the MMS.

- MMS' copyrighted content may not be used in any manner that implies endorsement, sponsorship, or promotion of any entity, product or service by the MMS or its publications. MMS cannot and does not authorize the use of any author's name on promotional materials; such approval must be obtained directly from the author.

- **CREDIT LINE:** This permission requires a full credit line either in close proximity to where MMS text or illustration appears, or on the copright page of any publication that incorporates the MMS' content. This credit line must include reference to the original article in standard citation format, together with a notice of copyright ownership, as follows: Copyright © *[year of publication] Massachusetts Medical Society. All rights reserved.*

- This permission is a one-time, non-exclusive grant limited only to the specific use, format(s), language(s) and edition(s) specified on the "Items Covered by Grant of Permission" page. It is<u>not</u> a "blanket" permission allowing unrestricted use of this material in future reproductions, editions, revisions, ancillary products, or other derivative works.

- This permission gives distribution rights throughout the world.

- Unless expressly stated otherwise, this grant of permission is issued for the material to be used only as originally published by MMS. Any adaptation or modification to the material must be reviewed and aproved by MMS prior to the issuance of a grant of permission. Approval of adaptations, if applicable, is noted on page three of this grant. Font and style changes are not considered adaptations.

- Any explanatory material or figure legends used by the requester must accurately reflect the material as originally published by MMS.

- Unless fees have been waived, this permission is contingent on payment in a timely manner of any fees associated with this use. **IMPORTANT**: Please reference MMS' original invoice number to ensure proper credit.

Publishing Division of the Massachusetts Medical Society
Department of Permissions & Licensing
860 Winter Street, Waltham, Massachusetts 02451-1413 USA
Tel: (781) 434 7382 · Fax: (781) 434 7633 · permissions@nejm.org

Items Covered by Grant of Permission

The Publishing Division
of the Massachusetts Medical Society

Department of Permissions & Licensing
860 Winter Street, Waltham, Massachusetts 02451-1413 USA
Telephone: (781) 434-7382 fax: (781) 434-7633

MMS Reference Number: PS - 2008 - 3499
MMS Invoice Number: RY - 2008 - 3499

Source Information							Further Conditions				
Source: The New England Journal of Medicine											
Volume	Pages	Pub. Date	Author(s)	Article Title	Type	Item	Format	Language	Adapted	Dollar Amount	Customer Reference
353	2477- 2490	12/8/2005	Cohen, McGovern	Renal-Cell Carcinoma	F	F1	Print & Electronic	English and French	Y	0.00	Fig 1.4B
353	2477- 2490	12/8/2005	Cohen, McGovern	Renal-Cell Carcinoma	F	F4	Print & Electronic	English and French	Y	0.00	Fig 1.5
356	185- 187	1/11/2007	Brugarolas	Renal-Cell Carcinoma -- Molecular Pathways and Therapies	F	F1	Print & Electronic	English and French	Y	0.00	Fig 1.6A

The following information has been provided for us in your letter of request.

End Use: introduction to doctoral thesis
User: Pierre-Alain Hueber
Sponsor: McGill University
Date of Use: 2008
Number of Copies:

Simply visit: http://www.sciencedirect.com/ and locate your desired content.
ɐn the abstract or summary and then click on the 'Request Permission' button to open the Rightslink web page
ɪich will launch you into the Rightslink application and then follow the steps below.

Select the way you would like to reuse the content
Create an account if you haven't already
Accept the terms and conditions and you're done

ɜase contact Rightslink Customer Care with any questions or comments concerning this service:
pyright Rightslink Customer Care
l (toll free): 877/622-5543 Tel: 978/777-9929
nail: customercare@copyright.com

evier Limited, a company registered in England and Wales with company number 1982084, whose registered office is The ulevard, Langford Lane, Kidlington, Oxford, OX5 1GB, United Kingdom.

ɔm: pa@hueber.com [mailto:]
nt: 27 March 2008 03:58
: Cancer Letters (ELS)
bject: Cancer Letters copyright permission

whom it may concern,

m writing concerning copyright permission for the following article that has been accepted for publication in ncer Letters :

vivo validation of PAX2 as a target for renal cancer therapy Cancer Letters 2008 in press

m the first author and wish to include this paper as part of my doctoral dissertation, since I completed this work ɪing the course of my graduate studies. The thesis is entitled « Pax2/Pax3 in normal kidney development and as ɪapeutic target for renal cancer » will be submitted to McGill University Montreal, Canada.

ɜase advise how I should proceed in obtaining copyright permission.

ank you.

ɪcerely

ɪrre-Alain Hueber

. Hueber

ɔntreal Children's
ɔ0 ste catherine west H2X2B4
514-412-4400 ext:22953

ɪs email is from Elsevier Limited, a company registered in England and Wales with company n
ɔse registered office is The Boulevard, Langford Lane, Kidlington, Oxford, OX5 1GB, United

RE: copyright permission for doctoral thesis

Inbox

"Overturf, Kyle" <kyle.overturf@aacr.org> show details Mar 28 | Reply

Dear Dr. Hueber,

Thank you for your recent correspondence regarding permission to reproduce figures from *Clinical Cancer Research.*

We do not require permission requests for the reproduction of articles or figures to be used in thesis. All information on our rules and regulations regarding reproductions can be found on our website at www.aacr.org.

If you have any questions or concerns regarding this, please do not hesitate to contact me.

Thanks,

Kyle Overturf

From: Pierre-Alain Hueber [mailto
Sent: Thursday, March 27, 2008 4:50 PM
To: permissions
Subject: copyright permission for doctoral thesis

To whom it may concern,

I am writing concerning copyright permission to use an image that has been published Clinical Cancer Research.

Figure 1 page 672
Identification of the Genes for Kidney Cancer: Opportunity for Disease-Specific Targeted Therapeutics Clinical Cancer Research 13, 671s-679s, January 15, 2007

I wish to include this image with modification as part of the Introduction of my doctoral thesis. Full credit (journal title, volume, year, pages and authors and original copyright) will be given

The thesis is entitled « Pax2/Pax3 in normal kidney development and as therapeutic target for renal cancer » and will be submitted to McGill University, Montreal, Canada.

Please find attached the completed permission form.

Thank you for considering my request.

Sincerely

Pierre-Alain Hueber

Montreal Children's Hospital- McGill University
4060 ste catherine west H2X2B4 Montreal
tel:514-412-4400 ext:22953

Please note that this e-mail and any files transmitted with it may be privileged, confidential, and protected from disclosure under applicable law. This information is intended only for the person or entity to which it is addressed and may contain confidential or privileged material. Any review, retransmission, dissemination, or other use of, or taking of any action in reliance upon, this information by persons or entities other than the intended recipient is prohibited. If you received this in error, please contact the sender and delete the material from any computer.

L'Hôpital de Montréal pour enfants
The Montreal Children's Hospital

Centre universitaire de santé McGill
McGill University Health Centre

October 31, 2007

Dr. Paul Goodyer
Pediatric Nephrology
Montreal Children's Hospital
Room E-222

Re: PED-07-035 **Molecular Pathogensis of Wilms' Tumor**

Dear Dr. Goodyer,

We are writing in response to your request for review by the Montreal Children Hospital Research Ethics Board of the research proposal entitled above.

We are pleased to inform you that the study was found to be within ethical guidelines for conduct at the McGill University Health Centre. Approval for the study to use samples from previous COG studies where consent was signed for banking for future studies was provided via expedited review of the Chair on Oct. 31, 2007, and will be reported to the Research Ethics Board (REB) at its meeting of Nov. 26, 2007, and will be entered accordingly into the minutes. At the MUHC, sponsored research activities that require US federal assurance are conducted under Federal Wide Assurance (FWA) 00000840.

All research involving human subjects requires review at a recurring interval and the current study approval is in effect until Oct. 30, 2008. It is the responsibility of the principal investigator to submit an Application for Continuing Review to the REB prior to the expiration of approval to comply with the regulation for continuing review of "at least once per year".

The Research Ethics Boards (REBs) of the McGill University Health Centre are registered REBs working under the published guidelines of the Tri-Council Policy Statement, in compliance with the "Plan d'action ministériel en éthique de la recherche et en intégrité scientifique" (MSSS, 1998) and the Food and Drugs Act (7 June, 2001), acting in conformity with standards set forth in the (US) Code of Federal Regulations governing human subjects research, and functioning in a manner consistent with internationally accepted principles of good clinical practice.

We wish to advise you that this document completely satisfies the requirement for Research Ethics Board Attestation as stipulated by Health Canada.

The project was assigned MUHC Study Number PED-07-035 that is required as MUHC reference when communicating about the research. Should any revision to the study, or other unanticipated development occur prior to the next required review, you must advise the REB without delay. Regulation does not permit initiation of a proposed study modification prior to REB approval for the amendment.